Methods in Molecular Biology 1748

Springer Protocols

Marco G. Alves
Pedro F. Oliveira *Editors*

Sertoli Cells

Methods and Protocols

EXTRAS ONLINE

Humana Press

METHODS IN MOLECULAR BIOLOGY

Series Editor
John M. Walker
School of Life and Medical Sciences
University of Hertfordshire
Hatfield, Hertfordshire, AL10 9AB, UK

For further volumes:
http://www.springer.com/series/7651

Sertoli Cells

Methods and Protocols

Edited by

Marco G. Alves

Department of Microscopy, Laboratory of Cell Biology and Unit for Multidisciplinary Research in Biomedicine (UMIB), Institute of Biomedical Sciences Abel Salazar (ICBAS), University of Porto, Porto, Portugal

Pedro F. Oliveira

Department of Microscopy, Laboratory of Cell Biology and Unit for Multidisciplinary Research in Biomedicine (UMIB), Institute of Biomedical Sciences Abel Salazar (ICBAS), University of Porto, Porto, Portugal; Department of Genetics, Faculty of Medicine, University of Porto, Porto, Portugal; i3S – Instituto de Investigação e Inovação em Saúde, University of Porto, Porto, Portugal; Department of Biosciences, Biotechnologies and Biopharmaceutics, University of Bari "Aldo Moro", Bari, Italy

Humana Press

Editors
Marco G. Alves
Department of Microscopy, Laboratory of Cell Biology and Unit for Multidisciplinary Research in Biomedicine (UMIB), Institute of Biomedical Sciences Abel Salazar (ICBAS)
University of Porto
Porto, Portugal

Pedro F. Oliveira
Department of Microscopy, Laboratory of Cell Biology and Unit for Multidisciplinary Research in Biomedicine (UMIB), Institute of Biomedical Sciences Abel Salazar (ICBAS)
University of Porto
Porto, Portugal

Department of Genetics, Faculty of Medicine
University of Porto
Porto, Portugal

i3S - Instituto de Investigação e Inovação em Saúde
University of Porto
Porto, Portugal

Department of Biosciences, Biotechnologies and Biopharmaceutics
University of Bari "Aldo Moro"
Bari, Italy

ISSN 1064-3745 ISSN 1940-6029 (electronic)
Methods in Molecular Biology
ISBN 978-1-4939-7697-3 ISBN 978-1-4939-7698-0 (eBook)
https://doi.org/10.1007/978-1-4939-7698-0

Library of Congress Control Number: 2018930253

Printed on acid-free paper

This Humana Press imprint is published by Springer Nature
The registered company is Springer Science+Business Media, LLC
The registered company address is: 233 Spring Street, New York, NY 10013, U.S.A.

Preface

We are proud to present this book dedicated to the somatic testicular Sertoli cell. These cells were first described by Enrico Sertoli in 1865. Since then, they have emerged as being pivotal for spermatogenesis and thus for male reproductive potential. These remarkable cells present some unique features that go far beyond the physical and nutritional support of spermatogenesis. That is why so many researchers have chosen to use them as models for a broad range of studies in many disciplines. This book was prepared not only for nonspecialists but also for experienced researchers that may be interested in a multidisciplinary approach to study these cells. The book is divided in 20 chapters, with only two review articles that introduce useful concepts for the understanding of the subsequent chapters, highlighting the mechanisms involved in two of the most relevant functions of these cells.

The use of Sertoli cells as models in male reproductive biology or as supporters for other cell types illustrates the need for standardized protocols for their in vitro culture. As expected, according to the species, there are small but crucial changes necessary to have these cells in culture (Chapter 1). After a successful culture, it is pivotal to characterize the cells and guarantee that the isolation was correct and the purity is as expected (Chapter 2). Most of the time, the visualization of the internal structures of the testis in sectioning material is mandatory. In that way, it is possible to have a detailed analysis of the seminiferous tubules, where Sertoli cells and germ cells establish an important relation, and the interstitial space. Thus, the specialized microenvironment can be analyzed by immunohistochemistry (Chapters 3 and 4).

Sertoli cells undergo proliferation and apoptosis during development, but it remains a matter of debate when they reach adulthood. In addition, that process, together with apoptosis, is altered by exposure to several substances and even hormones. It is then pivotal to study Sertoli cells' proliferation and apoptosis (Chapter 5). Many of those processes are mediated by protein-protein interactions, and to fully understand the relevance of Sertoli cell, it is essential to study those interactions being that co-immunoprecipitation is used many times (Chapter 6). The analysis and interpretation of interactome is complex, but it may open new insights on the molecular mechanisms that underlie Sertoli cell physiology and function (Chapter 7). Among the several novel processes identified in Sertoli cells, phagocytosis (Chapter 8), mitophagy (Chapter 9), and autophagy (Chapter 10) have emerged as biomarkers for health and disease.

The nutritional support of spermatogenesis (reviewed in Chapter 11) is an essential process in which the Sertoli cell produces the metabolic intermediates for the developing germ cells. Thus, assessing the metabolic activity of Sertoli cells (Chapter 12) and establishing their proteome (Chapter 13) enlighten a mechanistic action that may mediate subfertility or infertility in males. To further study Sertoli cell physiology and function, gene silencing or cell ablation is often used (Chapters 14 and 15).

The blood-testis barrier is composed of adjacent Sertoli cells being essential for spermatogenesis (reviewed in Chapter 16). Thus, the study of its integrity is a very valuable tool for researchers working on reproductive biology (Chapter 17). There is a long range of toxicants that affect the male reproductive system, and thus, novel computational methods

are being refined to evaluate their effect (Chapter 18). In addition, the water movement in Sertoli cells and the composition of the tubular fluid are a key element for a successful spermatogenesis (Chapter 19). Finally, we must also highlight the relevance of testis cryopreservation (Chapter 20).

We are hopeful that this volume dedicated to Sertoli cells will be a valuable resource for experienced researchers in reproductive biology, particularly andrologists, but also for future investigators and young students starting to study these remarkable cells. We thank all authors for their support and their contributions with key and useful notes. We also thank the production team and Springer for accepting this project. Their support and guidance were very useful. Finally, we would like to thank Dr. Raquel L. Bernardino for editorial checking and support at our laboratory. Finally, we thank the readers and we hope they can find this book useful.

Porto, Portugal

Marco G. Alves
Pedro F. Oliveira

Contents

Contributors

Marco G. Alves • *Unit for Multidisciplinary Research in Biomedicine (UMIB), Laboratory of Cell Biology, Department of Microscopy, Institute of Biomedical Sciences Abel Salazar (ICBAS), University of Porto, Porto, Portugal*

Yoni Baert • *Biology of the Testis, Research Laboratory for Reproduction, Genetics and Regenerative Medicine, Vrije Universiteit Brussel (VUB), Brussels, Belgium*

Barbara Banco • *Reparto di Anatomia Patologica, DiMeVet, Università degli Studi di Milano, Milan, Italy*

Ester Beltrán-Frutos • *Department of Cell Biology and Histology, School of Medicine, IMIB-Arrixaca, Regional Campus of International Excellence, Campus Mare Nostrum, University of Murcia, Murcia, Spain*

Raquel L. Bernardino • *Unit for Multidisciplinary Research in Biomedicine (UMIB), Laboratory of Cell Biology, Department of Microscopy, Institute of Biomedical Sciences Abel Salazar (ICBAS), University of Porto, Porto, Portugal*

Barbara Bilinska • *Department of Endocrinology, Institute of Zoology and Biomedical Research, Jagiellonian University, Krakow, Poland*

Nicolas Bourmeyster • *Laboratoire Signalisation et Transports Ioniques Membranaires, Université de Poitiers/CNRS, Poitiers, France; CHU de Poitiers, Poitiers, France*

Giuseppe Calamita • *Department of Biosciences, Biotechnologies and Biopharmaceutics, University of Bari "Aldo Moro", Bari, Italy*

Anne Cantereau • *Laboratoire Signalisation et Transports Ioniques Membranaires, Université de Poitiers/CNRS, Poitiers, France; Plateforme IMAGE-UP, Poitiers, France*

Rui A. Carvalho • *Department of Life Sciences, University of Coimbra, Coimbra, Portugal*

Haiqi Chen • *The Mary M. Wohlford Laboratory for Male Contraceptive Research, Center for Biomedical Research, Population Council, New York, NY, USA*

C. Yan Cheng • *The Mary M. Wohlford Laboratory for Male Contraceptive Research, Center for Biomedical Research, Population Council, New York, NY, USA; S.B.M. Pharmaceuticals Srl, Rome, Italy*

Luís Crisóstomo • *Unit for Multidisciplinary Research in Biomedicine (UMIB), Laboratory of Cell Biology, Department of Microscopy, Institute of Biomedical Sciences Abel Salazar (ICBAS), University of Porto, Porto, Portugal; Department of Genetics, Faculty of Medicine (FMUP), University of Porto, Porto, Portugal; i3S-Instituto de Investigação e Inovação em Saúde, University of Porto, Porto, Portugal*

Michael Curley • *MRC Centre for Reproductive Health, The Queen's Medical Research Institute, University of Edinburgh, Edinburgh, UK*

Annalucia Darbey • *MRC Centre for Reproductive Health, The Queen's Medical Research Institute, University of Edinburgh, Edinburgh, UK*

Nabil Eid • *Division of Life Sciences, Department of Anatomy and Cell Biology, Osaka Medical College, Osaka, Japan*

Margarida Fardilha • *Laboratory of Signal Transduction, Medical Sciences Department, Institute for Research in Biomedicine, University of Aveiro, Aveiro, Portugal*
Rita Ferreira • *QOPNA, Department of Chemistry, University of Aveiro, Aveiro, Portugal*
Concepción Ferrer • *Department of Cell Biology and Histology, School of Medicine, IMIB-Arrixaca, Regional Campus of International Excellence, Campus Mare Nostrum, University of Murcia, Murcia, Spain*
Maria João Freitas • *Laboratory of Signal Transduction, Medical Sciences Department, Institute for Research in Biomedicine, University of Aveiro, Aveiro, Portugal*
Hongyong Fu • *State Key Laboratory of Oncogenes and Related Genes, Renji-Med X Clinical Stem Cell Research Center, Ren Ji Hospital, School of Medicine, Shanghai Jiao Tong University, Shanghai, China*
María N. Galardo • *División de Endocrinología, Centro de Investigaciones Endocrinológicas "Dr César Bergadá" CONICET – FEI, Hospital de Niños Ricardo Gutiérrez, Ciudad Autónoma de Buenos Aires, Argentina*
Renshan Ge • *Institute of Reproductive Biomedicine, Wenzhou Medical University, Wenzhou, Zhejiang, China*
Patrizia Gena • *Department of Biosciences, Biotechnologies and Biopharmaceutics, University of Bari "Aldo Moro", Bari, Italy*
Ellen Goossens • *Biology of the Testis, Research Laboratory for Reproduction, Genetics and Regenerative Medicine, Vrije Universiteit Brussel (VUB), Brussels, Belgium*
Agostina Gorga • *CONICET-FEI-División de Endocrinología, Hospital de Niños Ricardo Gutiérrez, Centro de Investigaciones Endocrinológicas "Dr César Bergadá", Ciudad Autónoma de Buenos Aires, Argentina*
Valeria Grieco • *Reparto di Anatomia Patologica, DiMeVet, Università degli Studi di Milano, Milan, Italy*
Hitomi Hamaoka • *Division of Life Sciences, Department of Anatomy and Cell Biology, Osaka Medical College, Osaka, Japan*
Zuping He • *State Key Laboratory of Oncogenes and Related Genes, Renji-Med X Clinical Stem Cell Research Center, Ren Ji Hospital, School of Medicine, Shanghai Jiao Tong University, Shanghai, China; Shanghai Institute of Andrology, Ren Ji Hospital, School of Medicine, Shanghai Jiao Tong University, Shanghai, China; Shanghai Key Laboratory of Assisted Reproduction and Reproductive Genetics, Shanghai, China; Shanghai Key Laboratory of Reproductive Medicine, Shanghai, China*
Anna Hejmej • *Department of Endocrinology, Institute of Zoology and Biomedical Research, Jagiellonian University, Krakow, Poland*
Akio Horibe • *Division of Life Sciences, Department of Anatomy and Cell Biology, Osaka Medical College, Osaka, Japan*
Yuko Ito • *Division of Life Sciences, Department of Anatomy and Cell Biology, Osaka Medical College, Osaka, Japan*
Ivana Jarak • *Unit for Multidisciplinary Research in Biomedicine (UMIB), Laboratory of Cell Biology, Department of Microscopy, Institute of Biomedical Sciences Abel Salazar (ICBAS), University of Porto, Porto, Portugal; Department of Life Sciences, University of Coimbra, Coimbra, Portugal*
Bernard Jegou • *Université de Rennes/INSERM, IRSET, Rennes, France*

Pranitha Jenardhanan • *Centre for Bioinformatics, Pondicherry University, Puducherry, India*
Jehangir Khan • *Zoology Department, Buner Campus, Abdul Wali Khan University Mardan, Mardan, Pakistan*
Yoichi Kondo • *Division of Life Sciences, Department of Anatomy and Cell Biology, Osaka Medical College, Osaka, Japan*
Malgorzata Kotula-Balak • *Department of Endocrinology, Institute of Zoology and Biomedical Research, Jagiellonian University, Krakow, Poland*
Will M. Lee • *School of Biological Sciences, University of Hong Kong, Pokfulam, Hong Kong, China*
Nan Li • *The Mary M. Wohlford Laboratory for Male Contraceptive Research, Center for Biomedical Research, Population Council, New York, NY, USA*
Wei Li • *State Key Laboratory of Stem Cell and Reproductive Biology, Institute of Zoology, Chinese Academy of Sciences, Beijing, People's Republic of China*
Qingquan Lian • *Institute of Reproductive Biomedicine, Wenzhou Medical University, Wenzhou, Zhejiang, China*
Chao Liu • *State Key Laboratory of Stem Cell and Reproductive Biology, Institute of Zoology, Chinese Academy of Sciences, Beijing, People's Republic of China*
Wing-yee Lui • *School of Biological Sciences, University of Hong Kong, Pokfulam, Hong Kong, China*
Anna Maggio • *Department of Biosciences, Biotechnologies and Biopharmaceutics, University of Bari "Aldo Moro", Bari, Italy; Unit for Multidisciplinary Research in Biomedicine (UMIB), Laboratory of Cell Biology, Department of Microscopy, Institute of Biomedical Sciences Abel Salazar (ICBAS), University of Porto, Porto, Portugal*
Jesús Martínez-Hernández • *Department of Cell Biology and Histology, School of Medicine, IMIB-Arrixaca, Regional Campus of International Excellence, Campus Mare Nostrum, University of Murcia, Murcia, Spain*
Premendu P. Mathur • *Department of Biochemistry and Molecular Biology, Pondicherry University, Puducherry, India; KIIT University, Bhubaneshwar, Odisha, India*
Silvina B. Meroni • *División de Endocrinología, Centro de Investigaciones Endocrinológicas "Dr César Bergadá" CONICET – FEI, Hospital de Niños Ricardo Gutiérrez, Ciudad Autónoma de Buenos Aires, Argentina*
Nadia Messaddeq • *Institute of Genetics and Molecular and Cellular Biology, Illkirch, France; Centre National de la Recherche Scientifique, UMR7104, Illkirch, France; Institut National de la Santé et de la Recherche Médicale, U964, Illkirch, France; Université de Strasbourg, Strasbourg, France*
Annie-Claire Meunier • *Laboratoire Signalisation et Transports Ioniques Membranaires, Université de Poitiers/CNRS, Poitiers, France*
Dolores D. Mruk • *The Mary M. Wohlford Laboratory for Male Contraceptive Research, Center for Biomedical Research, Population Council, New York, NY, USA*
Minghui Niu • *State Key Laboratory of Oncogenes and Related Genes, Renji-Med X Clinical Stem Cell Research Center, Ren Ji Hospital, School of Medicine, Shanghai Jiao Tong University, Shanghai, China*
Peter O'Shaughnessy • *Institute of Biodiversity, Animal Health and Comparative Medicine, University of Glasgow, Glasgow, UK*

Pedro F. Oliveira • *Department of Microscopy, Laboratory of Cell Biology and Unit for Multidisciplinary Research in Biomedicine (UMIB), Institute of Biomedical Sciences Abel Salazar (ICBAS), University of Porto, Porto, Portugal; Department of Genetics, Faculty of Medicine, University of Porto, Porto, Portugal; i3S - Instituto de Investigação e Inovação em Saúde, University of Porto, Porto, Portugal; Department of Biosciences, Biotechnologies and Biopharmaceutics, University of Bari "Aldo Moro", Bari, Italy*

Jaime Onofre • *Biology of the Testis, Research Laboratory for Reproduction, Genetics and Regenerative Medicine, Vrije Universiteit Brussel (VUB), Brussels, Belgium*

Manivel Panneerselvam • *Centre for Bioinformatics, Pondicherry University, Puducherry, India*

Luis Miguel Pastor • *Department of Cell Biology and Histology, School of Medicine, IMIB-Arrixaca, Regional Campus of International Excellence, Campus Mare Nostrum, University of Murcia, Murcia, Spain*

Victor Quesada-Cubo • *Department of Cell Biology and Histology, School of Medicine, IMIB-Arrixaca, Regional Campus of International Excellence, Campus Mare Nostrum, University of Murcia, Murcia, Spain*

Diane Rebourcet • *MRC Centre for Reproductive Health, The Queen's Medical Research Institute, University of Edinburgh, Edinburgh, UK; Institute of Biodiversity, Animal Health and Comparative Medicine, University of Glasgow, Glasgow, UK*

María F. Riera • *División de Endocrinología, Centro de Investigaciones Endocrinológicas "Dr. César Bergadá" (CEDIE) CONICET – FEI, Hospital de Niños Ricardo Gutiérrez, Ciudad Autónoma de Buenos Aires, Argentina*

Gustavo Rindone • *División de Endocrinología, Centro de Investigaciones Endocrinológicas "Dr. César Bergadá" (CEDIE) CONICET – FEI, Hospital de Niños Ricardo Gutiérrez, Ciudad Autónoma de Buenos Aires, Argentina*

Vicente Seco-Rovira • *Department of Cell Biology and Histology, School of Medicine, IMIB-Arrixaca, Regional Campus of International Excellence, Campus Mare Nostrum, University of Murcia, Murcia, Spain*

Bruno Silvestrini • *S.B.M. Pharmaceuticals Srl, Rome, Italy*

Lee B. Smith • *MRC Centre for Reproductive Health, The Queen's Medical Research Institute, University of Edinburgh, Edinburgh, UK; School of Environmental and Life Sciences, University of Newcastle, Callaghan, NSW, Australia*

Mário Sousa • *Unit for Multidisciplinary Research in Biomedicine (UMIB), Laboratory of Cell Biology, Department of Microscopy, Institute of Biomedical Sciences Abel Salazar (ICBAS), University of Porto, Porto, Portugal; Centre for Reproductive Genetics Prof. Alberto Barros, Porto, Portugal*

Elizabeth I. Tang • *The Mary M. Wohlford Laboratory for Male Contraceptive Research, Center for Biomedical Research, Population Council, New York, NY, USA*

Fábio Trindade • *iBiMED, Department of Medical Sciences, University of Aveiro, Aveiro, Portugal; UnIC, Departamento de Cirurgia e Fisiologia, Faculdade de Medicina, Universidade do Porto, Porto, Portugal*

Dorien Van Saen • *Biology of the Testis, Research Laboratory for Reproduction, Genetics and Regenerative Medicine, Vrije Universiteit Brussel (VUB), Brussels, Belgium*

Rui Vitorino • *iBiMED, Department of Medical Sciences, University of Aveiro, Aveiro, Portugal; UnIC, Departamento de Cirurgia e Fisiologia, Faculdade de Medicina, Universidade do Porto, Porto, Portugal*

Hong Wang • *State Key Laboratory of Oncogenes and Related Genes, Renji-Med X Clinical Stem Cell Research Center, Ren Ji Hospital, School of Medicine, Shanghai Jiao Tong University, Shanghai, China*

Liping Wen • *State Key Laboratory of Oncogenes and Related Genes, Renji-Med X Clinical Stem Cell Research Center, Ren Ji Hospital, School of Medicine, Shanghai Jiao Tong University, Shanghai, China*

Qing Wen • *The Mary M. Wohlford Laboratory for Male Contraceptive Research, Center for Biomedical Research, Population Council, New York, NY, USA*

Xiang Xiao • *Department of Reproductive Physiology, Zhejiang Academy of Medical Sciences, Hangzhou, Zhejiang, China*

Marina G. Yefimova • *Laboratoire Signalisation et Transports Ioniques Membranaires, Université de Poitiers/CNRS, Poitiers, France; Sechenov Institute of Evolutionary Physiology and Biochemistry, Russian Academy of Sciences, St. Petersbourg, Russia*

Qingqing Yuan • *State Key Laboratory of Oncogenes and Related Genes, Renji-Med X Clinical Stem Cell Research Center, Ren Ji Hospital, School of Medicine, Shanghai Jiao Tong University, Shanghai, China*

Weihui Zhang • *State Key Laboratory of Oncogenes and Related Genes, Renji-Med X Clinical Stem Cell Research Center, Ren Ji Hospital, School of Medicine, Shanghai Jiao Tong University, Shanghai, China*

Fan Zhou • *State Key Laboratory of Oncogenes and Related Genes, Renji-Med X Clinical Stem Cell Research Center, Ren Ji Hospital, School of Medicine, Shanghai Jiao Tong University, Shanghai, China*

Chapter 1

Establishment of Primary Culture of Sertoli Cells

Raquel L. Bernardino, Marco G. Alves, and Pedro F. Oliveira

Abstract

The successful isolation and culture of Sertoli cells depend on a series of delicate processes of mechanical isolation and enzymatic digestion of the testicular tissue, taking advantage of an array of enzymes (such as DNAse, collagenase, and pancreatin) in order to digest the extracellular matrix components. The complexity of these processes may present some differences depending on the origin of the testicular sample (whole tissue or biopsy) and of the species in question. Rat and mouse Sertoli cells are obtained by a similar protocol, whereas bovine and human Sertoli cells require a more extensive mechanical and enzymatic processing.

Key words Enzymatic digestion, Mechanical dispersion, Primary cell culture, Sertoli cells

1 Introduction

In vitro experiments with living cells can be performed with cell derived from immortalized lines or from primary cultures. The studies available on the regulation and function of Sertoli cells are derived mainly from in vitro primary cultured Sertoli cells isolated from the testes [1–3]. This approach has some advantages and some disadvantages, being that the major drawbacks are the time spent to isolate and culture the cells and the continuous necessity to use fresh tissue [4].

The rat and mouse remain the preferred animals for this experimental procedure [5]. For primary cultures, Sertoli cells should be obtained from prepubertal animals [6], since proliferation of Sertoli cells occurs essentially before the birth and falls steadily after parturition [7]. The use of prepubertal testes favors a better adaptation of the Sertoli cells in vitro conditions, and the contamination by germ cells is lower because at this stage there are still few germ cells in seminiferous tubules [8]. It is known that inter-Sertoli junctions develop before the onset of puberty period [9, 10]. Rats [11] and mouse [12] with 20 days of age present a completed formation of the blood–testis barrier (BTB), as seen in adult animals,

Marco G. Alves and Pedro F. Oliveira (eds.), *Sertoli Cells: Methods and Protocols*, Methods in Molecular Biology, vol. 1748, https://doi.org/10.1007/978-1-4939-7698-0_1,

and have not yet started the spermatogenesis [11]. Hence, primary cultures of rat and mouse Sertoli cells are often made with animals about 20–22 days old. The bovines also are commonly used for in vitro studies with Sertoli cells [13], due to the high amount of testicular tissue per animal. Bulls reach the puberty at about 18 months [14], and for that reason Sertoli cell cultures must be made with tissue from animals before they reach this age. There are also several studies with primary cultures of human Sertoli cells; however, in this case, the vast majority are obtained from testicular biopsies, rather than the whole testicular tissue [15, 16].

In this protocol, the tissue dissociation conditions are selected to minimize damage to Sertoli cells and preserve their physiological and morphological characteristics. This procedure is described for obtaining essentially Sertoli cell cultures from rat and mouse, and alternatives are given for the protocol to obtain bovine and human Sertoli cell cultures, with the modifications on the enzymatic and mechanical procedures.

2 Materials

This procedure must be done in a sterile environment and ultrapure water should be used to prepare all solutions, which should be kept at 4 °C (unless indicated otherwise) (*see* **Note 1**).

2.1 Cell Culture

1. Hank's balanced salt solution (HBSS): 140 mM sodium chloride, 5 mM potassium chloride, 0.44 mM potassium phosphate monobasic anhydrous, 0.34 mM sodium phosphate dibasic, 6 mM D-glucose, and 4 mM sodium hydrogen carbonate. Weigh all the reagents into a 1 L graduated cylinder and dissolve in 900 mL of water (*see* **Note 2**). The pH should be adjusted to 7.4, using concentrated solutions of hydrochloric acid or/and sodium hydroxide. Adjust the volume to 1 L. Sterilize by filtering through a 0.2 μm mixed cellulose ester membrane filter using a vacuum filtration unit in the laminar flow chamber in a sterile environment, and store in a sterile bottle at 4 °C.
2. Phosphate-buffered saline solution (PBS): 140 mM sodium chloride, 3 mM potassium chloride, 10 mM sodium phosphate dibasic, and 1.8 mM potassium phosphate monobasic anhydrous. Weigh all reagents into a 1 L graduated cylinder and dissolve in 900 mL of water. The simplest method for making PBS is to prepare a 10× PBS stock solution (1.4 M sodium chloride, 0.03 M potassium chloride, 0.1 M sodium phosphate dibasic, and 0.18 M potassium phosphate monobasic anhydrous) in 1 L of water. To prepare a working solution of PBS, add 100 mL of 10× PBS stock to 900 mL water. If necessary, the pH of the solution should be adjusted to 7.4, using concentrated solutions

of hydrochloric acid or/and sodium hydroxide. Adjust the volume to 1 L. The PBS should be filtered through a 0.2 μm mixed cellulose ester membrane filter using a vacuum filtration unit in the laminar flow chamber in a sterile environment, and store in a sterile bottle at 4 °C (*see* **Note 3**).

2.2 Enzyme Solutions

1. Glycine solution: 100 mL HBSS, 50 U/mL penicillin and 50 mg/mL streptomycin, 1 M glycine, 2 mM EDTA, and 0.002% trypsin inhibitor. Adjust the pH to 7.2, using concentrated solutions of hydrochloric acid or/and sodium hydroxide and filter to sterilize.
2. DNase solution: Add 1 mg DNase (250 U) to 20 mL glycine solution. Filter to sterilize.
3. Collagenase solution 1: 20 mL HBSS, 1 mg DNase (250 U), and 4.5 mg collagenase type I. Filter to sterilize.
4. Collagenase solution 2: 12.5 mL HBSS, 3.5 mg collagenase type I, 3.5 mg DNase (250 U). Filter to sterilize.
5. Pancreatin solution: 10 mL HBSS, 2.5 mg pancreatin, and 2.5 mg DNase (250 U). Filter to sterilize.

2.3 Culture Medium

1. For the preparation of culture medium, you should start by adding Dulbecco's Modified Eagle's Medium (DMEM) (with glucose and L-glutamine) with Nutrient Mixture F-12 Ham (with glucose and L-glutamine) and dissolve in 900 mL of water according to the manufacturer's recommendations (*see* **Note 4**). After add 14 mM sodium hydrogen carbonate and 15 mM HEPES.
2. If low-glucose DMEM is used, it should be supplemented with D-glucose until reaching a final concentration of 18 mM.
3. The pH of the medium should be adjusted to 7.4, using concentrated solutions of hydrochloric acid or/and sodium hydroxide. Adjust the volume to 1 L.
4. This solution should be filtered through a 0.2 μm mixed cellulose ester membrane filter using a vacuum filtration unit in the laminar flow chamber in a sterile environment,
5. Add to the sterile medium 100 mL fetal bovine serum (FBS) (10%), 50 μg/mL gentamicin, 50 U/mL penicillin, and 50 mg/mL streptomycin (all these reagents should be sterile) (*see* **Note 5**). Store in a sterile bottle at 4 °C.

3 Methods

These methods are essentially for the isolation of rat and mouse Sertoli cells. However, some alternatives will be given to the protocol for bovine and human Sertoli cell cultures (*see* **Note 6**)

(Fig. 1). The tissue dissociation conditions are chosen to minimize damage to Sertoli cells throughout the sequential enzymatic and mechanical. First, soak the outside of the skin of the euthanized animal in ethanol 70% and remove the testes as aseptically as possible. After removal of the testes, the all protocol should be done inside a laminar chamber, in a sterile environment.

3.1 Mechanical Dispersion

1. Place the right and left testis of the same animal (if rat or mouse) in a 50 mL conical tube with 20 mL HBSS a 4 °C.
2. Wash twice with HBSS at 4 °C, shaking gently.
3. Place the testes in petri dish at 4 °C in sterile environment. With the support of tweezers and a scissor, remove the tunica albuginea, as well as the testicular blood vessels (*see* **Note 7**).
4. Wash twice with HBSS at 4 °C, shaking gently.

   For bovine testis only: The tissue should be cut into small pieces. An amount of tissue corresponding to 1 g should be placed in 25 mL of HBSS and shaken vigorously during 1 min. The tissue should be let to settle on ice for 5 min and the supernatant removed. Repeat this process three times (*see* **Note 8**).
5. Wash once with glycine solution (*see* **Note 9**).

   For bovine testis only: This and the subsequent step are not to be taken into account when performing bovine Sertoli cell cultures.

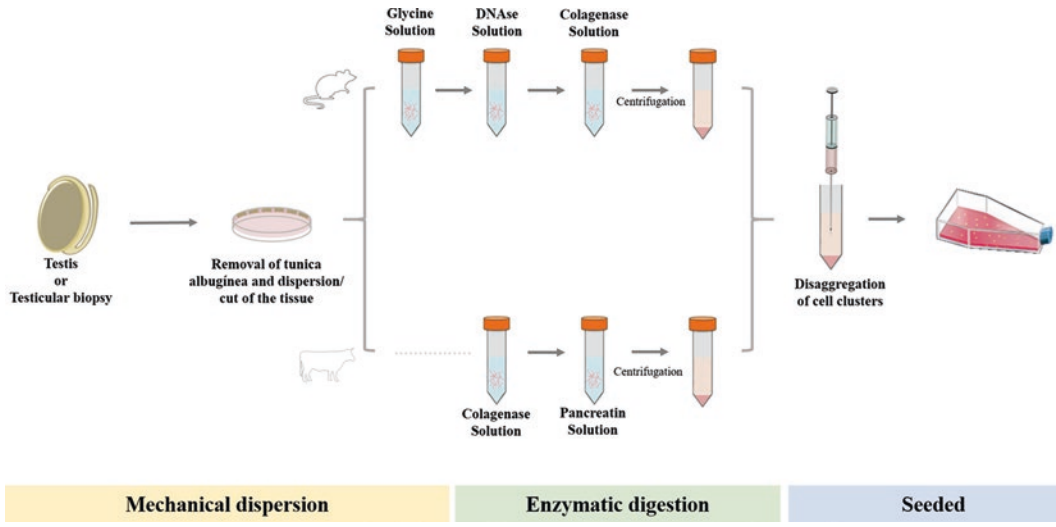

Fig. 1 Simplified schematic representation of methodological approach of primary culture of Sertoli cells. The testis (rat, mouse, or bovine) or testicular biopsy (bovine or human) is collected, and the tunica albuginea is removed and then the tissue is fragmented. The testes obtained from rats and mice undergo an osmotic shock with the glycine solution and then enzymatic digestion with a solution of DNase and collagenase. In case of the bovine or human sample, the enzymatic digestion is made with collagenase and pancreatin solution. Before seeding the cells in the flask, the pellet is passed through a needle for disaggregation of the clusters

6. Place the testicular tissue in a petri dish and carefully disperse the seminiferous tubules with the help of tweezers.

3.2 Enzymatic Digestion of Rat and Mouse Testicular Tissue

1. Place the seminiferous tubules in 50 mL conical tubule with 20 mL DNase solution in a sterile environment, and incubate for 10 min at room temperature.
2. Gently pipette the tubules through a large-bore glass Pasteur pipette. This procedure allows the release of the cells of the testicular interstitial tissue, Leydig and peritubular cells. Pellet the loosen tubules by gravity and discard the supernatant.
3. Wash three times with HBSS, allowing tubules to settle by gravity. Pellet the loosen tubules by gravity and discard the supernatant.
4. Resupend the pellet obtained at the last wash in 20 mL collagenase solution 1 and incubate at room temperature during 20 min (*see* **Note 10**).
5. Centrifuge at 300 × *g* during 3 min at room temperature and discard the supernatant.
6. Wash three times with HBSS by centrifuging at 300 × *g* during 3 min, and discard the supernatant.
7. Resuspend the pellet in culture medium and centrifuge at 300 × *g* during 3 min.
8. Resuspend the resulting pellet in 5 mL culture medium and force the remaining tissue through a 20 G needle, in order to disaggregate the cell clusters (*see* **Note 11**).

3.3 Enzymatic Digestion of Bovine Testicular Tissue

1. Resuspend the pellet obtained in the last wash in 12.5 mL collagenase solution 2 and shake (160 oscillations/min) during approximately 30 min at 32 °C.
2. Wash the digested tissue with HBSS and discard the aggregate formed saving the intact tissue and the washing medium.
3. Centrifuge the resulting suspension (intact tissue and washing medium) at 250 × *g* during 3 min and wash twice in HBSS.
4. Resuspend the pellet obtained in 10 mL pancreatin solution and shake (160 oscillations/min) during 15–25 min at 32 °C, until a new aggregate is formed (*see* **Note 12**).
5. Reserve the cellular suspension and wash the aggregate with 10 mL of HBSS. Add the washing solution to the previous cellular suspension and discard the aggregate.
6. Add 0.2 mL of FBS to the suspension and centrifuge at 250 × *g* during 3.5 min (*see* **Note 13**).
7. Wash the pellet three times with 10 mL of HBSS by centrifuging at 250 × *g* during 3.5 min.
8. Resuspend the pellet in 5 mL of HBSS with 5% FBS and put at 4 °C during 5 min.

9. Centrifuge at 250 × *g* during 4 min at room temperature and discard supernatant.
10. Wash the pellet with 10 mL of HBSS and centrifuge 250 × *g* during 4 min (*see* **Note 14**).
11. Resuspend the resulting pellet in 5 mL of culture medium and force through a 20 G needle, in order to disaggregate the cell clusters.

3.4 Seeding

1. Seed the cells in tissue culture flasks and incubate at 33 °C (5% CO_2).
2. Cell cultures should be allowed to stand undisturbed for 2 days, and thereafter should be inspected under the microscope. The culture medium should be replaced as frequently as necessary (*see* **Note 15**).

3.5 Maintenance of Cell Cultures

1. Observe the cells using an inverted optical microscope (*see* **Note 16**).
2. Discard the culture flask medium under sterile conditions.
3. Wash three times with sterile PBS (33–37 °C) (*see* **Note 17**).
4. Replace with fresh culture medium preheated (33–37 °C) and place the cell in the incubator.

4 Notes

1. All solutions should be prepared the day before the Sertoli cells culture.
2. Add about 500 mL water to a 1 L graduated cylinder and add one chemical at a time, while shaking, to dissolve the salts easier. The sodium hydrogen carbonate should be the last to be added when the salts are dissolved, for it not to precipitate.
3. This solution can be purchased already prepared and sterile.
4. DMEM and F12 can be acquired in powder or in liquid form. If acquired as powder, consult the manufacturer's instructions in order to know in which volume of water the powder must be dissolved.
5. Antimycotics may also be added to the culture medium (e.g., 0.5 mg/mL amphotericin B) but these are not essential for the cell culture.
6. For primary cultures of human Sertoli cells, if using small testicular samples (biopsies), perform only **items 10** and **11** of Subheading 3.3, and proceed to Subheading 3.4. If using a large sample of testicular tissue or the entire testis, you should

follow the protocol described for the isolation of bovine Sertoli cells.

7. To maintain the temperature at 4 °C during the mechanical dispersion, place an ice pack under the petri dish plate.
8. This step is performed to remove erythrocytes and free Leydig cells.
9. The alteration of osmolality caused by glycine solution (hyperosmotic) will lyse some testicular cell types, particularly those outside the blood–testis barrier (e.g., spermatogonia). It also makes it easier to remove cells from the basement membranes during enzymatic dissociation. EDTA is a chelating agent, i.e., it has the ability to binds to calcium and magnesium. The trypsin inhibitors protect the cells against proteolytic degradation.
10. Collagenase is essential for degrading the extracellular matrix. It plays a crucial role in the dissociation of tissues, thus contributing to the yield and viability of the cells.
11. The culture medium must be previously placed in a water bath at a temperature between 33 and 37 °C.
12. Be careful with overdigestion.
13. The solution can be divided into four tubes of 15 mL to facilitate centrifugation.
14. Wash with a medium-soaked glass Pasteur pipette to release germ cells from agglomerates.
15. Every 2 days, the cells should be observed under the microscope to observe the status of the cultures and confluence. The culture medium should also be observed, for if it is a medium containing a pH indicator, such as phenol red, it will change color when it is necessary to replace it.
16. This step is essential, not only to assess confluence but also to detect any contamination in the cell culture.
17. The washes should be done gently with care. PBS should not be directly added to the bottom of the flasks, where the cells adhere, so that they do not come loose. The flask should be shaken gently. If the cells are released during the washes, you can replace PBS with PBS supplemented with calcium chloride (0.9 mM) and magnesium chloride (0.49 mM).

Acknowledgments

This work was supported by the "Fundação para a Ciência e a Tecnologia"–FCT (PTDC/BBB-BQB/1368/2014), UMIB (PEst-OE/SAU/UI0215/2014). R.L. Bernardino was also financed by (SFRH/BD/103105/2014).

References

1. Welsh MJ, Wiebe JP (1975) Rat Sertoli cells: a rapid method for obtaining viable cells. Endocrinology 96(3):618–624
2. Bernardino RL, Martins AD, Jesus TT, Sá R, Sousa M, Alves MG, Oliveira PF (2015) Estrogenic regulation of bicarbonate transporters from SLC4 family in rat Sertoli cells. Mol Cell Biochem 408(1–2):47–54
3. Jesus TT, Bernardino RL, Martins AD, Sá R, Sousa M, Alves MG, Oliveira PF (2014) Aquaporin-9 is expressed in rat Sertoli cells and interacts with the cystic fibrosis transmembrane conductance regulator. IUBMB Life 66(9):639–644
4. Mather JP, Roberts PE (1998) Introduction to cell and tissue culture: theory and technique. Springer, Boston, MA. https://doi.org/10.1007/b102298
5. Dutta S, Sengupta P (2016) Men and mice: relating their ages. Life Sci 152:244–248
6. Steinberger A, Heindel J, Lindsey J, Elkington J, Sanborn B, Steinberger E (1975) Isolation and culture of FSH responsive Sertoli cells. Endocr Res Commun 2(3):261–272
7. Orth JM (1982) Proliferation of Sertoli cells in fetal and postnatal rats: a quantitative autoradiographic study. Anat Rec 203(4):485–492
8. Majumdar SS, Tsuruta J, Griswold MD, Bartke A (1995) Isolation and culture of Sertoli cells from the testes of adult Siberian hamsters: analysis of proteins synthesized and secreted by Sertoli cells cultured from hamsters raised in a long or a short photoperiod. Biol Reprod 52(3):658–666
9. Nagano T, Suzuki F (1976) The postnatal development of the junctional complexes of the mouse Sertoli cells as revealed by freeze-fracture. Anat Rec 185(4):403–417
10. Hatier R, Grignon G (1980) Ultrastructural study of Sertoli cells in rat seminiferous tubules during intrauterine life and the postnatal period. Anat Embryol 160(1):11–27
11. Bergmann M, Dierichs R (1983) Postnatal formation of the blood-testis barrier in the rat with special reference to the initiation of meiosis. Anat Embryol 168(2):269–275
12. Meng J, Holdcraft RW, Shima JE, Griswold MD, Braun RE (2005) Androgens regulate the permeability of the blood–testis barrier. Proc Natl Acad Sci U S A 102(46):16696–16700
13. Oliveira PF, Sousa M, Barros A, Moura T, Costa AR (2009) Membrane transporters and cytoplasmatic pH regulation on bovine Sertoli cells. J Membr Biol 227(1):49–55
14. Reinhardt V, Mutiso F, Reinhardt A (1978) Social behaviour and social relationships between female and male prepubertal bovine calves (Bos Indicus). Appl Anim Ethol 4(1):43–54
15. Bernardino RL et al (2016) Estradiol modulates Na+−dependent HCO3− transporters altering intracellular pH and ion transport in human Sertoli cells: a role on male fertility? Biol Cell 108(7):179–188
16. Meneses M et al (2016) Pioglitazone increases the glycolytic efficiency of human Sertoli cells with possible implications for spermatogenesis. Int J Biochem Cell Biol 79:52–60

Chapter 2

Evaluation of the Purity of Sertoli Cell Primary Cultures

Raquel L. Bernardino, Marco G. Alves, and Pedro F. Oliveira

Abstract

The purity of the primary cultures of Sertoli cells is a factor for the validation of the studies using this methodological approach. There is a probability of contamination of these cultures with other testicular cellular types, such as peritubular cells and germ cells (that represent a large percentage of the volume of the seminiferous tubules).

For the evaluation of the purity of cultures, the immunocytochemistry technique (immunoperoxidase or immunofluorescence) is frequently used to label a protein marker specific for the Sertoli cells within the testicular environment. The expression of several protein markers can be used, with different particularities, being that vimentin is often used as a marker for Sertoli cells. Vimentin is expressed independently of the differentiation state of the cells and is observed around the nuclei and in the cytoplasm of Sertoli cells.

Key words Antibody, Immunocytochemistry, Immunofluorescence, Immunoperoxidase, Prepubertal stage, Culture purity, Sertoli cells, Vimentin

1 Introduction

Sertoli cell cultures are obtained from samples of total testis or from small explants of testicular tissue (biopsies). These cultures are prepared taking advantage of enzymatic and mechanical processes for removal of interstitial and peritubular tissues and cells, such as germ cells and somatic cells of peritubular origin [1, 2]. The germ cells constitute the more frequent contaminants in Sertoli cell primary cultures, representing sometimes more than 25% of the cultured cells even when cells are obtained from prepubertal mice [3]. If the cells are obtained from older animals, the percentage of cell contaminants increases. These contaminants generally are removed with the exposure to conditions to which the Sertoli cell cultures are more resistant [4, 5].

Immunocytochemistry is a technique for detecting molecules of interest within cells by means of immunological and chemical reactions. This technique is highly specific and sensitive and can detect a large variety of antigens [6]. Usually, in this technique, the antigen is recognized by a specific primary antibody, to which the

Marco G. Alves and Pedro F. Oliveira (eds.), *Sertoli Cells: Methods and Protocols*, Methods in Molecular Biology, vol. 1748, https://doi.org/10.1007/978-1-4939-7698-0_2,

secondary antibody binds. Then a reagent that will bind to the secondary antibody is added, which contains an enzymatic portion that will convert a substrate (e.g., DAB) into a colored product. The color will appear in the same location where the primary antibody recognized that antigen of interest [7]. Alternatively, the antigen of interest can be observed using secondary antibody linked to a fluorophore (e.g., FITC) [1], which is detected in a fluorescence microscope.

Immunocytochemistry is used for evaluating the purity of Sertoli cell cultures as this is a crucial factor for the validation of studies involving this experimental approach. The purity of the Sertoli cell cultures can be assessed by the immunocytochemistry, through the detection of protein marker specific for the Sertoli cells within the testicular environment [8, 9].

Vimentin is the common intermediate filament protein that supports desmosome function. It is formed by polymerization of 57 kDa vimentin monomers and is an essential component of the Sertoli cell cytoskeleton [10, 11]. It is known that this protein has an important role in anchoring germ cells to the seminiferous epithelium with consequent importance for normal spermatogenesis [12]. This protein is regularly present in Sertoli cells independent of spermatogenesis phase or the state of Sertoli cell differentiation [13]. At the structural level, vimentin is observed around the nuclei, in cytoplasm along fibrillary material and at the ectoplasmic specializations, and also in the periphery of the Sertoli cell processes [10, 13]. Hence, this filament protein is often used as a specific marker for Sertoli cells [4, 7].

In this protocol two possible procedures are described for evaluating the purity of the primary cultures of Sertoli cells through the detection of a specific protein marker, vimentin. They involve the examination of cell cultures by microscopy techniques and their selection based on the presence of other testicular cell contaminants below 10–5%. Only under these conditions one can state to have a pure culture of Sertoli cells.

2 Materials

All the solutions used in this procedure should be prepared with ultrapure water and stored at room temperature or kept at 4 °C (unless indicated otherwise).

2.1 Working Solutions

1. Phosphate-buffered saline solution (PBS): 140 mM sodium chloride, 3 mM potassium chloride, 10 mM sodium phosphate dibasic, and 1.8 mM potassium phosphate monobasic anhydrous. Weigh all the chemicals into a 1 L graduated cylinder and dissolve in 900 mL of water. If necessary, the pH of the solution should be adjusted to 7.4, using concentrated

solutions of hydrochloric acid and/or sodium hydroxide. Adjust the volume to 1 L.

2. Phosphate-buffered saline solution with Tween 20 (PBS-T): Prepare PBS as referred above and add 2 mL Tween 20.
3. Fixing solution: PBS with 4% (w/v) paraformaldehyde, pH 7.4.
4. Antigen retrieval buffer: 10 mM sodium citrate solution diluted in ultrapure water, pH 6.
5. Inhibition solution: Methanol with 3% (v/v) hydrogen peroxide.
6. Permeabilization solution: PBS with 0.1% (v/v) Triton X-100.
7. Blocking solution: PBS-T with 1% (w/v) BSA or PBS-T with 10% (v/v) serum from the species from which the secondary antibody was obtained.
8. Extravidin-peroxidase complex solution (2–2.5 mg/mL).
9. 3,3′-Diaminobenzidine (DAB) substrate solution.
10. DAPI or Hoechst 33342 solution (10 mg/mL).
11. *Hematoxylin solution* (1 mg/mL) diluted in ethanol.
12. Primary antibody (anti-vimentin) solution (1 mg/mL).
13. Fluorophore-conjugated secondary antibody or horseradish peroxidase (HRP)-conjugated secondary antibody solution.

3 Methods

Sertoli cell culture's purity can be revealed by immunocytochemistry by fluorescence (Protocol *A*) or by immunoperoxidase technique (Protocol *B*). Cultures can be examined by fluorescence microscopy or by phase-contrast microscopy and can be used if the other cell contaminants are below 5–10%.

3.1 Preparing the Slide (Protocols A and B)

1. Sterilize glass coverslips by dipping them in 90% ethanol and carefully drying in the laminar flow.
2. Place each coverslip in sterile 6-well culture plates.
3. Add about 1 mL of cell suspension over each coverslip in the plate.
4. Grow cells on glass coverslips at 33 °C in an incubator (5% CO_2) during 96 h.
5. Aspirate the culture medium from each well, and gently rinse the cells three times in PBS at room temperature (*see* **Note 1**).

3.2 Fixation (Protocols A and B)

1. Incubate the cells with fixing solution for 10 min at room temperature.
2. Wash the cells three times with ice-cold PBS (*see* **Note 2**).

3.3 Antigen Retrieval (See Note 3) (Protocols A and B)

1. Heat the antigen retrieval buffer to 98 °C (*see* **Note 4**).
2. With the help of one tweezer, dip the coverslips in the buffer, being careful to know which side of the coverslip has the cells.
3. Heat the coverslips at 98 °C for 10 min.
4. Remove the coverslips from the antigen retrieval buffer, and put them in the 6-well culture plates with the cells facing up.
5. Wash the coverslips with cells three times in PBS, 5 min each wash.

3.4 Permeabilization (Protocols A and B)

1. Incubate the coverslips with the cells in permeabilization solution for 15 min at room temperature (*see* **Note 5**).
2. Wash the coverslips with cells three times in PBS, 5 min each wash.

3.5 Inhibition of Endogenous Peroxidases (Protocol B)

1. Incubate the cells with inhibition solution for 10 min at room temperature.
2. Wash the coverslips with cells two times in PBS-T, 5 min each wash.

3.6 Blocking and Immunostaining (Protocol A)

1. Incubate the coverslips with the blocking solution for 1 h at room temperature to block unspecific binding of the antibodies.
2. Wash the coverslips with cells three times in PBS-T, 5 min each wash.
3. Incubate the coverslips with primary antibody (anti-vimentin) diluted in blocking solution, with an appropriate dilution, overnight at 4 °C in a humidified chamber (*see* **Note 6**). Use a humidity chamber for all incubations to prevent evaporation. The final volume of the antibody solution should be sufficient to cover each coverslip (*see* **Note 7**).
4. Wash the coverslips with cells three times in PBS-T, 5 min each wash.
5. Incubate the coverslips with the fluorophore-conjugated secondary antibody diluted in blocking solution with a respective dilution 1 h at room temperature in the dark (*see* **Note 8**).
6. Wash the coverslips with cells three times in PBS-T, 5 min each wash.
7. Incubate the coverslips with DAPI or 3 μg/mL Hoechst 33342 stain for 10 min (*see* **Note 9**).
8. Wash the coverslips with cells three times in PBS-T, 5 min each wash.

3.7 Blocking and Immunostaining (Protocol B)

1. Incubate the coverslips with blocking solution for 1 h at room temperature to block unspecific binding of the antibodies.
2. Wash the coverslips with cells two times in PBS-T, 5 min each wash.

3. Incubate cells with primary antibody (anti-vimentin), diluted in blocking solution with an appropriate dilution, overnight at 4 °C in a humidified chamber (*see* **Note 6**). Use a humidity chamber for all incubations to prevent evaporation. The final volume of the antibody solution should be sufficient to cover each coverslip (*see* **Note 7**).
4. Wash the coverslips with cells three times in PBS-T, 5 min each wash.
5. Incubate coverslips with HRP secondary antibody solution, diluted in blocking solution with an appropriate dilution, during 1 h at room temperature.
6. Wash the coverslips with cells three times in PBS-T, 5 min each wash.
7. Incubate the coverslips with the extravidin-peroxidase complex diluted in blocking solution for 30 min (see dilution and incubation time recommended by the manufacturer).
8. Wash the coverslips two times in PBS-T, 5 min each wash.
9. Add the DAB substrate solution (*see* **Note 10**) to the coverslips, and incubate until the desired development is achieved (a brownish color appears). Typical incubations are 5–15 min long (*see* **Note 11**).
10. Stop the reaction by washing the coverslips with water for 2 min.
11. Immerse four times in hematoxylin solution for 10 s to stain cell nuclei (optional step) (*see* **Note 12**).
12. Wash the coverslips under running water.

3.8 Mounting of the Coverslips and Visualization (Protocols A and B)

1. Mount the coverslips in a slide with a drop of mounting medium (*see* **Note 13**).
2. Seal the coverslips on the slides with nail polish to prevent drying and movement.
3. Visualize the cells using a fluorescence microscope with the appropriate filters (Protocol *A*) or optical microscope (Protocol *B*) (Fig. 1). Store the coverslips in the dark at −20 °C.

4 Notes

1. PBS must be preheated to prevent the releasing of the cells from the coverslip.
2. The coverslips containing the cells can be stored in PBS with 0.02% sodium azide in PBS at 4 °C for a few days.
3. This step is optional. Antigen retrieval is a methodological approach that increases the availability of epitopes that can be

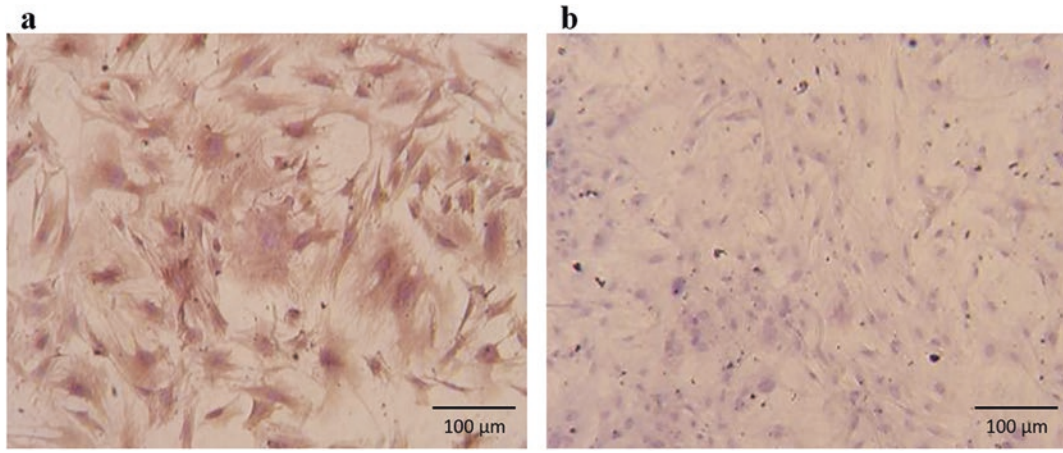

Fig. 1 Immunocytochemistry of a culture of Sertoli cells. (**a**) Marking of vimentin in Sertoli cells observed under the optical microscope. (**b**) Negative control, without adding any antibodies and nuclei stained with hematoxylin

bound by the specific primary antibody. Some antibodies bind better when cells are heated in antigen retrieval buffer. Check the product data sheet recommendations.

4. The heating of the solution should be done in a water bath to maintain the temperature constant during incubation. In this step, one must be careful with the temperature, because when heating methods such as microwave are utilized, this can result in unbalanced epitope retrievals due to a creation of cold and hot spots. A temperature too high may also cause the cell dissociation from the coverslip.
5. Triton X-100 is the detergent more frequently used for permeabilization. However, this method tends to destroy some of the membranes, and for that reason it is not appropriated for membrane-associated antigens. Digitonin and saponin are also agents that improve the penetration of the antibody and which can replace Triton X-100.
6. If the antibodies used have not been previously assayed for these cells, specific control experiments should be performed to evaluate if the antibodies react with all isotypes, which are:
   - Perform the entire protocol without adding any antibodies. Any fluorescence observed is due to the autofluorescence of the sample.
   - Perform the entire protocol without adding the primary antibody. Any observed fluorescence is due to nonspecific binding of the secondary antibody.
7. It is advisable to use a hydrophobic pen so that the antibody will not spread as easily over the coverslip.
8. After this step, all procedures must be performed in the dark, so that no fluorescence is lost, and at room temperature.

9. DAPI or Hoechst 33342 will stain the nuclei of the cells.
10. DAB substrate can be purchased in powder or liquid form. If bought in powder, dissolve in 50 mM Tris, pH 7.2 at 1 mg/mL. The manufacturer's instructions should be followed to make the solution.
11. DAB reaction produces brown bands or spots at sites of reaction with HRP-conjugated antibodies.
12. If the staining is too strong, the immersion times in hematoxylin can be reduced.
13. Take out the coverslips with tweezers and place them on the mounting medium, with the cell-side face down.

Acknowledgments

This work was supported by the "Fundação para a Ciência e a Tecnologia" (FCT) (PTDC/BBB-BQB/1368/2014) and UMIB (PEst-OE/SAU/UI0215/2014). R.L. Bernardino was also financed by FCT (SFRH/BD/103105/2014).

References

1. Bernardino RL et al (2016) Estradiol modulates Na+−dependent HCO3− transporters altering intracellular pH and ion transport in human Sertoli cells: a role on male fertility? Biol Cell 108(7):179–188
2. Bernardino RL, Martins AD, Jesus TT, Sá R, Sousa M, Alves MG, Oliveira PF (2015) Estrogenic regulation of bicarbonate transporters from SLC4 family in rat Sertoli cells. Mol Cell Biochem 408(1–2):47–54
3. Palombi F, Ziparo E, Rommerts F, Grootegoed J, Antonini M, Stefanini M (1979) Morphological characteristics of male germ cells of rats in contact with Sertoli cells in vitro. J Reprod Fertil 57(2):325–330
4. Rato L, Alves MG, Socorro S, Carvalho RA, Cavaco JE, Oliveira PF (2012) Metabolic modulation induced by oestradiol and DHT in immature rat Sertoli cells cultured in vitro. Biosci Rep 32(1):61–69
5. Orth JM (1982) Proliferation of Sertoli cells in fetal and postnatal rats: a quantitative autoradiographic study. Anat Rec 203(4):485–492
6. Polak JM, Van Noorden S (2014) Immunocytochemistry: practical applications in pathology and biology. Butterworth-Heinemann, Bristol
7. Alam MS, Kurohmaru M (2014) Disruption of Sertoli cell vimentin filaments in prepubertal rats: an acute effect of butylparaben in vivo and in vitro. Acta Histochem 116(5):682–687
8. Griswold MD (2014) Sertoli cell biology, 2nd edn. Academic Press, Amsterdam
9. Yakimchuk K (2013) Cell markers. Materials and Methods 3:183. https://doi.org/10.13070/mm.en.3.183
10. Mruk DD, Bonanomi M, Silvestrini B (2016) Lonidamine-ethyl ester-mediated remodelling of the Sertoli cell cytoskeleton induces phosphorylation of plakoglobin and promotes its interaction with α-catenin at the blood–testis barrier. Reprod Fertil Dev 29(5):998–1011
11. Franke WW et al (1982) Differentiation-related patterns of expression of proteins of intermediate-size filaments in tissues and cultured cells. Cold Spring Harbor Symp Quant Biol 46(Pt 1):431–453
12. Amlani S, Vogl A (1988) Changes in the distribution of microtubules and intermediate filaments in mammalian Sertoli cells during spermatogenesis. Anat Rec 220(2):143–160
13. Aumüller G, Steinbrück M, Krause W, Wagner H-J (1988) Distribution of vimentin-type intermediate filaments in Sertoli cells of the human testis, normal and pathologic. Anat Embryol 178(2):129–136

Chapter 3

Preparation of Testicular Samples for Histology and Immunohistochemistry

Barbara Bilinska, Anna Hejmej, and Malgorzata Kotula-Balak

Abstract

One approach to visualize internal structures of the testis is histological sectioning of the material. The use of testicular samples allows a detailed analysis of the structure of both seminiferous tubules and the interstitial space. It is worth noting that key role in the control of germ cell development is assigned to Sertoli cells. Thus, in this chapter the special reference is made on visualization of Sertoli cells in the seminiferous epithelium in which they create a specialized microenvironment to support the germ cell development through the formation of the blood-testis barrier (BTB). The use of transmission electron microscopy (TEM) allows a deeper insight into the BTB morphology, especially the organization of the basal ectoplasmic specialization (ES) and coexisting intercellular junctions.

Equally important, immunohistochemistry (IHC) is an appropriate technique to detect the localization of various proteins in paraffin-embedded and fixed tissues, i.e. testicular samples. A proper fixation allows to stabilize structure of the seminiferous tubules and preserve cells against irreversible damage. As such localization of various junction proteins connecting adjoined Sertoli cells and present in germ cell-Sertoli cell interfaces is possible. Also immunofluorescence (IF) is helpful to detect the distribution and relative abundance of the junctional proteins, while immunocytochemistry (ICC) is a valuable technique to show a protein distribution within a single cell (e.g. in Sertoli cell culture).

Key words Testis, Histology, Ultrastructure, Immunohistochemistry, Immunocytochemistry, Sertoli cell, Blood–testis barrier, Intercellular junctions

1 Introduction

Spermatogenesis is a highly regulated process of germ cell differentiation where spermatozoa are produced from spermatogonia. Its successful completion depends on signals provided by the local testicular environment. It should be emphasized that testosterone, a main androgen, is necessary for the initiation, maintenance, and regulation of spermatogenesis [1, 2].

Testosterone acts through its own, highly specific receptors, called androgen receptors (AR). Importantly, the major cellular target and translator of testosterone signals to developing germ cells are Sertoli cells [3]. Throughout spermatogenesis, developing

Marco G. Alves and Pedro F. Oliveira (eds.), *Sertoli Cells: Methods and Protocols*, Methods in Molecular Biology, vol. 1748, https://doi.org/10.1007/978-1-4939-7698-0_3,

germ cells remain in close contact with Sertoli cells, forming dynamic associations within the seminiferous epithelium. Sertoli cells form a single layer, which extends from the basement membrane to the lumen of a seminiferous tubule. Thin cytoplasmic processes of Sertoli cells support differentiating germ cells and play a role in nourishing, positioning, and transport of the cells toward the lumen of a seminiferous tubule. Contacts between Sertoli and germ cells are constituted by specialized junction complexes: apical ectoplasmic specialization (aES), desmosome-like junctions (DJs), gap junctions (GJs), and tubulobulbar complex. Additionally, Sertoli cells contribute to the formation of the blood–testis barrier (BTB), dividing the seminiferous epithelium into a basal and an apical compartment, thereby conferring cell polarity and creating unique environments for germ cell development [4, 5]. Sertoli cells as an important component of the seminiferous epithelium are presented in Fig. 1A. The unique feature of the BTB, when compared with other epithelial barriers, is its ability to open transiently to allow passage of preleptotene spermatocytes into the adluminal compartment. The BTB is composed of basal ectoplasmic specialization (bES), coexisting tight junctions (TJs), DJs, and GJs. Maintenance of structure and function of these protein complexes is essential for the BTB integrity and, in consequence, for male fertility [6, 7]. It should be added that in vitro experiments employing cultures of Sertoli cells are useful for studying androgen regulation of the intercellular interaction in testicular cells [8]. Several reports of Cheng and Mruk [9, 10] on physical interactions between TJs, GJs, and bES proteins pointed out the significance of intercellular communication with respect to Sertoli cell function. Understanding the factors that influence Sertoli–Sertoli and Sertoli–germ cell interactions is therefore of special importance. Such studies require methods which ensure the preservation of tissue architecture and cell morphology, as well as the maintenance antibody binding capability.

Histology is particularly important to characterize histological alterations within seminiferous tubules of the testis that result from experimental treatments or appear as a consequence of environmental conditions [11–13]. Thus, high-quality tissue processing is critical for accurate assessment of normal and abnormal structures. Since the structure of the tissue is determined by the shapes and sizes of proteins inside the cell, fixation terminates any ongoing biochemical reactions. Paraffin is an agent the tissue specimen can be infiltrated with; its subsequent converting from a liquid into a solid allows thin sectioning. The objective of testis fixation is to preserve morphology, minimize the loss of molecular components, prevents autolysis, and to do this in such a way as to allow for the preparation of thin, stained sections [14].

As testicular microenvironment depends on the formation of the BTB, its impermeability (or partial permeability) in physiological

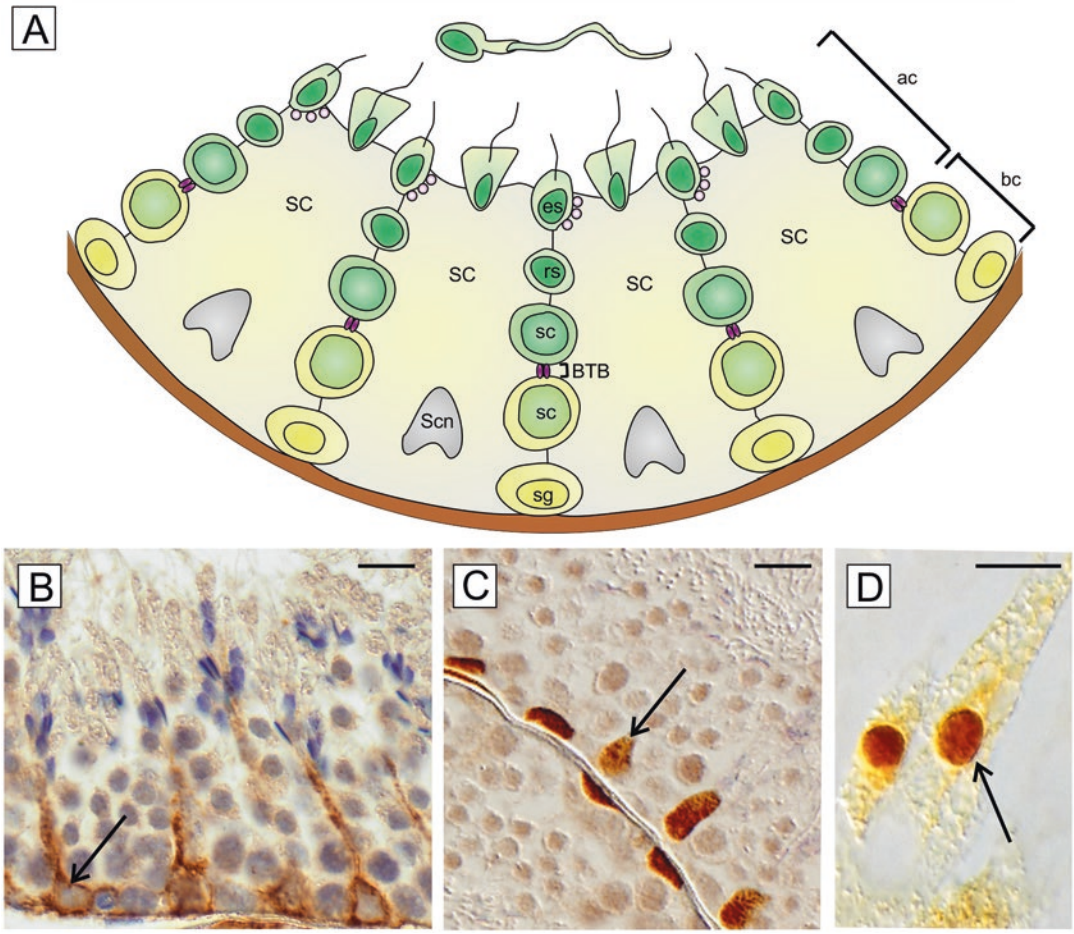

Fig. 1 (**A**-**C**) Schematic representation of the seminiferous tubule organization. (**A**) The figure illustrates Sertoli cells (SC) supporting germ cells structurally until they are released from seminiferous epithelium as spermatozoa. From the basement membrane to the lumen, spermatogonia (sg), spermatocytes (sc), round spermatids (rs), and elongated spermatids (es) are depicted. Sertoli cell nucleus (Scn) is situated close to the basement membrane, while Sertoli cell cytoplasm extends toward the lumen being in close contact with the other germ cell types. Blood-testis barrier (BTB) divides seminiferous tubule into two separate compartments: basal compartment (bc) and apical compartment (ac). (**B**) Representative micrograph of immunohistochemical localization of vimentin in bank vole testis. Scale bars represent 15 μm. Paraffin sections were fixed using 4% PFA. Positive signal is localized to the Sertoli cell cytoplasm only; therefore, vimentin frequently serves as a useful marker of Sertoli cells (arrows). In negative controls (not shown), primary antibodies were replaced with normal serum (*see* **Note 26**). (**C**, **D**) Representative micrographs of immunohistochemical localization of androgen receptor (AR) in bank vole testis (**C**) and mouse Sertoli cells in vitro (**D**). Scale bars represent 15 μm. Paraffin section was fixed with 4% PFA, whereas cultured cells were fixed with methanol for 5 min and acetone for 3 min. Only Sertoli cell nuclei show a positive signal for AR (arrows) which serves as a marker for identification of Sertoli cells within the seminiferous epithelium (**C**)

and/or experimental conditions is of special interest for researchers interested in the functioning of the male gonad. In this context, we developed a method allowing "visualization" of functional state of the BTB at the level of electron microscopy [15] that guaranties the highest resolution of obtained images. A critical step during sample preparation for TEM is fixation and postfixation to maintain the architecture of the tissue in its natural status. The method we developed is based on protocols proposed by Russell [16, 17] and involves fixation and postfixation in modified two-component fixatives. It improves the quality of fixation of the basal ES and enhances the contrast of plasma membranes. What is more, potassium ferrocyanide (contained in our Fixative 2—*see* Subheading 2.3) contrasts only "open" intercellular spaces and does not penetrate between membranes of the basal ES sealed with the TJs, allowing assessment of the permeability of the BTB.

Taken together, in this chapter we present the protocols for testis histology at the light and electron microscopy level. A few methodological points are devoted to fixation of cultured Sertoli cells. We also give an overview of the main procedures for immunostainings of testicular sections and Sertoli cell cultures. Visualization of specific proteins, namely, those that are components of intercellular junctions within the seminiferous epithelium and others that can be used as markers for Sertoli cells is presented in Fig. 1B–D, Fig. 5B–E, and Fig. 6A–F.

These protocols have been adapted from methods used in our laboratory [12, 15, 18–24] and can be further adapted to be used in other animal models.

2 Materials

Prepare all solutions with ultrapure water. All glassware should be clean, smooth, and free from scratches. Handle all solutions in accordance with safety regulations.

Notes are explanatory, give practical advice, and discuss details of specific steps of the solution preparation.

2.1 Washing Buffers

1. Phosphate-buffered saline (PBS): 137 mM NaCl, 2.7 mM KCl, 10 mM Na_2PO_4, 1.8 mM KH_2PO_4. Weigh 8 g NaCl, 0.2 g KCl, 1.42 g Na_2PO_4, and 0.24 g KH_2PO_4. Transfer weighed reagents to the 1-L flask and dissolve in 800 mL distilled water (dH_2O) to a final volume of 1 L. Adjust the pH to 7.4 with HCl and add dH_2O to 1 L. Store at 4 °C (*see* **Note 1**).
2. 10× Tris-buffered saline (TBS): 0.05 M Tris–HCl, 0.15 M NaCl, pH 7.6. Weigh 61 g Trizma base and 90 g NaCl and add dH_2O to 1 L. Mix to dissolve and adjust pH to 8.4 using concentrated HCl. Store at room temperature. Dilute 1:10 with distilled water before use and adjust pH if necessary.

3. Tris-buffered saline—0.1% Tween 20 (TBST): Dilute 100 mL 10× TBS with 900 mL dH_2O and add 1 mL Tween 20.

2.2 Fixation, Embedding, and Staining for Histology

1. Bouin's fixative: saturated picric acid, formalin, and glacial acetic acid at 15:5:1 proportions.

   Add 75 mL of saturated aqueous solution of picric acid (*see* **Note 1**), 25 mL of 37% formaldehyde, and 5 mL of glacial acetic acid. Store at room temperature (*see* **Note 2**).
2. Tissue dehydration/rehydration reagent: A graded series of ethanol (50, 70, 80, 90, 96, and 100%)
3. Tissue clearing reagent: Three changes of xylene for clearing the tissue.
4. Tissue embedding: Paraplast Plus, Glycid Ether 100 resin for tissue embedding, Tissue-Tek for tissue snap freezing.
5. Reagents for hematoxylin and eosin staining (H-E): Delafield's alum hematoxylin and 1% eosin. Dissolve 4 g hematoxylin in 25 mL absolute ethanol, and add 375 mL 10% ammonium alum solution. Leave in uncovered container, in a warm, sunlit place for 1 week. Filter, and then add the 200 mL glycerol and 100 mL methanol. Leave for a week. Filter and dilute 1:10 in dH_2O. Store in a tightly stoppered container in the dark at room temperature. Dissolve 1 g ethyl eosin in 100 mL 90% ethanol and filter (*see* **Note 3**).
6. Reagents for trichrome Goldner staining:
   (a) Weigert's iron hematoxylin—Solution A: Dissolve 1 g hematoxylin in 100 mL 96% ethanol. Solution B: Mix 4 mL 10% $FeCl_2$, 1 mL HCl, and 100 mL dH_2O. Mix solutions A and B (1:1) before use.
   (b) Ponceau 2R/acid fuchsin solution—Solution A: Dissolve 1 g ponceau 2R in 100 mL dH_2O. Solution B: Dissolve 1 g acid fuchsin in 100 mL dH_2O. Solution C: Dilute 2 mL acetic acid in 100 mL dH_2O. Before use mix 6 mL solution A, 2 mL solution B, and 9 mL solution C. Add 3 mL dH_2O.
   (c) Orange G/phosphomolybdic acid solution: Dissolve 5 g phosphomolybdic acid and 2 g orange G in 100 mL dH_2O.
   (d) Light green solution: Dissolve 300 mg light green in 100 mL dH_2O.
7. Counterstaining: Mayer's hematoxylin solution.
8. Mounting media: DPX.

2.3 Fixatives for Electron Microscopy (EM)

1. Fixative 1: Mixture of 2% formaldehyde and 2.5% glutaraldehyde in 0.1 M phosphate buffer, pH 7.3.
2. Fixative 2: Mixture of 2% osmium tetroxide and 0.8% potassium ferrocyanide in 0.1 M phosphate buffer (*see* **Notes 4** and **5**).

2.4 Fixatives for Immunohistochemistry/ Immunocytochemistry and Immunofluorescence

1. 4% paraformaldehyde solution (PFA) in PBS: Add 800 mL of PBS to a glass beaker on a stir plate and heat while stirring to approximately 60 °C (*see* **Notes 1** and **2**). Add 40 g of paraformaldehyde powder to the heated PBS solution; it will not immediately dissolve into solution. Slowly raise the pH to 6.9 by adding 1 N NaOH dropwise from a pipette until the solution clears. The solution is ready to be cooled and filtered after the paraformaldehyde is dissolved. Adjust the volume of the solution to 1 L with PBS (*see* **Notes 6** and **7**).
2. 10% neutral buffered formalin (10% NBF): Add 100 mL 37% formaldehyde, 900 mL dH_2O, 4.0 g $NaH_2PO_4 \cdot H_2O$, and 6.5 g Na_2HPO_4. Mix to dissolve and store at room temperature (*see* **Note 8**).

2.5 Antigen Retrieval Buffers

Antigen retrieval step is used with paraffin-embedded and formalin- or paraformaldehyde-fixed tissues. The retrieval step breaks the formalin/paraformaldehyde cross-links that are formed during fixation so that the antigen is unmasked.

1. 10 mM citrate buffer:
   Solution A: Weigh 2.1 g citric acid and transfer to 100 mL dH_2O. Solution B: Weigh 2.9 g sodium citrate and transfer to 100 mL dH_2O. Mix 9 mL solution A and 41 mL solution B. Add dH_2O to a volume of 500 mL and adjust to pH 6.0 with HCl (12 N). Store at 4 °C.
2. Tris–EDTA buffer: 10 mM Tris containing 1 mM EDTA and 0.05% Tween 20; pH 9.0.
   Mix 1.21 g Tris base and 0.37 g of EDTA in 1 L of dH_2O. Adjust the pH to 9.0 with 1 N NaOH and then add 0.5 mL of Tween 20. Store at room temperature for up to 3 months (*see* **Notes 9** and **10**).
3. Permeabilization: Triton X-100, Tween 20.

2.6 Blocking Reagents

1. 0.3% H_2O_2 in methanol or PBS: Add 9.9 mL methanol or PBS and 0.1 mL 30% of H_2O_2 to a glass jar covered with aluminum foil.
2. Polyvalent blocking serum (5–10% normal goat/horse serum) to reduce nonspecific background staining.

2.7 Antibodies and Reagents for Antigen Visualization

1. Primary antibody. The antibody that binds to the studied protein (*see* **Note 11**).
2. Biotinylated secondary antibody (for IHC and ICC). The antibody that binds to the Fc domain of the primary antibody with its Fab domain. The Fc domain of the secondary antibody is conjugated with biotin that binds to streptavidin to amplify the reaction (*see* **Note 11**).
3. Alexa Fluor-conjugated secondary antibody (for IF) (*see* **Note 11**).

4. Ready-to-use streptavidin conjugated with horseradish peroxidase (HRP), e.g., VECTASTAIN Elite ABC HRP Kit: Dilute Reagent A and Reagent B in TBS (1:1:100). Mix immediately and allow to stand for about 30 min before use.
5. Chromogenic substrate solution: 0.02% 3,3′-diaminobenzidine (DAB) in TBS containing 0.03% H_2O_2 and 0.07% imidazole. Weigh 5 mg DAB and 6.8 mg imidazole and transfer to 10 mL TBS. Add 10 μL H_2O_2. The solution should be prepared just before use (*see* **Note 12**).

2.8 Mounting and Embedding Media

1. DPX, glycerol-based mounting medium, VECTASHIELD® Antifade Mounting Medium.

3 Methods

The methods described below are for testicular sample histology at the light and electron microscopy level, immunohistochemistry including immunofluorescence (both in paraffin and frozen sections), and immunocytochemistry of cultured Sertoli cells.

Notes, where appropriate, discuss details of, and reasoning of, specific steps in the protocol. Notes also indicate where the protocol can be modified to optimize the staining.

3.1 Light Microscopy: Histology of the Testis

3.1.1 Tissue Processing

1. Fix the tissue with Bouin's solution or 10% NBF for 24 h–48 h at 4 °C (*see* **Notes 13–15**).
2. Wash with dH_2O or PBS.
3. Place into increasing concentrations of ethanol (50, 70, 80, and 90%) for 1 h each.
4. Place into three changes of absolute alcohol for 1 h each and fourth change for 24 h.
5. Clear with two changes of xylene for 30 min each.
6. Incubate in two changes of liquid paraffin wax at 56–59 °C for 24 h each (*see* **Note 16**).
7. Embed tissues in paraffin blocks.
8. Cut sections of 4–5 μm in thickness and mount on the slides (*see* **Note 17**).

3.1.2 H-E Staining (See Note 18)

1. Deparaffinize slides in two changes of xylene for 10 min each.
2. Hydrate slides to water by dipping them in two changes of absolute ethanol (for 10 min each), two changes of 96% ethanol, and one of 70% ethanol for 5 min each.
3. Wash in dH_2O.
4. Stain with hematoxylin for 30–60 s (*see* **Note 19**).

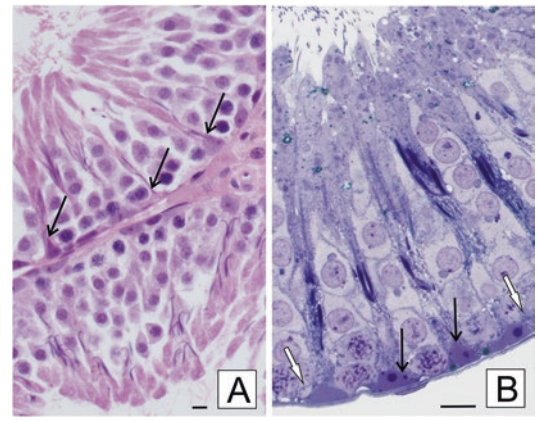

Fig. 2 (**A**, **B**) Representative micrographs of rat testis fixed with Bouin's fixative and stained by hematoxylin-eosin (**A**) and semi-thin section immersed in ice-cold pre-fixative (fixative 1) and stained by 1% methylene blue (**B**). Scale bars represent 15 μm. Both cross sections (**A**, **B**) illustrate all germ cell types present during spermatogenesis. Sertoli cells are depicted by arrows. This is an example of well-fixed tissue showing good nuclear and cytoplasmic morphology. Note a distribution of ectoplasmic specialization (open arrows) close to the basement membrane

5. Rinse with 3–4 changes of tap water for 15 min.
6. Dip slides sequentially in ethanol (50, 70, 80, and 96%) for 5 min each.
7. Stain in eosin for 20–30 s.
8. Dehydrate through two changes of absolute ethanol for 10 min each.
9. Clear through two changes of xylene for 10 min each and coverslip with a DPX medium.
10. Clear the tissue slides in two changes of xylene for 10 min each and coverslip using a DPX mounting medium.

Here we show rat testis histology (Fig. 2).

3.1.3 Trichrome Goldner Staining (See Note 18)

The Goldner staining can be used for the differentiated visualization of connective tissue. In this method three different dyes of different molecular size are used. Due to the trichrome staining, collagen, erythrocytes, and muscles can be selectively visualized. The nuclei have to be stained with Weigert's iron hematoxylin because nuclei stained with ordinary hematoxylin solutions are decolored (Fig. 3).

1. Deparaffinize slides in two changes of xylene for 10 min each.
2. Hydrate slides to water by dipping them in two changes of absolute ethanol (for 10 min each), two changes of 96% ethanol, and one of 70% ethanol (for 5 min each).

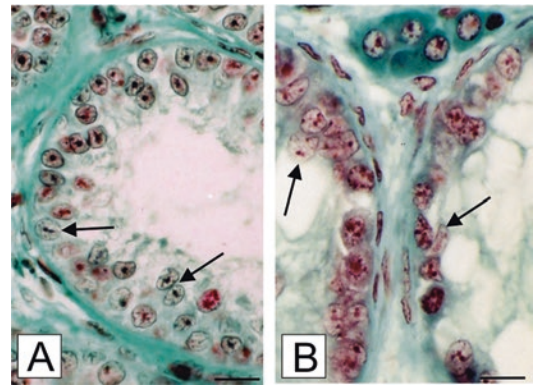

Fig. 3 (**A**, **B**) Representative micrographs of immature European bison testis and that of cryptorchid horse fixed with Bouin's solution and stained with Goldner trichrome. Sertoli cells and premeiotic germ cells are visible in (**A**), while Sertoli cells and spermatogonia are present in (**B**). Connective tissue is stained green and nuclear chromatin is brownish dark. Sertoli cells are depicted by arrows. Scale bars represent 20 μm

3. Place into Weigert's iron hematoxylin for 4 min.
4. Place into tap water for 10 min.
5. Place into dH_2O for 1 min.
6. Place into ponceau 2R/acid fuchsin solution for 3 min.
7. Wash in dH_2O.
8. Place into orange G/phosphomolybdic acid solution for 4 min.
9. Wash in dH_2O.
10. Place into light green solution for 7 min.
11. Wash in dH_2O.
12. Dehydrate rapidly with 70% ethanol for 1 min, 96% ethanol for 2 min, and absolute ethanol—three changes for 2.5 min each.
13. Clear with two changes of xylene (for 5 min each) and coverslip using a DPX mounting medium.

3.2 TEM: Contrast Enhancement of Basal Ectoplasmic Specialization in Sertoli Cells

The interstitial tissue around the seminiferous tubules must be carefully removed under a stereomicroscope for better fixation of the tubules. The steps of the procedure developed in our laboratory are as follows:

1. Fix in fixative 1 for 1–1.5 h at 4 °C (*see* **Note 20**).
2. Wash in 0.1 M phosphate buffer, pH 7.3–7.4, 3 × 15 min at 4 °C.
3. Fix in fixative 2 for 30–60 min at 4 °C (*see* **Note 21**).
4. Rinse with three changes of tap water (30 min for each) at room temperature.

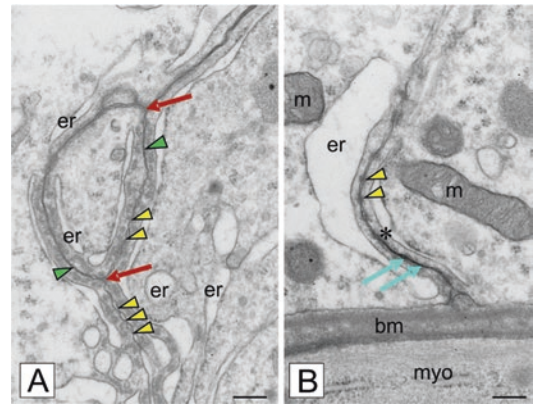

Fig. 4 (**A**, **B**) Representative transmission electron micrographs of basal ectoplasmic specialization connecting adjoined Sertoli cells in rat. Scale bars represent 0.5 μm. Tangential section through the junctional complex (sandwiched between endoplasmic reticulum cisternae) located next to nonspecialized membranes (**A**). Note that electron-dense tracer penetrates only between nonspecialized membranes (blue arrows in **B**) and is stopped at the basal limit of ectoplasmic specialization (asterisks in **B**). Basement membrane, bm; endoplasmic reticulum, er; mitochondrion, m; Sertoli cell nucleus, nu; myoid cell, myo. Red arrows indicate three membrane junctions, green arrowheads gap junctions, and yellow arrowheads tight junctions

5. Dehydrate in increasing concentrations of ethanol (30%, two changes, for 10 min each; 50, 70, 90, 96% for 15 min each; 100%, two changes, for 15 min each) and in acetone (three changes, for 10 min each), all steps at room temperature.
6. Embed in Epon 812 or its equivalents (e.g., Glycid Ether 100 resin) (*see* **Note 22**).
7. Cut blocks into ultrathin (gray or silver) sections.
8. Contrast sections with uranyl acetate (saturated aqueous solution) and lead citrate according to standard protocol.

Here we show ultrastructure of basal ectoplasmic specialization connecting adjoined Sertoli cells (Fig. 4).

3.3 Immunohistochemical Staining

Immunohistochemistry (IHC) is a method for demonstrating the localization of the protein of interest in tissue sections. The method is accomplished with antibodies that recognize the target protein and then visualized using chromogenic detection (*see* **Note 17**).

1. Deparaffinize slides in two changes of xylene for 10 min each.
2. Hydrate slides to water by dipping them in two changes of absolute ethanol (for 10 min each), two changes of 96% ethanol, and one of 70% ethanol (for 5 min each).
3. Immerse the sections on the slides in citrate buffer and heat in a microwave oven (8 min, 700 W).

4. Wash the slides with TBS twice for 5 min each (*see* **Note 23**).
5. Block endogenous peroxidase activity with 0.3% H_2O_2 in methanol for 15 min (*see* **Note 24**).
6. Wash the slides in TBS three times for 5 min each.
7. Block nonspecific binding sites with 5–10% normal serum for 20 min at room temperature (*see* **Notes 25** and **26**).
8. Do not wash the slides. Shake off excess fluid with a brisk motion and carefully wipe each slide around the sections.
9. Incubate the sections overnight at 4 °C in the presence of a primary antibody (*see* **Notes 27** and **28**).
10. Perform negative controls on each slide replacing the primary antibody with TBS or normal serum.
11. Wash the slides with TBS three times for 5 min each.
12. Incubate the sections for 60 min at room temperature in the presence of a secondary biotinylated antibody.
13. Wash the slides with TBS three times for 5 min each.
14. Apply ABC solution in TBS for 30 min to the sections to amplify signals (*see* **Note 29**).
15. Apply DAB substrate solution for 3–6 min (or until desired color reaction is observed) to the sections to reveal the color of the antibody staining (*see* **Notes 30** and **31**).
16. Wash the slides in dH_2O.
17. Counterstain the slides with Mayer's hematoxylin for 15–30 s (*see* **Note 19**).
18. Rinse the slides in running tap water for 1–2 min.
19. Dehydrate the sections through a graded series of ethanol (70, 80, 90, and 100%) for 5 min each.
20. Clear the sections on the slides in two changes of xylene (5 min for each) and coverslip using mounting solution (e.g., DPX).

Here, we present schematic diagram illustrating the complexity of intercellular junctions in the basal and apical testis compartments to better explain localization of the junction proteins within the seminiferous epithelium and microphotographs showing junction proteins' immunoexpression in testes (Fig. 5).

3.4 Immunofluorescence Staining of Paraffin Sections

Immunofluorescence (IF) rely on the use of antibodies to label a specific target antigen with a fluorescent dye also called fluorophores or fluorochromes. The fluorophore allows visualization of the target distribution in the sample under a fluorescent microscope (e.g., epifluorescence and confocal microscopes).

1. Deparaffinize slides in two changes of xylene for 10 min each.

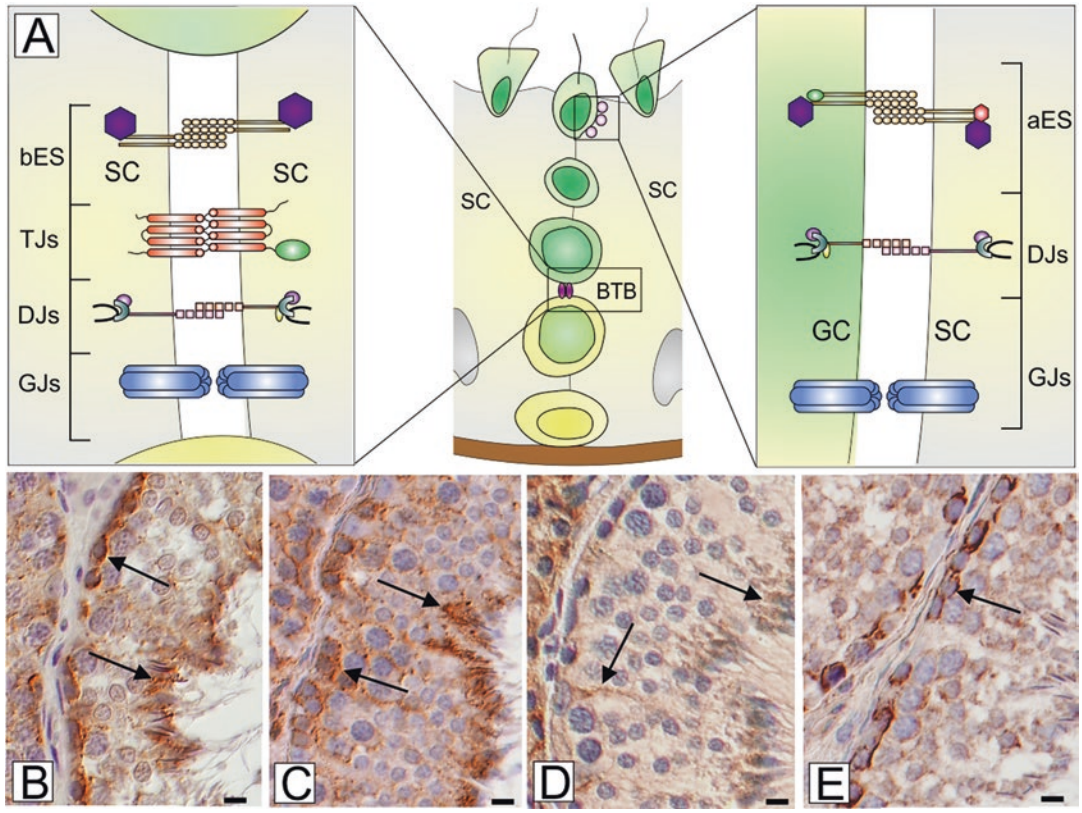

Fig. 5 (**A**–**E**) Schematic drawing illustrating the molecular architecture of intercellular junctions in the basal and apical compartments. (**A**) In the basal compartment, the BTB includes basal ectoplasmic specialization (bES), tight junctions (TJs), desmosome-like junction (DJs), and gap junctions (GJs), while in the apical compartment, the apical ectoplasmic specialization (aES), desmosome-like junctions, and gap junctions (GJs) are located between Sertoli cells (SC) and germ cells (GC). Color shapes depict intercellular junction proteins presented in (**B**–**E**). Representative micrographs of immunohistochemical localization of N-cadherin (**B**), β-catenin (**C**), connexin 43 (Cx43) (**D**), and zonula occludens (ZO-1) (**E**) in boar testis. Nomarski microscopy (*see* **Note 32**). Scale bars represent 10 μm. Paraffin sections were fixed using 10% NBF, and junction proteins were detected with monoclonal or polyclonal antibodies. Signals were visualized using ABC and DAB as a substrate. All sections were counterstained with Mayer's hematoxylin. Positive signals are located at membrane appositions of Sertoli-Sertoli cells and Sertoli-germ cells (arrows). In negative controls (not shown), primary antibodies were replaced with normal serum (*see* **Note 26**)

2. Hydrate slides to water by dipping them in two changes of absolute ethanol (for 10 min each), two changes of 96% ethanol, and one of 70% ethanol (for 5 min each).
3. Immerse the sections on the slides in citrate buffer and heat in a microwave oven (8 min, 700 W).
4. Wash the slides with TBS twice for 5 min each (*see* **Note 23**).
5. Block nonspecific binding sites with 5–10% normal serum for 20 min at room temperature (*see* **Notes 25** and **26**).
6. Do not wash the slides. Shake off excess fluid with a brisk motion and carefully wipe each slide around the sections.

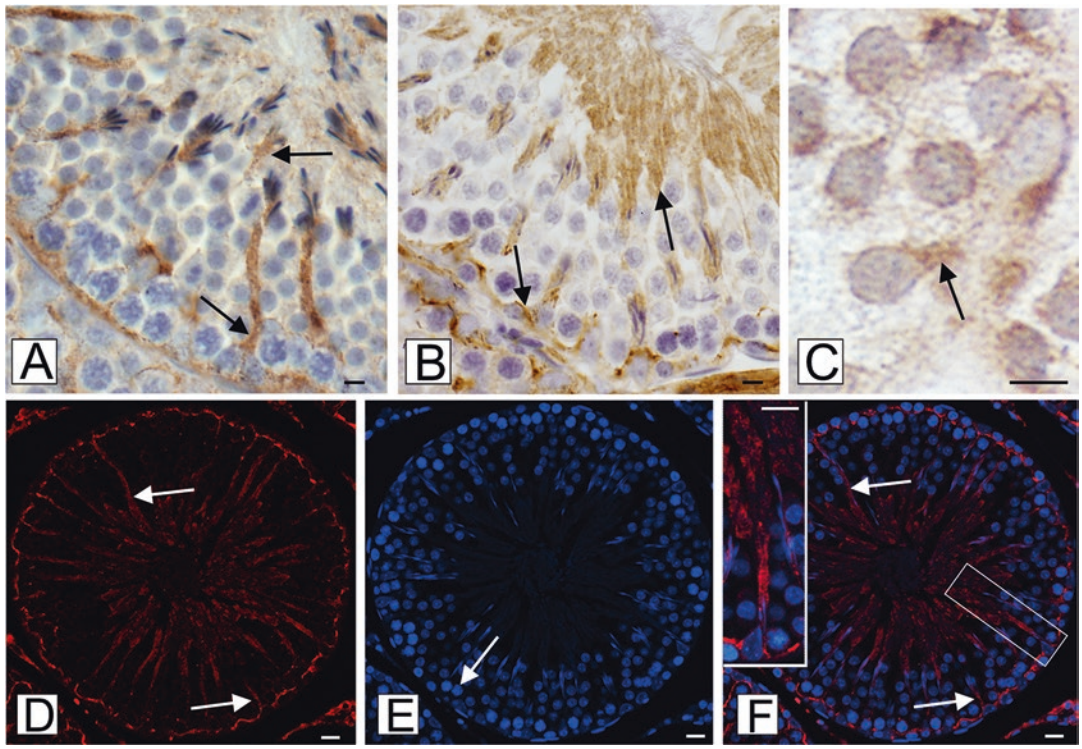

Fig. 6 (**A**–**F**) Representative micrographs of Cx43 immunostaining in rat (**A**) and bank vole (**B**) testes and primary rat Sertoli cell culture (**C**). Scale bars represent 10 μm. Paraffin sections were fixed using 10% NBF (**B**, **B**) and Bouin's solution (**D**–**F**), while cultured cells were fixed with methanol/acetone (as in Fig. 1D), and Cx43 was detected with polyclonal antibody against Cx43 protein. Sections A and B were counterstained with Mayer's hematoxylin. Immunofluorescence signal (**D**–**F**) was visualized using secondary Alexa Fluor-conjugated antibody and VECTASHIELD medium without DAPI (**D**), only DAPI staining (**E**), and merge image (**F**). Scale bars represent 25 μm. Positive signal is located at membrane appositions of Sertoli-Sertoli cells and Sertoli-germ cells (arrows). See the signal also at higher magnification (insert in **F**). In negative controls (not shown), primary antibody was replaced with normal serum (*see* **Note 26**)

7. Incubate the sections overnight at 4 °C in the presence of a primary antibody (*see* **Notes 27** and **28**).
8. Perform negative controls on each slide replacing the primary antibody with TBS or normal serum.
9. Wash the slides with TBS three times for 5 min each.
10. Incubate the sections in the presence of a secondary antibody conjugated with fluorochrome for 90 min in dark at room temperature.
11. Wash the slides with TBS five times for 3 min each in dark.
12. Add two drops of VECTASHIELD reagent without DAPI or with DAPI to the slide and mount the coverslip (*see* **Notes 33** and **34**).

Here we present immunostaining visualized by ABC-DAB and Alexa Fluor (Fig. 6).

3.5 Rapid Immunofluorescence Staining of Frozen Sections

1. Snap freeze fresh tissue in liquid nitrogen, embed in Tissue-Tek, cut 7-μm-thick cryostat sections, and mount on Superfrost Plus slides (*see* **Note 35**). The slides are ready to use (*see* **Note 36**).
2. Fix the sections in Bouin's solution for 5 min (*see* **Notes 2** and **37**).
3. Wash the slides with PBS twice for 5 min each.
4. Incubate the sections with 0.1% Triton X-100 in PBS for 10 min for permeabilization (*see* **Note 38**).
5. Wash the slides with PBS three times for 5 min each.
6. Block nonspecific binding sites with 10% normal serum for 30 min at room temperature (*see* **Notes 25** and **26**).
7. Do not wash. Shake off excess fluid with a brisk motion and carefully wipe each slide around the sections.
8. Incubate the sections overnight at 4 °C in the presence of the diluted primary antibody (*see* **Notes 27** and **28**).
9. Perform negative controls on each slide replacing the primary antibody with TBS or normal serum.
10. Wash the slides in PBS three times for 5 min each.
11. Incubate the sections in the presence of a secondary antibody conjugated with fluorochrome in humidified chamber for 90 min in dark at room temperature (*see* **Note 39**)
12. Wash the slides with PBS five times for 3 min in dark.
13. Add two drops of VECTASHIELD reagent (with DAPI or without DAPI) to the slide and mount the coverslip (*see* **Notes 33** and **34**).

Here we show immunofluorescence in frozen rat testes (Fig. 7).

3.6 Immunocytochemical Staining

For immunocytochemistry Sertoli cells are to be cultured directly on the bottom of the plastic plates or on the round glass coverslips in 24-well plastic plates (*see* **Note 40**).

1. Wash the cells three times with PBS for 5 min each.
2. By using a pair of forceps lift the coverslips (which contain the attached cells) and put them into a Petri dish.
3. Fix the cells with 4% PFA (*see* **Note 41**).
4. Wash the cells three times with PBS for 5 min each (*see* **Note 42**).
5. Incubate the cells for 1 min with PBS containing either 0.1% Triton X-100 or equivalents (*see* **Notes 43** and **44**).
6. Block endogenous peroxidase activity with 0.3% H_2O_2 in PBS for 15 min (*see* **Note 24**).
7. Wash the slides in PBS three times for 5 min each.

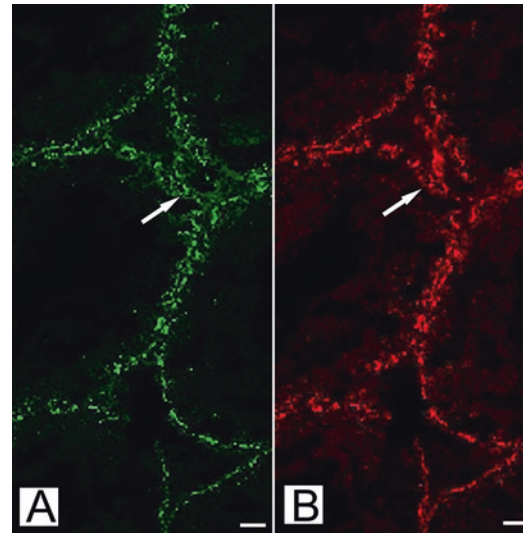

Fig. 7 (**A**, **B**) Representative micrographs of immunofluorescence localization of N-cadherin (**A**) and β-catenin (**B**) in rat testis. Scale bars represent 15 μm. Frozen sections were fixed using Bouin's solution for 5 min. Immunofluorescence signal was visualized using secondary Alexa Fluor-conjugated antibodies and VECTASHIELD medium without DAPI. Positive signals are depicted by arrows. In negative controls (not shown), primary antibodies were replaced with normal serum (*see* **Note 26**)

8. Block nonspecific binding sites with 5 to 10% normal serum for 20 min at room temperature (*see* **Notes 25** and **26**).
9. Do not wash the coverslips. Lift the coverslips and put them (upside-down) onto a 30 μL drop of a primary antibody on a sheet of Parafilm, and incubate the cells overnight at 4 °C (*see* **Note 45**).
10. Perform negative controls replacing the primary antibody with TBS or normal serum.
11. Lift the coverslips, put them into the plastic plate and wash with PBS three times, for 5 min each
12. Lift the coverslips and put them (upside-down) onto a 30 μL drop of a secondary antibody on a sheet of Parafilm.
13. Incubate the cells for 30 min at 37 °C.
14. Wash coverslips three times with PBS for 5 min each (*see* **Note 46**).
15. Lift the coverslips, and put them (upside-down) onto a 30 μL drop of ABC solution for 30 min to the sections to amplify signals (*see* **Note 29**).
16. Wash coverslips three times with PBS for 5 min each.

17. Apply DAB substrate solution for 3–6 min (or until desired color reaction is observed) to the cells to reveal the color of the antibody staining (*see* **Notes 30** and **31**).
18. Wash the coverslips with dH_2O.
19. Counterstain the slides with Mayer's hematoxylin for 15–30 s (*see* **Note 19**).
20. Rinse the slides in tap water for 1 min.
21. Mount the coverslips with a drop of glycerol-based mounting medium. They are ready for microscopic observation.

Here, we present immunocytochemical localization of androgen receptor and connexin 43 in primary mouse and rat Sertoli cell cultures, respectively (*see* Figs 1D and 6C).

4 Notes

1. PBS can be prepared as a 10× stock: 80 g NaCl, 2.0 g KCl, 14.4 g Na_2PO_4, and 2.4 g KH_2PO_4 dissolved in 800 mL dH_2O. Adjust the pH to 7.4 with HCl and add dH_2O to 1 L.
2. Filter the picric acid with a filter paper before adding the fixative to avoid any remaining undissolved particles.
3. Filter the hematoxylin with a filter paper to avoid any remaining undissolved particles.
4. The mixture of osmium tetroxide and potassium ferrocyanide should be prepared just before use and kept at 4 °C. Properly prepared mixture is transparent and light-brown, and it should not be used if it turns dark or black.
5. The contrast ensured by this method is high enough to visualize ectoplasmic specializations even in semi-thin (0.7–1 μm thick) sections at the level of light microscope.
6. Take care that the solution does not boil.
7. Use gloves and protect eyes.
8. It is recommended to use 10% NBF solution no longer than 3 months after it was prepared.
9. For extended storage, store at 4 °C.
10. Tris-EDTA buffer is recommended to improve staining with low-abundance epitopes or with antibodies that have weak affinity. It enhances staining for numerous antibodies, although background staining is often increased.
11. The antibody must be diluted (not always as recommended by the manufacturer).
12. DAB is a carcinogen. Handle with care, protect eyes, and work with gloves, laboratory coat, and laboratory glasses.

13. In animals larger than a mouse (rats, pigs, etc.), testes will need to be cut into smaller pieces (no thicker than 5 mm) before fixation.
14. It is important to fix testis specimens at the site of removal as soon as possible after dissection.
15. The volume of fixative must be 15–20 times over the sample volume, and the tissue must be completely immersed in the solution.
16. Do not let the paraffin exceed 60 °C for prolong periods of time because this will degrade the paraffin polymers and make it hard and brittle.
17. Use slides coated with 3-aminopropyltriethoxysilane solution (APES) to make the slides more adhesive for fixed tissue and reduce the background staining of glass surface.
18. Carry out all procedures at room temperature unless otherwise specified. 5 μm paraffin sections of 10% NBF or Bouin's solution-fixed testicular tissue are suitable.
19. Control the intensity of the hematoxylin staining under the microscope to obtain the desire intensity.
20. Dissected testes should be placed in excessive amount of fixative 1 and pierced with a fine needle. After 10–15 seminiferous tubules should be cut into small fragments (2–4 mm) and transferred into fresh cold fixative.
21. Fixation time in fixative 2 strongly depends on the material (analyzed species, size of samples) and must be determined experimentally.
22. The Glycid Ether 100 resin is a commercial name of Epon 812.
23. TBST is often used for washing steps.
24. Add enough H_2O_2 to completely cover the slides and keep them in dark.
25. Circle each section on the slide using a hydrophobic pen (PAP Pen) in order to avoid leaking reagent from the slide.
26. Use normal serum from the same species as the host of the secondary antibody.
27. All incubations should be carried out in the humidified chamber to avoid drying of the tissue.
28. Drying at any stage of the procedure will lead to nonspecific staining, mainly high background.
29. For detection of low-abundance proteins, amplify signals by using ABC method. Conjugation of biotin to antibodies and reporter enzymes or fluorophores provides a powerful means to amplify signals.

30. Observe the color of the antibody staining in the tissue sections under a light microscope.
31. Store the slides at 4 °C to delay fading of the DAB reaction.
32. The use of differential interference contrast (DIC) microscopy (known as Nomarski microscopy) allows the researcher to distinguish more easily germ cell types and Sertoli cells within the seminiferous epithelium.
33. VECTASHIELD® Antifade Mounting Medium does not solidify, but remains a liquid on the slide and can be stored without sealing. If desired, coverslips can be permanently sealed with clear nail polish. Alternatively, VECTASHIELD® HardSet Antifade Mounting Medium may be used.
34. Mounted slides should be stored at 4 °C protected from light.
35. Snap freezing is the process of rapid cooling of a tissue to temperature below −70 °C.
36. Alternatively, the slides may be stored at −80 °C until needed.
37. Alternatively, 4% paraformaldehyde in PBS for 5–10 min or methanol (chilled at −20 °C) for 5 min may be used.
38. Alternatively, acetone (chilled at −20 °C) for 5 min may be used.
39. Secondary antibody may be diluted in PBS, 1% BSA or 10% NGS.
40. Glass coverslips are needed for methanol/acetone fixation
41. If the target protein is intracellular, it is very important to permeabilize the cells (*see* Fig. 1c, d). Methanol-acetone-fixed samples do not require permeabilization.
42. During a whole procedure, note of which side of the coverslips the cells are on.
43. Triton X-100 is the most popular detergent for improving the penetration of the antibody. However, it is not appropriate for membrane-associated antigens since it destroys membranes.
44. The optimal percentage of Triton X-100 should be determined for each protein of interest
45. Duration of fixation is depended on antigenicity. If antigen is sensitive to fixation, fixation time can be shorter or be done at 4 °C.
46. If needed, most wash steps within this protocol can be extended beyond the time specified.

Acknowledgments

The authors would like to acknowledge Dr. Katarzyna Chojnacka, Dr. Marta Zarzycka, Dr. Ilona Kopera-Sobota, and Dr. Ewelina Gorowska-Wojtowicz (former PhD students of B.B.) for their work and involvement in improving methods presented herein. Special thanks are expressed to Dr. Ewelina Gorowska-Wojtowicz for illustrations. Several methods described here were obtained from the studies supported by a HARMONIA 3 grant (2012/06/M/NZ4/00146) from the National Science Centre (to B.B.)

References

1. Su L, Kopera-Sobota IA, Bilinska B et al (2013) Germ cells contribute to the function of the Sertoli cell barrier. Spermatogenesis 3:e26460
2. O'Hara L, Smith LB (2015) Androgen receptor roles in spermatogenesis and infertility. Best Pract Res Clin Endocrinol Metab 29:595–605
3. França LR, Hess RA, Dufour JM et al (2016) The Sertoli cell: one hundred fifty years of beauty and plasticity. Andrology 4:189–212
4. Mruk DD, Cheng CY (2004) Sertoli-Sertoli and Sertoli-germ cell interactions and their significance in germ cell movement in the seminiferous epithelium during spermatogenesis. Endocr Rev 25:747–806
5. Kopera I, Bilinska B, Cheng CY et al (2010) Sertoli-germ cell junctions in the testis – a review of recent data. Philos Trans R Soc Lond Ser B Biol Sci 365:1593–1605
6. Mruk DD, Cheng CY (2015) The mammalian blood–testis barrier: its biology and regulation. Endocr Rev 36:564–591
7. Stanton PG (2016) Regulation of the blood-testis barrier. Semin Cell Dev Biol 59:166–173
8. Chojnacka K, Zarzycka M, Hejmej A et al (2016) Hydroxyflutamide affects connexin 43 via the activation of PI3K/Akt- dependent pathway but has no effect on the crosstalk between PI3K/Akt and ERK1/2 pathways at the Raf-1 kinase level in primary rat Sertoli cells. Toxicol In Vitro 31:146–157
9. Cheng CY, Mruk DD (2002) Cell junction dynamics in the testis: Sertoli-germ cell interactions and male contraceptive development. Physiol Rev 82:825–874
10. Mruk DD, Cheng CY (2011) An in vitro system to study Sertoli cell blood-testis barrier dynamics. Methods Mol Biol 763:237–252
11. Hejmej A, Kotula-Balak M, Galas J et al (2011) Effects of 4-tert-octylphenol on the testes and seminal vesicles in adult male bank voles. Reprod Toxicol 31:95–105
12. Kopera I, Durlej M, Hejmej A et al (2011) Differential expression of connexin 43 in adult pig testes during normal spermatogenic cycle and after flutamide treatment. Reprod Domest Anim 46:1050–1060
13. Hejmej A, Bilinska B (2014) A role of junction-mediated interactions in cells of the male reproductive tract: impact of prenatal, neonatal, and prepubertal exposure to anti-androgens on adult reproduction. Histol Histopathol 29:815–830
14. Hopwood D (1996) Fixation and fixatives. In: Bancroft J, Stevens A (eds) Theory and practice of histological techniques. Churchill Livingstone, New York
15. Chojnacka K, Hejmej A, Zarzycka M et al (2016) Flutamide induces alterations in the cell-cell junction ultrastructure and reduces the expression of Cx43 at the blood-testis barrier with no disturbance in the rat seminiferous tubule histology. Reprod Biol Endocrinol 14:14
16. Russell LD, Burguet S (1977) Ultrastructure of Leydig cells as revealed by secondary tissue treatment with a ferrocyanide-osmium mixture. Tissue Cell 9:751–766
17. Perreira GG, Melo RCN, Russell LD (2002) Relationship of Sertoli-Sertoli tight junctions to ectoplasmic specialization in conventional and en face views. Biol Reprod 67:1232–1241
18. Hejmej A, Wiszniewska B, Kosiniak-Kamysz K et al (2006) The presence of androgen receptors in the epididymis and prostate of the stallion and cryptorchid horse - a preliminary study. Vet J 171:373–379
19. Hejmej A, Kotula-Balak M, Sadowska J et al (2007) Expression of connexin 43 protein in testes, epididymides and prostates of stallions. Equine Vet J 39:122–127

20. Hejmej A, Kopera I, Kotula-Balak M et al (2009) Age-dependent pattern of connexin43 expression in testes of European bison *(Bison bonasus,* L.) J Exp Zool A 311A: 667–675
21. Lydka M, Kotula-Balak M, Kopera-Sobota I et al (2011) Vimentin expression in testes of Arabian stallions. Equine Vet J 43:184–189
22. Hejmej A, Kopera I, Kotula-Balak M et al (2012) Are expression and localization of tight and adherens junction proteins in testes of adult boar affected by fetal and neonatal exposure to flutamide? Int J Androl 35:340–352
23. Hejmej A, Kotula-Balak M, Chojnacka K et al (2013) Photoperiod-dependent effects of 4-tert-octylphenol on adherens and gap junction proteins in bank vole seminiferous tubules. Int J Endocrinol 2013:134589
24. Zarzycka M, Chojnacka K, Mruk D et al (2015) Flutamide alters distribution of c-Src and affects cell adhesion function in the adult rat seminiferous epithelium. Andrology 3:569–581

Chapter 4

Rabbit Sertoli Cells: Immunohistochemical Profile from Neonatal to Adult Age

Valeria Grieco and Barbara Banco

Abstract

Immunohistochemistry (IHC) on formalin-fixed paraffin-embedded tissue specimens is a widely used laboratory technique that allows the demonstration and the direct microscopical observation of antigens within tissue sections by means of specific antibodies. IHC is one the best tools to define the immunophenotype of a cell during maturation or neoplastic transformation.

To investigate the immunophenotype of postnatal rabbit Sertoli cell, from neonatal to adult age, in this chapter, the immunohistochemical protocol described is one of the most common: the avidin-biotin complex (ABC) method.

Key words Formalin-fixed specimens, Sertoli cells, Antigens, Antibodies, Chromogen

1 Introduction

Sertoli cells are fundamental for testis development and function: they physically support the germ line, permitting the maturation of germ cells, thanks to growth factors, hormones, and proteins that are the base of the so-called Sertoli cells and germ cell interaction [1]. The reduction in Sertoli cells number and function critically affects the testicular function, causing an impairment of spermatogenesis that predispose to neoplastic transformation.

In this condition, both Sertoli and germ cells are affected, and both can be characterized by an altered phenotype characterized by cellular dedifferentiation and re-expression of markers of immaturity, naturally lost during testicular maturation [2]. For this reason, the study of the normal immunophenotype of Sertoli cell, from immature (neonatal and pubertal) to mature testis, could improve our knowledge about their normal, physiological phenotype, allowing a comparison with the pathological counterpart (neoplastic, toxic, and degenerative changes) [3].

Rabbit species (*Oryctolagus cuniculus*) is widely used for scientific purposes including research on human male reproductive

Marco G. Alves and Pedro F. Oliveira (eds.), *Sertoli Cells: Methods and Protocols*, Methods in Molecular Biology, vol. 1748, https://doi.org/10.1007/978-1-4939-7698-0_4,

system toxicology [4, 5]. In addition, the rabbit is increasingly common as pet species, and numerous pre-neoplastic and neoplastic testicular lesions have ben already signaled [6–10].

Immunohistochemistry (IHC) on formalin-fixed paraffin-embedded tissue samples is a valid technique widely used, for diagnosis and investigation as well. IHC is a simple technique allowing the demonstration of antigens within tissue sections by means of specific antibodies [11]. IHC is one the best tools to define the immunophenotype of a date cell and to understand its changes during maturation or neoplastic transformation. Antigen detection systems in immunohistochemistry include fluorescence and enzyme-antibody conjugate methods.

The enzymatic immunohistochemistry described in this chapter is realized by using one of the most common immunohistochemical methods: the avidin-biotin complex (ABC) method [12]. This method is based on the capacity of a tetrameric protein present in the chicken egg to bind biotin. Due to this affinity, the protein has been called "avidin." In this method, after the primary antibody, directed against the target antigen, a secondary biotinylated antibody is applied. After this, a third reagent is employed: a complex of avidin mixed with biotin, linked with appropriate enzyme label (in this case peroxidase). Anyway, other non-avidin-biotin methods can be employed [11].

Independently from the system considered, IHC is an easy technique, which can be performed in a basic laboratory, simply provided by tap water, a microwave oven (MW), a fume hood for chemistry, and a very basic optical microscope. These characteristics, together with the possibility to directly observe the presence of in antigens within histologic sections, allowed IHC, created about 70 years ago, to still represent a valid and reliable laboratory assay.

2 Materials

Prepare and store your reagents at room temperature (unless indicated otherwise).

Among materials, fresh rabbit testes are included: take care to follow animal welfare and legal regulations of your country to acquire and manage animal tissue samples.

Diligently follow all waste disposal regulations when disposing waste material.

2.1 Tissues

Testes from rabbits of various ages to be immersed in formalin (*see* **Note 1**).

2.2 Formalin

1. Commercially available 10% neutral buffered formalin to fix testes (*see* **Note 2**). Formalin can be also prepared in the

laboratory. To prepare 500 mL of 10% neutral buffered formalin, in a 500 mL graduated cylinder, put 50 mL of 37% formaldehyde and then add 450 mL of distilled water, 2 g of sodium phosphate monobasic (NaH_2PO_4), and 3.25 g of sodium phosphate dibasic (Na_2HPO_4), and mix well. The solution is stable for long time at room temperature.

2.3 Tissue Processing and Paraffin Embedding

1. Plastic tissue processing/embedding cassettes for histology.
2. Alcohols. Absolute 100% ethanol and graded ethanol (95% and 70%). Absolute 100% ethanol is commercially available. Alcohol 95% and 70% can be bought or obtained by diluting 100% ethanol. To prepare 95% ethanol, add 50 mL of distilled water to 950 mL of absolute ethanol. To prepare 70% ethanol, add 300 mL of distilled water to 700 mL of absolute ethanol.
3. Xylene.
4. Paraffin wax.
5. Tissue processing machine for histology (*see* **Note 3**).
6. Paraffin embedding machine (*see* **Note 4**).
7. Microtome to cut histologic sections from paraffin blocks (*see* **Note 5**).
8. Poly-L-lysine- or silane-coated slides (*see* **Note 6**).

2.4 Immunohistochemistry

1. Staining dishes/jars for histology to hold approximately 250 mL and plastic staining racks (each rack vertically holds more than 20 slides).
2. Fridge.
3. Incubator.
4. Basic microwave oven and microwavable plastic or pyrex staining dishes for histology to hold, approximately, 250 mL of sodium citrate pH 6.0 (0.01 M) antigen retrieval buffer.
5. Xylene (for section deparaffinization).
6. Ethanol absolute, 95% and 70% ethanol for sections rehydration.
7. TRIS 10× concentrate solution and working solution. To obtain concentrate solution, in 1 L graduated cylinder, put 370 mL hydrochloric acid (1 mol), and then add 630 mL of distilled water. Weight 56.5 g of Tris (hydroxymethyl) aminomethane powder and transfer to a glass beaker. Add the solution of water and hydrochloric acid to the powder and mix well to dissolve. Store at 4 °C. To obtain the working solution (pH 7.6): dilute the concentrate solution in distilled water (1/10). Mix well. Store this solution at room temperature.
8. Micropipette (0.5–10 µL, 10–100 µL, 20–200 µL, 100–1000 µL) and related pipette tips.

9. Peroxidase inhibition reagent: add 2 mL of 30% hydrogen peroxide in 200 mL of methanol. Reagent should be prepared each time just before use and then trashed.
10. Pepsin solution digest-all (ready to use) for enzymatic antigen retrieval.
11. Antigen retrieval sodium citrate pH 6.0 (0.01 M) buffer solution. Prepare the following A and B solutions. *Solution A*: weight 29.41 g of tri-Sodium citrate dihydrate powder and transfer to a glass beaker. Add 1000 mL of distilled water. Mix well to dissolve. Store this solution at 4 °C. *Solution B*: weight 22 g of citric acid powder and transfer to a glass beaker. Add 1000 mL of distilled water. Mix well to dissolve. Store this solution at 4 °C. To prepare sodium citrate working solution, add 81 mL of solution A to a 100 mL graduated cylinder, and then add 19 mL of solution B. This solution will be diluted 1/10 in a 1 L cylinder adding 900 mL of distilled water. Mix well and store this solution at room temperature.
12. A PAP Pen Liquid Blocker to encircle sections (*see* **Note 7**).
13. Wet chamber. Wet chambers are commercially available; however, a simple and useful wet chamber can be built with materials already present in most laboratories (*see* **Note 8**).
14. Background blocking solution. Normal serum of several species, commercially available, is used for this purpose. Select and dilute the normal serum of the species in which the biotinylated secondary antibody has been produced in TRIS buffer.
15. Primary antibodies. Monoclonal antibodies made in mouse and polyclonal antibodies made in other species except the rabbit are preferable. For use, antibodies will be diluted in TRIS buffer at the optimal working dilution (*see* **Note 9**).
16. Secondary biotinylated antibodies diluted in TRIS buffer, raised against the IgG of the animal used for primary antibody production.
17. Avidin/biotinylated enzyme complex (ABC) (*see* **Note 10**).
18. For detection of the immune reaction with developing reagent: aminoethylcarbazole (AEC) or 3,3-diaminobenzidine (DAB) to prepare immediately before use, according to the manufacturer's instructions.
19. Mayer's hematoxylin solution (commercially available) for counterstaining.
20. Cover slips (24 × 40 mm–24 × 60 mm).
21. Aqueous mounting medium (*see* **Note 11**).

3 Methods

Unless specified, all procedure is carried out at room temperature.

During all immunohistochemical protocol, do not let the sections dry out.

For immunohistochemistry consider negative and positive controls of the immunolabeling (*see* **Note 12**).

3.1 Preparation of Paraffin Sections

1. Fix tissue samples in neutral buffered formalin for at least for 72 at room temperature (*see* **Note 13**).
2. After fixation, tissues are processed through a series of graded alcohols before to be clarified in xylene and paraffin embedded, as routinely in histology practices. Paraffin blocks can be stored at room temperature.
3. Cut blocks with a microtome to obtain sections approximately 5 μm thick, and then mount them onto polylysine-coated slides.
4. To make the section adhering to the slide, dry slides at room temperature overnight, or incubate them at 50 °C, for at least 2 h, in an oven.

3.2 Immunohistochemical Protocol

1. Deparaffinization (*see* **Note 14**). Prepare three jars/dishes for histology, and fill two of them with xylene and one with 100% ethanol. Place the slides in a rack, and perform the following washes, passing the rack jar by jar: xylene 1 (30 min), xylene 2 (30 min), and 100% ethanol (5 min).
2. Block of the endogenous peroxidase activity (*see* **Note 15**). To irreversibly inhibit endogenous peroxidase, slides should be placed in a bath of hydrogen peroxide and methanol for at least 30 min. The bath of 200 mL absolute methanol plus 2 mL of 30% hydrogen peroxide must be made up fresh just before the use and then trashed.
3. Sections rehydration. As in Subheading 3.2, **step 1**, prepare three histology jars/dishes, respectively, containing 100% ethanol, 95% ethanol, and 70% ethanol. In each jar, the rack with sections will stay at least 3 min.
4. After rehydration, put slides in TRIS buffer (0.05 M, pH 7.6) for at least 5 min.
5. Enzymatic epitope retrieval (*see* **Note 16**). Wipe away excess liquid around the section on the glass slide with tissue paper. Encircle the tissue section with the PAP Pen Liquid Blocker and let dry (5–15 s). Be careful not write too close to the sample margins. Among the antibodies employed for the present chapters, those directed against cytokeratins and desmin require enzyme-induced epitope retrieval. For enzymatic digestion: put the slides in a wet chamber, laying the slides flat.

Cover each section (already encircled with PAP pen) with 100–200 μL of Pepsin digest-all (ready to use) solution, close the wet chamber with its cover, and incubate for 12–14 min at 37 °C. Then rinse slides in TRIS buffer and leave them in.

6. Heat-induced epitope retrieval (*see* **Note 16**). Among the antibodies employed for the present chapters, those directed against anti-Müllerian hormone and vimentin (this latter particularly if sections derive from overfixed samples) require heat-induced epitope retrieval. Place slides (not encircled with PAP-pen) in a plastic rack and in a microwaveable plastic or pyrex staining jar for histology to hold approximately 250 mL of antigen retrieval buffer. Also pyrex coplin jars can be used. Immerge and cover the slides with abundant antigen retrieval buffer (e.g., buffer solution sodium citrate, pH 6). Place the plastic jar inside the microwave, covered with its cover, and set the microwave for heating the slides (650 W for 10 min). Be sure to monitor for evaporation and watch out for boiling over during the procedure, and do not allow the slides to dry out. When 10 min has elapsed, remove the plastic jar from the microwave, and put at room temperature until decooling is obtained. Then transfer the slides from antigen retrieval buffer to the TRIS buffer.
7. Encircle the sections as described in Subheading 3.2, **step 5**, and then put all sections (from both **steps 5** and **6**) in the same jar with TRIS buffer.
8. Dilute the blocking serum.
9. Remove slides from bath and wipe away the excess liquid from the section. Place the slides in a wet chamber, laying the slides flat, and apply 100–200 μL of the blocking serum on each sample. Close the wet chamber with its cover and incubate for 20 min at room temperature.
10. Dilute the primary antibodies (vimentin, CK AE1-AE3, desmin, and anti-Müllerian hormone) in TRIS buffer (*see* **Note 9**).
11. Cover the sections with primary antibody. To do this step: tap off normal serum and wipe away excess. Do not wash in TRIS buffer. Lay the slide flat and apply the primary antibody.
12. Incubate for 18 h at 4 °C.
13. Rinse slides three times (3 min each) in TRIS buffer.
14. Dilute the secondary biotinylated antibody in TRIS buffer, and prepare the avidin-biotin complex (ABC) following manufacturer instructions.
15. Remove slides from bath and wipe away the excess liquid from the section. Do not let them dry. Place the slides again in the wet chamber, laying the slides flat, and apply 100–200 μL of

the secondary biotinylated antibody directed against the immunoglobulins of the species in which the primary antibody has been produced. Close the wet chamber with its cover.

16. Incubate for 30 min at room temperature.
17. Rinse slides three times (3 min each) in TRIS buffer.
18. Remove slides from bath and wipe away the excess liquid from the section. Do not let them dry. Place the slides again in the wet chamber, laying them flat, and apply 100–200 μL of ABC complex (avidin-biotin-peroxidase complex). Close the wet chamber with its cover.
19. Incubate for 30 min, at room temperature.
20. Rinse slides with TRIS buffer (three times, 3 min each).
21. Detection of the immune reaction with developing reagents (e.g.,amino-9-ethylcarbazole[AEC])or3,30-diaminobenzidine tetrachloride (DAB). Dilute the chromogen according to the manufacturer's instructions. Place the slides again in the wet chamber, laying the slides flat, and cover them with the diluted chromogen. Optimal development times should be determined (*see* **Note 17**).
22. Prepare a jar with filled with tap water and put an empty rack into. Stop reaction in tap water by immerging slides, rapidly one by one, in the jar where all the slides included in the immunohistochemical test will be finally collected.
23. Wash sections putting the jar under running tap water for 3 min.
24. Counterstain sections (1–2 min) by immersing the rack containing them in a jar filled with Mayer's hematoxylin. Then put the rack in a jar filled with tap water and rinse in running tap water for 5 min.
25. Remove slides from bath and wipe away the excess liquid from the sections.
26. Mounting cover slips. Place a drop of mounting media over the section and gently apply a cover slip.

4 Notes

1. Depending on the age and the breed of the rabbit, testes could vary in size. Considering this, testes measuring more than 1 cm in diameter should be cut longitudinally before the immersion in formalin. Small-sized testicles (neonates or pet rabbits) can be fixed entirely to avoid to damage tissue with the blade. In improperly fixed testes, Sertoli cells detach from basal membranes and autolytic germ cells condense in groups or aggregates within the lumen of the seminal tubules.

2. Neutral 10% buffered formalin is the most common chemical fixative. Fixation of tissues is necessary to preserve cellular components, prevent tissue autolysis, and facilitate conventional staining and immunostaining [13]. Timing of formalin fixation is important. For rabbit testes, 2 days of fixation will be optimal. Overfixation and underfixation adversely affects the immunostaining results. Reduction in immunostaining and/or antigen decay and loss of antigenicity can occur, increasing the possibility of false negative interpretations. On the other hand, underfixed tissues can be easily damaged by antigen retrieval methods. Moreover, for largest testes, not appropriately fixed, immunohistochemical reaction could be present only at the periphery of the specimen, while the central part, not well fixed due to uncomplete penetration of formalin, could be unreactive leading to false negative results.
3. Two main types of these machines are available over the counter. One is the "carousel" type, represented by a carousel containing a metallic cage in which the cassettes containing the trimmed tissues are placed. The carousel is composed by several glass beakers containing absolute/graded ethanol, or xylene, or paraffin wax. The carousel turns the cage containing the tissue cassettes in the beakers until the end of processing. The second type is composed by a fix chamber in which is placed the metallic cage containing cassettes. In and out of this chamber, the differed solutions are pumped. The tissue processing generally runs overnight.
4. Several paraffin embedding machines are available over the counter. They are generally composed by three modules (two hot and one cool). The first heating module is composed by a chamber filled of melted paraffin in which the tissue cassettes are placed. The same module contains a tank of melted paraffin connected to a paraffin dispenser. The second heating module contains metal molds for realizing paraffin blocks. The third module is a cooling plate where hot paraffin blocks are placed. Once cooled, paraffin blocks will be detached from theirs molds and will be ready to use.
5. Seriated sections from paraffin blocks should be cut at the thickness of 4–5 μm on a microtome. Place the blocks on a cold plate for few minutes. Cut the sections, and place them onto the water surface. Float the sections on a cold (room temperature) water bath and then on a 40 °C water bath containing distilled water. Once sections are flattened, remove them vertically from the water taking them with a poly-L-lysine slide. Drain excess water from beneath the section before drying and store slides in racks in an upright position, and then dry in an oven (drying temperatures should not exceed 55 °C). Store paraffin sections in a dust-free box at room temperature

(slides should be taken in a dry environment, not exposed to the sun light, at room temperature).

6. During the immunohistochemical test, sections needs to be always wet. Moreover, they generally undergo enzymatic or MW antigen retrieval; thus, to avoid detachment, to place them onto slides coated by an adhesive, such as poly-L-lysine or silane, will be extremely useful.
7. The hydrophobic properties of the liquid contained into the pen allows, after deparaffinization, to draw barriers on the slide and to confine the presence of the reagents within a defined and limited area.
8. For a homemade wet chamber, put paper towels wet with tap water or distilled water into a plastic slide box for slide storage. Put the slides lying flat in the wet chamber, covered with the reagent, and close the box cover. Wet chambers can be used at room temperature, or they can be put into the fridge or into the incubator.
9. The optimal working dilution of the primary antibody should be determined applying a dilution series of the primary antibody on serial sections of a known positive control. The optimal dilution is obtained when the strongest positive reaction is present in the absence of background staining. Take care your antibody is cross-reactive for the rabbit species, and test the optimal dilution of your antibody; this can vary depending on the source/manufacturer and sometimes depending on the antibody lot.
10. The components of the avidin-biotin complex are commercially available in kits that generally provide two reagents to be mixed and diluted in buffer. Follow the manufacturer instruction. The complex can be used with any of biotinylated antibodies.
11. Several mounting media are commercially available. To avoid discoloration, aqueous media must be used when the detection of the immune reaction is performed with aminoethylcarbazole (AEC).
12. Negative and positive controls. For each sample, negative control could be represented by a serial section in which the primary antibody is substituted by normal serum horse serum diluted in TRIS buffer. For the antibodies employed in this chapter, except for that directed against anti-Müllerian hormone, positive internal control structures were present in testes sections. Internal positive controls were represented by rete testis for cytokeratins, interstitial connective tissue for vimentin, and vessel walls for desmin. As positive control for anti-Müllerian hormone (AMH), which is strongly expressed in

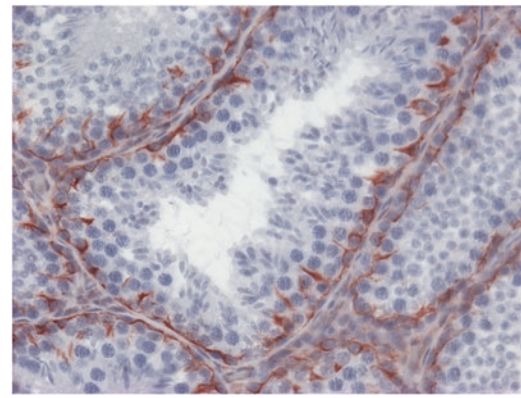

Fig. 1 Mature rabbit testis. Vimentin immunolabeling. Diffuse and strong expression of vimentin in the cytoplasm of Sertoli cells without background staining. ABC method, AEC chromogen, Mayer's hematoxylin counterstain. Magnification 200×

neonatal Sertoli cells, a section of neonatal rabbit testis was included in each immunohistochemical test.

13. For an optimal fixation, the tissue sample should not exceed 7 mm in thickness and immersed in abundant formalin.
14. To remove paraffin from the section is a key step. Not totally removed paraffin wax causes poor, irregular labeling or negative staining.
15. The substrate chromogen reaction used to visualize peroxidase cannot distinguish between the enzyme immunologically localizing the antigen and the endogenous peroxidase activity already present within the specimen (confined mostly to the red blood cells).
16. Overfixation in formalin causes formation of aldehyde linkages that mask the antigen preventing its localization by the primary antibody. To unmask the antigen sites, aldehyde bonds can be eliminated with proteolytic enzymes or high-temperature heating.
17. The optimal time of development (that can be easily controlled by a microscope) is reached when the immunolabeled antigen is well visible with absent/low background staining (Fig. 1). Generally, if DAB is used as chromogen, the reaction will develop soon (1–2 min max), while the reaction of AEC is slower (7–15 min). The interpretation of the results is not always straightforward: several artifacts can mimic the positive reaction. To avoid false-positive results, check the corresponding negative control sections. Moreover, several artifacts can be found and interfere with correct interpretation of the immunostaining, such as precipitates, chromogen granules, and counterstaining pigments. Tissue artifacts also occur when the sections are too thick or where the tissue is folded. Take

into account that only the staining pattern of viable cells should be considered for interpretation, avoiding to consider necrotic and detached cells as positively labeled.

With the present method and primary antibodies employed, rabbit Sertoli cells will be positive for VIM from neonatal to adult age. Cytokeratins and AMH will be visualized exclusively in immature testes and diffusely and strongly positive in neonates (0–7 days of life) and will progressively decrease in prepubertal testes indicating an immature Sertoli cell status. Desmin will be not expressed [3] (as in other species, including man, this markers should be expressed only by early fetal Sertoli cells [14]).

References

1. Griswold MD (1995) Interactions between germ cells and Sertoli cells in the testis. Biol Reprod 52:211–216
2. Sharpe RM, McKinnell C, Kivlin C, Fisher JS (2003) Proliferation and functional maturation of Sertoli cells, and their relevance to disorders of testis function in adulthood. Reproduction 125:769–784
3. Banco B, Grilli G, Giudice C, Marques AT, Cotti Cometti S, Visigalli G, Grieco V (2016) Immunophenotyping of rabbit testicular germ and Sertoli cells across maturational stages. J Histochem Cytochem 64:715–726
4. Williams J, Gladen BC, Turner TW, Schrader SM, Chapin RE (1991) The effects of ethylene dibromide on semen quality and fertility in the rabbit: evaluation of a model for human seminal characteristics. Fundam Appl Toxicol 16:687–700
5. Attardi BJ, Engbring JA, Gropp D, Hild SA (2011) Development of dimethandrolone 17beta-undecanoate (DMAU) as an oral male hormonal contraceptive: induction of infertility and recovery of fertility in adult male rabbits. J Androl 32:530–540
6. Brown PJ, Stafford RA (1989) A testicular seminoma in a rabbit. J Comp Pathol 100:353–355
7. Veeramachaneni DN, Vandewoude S (1999) Interstitial cell tumour and germ cell tumour with carcinoma in situ in rabbit testes. Int J Androl 22:97–101
8. Roccabianca P, Ghisleni G, Scanziani E (1999) Simultaneous seminoma and interstitial cell tumour in a rabbit with a previous cutaneous basal cell tumour. J Comp Pathol 121:95–99
9. Banco B, Stefanello D, Giudice C, D'Acierno M, Di Giancamillo M, Grieco V (2012) Metastasizing testicular seminoma in a pet rabbit. J Vet Diagn Investig 24:608–611
10. Banco B, Ferreira da Silva J, Cotti Cometti S, Stefanello D, Grieco V (2017) Immunohistochemical expression of placental alkaline phosphatase in five cases of seminoma in rabbits. J Comp Pathol 156:366–370
11. Ramos-Vara JA, Miller MA (2014) When tissue antigens and antibodies get along: revisiting the technical aspects of immunohistochemistry--the red, brown, and blue technique. Vet Pathol 51:42–87
12. Hsu SM, Raine L, Fanger H (1981) Use of avidin-biotin-peroxidase complex (ABC) in immunoperoxidase techniques: a comparison between ABC and unlabeled antibody (PAP) procedures. J Histochem Cytochem 29:577–580
13. Hayat MA (2002) Fixation and embedding. In: Microscopy, immunohistochemistry, and antigen retrieval methods for light and electron microscopy. Kluwer Academic, New York, pp 71–93
14. Rogatsch H, Jezek D, Hittmair A, Mikuz G, Feichtinger H (1996) Expression of vimentin, cytokeratin, and desmin in Sertoli cells of human fetal, cryptorchid, and tumour-adjacent testicular tissue. Virchows Arch 427:497–502

Chapter 5

Identification of Proliferative and Apoptotic Sertoli Cells Using Fluorescence and Confocal Microscopy

Jesús Martínez-Hernández, Vicente Seco-Rovira, Ester Beltrán-Frutos, Victor Quesada-Cubo, Concepción Ferrer, and Luis Miguel Pastor

Abstract

Sertoli cells, the testicular somatic cells of the seminiferous epithelium, are vital for the survival of the epithelium. They undergo proliferation and apoptosis during fetal, neonatal, and prepubertal development. Apoptosis is increased in certain situations such as exposure to many substances, for example, toxics, or short photoperiod in the non-breeding season of some mammals. Therefore, it has always been considered that Sertoli cells that reach adulthood are quiescent cells, that is to say, nonproliferative, do not die, are terminally differentiated, and whose numbers remain constant. Recently, a degree of both proliferation and apoptosis has been observed in normal adult conditions, suggesting that consideration of this cell as quiescent may be subject to change. All this make it necessary to use histochemical techniques to demonstrate whether Sertoli cells are undergoing proliferation or apoptosis in histological sections and to allow the qualitative and quantitative study of these. In this chapter, we present two double-staining techniques that can be used for identifying Sertoli cells in proliferation or apoptosis by fluorescence microscopy. In both, the Sertoli cells are identified by an immunohistochemistry for vimentin followed by an immunohistochemistry for PCNA or a TUNEL histochemistry.

Key words Proliferation, Confocal, Fluorescence, Sertoli cell, Apoptosis, Seminiferous epithelium, Testis, Syrian hamster

1 Introduction

One of the most fascinating cells in the field of reproductive cell biology, the Sertoli cell, was discovered 150 years ago. Since then, the more it has been studied, the more changes there have been in our understanding of it. Even today, it continues to be the subject of numerous investigations because of its central role in the biology of the testicular seminiferous epithelium and, consequently, its relevance in testicular pathology [1]. Professor Enrico Sertoli discovered the Sertoli cell in 1865 as an isolated cell with a characteristic morphology. The cell in question was characterized by having a cytoplasm composed of elongated "branches," something

Marco G. Alves and Pedro F. Oliveira (eds.), *Sertoli Cells: Methods and Protocols*, Methods in Molecular Biology, vol. 1748, https://doi.org/10.1007/978-1-4939-7698-0_5,

that had not been observed in any other cell previously [2]. Together with this unique characteristic, histologically it is the only somatic cell found in the epithelium of the seminiferous tubules of the testes, where it plays a key role in offering structural, metabolic, and protective support to the rest of the cellular components [3].

It is known that Sertoli cells, like other cells, have proliferative activity, although, in their case, quite limited. There is consensus that in all the species studied, such proliferative activity takes place during the embryogenic-fetal-neonatal period and, while it may also occur in the prepuberal period, it is always more important in the first [4]. In the case of some species such as rodents, this first period is continuous, and the proliferative activity extends until puberty [5]. Proliferation may also be observed in some seasonally reproducing rodents [6]. In the case of humans, these periods (neonatal and prepuberal) are separated by more than 10 years. Such proliferation of Sertoli cells conditions both the testicular size and the daily production of sperm [7], both having, in the case of humans, a direct relationship [8]. In contrast, in other nonmammalian species such as *Squalus acanthias* or in insects such as *Drosophila melanogaster*, the Sertoli cell equivalent proliferates throughout adult life [9].

Subsequently, Sertoli cells undergo a series of morphological and functional changes in the period near the onset of puberty that will condition their maturity, helping them to become stable and nonproliferative (mature). Thus, these mature cells, with a more prominent nucleus and with close connections between them, will form an adluminal compartment. In this compartment, the germinal cells will become more directly dependent on the secretion of certain factors by the Sertoli cells. Factors affecting such maturation are thyroid hormone T3 (triiodothyronine), follicle-stimulating hormone (FSH), androgens, inhibin B [10], as well as the presence or absence of newly differentiated germ cells [11]. Whatever the case, it is a progressive process, with multiple and different maturation times, depending on the species and during which the main marker proteins associated with Sertoli cell immaturity change. Therefore, most authors believe that the presence of Sertoli cells with immature characteristics in adults is due to failure in early stages of development, which compromises the remaining steps toward maturation [12]. A special case is the changes that take place in the proliferation of Sertoli cells during the breeding seasons of the Siberian hamster. In these animals, it has been observed that the mature characteristic of Sertoli cells is maintained until the loss of meiotic germ cells in regression due to a short photoperiod. Subsequently, during recrudescence, with the increase in FSH, the Sertoli cells with immature phenotype proliferate [13]. Sertoli cells have long been considered as quiescent, nonproliferative, and terminally differentiated cells [14]. This paradigm has been questioned in recent years because it has been

shown that in vitro populations of Sertoli cells can transiently act similarly to cells with active proliferation [15]. The proliferation of these cells in adult mammals has also been observed in vivo. Thus, the positivity of Sertoli cells toward proliferating cell nuclear antigen (PCNA) after FSH administration suggests that they proliferate rather than the existence of a subpopulation of proliferating stem Sertoli cells [6]. On the other hand, under specific in vitro conditions, the arrest of cell division can be avoided [16], as also studied in humans [17]. Accordingly, it follows that the molecular mechanisms necessary for proliferation persist in the adult and can be set in motion by appropriate stimuli and conditions. This means that in the adult Sertoli cell population, cells with both immature and adult phenotypes may coexist, as can cells phenotypically in an intermediate or transitional state [6]. All this would imply that, contrary to what has always been postulated with respect to adult Sertoli cells, they may undergo proliferation and be induced through hormonal actions or through the activation of specific genes.

In order to achieve an adequate degree of development and ratio between Sertoli cells and adult germ cells, it is necessary to achieve, during postnatal development, a balance between the proliferation and the death of Sertoli cells [5]. Most authors have concluded that the death of Sertoli cells is due primarily to a process of apoptosis, and numerous histochemical investigations have been carried out using the TUNEL technique (TdT-mediated dUTP in situ nick end labelling) [18, 19], both in vitro and in vivo, to demonstrate this.

Sertoli cell apoptosis has also been described during testicular regression due to short photoperiod in the seasonal reproduction of hamster, during which there is an FHS deficit (under normal physiological conditions) [20], and when such a deficit occurs in hypogonadotropic rats (under pathological conditions) [21]. To date, then, the apoptosis of Sertoli cells has been described in relation to both special physiological (postnatal development and testicular regression in seasonal reproduction) or pathological (mainly toxic) conditions [19, 22, 23]. In addition, several studies suggest that Sertoli cells decrease with age [8, 24] and only recently has it been suggested that they undergo apoptosis during adulthood [25].

Evidence that the Sertoli cell is not quiescent, as it was previously thought to be in the adult state, implies the need to generate histochemical techniques that permit Sertoli cells both in proliferation and apoptosis to be identified in histological sections. Such techniques will throw light on the balance of both phenomena that are essential for determining the final population of these cells that are important for maintaining the function of the seminiferous epithelium. In this chapter, we explain two techniques that combine an immunohistochemistry for vimentin, a Sertoli cell specific

marker [26], with the classic histochemical TUNEL technique for the identification of cells in apoptosis or the immunohistochemistry for PCNA for the identification of proliferating cells. The observations described were made by both conventional and confocal fluorescence microscopy.

2 Materials

1. Methacarn fixative: chloroform, methanol, and acetic acid in a 6:3:1 ratio.
2. Graded series of ethanol (100°, 90°, 70°).
3. O-xylene for dewaxing sections of TUNEL and xylene for vimentin and PCNA immunofluorescence.
4. Poly-L-lysine-coated glass slides: dilute poly-L-lysine solution 1:10 with deionized water prior to coating slides, and store at room temperature prior to use or in a refrigerator for 2–3 months. Place clean slides in diluted working poly-L-lysine solution for 5 min. Drain slides and dry in oven for 1 h at 60 °C or overnight at room temperature (18–26 °C).
5. Coplin Jars.
6. Humidity chambers (*see* **Note 1)** for the incubation of samples.
7. DNase-Free H_2O for the preparation of all solutions (*see* **Note 2**).
8. Phosphate buffered saline (PBS) made using DNase-free H_2O. In our lab, we prepare the PBS at a concentration of 10× and, when necessary, dilute it to a concentration of 1×. For 1 L of 10× PBS, add 87 g of NaCl, 2.72 g of KH_2PO_4, and 11.36 g of Na_2PO_4 (or 26.9 g of $NaHPO_4 \times 12H_2O$) to 1 L H_2O distillate or 1 L DNase-free H_2O. When everything is completely dissolved, adjust the pH to 7.4 (*see* **Note 3**).
9. PBS-glycine at 0.02 M (*see* **Note 4**).
10. Primary antibodies: monoclonal mouse anti-vimentin clone V9 and PCNA (c-20) goat-polyclonal IgG.
11. Secondary antibodies: Alexa Fluor 488 rabbit anti-mouse IgG and rabbit anti-goat IgG biotin.
12. Alexa Fluor 555-conjugate streptavidin.
13. PBS with 0.1% of bovine serum albumin (*see* **Note 5**).
14. Cardio TACS in situ apoptosis detection kit. The kit contains all the reagents and buffers for detecting apoptotic cells by TUNEL. The kit provides the Cytonin to permeabilize membranes.
15. 1.5 mL microtubes.
16. Fluorescent Mounting Medium.

3 Methods

For this study, testicular samples of Syrian hamster (*Mesocricetus auratus*) that had been exposed to a short photoperiod of 8:16 LD for 21 weeks were used. During this period, the animals were kept at the animal facility of the University of Murcia at a constant temperature of 21 ± 1 °C and with food and water provided ad libitum. The animals were killed by CO_2 overdose in a closed chamber. Then, the testes were fixed in methacarn for 8 h (*see* **Note 6**). Once the samples were properly fixed, they were embedded in paraffin using an automatic tissue processor (*see* **Note 7**) before preparing paraffin blocks for slicing (5 μ thickness) using a microtome (*see* **Note 8**). Tissue sections were placed on slides (*see* **Note 9**) for later use in the various histochemical techniques described in this chapter.

As a general rule, all steps should be performed at room temperature unless otherwise specified.

3.1 Vimentin Immunofluorescence Technique

1. Deparaffinize the slides in xylene, 3 × 5 min.
2. Rehydrate with ethanol of decreasing gradation (100°, 90°, 70°), 3 × 5 min each.
3. Wash in distilled water, 2 × 2 min.
4. Wash in PBS (1×), 1 × 5 min.
5. Block the samples in PBS-glycine for 10–30 min (*see* **Note 10**).
6. Wash in PBS (1×), 1 × 5 min.
7. Incubate with Cytonin: put a drop (50 μL) of Cytonin per section for 30–60 min in a humidity chamber (*see* **Note 11**).
8. Wash in PBS (1×), 1 × 5 min.
9. Incubate with primary antibody mouse monoclonal anti-vimentin IgG_1 in PBS/BSA 0.1% (dilution 1/50) in humidity chamber at 4 °C overnight (*see* **Note 12).**
10. Wash in PBS (1×), 3 × 5.
11. Incubate the samples with secondary antibody Alexa Fluor 488 rabbit anti-mouse in PBS/BSA 0.1% (dilution 1/200) in humidity chamber for 45 min (*see* **Note 13**).
12. Wash in PBS (1×), 3 × 5 min.
13. Mount with Fluorescent Mounting Medium and keep in darkness (*see* **Note 14**).

3.2 TUNEL Histochemical Technique

It is very important to use DNase-free H_2O with this technique for both the buffers and whenever the use of water is specified and o-xylene for deparaffinizing the sections.

As a general rule, all steps should be performed at room temperature unless otherwise specified. The general protocol for TUNEL technique is described below:

1. Deparaffinize the slides with o-xylene, 3 × 5 min (*see* **Note 15**).
2. Rehydrate with ethanol of decreasing gradation (100°, 90°, 70°), 3 × 5 min each.
3. Wash in DNase-free H_2O, 2 × 2min.
4. Wash in PBS (1×) 1 × 5 min.
5. Incubate with PBS-glycine 0.02 M, 10–30 min (*see* **Note 10**).
6. Incubate with Cytonin: put a drop of 50 μL of Cytonin per section in a humidity chamber for 30–60 min (*see* **Note 11**).
7. In a Coplin jar, wash the slides in DNase-free H_2O, 1 × 2 min.
8. In a Coplin jar, incubate the slides with 1× TdT labelling buffer for 5 min (*see* **Note 16**).
9. Prepare in a 1.5 mL microtube the labelling reaction mix containing 1 μL of TdT dNTP Mix**,** 1 μL of 50 × Mn^{+2}, 50 μL 1×TdT labelling buffer (*see* **step 8**), and 1 μL of TdT enzyme (taken directly from the freezer) per sample (*see* **Note 17)**.
10. Put a drop (50 μL) of the labelling reaction mix on each section, and incubate in a humidity chamber for 1 h at 37 °C.
11. In a Coplin jar, dip the slides for 5 min in the stop solution (5 mL TdT Stop Buffer +45 mL DNase-free H_2O).
12. Wash in PBS (1×), 2 × 5 min.
13. Incubate with Alexa Fluor 555-conjugated streptavidin in PBS/BSA 0.1% (dilution 1/600) in humidity chamber for 20 min (*see* **Note 13**).
14. Wash in PBS (1×), 2 × 5 min.
15. Mount with Fluorescent Mounting Medium and keep in darkness (*see* **Note 14**).

3.3 TUNEL-Vimentin Fluorescence Technique

As in the TUNEL technique, it is necessary for the reagents to be diluted using DNase-free H_2O, and sections must be deparaffinized with o-xylene. These specifications do not affect the vimentin immunofluorescence technique. As a general rule, all steps should be performed at room temperature unless otherwise specified.

1. Deparaffinize the slides in o-xylene, 3 × 5 min (*see* **Note 15**).
2. Rehydrate with ethanol of decreasing gradation (100°, 90°, 70°), 3 × 5 min each.
3. Wash in DNase-free water, 2 × 2 min.
4. Wash in PBS (1×), 1 × 5 min.
5. Block the samples in PBS-glycine for 10–30 min (*see* **Note 10**).

6. Wash in PBS (1×), 1 × 5 min.
7. Incubate with Cytonin: put one drop (50 μL) of Cytonin per section, and place in a humidity chamber for 30–60 min (*see* **Note 11**).
8. Wash in PBS (1×), 1 × 5 min.
9. Incubate with primary antibody mouse monoclonal anti-vimentin IgG_1 in PBS/BSA 0.1% (dilution 1/50) in humidity chamber at 4 °C overnight (*see* **Note 12)**.
10. Wash in PBS (1×), 3 × 5.
11. Incubate the slides in a Coplin jar with 1× TdT labelling buffer for 5 min (*see* **Note 16**).
12. In a 1.5 mL microtube, prepare the labelling reaction mix containing 1 μL of TdT dNTP Mix**,** 1 μL of 50 × Mn^{+2}, 50 μL of 1× TdT labelling buffer (*see* **step 8**), and 1 μL of TdT enzyme (taken directly from the freezer) per sample (*see* **Note 17)**.
13. Put a drop (50 μL) of the labelling reaction mix on each section, and incubate in a humidity chamber for 1 h at 37 °C.
14. In a Coplin jar, dip the slides for 5 min in the stop solution (5 mL TdT Stop Buffer +45 mL DNase-free H_2O).
15. Wash in PBS (1×), 3 × 5.
16. Incubate the samples with secondary antibody Alexa Fluor 488 rabbit anti-mouse in PBS/BSA 0.1% (dilution 1/200) in a humidity chamber for 45 min (*see* **Note 13**).
17. Wash in PBS (1×), 3 × 5.
18. Incubate with Alexa Fluor 555-conjugated streptavidin in PBS/BSA 0.1% (dilution 1/600) in a humidity chamber for 20 min (*see* **Note 13**).
19. Wash in PBS (1×), 3 × 5.
20. Mount with Fluorescent Mounting Medium and keep in darkness (*see* **Note 14**).

3.4 Vimentin-PCNA Immunofluorescence Technique

Follow **steps 1–12**, as described in Subheading 3.1. The PCNA steps continue as below (*see* **Note 18**):

1. Incubate with primary antibody PCNA goat-polyclonal IgG in PBS/BSA 0.1% (dilution 1/50) in humidity chamber at 4 °C overnight.
2. Wash in PBS (1×), 3 × 5.
3. Incubate the samples with the secondary antibody rabbit anti-goat biotinylated in PBS/BSA 0.1% (dilution 1/200) in a humidity chamber for 45 min.
4. Wash in PBS (1×), 3 × 5 min.

5. Incubate the samples with Alexa Fluor 555-conjugated streptavidin in PBS/BSA 0.1% (dilution 1/600) in a humidity chamber for 20 min (*see* **Note 13**).
6. Wash in PBS (1×), 3 × 5 min.
7. Mount with Fluorescent Mounting Medium and keep in darkness (*see* **Note 14**).

3.5 Observation of TUNEL+/Vimentin+ and Vimentin+/PCNA + Sertoli Cells

The techniques described above enabled the observation and reliable identification of Sertoli cells in two very important cell states, although neither has been much studied under normal physiological conditions in adult individuals: cell death by apoptosis and proliferation. Using dark-field microscopy, it is easy to differentiate Sertoli cells from germ cells through their positivity to vimentin (green) (Fig. 1a, d). In addition, simply by changing the excitation filter of the light source, it is possible to identify the cells that are TUNEL + or PCNA + (red) (Fig. 1b, e). Although fluorescence microscopy gives very reliable results, it has the disadvantage that it is necessary to take photographs with each of the filters individually and then to superpose both photos by means of image processing software (Fig. 1a–c). In contrast, confocal microscopy allows images to be obtained with each channel individually (Fig. 1d, e) and with both channels (green and red) at the same time (Fig. 1f), which facilitates identification of the Sertoli cells (green) that are TUNEL + or PCNA + (red). Thus, we can conclude that although the final results are very similar and both types of microscope can be used interchangeably, the versatility offered by the confocal microscope makes it the most suitable choice for both qualitative and quantitative studies.

The techniques described above enabled Sertoli cells to be observed and reliably identified in two important cell stages (death by apoptosis and proliferation), which have been little studied in normal adult individuals. Using dark-field microscopy, it was easy to differentiate the Sertoli cells based on their positivity toward vimentin (green) (Fig. 1a, d). Moreover, by simply changing the filter light source, it was possible to localize cells that were TUNEL+ or PCNA+ (red) (Fig. 1b, e). Although fluorescence microscopy also provides reliable results, it has the disadvantage that photographs must be taken with each of the filters individually before they are superimposed by means of an image treatment software (Fig. 1a–c). By contrast, confocal microscopy enables images to be obtained individually (Fig. 1d, e) and images with both channels (green and red) simultaneously (Fig. 1f), facilitating the identification of Sertoli (green) cells that are also TUNEL+ or PCNA+. While the final results obtained by both techniques are very similar and bot microscopes can be used indistinctively, the versatility of confocal microscopy makes it the most useful for both qualitative and quantitative studies.

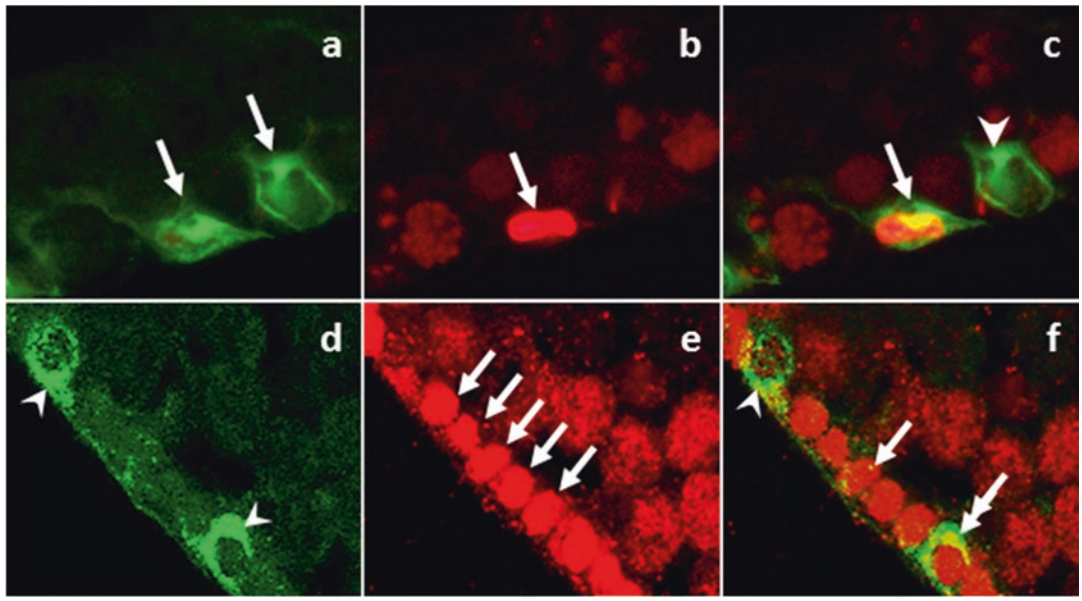

Fig. 1 (**a**–**c**) Fluorescence microscopy for the detection of Sertoli cells. (**a**) Vimentin immunofluorescence technique (green), where two vimentin + cells (arrows) can be observed, corresponding to Sertoli cells. (**b**) Histochemistry of TUNEL, where a TUNEL + cell can be observed (arrow). (**c**) By merging both images, it is observed that the TUNEL+ cell is also vimentin + (arrow), corresponding to a Sertoli cell in apoptosis. A Sertoli cell vimentin+/TUNEL- (arrowhead) can also be observed. (**d**–**f**) Confocal microscopy for the detection of Sertoli cells. (**d**) Vimentin immunofluorescence technique (green), showing vimentin + cells (arrowheads). (**e**) Immunofluorescence of PCNA antigen (red). Several PCNA positive cells are observed, but it cannot be determined whether they are spermatogonia or Sertoli cells (arrows). (**f**) Superposing the green and red channels allows vimentin+/PCNA+ cells corresponding to proliferating Sertoli cell to be identified (double arrow), compared with a vimentin−/PCNA+ cell corresponding to a spermatogonia (arrow) and a vimentin+/PCNA- cell corresponding to a nonproliferative Sertoli cell (arrowhead)

4 Notes

1. The humidity chambers can be made using Petri dishes. Place paper on the dish bottom and two glass rods to prevent the slides from directly touching the paper. Before use, wet the paper with water and remove the excess.
2. The DNase-free H_2O can be purchased commercially, or ultrapure water can be used. In our lab, we use distilled water boiled for 30 min. When cooled to room temperature, it can be used as solvent for buffers and reagents.
3. Phosphates (KH_2PO_4, Na_2PO_4. $NaHPO_4 \times 12H_2O$) must be added slowly to prevent them from precipitating. If precipitation occurs, it makes their dissolution more difficult.
4. It is advisable to prepare a large volume (for example 100 mL) and divide into microtubes of 1.5 mL. Freeze the aliquots at −20 °C and thaw when needed.

5. As in **Note 4**, 0.1% PBS/BSA can be frozen in aliquots of 1.5 mL at −20 °C and thawed when needed.
6. After about 30 min, cut the testis into two or three pieces to allow proper fixation of the central portion. If sample processing is not continued, change the fixative solution for PBS buffer in order to prevent overfixation.
7. The times of paraffin embedding may vary with the model of tissue processor. We recommend a minimum time of 15 h to ensure proper inclusion.
8. If the tissue used is testis, the sections should not be more than 5 μ thick to prevent overlapping of cell nuclei and elements that could be positive in the techniques used but belonging to cells that are at different depths.
9. The slides must be previously dipped in poly-L-lysine to prevent the tissue section from coming off the slide when the histochemical techniques are being carried out. Moreover, once the tissue sections have been placed on the slides, it is strongly recommended to wait at least 24 h for correct fixing to the slide.
10. For a total volume of 100 mL of PBS, and considering the molecular weight of glycine, take 0.15 g of glycine and dilute in 100 mL of PBS to obtain a final concentration of 0.02 M.
11. Permeabilization can be also carried out using PBS-saponin 0.1% for 10–30 min at room temperature.
12. Both the dilution and the time of incubation are adjusted to our samples, but these parameters may change depending of the fixation method or the tissue used. Samples can be incubated for 2 h at room temperature giving similar results.
13. When the fluorescent antibody is used, all the steps must be carried out using the lowest ambient light possible. In our lab, all the material used (Coplin jars, humidity chambers and microtubes) are covered by foil to protect the samples and the antibody against the light.
14. Check that there are no air bubbles in the tissue. If there are any, press the tissue next to the bubble gently with the end of tweezers. Never move the cover slip because you can tear the tissue.
15. Dewaxing is also possible in o-xylene (15 min in a Coplin jar). The o-xylene can be reused several times (five to eight times) according to how many slides have been dewaxed.
16. Prepare 45 mL DNase-free H_2O + 5 mL 10× TdT labelling buffer. Important! Take 50 μL per sample for the next step. For example, if you have ten samples, use a microtube to take 500 μL of 1× TdT labelling buffer for **step 8**.

17. Both the TdT dNTP Mix and 50× Mn^{+2} are frozen, so remove from freezer a few minutes before use.
18. Because the first part (vimentin technique) has the fluorescent secondary antibody built-in, the part corresponding to PCNA should be made with the lowest possible ambient light, and the material used should be protected from light (as described in **Note 13**).

Acknowledgment

This work was supported by GERM 19892/15 from Fundación Seneca CARM.

References

1. Sharpe RM, McKinnell C, Kivlin C, Fisher JS (2003) Proliferation and functional maturation of Sertoli cells, and their relevance to disorders of testis function in adulthood. Reproduction 125:769–784
2. Ebner V (1888) Zur Spermatogenese bei den Säugethieren. Arch Mikr Anat 31:236–291. Cited by França LR, Hess RA, Dufour JM, Hofmann MC, Griswold MD (2016). The Sertoli cell: one hundred fifty years of beauty and plasticity. Andrology 4:189–212
3. França LR, Hess RA, Dufour JM, Hofmann MC, Griswold MD (2016) The Sertoli cell: one hundred fifty years of beauty and plasticity. Andrology 4:189–212
4. Plant TM, Marshall GR (2001) The functional significance of FSH in spermatogenesis and the control of its secretion in male primates. Endocr Rev 22:764–786
5. Kluin PM, Kramer MF, de Rooij DG (1984) Proliferation of spermatogonia and Sertoli cells in maturing mice. Anat Embryol (Berl) 169:73–78
6. Tarulli GA, Stanton PG, Lerchl A, Meachem SJ (2006) Adult Sertoli cells are not terminally differentiated in the Djungarian hamster: effect of FSH on proliferation and junction protein organization. Biol Reprod 74:798–806
7. Sharpe RM, Turner KJ, McKinnell C, Groome NP, Atanassova NN, Millar MR et al (1999) Inhibin-B levels in plasma of the male rat from birth to adulthood: effect of experimental manipulation of Sertoli cell number. J Androl 20:94–101
8. Johnson L, Zane RS, Petty CS, Neaves WB (1984) Quantification of the human Sertoli cell population: its distribution, relation to germ cell numbers and age-related decline. Biol Reprod 3:785–795
9. McClusky LM (2005) Stage and season effects on cell cycle and apoptotic activities of germ cells and Sertoli cells during spermatogenesis in the spiny dogfish (*Squalus acanthias*). Reproduction 129:89–102
10. Anderson RA, Sharpe RM (2000) Regulation of inhibin secretion in the human male and its clinical applications. Int J Androl 23:136–144
11. Maymon BB-S, Paz G, Elliott DJ, Hammel I, Kleiman SE, Yogev L et al (2000) Maturation phenotype of Sertoli cells in testicular biopsies of azoospermic men. Hum Reprod 15:1537–1542
12. Sharpe RM, McKinnell C, Kivlin C, Fisher JS (1987) Proliferation and functional maturation of Sertoli cells, and their relevance to disorders of testis function in adulthood. Reproduction 125:769–784
13. Bergmann M (1987) Photoperiod and testicular function in Phodopus Sungorus. Adv Anat Embryol Cell Biol 105:1–76
14. Hayrabedyan S, Todorova K, Pashova S, Mollova M, Fernández N (2012) Sertoli cell quiescence - new insights. Am J Reprod Immunol 68:451–455
15. Chaudhary J, Sadler-Riggleman I, Ague JM, Skinner MK (2005) The helix-loop-helix inhibitor of differentiation (ID) proteins induce post-mitotic terminally differentiated Sertoli cells to re-enter the cell cycle and proliferate. Biol Reprod 72:1205–1217
16. Ahmed EA, Barten-van Rijbroek AD, Kal HB, Sadri-Ardekani H, Mizrak SC, van Pelt AM et al

(2009) Proliferative activity in vitro and DNA repair indicate that adult mouse and human Sertoli cells are not terminally differentiated, quiescent cells. Biol Reprod 80:1084–1091

17. Chui K, Trivedi A, Cheng CY, Cherbavaz DB, Dazin PF, Huynh ALT et al (2011) Characterization and functionality of proliferative human Sertoli cells. Cell Transplant 20:619–635
18. Sasso-Cerri E, Miraglia SM (2002) In situ demonstration of both TUNEL-labeled germ cell and Sertoli cell in the cimetidine-treated rats. Histol Histopathol 17:411–417
19. Berensztein EB, Sciara MI, Rivarola MA, Belgorosky A (2002) Apoptosis and proliferation of human testicular somatic and germ cells during Prepuberty: high rate of testicular growth in newborns mediated by decreased apoptosis. J Clin Endocrinol Metab 87:5113–5118
20. Seco-Rovira V, Beltrán-Frutos E, Ferrer C, Sáez FJ, Madrid JF, Pastor LM (2014) The death of Sertoli cells and the capacity to phagocytize elongated spermatids during testicular regression due to short photoperiod in Syrian hamster (*Mesocricetus auratus*). Biol Reprod 90:1–10
21. Yagi M, Suzuki K, Suzuki H (2006) Apoptotic Sertoli cell death in hypogonadic (hgn/hgn) rat testes during early postnatal development. Asian J Androl 8:535–541
22. Gong Y, Wu J, Huang Y, Shen S, Han X (2009) Nonylphenol induces apoptosis in rat testicular Sertoli cells via endoplasmic reticulum stress. Toxicol Lett 186:84–95
23. Sasso-Cerri E, Cerri PS (2008) Morphological evidences indicate that the interference of cimetidine on the peritubular components is responsible for detachment and apoptosis of Sertoli cells. Reprod Biol Endocrinol 6:18
24. Petersen PM, Seierøe K, Pakkenberg B (2015) The total number of Leydig and Sertoli cells in the testes of men across various age groups - a stereological study. J Anat 226:175–179
25. Martinez-Hernandez J, Seco-Rovira V, Beltran-Frutos E, Ferrer C, Quesada-Cubo V, Pastor LM (2016) Apoptosis of Sertoli cells in the Syrian hamster (*Mesocricetus auratus*) during testicular recrudescence after exposure a short photoperiod. Reprod Domest Anim 51(S2):114–115
26. Aumüller G, Steinbrück M, Krause W, Wagner HJ (1988) Distribution of vimentin-type intermediate filaments in Sertoli cells of the human testis, normal and pathologic. Anat Embryol (Berl) 178:129–136

Chapter 6

Sertoli Cell Preparation for Co-immunoprecipitation

Maria João Freitas and Margarida Fardilha

Abstract

Most techniques to study protein-protein interactions, gene expression or signal transduction, among others, in Sertoli cells, depend on obtaining a protein extract of such cells. This is accomplished by lysing the Sertoli cells and solubilizing the intracellular proteins. Depending on the purpose of your study, the technique used to lyse and consequently obtain protein extracts from Sertoli cells must be considered. In this chapter, we will focus on how to obtain a protein Sertoli cell extract suitable for co-immunoprecipitation technique.

Key words Lysis buffer, Protein quantification, Co-immunoprecipitation, Sertoli cells, Western blot

1 Introduction

Most interactomic and proteomic studies rely on obtaining an enriched protein sample from Sertoli cells. To achieve that, it is necessary to disrupt the plasma membrane and solubilize the proteins. Moreover, if the goal of the researcher is to obtain proteomic or protein-protein interaction information of a specific organelle (e.g., nucleus, mitochondria, etc.), a specific lysis buffer must be used which extracts only the proteins within the organelle or at least an enriched fraction.

Most cell lysis buffers rely on detergents to solubilize the plasma membrane and release the protein content within the cell. Depending on the nature of the detergent, percentage of the detergent, and conjugation with other disruption methods (such as sonication), the strength of cell lysis can be controlled. Therefore, according to the goal of the experiment, the researcher can choose the most suitable lysis buffer. Besides solubilizing the plasma membrane, some lysis buffers disturb cellular components, such as the cytoskeleton, releasing associated proteins. It is noteworthy to mention that, for methodologies that require maintenance of protein-protein interactions, a non-denaturing lysis buffer must be used (*see* **Note 1**). Also, we suggest the researcher to add protease

Marco G. Alves and Pedro F. Oliveira (eds.), *Sertoli Cells: Methods and Protocols*, Methods in Molecular Biology, vol. 1748, https://doi.org/10.1007/978-1-4939-7698-0_6,

inhibitors while performing cell lysis. This prevents general proteolysis (*see* **Note 2**).

After cell lysis, some proteomic and interactomic methods require quantification of the protein extracted. Choosing a method for protein quantification depends on compatibility of the substances present in the protein sample with the method, amount of protein available, detection limit of the method, simplicity, and time required for the method. Although the options for protein quantification are vast, from colorimetric, UV analysis, and amino acid analysis to densitometry and mass spectrometry, we believe that there are two methods that stand out. Colorimetric and UV analysis are inexpensive and easy to execute [1]. Therefore, we recommend colorimetric, specifically the Smith bicinchoninic acid (BCA) method and UV absorbance at 280 nm.

In the BCA method, copper interacts with four nitrogen atoms present in peptides. These forms the cuprous complexes, which in turns reacts with bicinchoninic acid, forming a deep purple color (which is read at 562 nm). The major advantage of the BCA method is the detection range (0.2–50 μg) and its compatibility with several detergents [2]. On the other hand, the absorbance at 280 nm method relies on the fact that amino acid residues with aromatic rings (tryptophan and tyrosine) absorb light. The absorbance of light is proportional to the concentration of tryptophan and tyrosine residues and therefore the quantity of protein. The range of detection of this method is 20–3000 μg. Note that if there is a nucleic acid contamination, the absorbance at 280 nm can be altered [3] (*see* **Note 3**).

2 Materials

2.1 Sertoli Cell Lysis

1. Lysis buffer. Please choose the lysis buffer according the future application (*see* **Notes 1** and **2**).
2. Ice.
3. Sertoli cells (either cultured or isolated).
4. Centrifuge (must reach 16,000 × *g* and refrigerate).
5. Ice-cold PBS1× (137 mM NaCl; 2.7 mM KCl; 10 mM Na_2HPO_4; 1.8 mM KH_2PO_4).

2.2 Ultraviolet Absorption at 280 nm Method

1. Spectrophotometer absorbing at UV.
2. Quartz cuvettes. Nowadays plastic cuvettes are available that do not absorb at 280 nm, so they can be used.
3. Blank solution: solution of the buffer and all components except the protein.

2.3 BCA Method

1. Microplate (96-well plate).
2. Bovine serum albumin (BSA) solution (typically 2 mg/mL).
3. Spectrophotometer absorbing in the visible range.
4. BCA reagent A: 1 g sodium bicinchonivate, 2 g Na_2CO_3, 0.16 g sodium tartrate, 0.4 g NaOH, and 0.95 g $NaHCO_3$, made up to 100 mL. Adjust the pH to 11.25. Store at room temperature indefinitely.
5. BCA reagent B: 0.4 g $CuSO_4$. Made up to 10 mL. Store at room temperature indefinitely.
6. BCA Working solution: 50 parts of reagent A and 1 parts of reagent B. The solution is green and stable for a week at room temperature.

3 Methods

Carry all experiments at room temperature in the laboratory bench unless otherwise specified.

3.1 Sertoli Cell Lysis

1. 15 min before starting the experiment, prepare the lysis buffer (*see* **Notes 1** and **2**). Keep the lysis buffer one ice.
2. Resuspend the Sertoli cells gently in ice-cold PBS1× (500 µL–1 mL).
3. Centrifuge the Sertoli cells 5 min at 400 × *g*, 4 °C. Aspirate the supernatant.
4. Repeat **steps 2** and **3**, two more times.
5. Resuspend gently the Sertoli cells in ice-cold lysis buffer (*see* **Notes 4** and **5**).
6. Incubate on ice for 30–60 min. Tap the tube every 10 min.
7. Centrifuge the Sertoli cell extract at 16,000 × *g*, 15 min, 4 °C.
8. Recover the supernatant (typically called soluble fraction). The supernatant is rich in proteins.
9. To the pellet add 1% SDS (we suggest the same amount of lysis buffer used).
10. Incubate on ice 10–20 min. Tap the tube once in a while.
11. Centrifuge at 16,000 × *g*, 15 min, 4 °C.
12. Recover the supernatant and storage it at −20 °C (*insoluble fraction*).
13. Depending on the application, the soluble fraction can be frozen at −20 °C or −80 °C or used immediately.
    - *Western blot*: freeze at −20 °C for short periods of time or at −80 °C for longer storage.

- *Immunoprecipitation*: depending on what the researcher wants to evaluate, the sample can be frozen (−80 °C) or used immediately. If proteins must be kept active, do not freeze.
- *Co-IP*: Use immediately or if not possible keep on ice for no more than 1 h.

3.2 Protein Quantification: Ultraviolet Absorption at 280 nm

1. Turn on the spectrophotometer and set to read at 280 nm. Allow the instrument to equilibrate for 15 min.
2. Place the blank solution into the cuvette and take a reading. Alternatively, blank the instrument using the blank solution.
3. Place the protein solution in the cuvette and take a reading. Repeat this step one more time to obtain duplicate readings. Also, if the absorbance value is greater than 2, dilute the protein (we suggest 1:10) (*see* **Note 6**).

3.3 Protein Quantification: BCA (See Note 7)

1. Prepare 25 μL of the standards with bovine serum albumin (BSA) and your samples in duplicate.
   - There must be at least four standards with BSA quantities between ranging from 0 to 50 μg.
   - Your samples may need to be diluted. If so, dilute them in the buffer they are in. Depending if your protein sample came from cultures or isolated Sertoli cells, dilution must vary. We suggest a 1:5 dilution.
2. Pipete the protein samples and the standards into a microplate. Do not forget to register the location of each sample and standard.
3. Add 200 μL of working BCA solution to each well.
4. Incubate at 37 °C for 30 min (preferentially with the lid, to minimize sample evaporation).
5. Turn on the spectrophotometer and set to read at 562 nm. Allow the instrument to equilibrate for 15 min.
6. After 30 min, let the samples stand for 5 min at room temperature. Measure the absorbance at 562 nm of all samples and standards (preferentially at the same time). Register the absorbance values. Using the absorbance values of the BSA standards, it is possible to determine the protein concentration of your samples.

In Table 1 is listed the BCA results of protein concentration obtained when approximately 80×10^6 Sertoli cells (human primary culture) were lysed in 70 μL of different lysis buffers (*see* **Note 6**).

As is shown in Table 1, the lysis with LB1 is very mild, and almost no protein was recovered. This was expected, since only

Table 1

Protein concentration obtained with different lysis buffers from human Sertoli cells

Lysis buffer	Sertoli cells protein extract concentration (μg/μL)
Lysis buffer 1	0.059
Lysis buffer 2	0.48
Lysis buffer 3	0.56
Lysis buffer 4	0.45
Lysis buffer 5	3.79

Sertoli cells were lysed in 70 μL of diferent lysis buffers. Lysis buffer 1 (LB1): 20 mM Tris–HCl, pH 7.5, 1 mM EDTA. Lysis buffer 2 (LB2): 50 mM Tris–HCl, pH 7.5, 150 mM NaCl, 1% NP-40%. Lysis buffer 3 (LB3): RIPA 1× (50 mM Tris–HCl, pH 7.4, 150 mM NaCl, 1 mM EDTA, 0.25% deoxycholic acid, 1% NP-40% (ref: 20–188, Merck Millipore). Lysis buffer 4 (LB4): 10 mM Tris–HCl, pH 7.5, 100 mM NaCl, 1 mM EDTA, 1% Triton X-100, 0.1% SDS, 10% glycerol. Lysis buffer 5: 1% SDS

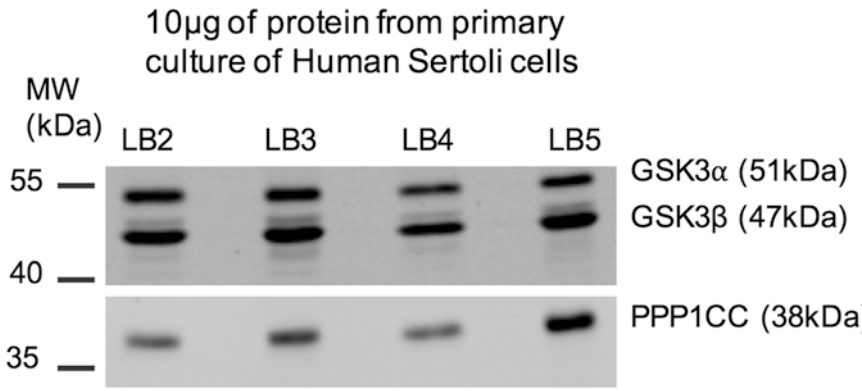

Fig. 1 Solubilization of GSK3 and PPP1CC in Sertoli cells. Human Sertoli cells (primary culture) were lysed in the lysis buffers listed in Table 1, and 10 μg of protein was resolved in a SDS-PAGE and immunoblotted with anti-GSK3α/β antibody and anti-PPP1CC

soluble proteins present in the cytoplasm are recovered with the Tris–HCl lysis buffer. On the other hand, LB5 (1% SDS) was the most efficient lysis buffer. To evaluate the solubilization of specific proteins with each lysis buffer, 10 μg of total protein was resolved by SDS-PAGE, and phosphoprotein phosphatase 1 gamma catalytic subunit (PPP1CC) and glycogen synthase kinase 3 (GSK3) protein were detected by immunoblotting (Western blot). Due to the very low protein concentration obtained with the Tris–HCl lysis buffer, further Western blot analysis was not possible.

Figure 1 illustrates the recovery of PPP1CC and GSK3 isoform alpha and isoform beta of primary culture of human Sertoli

cells using the different lysis buffers listed in Table 3. After, densitometry studies were performed (Quantity One Software, BioRad). For PPP1CC, LB5 solubilizes between 30 and 50% more protein than the other lysis buffers suggesting that part of PPP1CC may be associated with cytoskeletal structures and requires a strong lysis buffer to be solubilized. Nevertheless, all other lysis buffers also solubilize PPP1CC, specially LB3, suggesting that PPP1CC is distributed throughout the entire cell. Regarding GSK3α, LB5 is not the most efficient lysis buffer. LB3 solubilizes 30% more GSK3α than LB5. The fact that LB5 is a strong lysis buffer results in solubilization of a wide range of protein. Consequently in 10 μg more proteins are represented, which may result in underrepresentation of GSK3α. Particularly for GSK3β, all lysis buffers perform similarly (only 20% of protein recover difference between lysis buffer). The results show the performance of different lysis buffers in Sertoli cells, and depending on the protein of interest, the most suitable lysis buffer can vary. Besides, this type of experiment is crucial to determine the best suitable lysis buffer for applications such as Co-IP.

4 Notes

1. The most commonly used detergents as well as the group of proteins they solubilize are shown in Table 2 (adapted from [4–6]).
2. We strongly suggest the researcher to add protease inhibitors to any lysis reagent used. The most common protease inhibitors used are shown in Table 3 (adapted from [7, 8]).
3. There are several reagents/substances described that interfere with measuring proteins concertation when using BCA or absorbance at 280 nm. Therefore, the researcher must choose the method which better suits your situation. The reagents and substances are shown in Table 4 (adapted from [8]).
4. The amount of lysis buffer can vary. The researcher can choose one of two options: either add a fixed amount of lysis buffer per million of cells or previously test a range of lysis buffers. For immunoprecipitation, 1–2 × 10^7 cells require around 1 mL of lysis. If the researcher chooses to determine the protein concentration, for example, for Co-IP in Sertoli cells, 600–800 μg of total protein usually gives good results [9–11]. So, the researcher must add a range of lysis buffers and determine which volume gives a suitable protein concentration for Co-IP.
5. Other disruption methods can be added. Typically, if a harsh lysis is required, mechanical/physical methods, such as sonication,

Table 2
Lysis buffers

Lysis reagents	Type of proteins solubilized	How proteins are solubilized
20–50 mM Tris–HCl, pH 7.4	Cytoplasmic soluble proteins	The high ionic strength leads to cell implosion. Do not denature proteins or break protein-protein interactions
0.5–2% NP-40	Cytoplasmic soluble proteins. Membrane-bound proteins. At higher percentage, can lyse nuclear membrane	Nonionic detergent. Breaks protein-lipid and lipid associations (membrane). Do not denature proteins or break protein-protein interactions at lower concentrations. If >1%, protein-protein interactions can be compromised
Triton X-100	Cytoplasmic protein bound to cytoskeletal structures. At higher percentage, can lyse nuclear membrane	Nonionic detergent. Break protein-lipid and lipid associations (membrane). Do not denature proteins or break protein-protein interactions at lower concentrations. If >1% protein-protein interactions can be compromised
Digitonin or n-dodecyl-β-D-maltoside (DDM)	Cytoplasmic and plasma membrane proteins	Nonionic detergent. Selectively permeabilizes the plasma membrane leaving the nuclear and mitochondrial membranes intact [13]
CHAPS	Cytoplasmic proteins, cytoskeletal-bound proteins, and membrane proteins	Zwitterionic detergent (neutral detergent). Harsher than nonionic detergents and can destroy some protein-protein interactions. Most suitable for protein solubilization for 2D-PAGE gels
Sodium deoxycholate	Cytoplasmic proteins, cytoskeletal-bound proteins, membrane proteins	Ionic detergent. Proteins are completely denatured and protein-protein interaction are lost (at concentrations higher than 0.25%)
0.1–1% SDS	Cytoplasmic proteins, cytoskeletal-bound proteins, membrane proteins, and cytoskeletal proteins (whole cell)	Ionic detergent. Normally used to solubilize all proteins and it's considered the harsher lysis buffer. Protein-protein interactions are lost
Lysis buffer	*Type of proteins solubilized*	*How proteins are solubilized*
RIPA (immunoprecipitation assay)	Cytoplasmic proteins, cytoskeletal-bound proteins, membrane proteins, and cytoskeletal proteins (whole cell). Particularly useful for nuclear extracts	25 mM Tris–HCl, 150 mM NaCl, 0.1% SDS, 0.5% sodium deoxycholate, 1% Triton X-100, or NP-40. The combination of SDS and sodium deoxycholate ensures that all proteins are solubilized

(continued)

Table 2
(continued)

Lysis reagents	Type of proteins solubilized	How proteins are solubilized
RIPA (Co-IP assay)	Cytoplasmic proteins, cytoskeletal-bound proteins, membrane proteins, and cytoskeletal proteins (whole cell)	50 mM Tris–HCl, 150 mM NaCl, 0.25% sodium deoxycholate, 1% NP-40 The low amount of sodium deoxycholate and the absence of SDS ensure that this RIPA can be used for most Co-IP experiments
What else to add		
Reagent	*Function*	
100 mM NaCl	The presence of NaCl in physiological concentrations helps dissolve the proteins	
10% glycerol	Increases protein solubility and stability	
Protease inhibitors	Prevents the degradation of the proteins by proteases. See Table 3	

The most commonly used detergents are listed, as well as the group of proteins they solubilize. Adapted from [4–6]

Table 3
Main protease inhibitors for each class

Inhibitor	Protease class[a]	Characteristics	Range of working concentrations	Typical stock solutions
Aprotinin	Serine	Inhibits plasmin, trypsin, chymotrypsin. Does not act on thrombin or factor X	1–100 μM	10 mM in water or aqueous buffers (e.g., 0.1 M Tris–HCl, pH 8.0) (6 months at −20 °C)
TPCK (tosyl phenylalanyl chloromethyl ketone)	Serine	Inhibits trypsin-like proteases	10–100 μM	10 mM in ethanol, stable at 4 °C
Benzamidine	Serine	Inhibits trypsin and trypsin-like enzymes	0.5–4.0 mM	50 mg/mL in water
Chymostatin	Cysteine	Specific inhibitor for α-,β-,γ-,δ-chymotrypsin. It also inhibits papain and lysosomal cysteines	10–100 μM	20 mg/mL in DMSO, stable at −20 °C for 1 month

(continued)

Table 3
(continued)

Inhibitor	Protease class[a]	Characteristics	Range of working concentrations	Typical stock solutions
Antipain	Serine, cysteine	Inhibits plasmin, thrombin, and trypsin as well as calpain and papain	10–100 μM	10 mM in water, stable for 1 month at −20 °C
Leupeptin	Serine, cysteine	Inhibits trypsin-like proteases and calpain and papain	10–100 μM	10 mM in water, stable 6 months at −20 °C
PMSF (α-toluenesulfonyl fluoride; phenylmethylsulfonyl fluoride)	Serine, cysteine	Broad spectrum of serine protease and some cysteine protease such as papain	0.1–10 mM	200 mM in isopropanol, prepare freshly
Pepstatin A	Aspartic	Inihibts pepsin, renin, cathepsin, and many microbial proteases	1 μM	1 mM in methanol or DMSO, stable −20 °C
EDTA	Metalloproteinase	Broad-spectrum metalloproteinase	1–10 mM	Soluble in water, prepare freshly
EGTA	Metalloproteinase	Specifically inhibits Ca^{2+}-dependent proteases	1 mM–10 mM	Soluble in water, prepare freshly
α_2-Macroglobulin	Serine, cysteine, aspartic, metalloproteinse	Broad-spectrum protease inhibitor	Equimolar	Soluble in water, stable at −20 °C

Please note that there are commercially options of combinations of protease inhibitors. Typically, these protease inhibitor cocktails present a protease inhibitor from each class. Adapted from [7, 8]
[a]Refers to the class of proteases that the inhibitor acts on

can be performed [12]. Note that most protein-protein interactions will be disrupted.

6. Currently, there are spectrophotometers that only require 1–2 μL of protein sample to obtain an accurate reading; therefore, the loss of sample is minimal. There is no need for cuvettes and the sample is loaded directly into the spectrophotometer.
7. The protocol presented is suitable for microplate (96-well plate). Also, there are several commercial available BCA kits.

Table 4
Substance compatibility for protein quantification methods

Substance	BCA	UV Abs_{280nm}
Detergents		
CHAPS	5%	10%
Sodium deoxycholate	5%	0.3%
Nonidet P-40	5%	Do not use
SDS	5%	0.1%
Triton X-100	5%	0.02%
Tween-20	5%	0.3%
Chelators		
EDTA[a]	10 mM	30 mM
Buffers		
PBS	Undiluted	Undiluted
Tris–HCl	250 mM	500 mM
Sodium chloride	1 M	>1 M
Solvents and others		
Urea	3 M	>1 M
PMSF	1 mM	No data
DTT	1 mM	3 mM

The maximum concentration of each substance in the BCA and UV Abs_{280nm}. Adapted from [8]

[a]Another frequently used chelator is EGTA. However, EGTA interferes with both BCA and UV Abs_{280nm} measurements. Therefore, we recommend the use of EDTA. Still if EGTA is necessary, use the Bradford method to determine protein concentration

Acknowledgments

This work was supported by FEDER funds through the "Programa Operacional Competitividade e Internacionalização (COMPETE 2020)" and by national funds through the FCT (Fundação para a Ciência e Tecnologia), Projects PTDB/BBB-BQB/3804/2014 and PTDC/DTP-DES/6077/2014. We are thankful to the Institute for Biomedicine (iBiMED) (UID/BIM/04501/2013) for supporting this project. iBiMED is supported by the Portuguese Foundation for Science and Technology (FCT), Compete2020, and FEDER fund. This work was also supported by an individual grant from FCT of the Portuguese Ministry of Science and Higher Education to M.J.F. (SFRH/BD/84876/2012).

References

1. Goldring JP (2012) Protein quantification methods to determine protein concentration prior to electrophoresis. Methods Mol Biol 869:29–35. https://doi.org/10.1007/978-1-61779-821-4_3
2. Smith PK, Krohn RI, Hermanson GT, Mallia AK, Gartner FH, Provenzano MD, Fujimoto EK, Goeke NM, Olson BJ, Klenk DC (1985) Measurement of protein using bicinchoninic acid. Anal Biochem 150(1):76–85
3. Fasman GD (1989) Practical handbook of biochemistry and molecular biology. CRC Press, Boca Raton, FL
4. EMBL (2017) Protein purification - extraction and clarification choice of lysis buffer and additives. https://www.embl.de/pepcore/pepcore_services/protein_purification/extraction_clarification/lysis_buffer_additives/. Accessed 5 Mar 2017
5. Linke D (2009) Detergents: an overview. Methods Enzymol 463:603–617. https://doi.org/10.1016/s0076-6879(09)63034-2
6. Paasch U, Heidenreich F, Pursche T, Kuhlisch E, Kettner K, Grunewald S, Kratzsch J, Dittmar G, Glander HJ, Hoflack B, Kriegel TM (2011) Identification of increased amounts of eppin protein complex components in sperm cells of diabetic and obese individuals by difference gel electrophoresis. Mol Cell Proteomics 10(8):M110 007187. https://doi.org/10.1074/mcp.M110.007187
7. Hooper NM (1990) Proteolytic enzymes: a practical approach Edited by R J Beynon and J S Bond. pp 259. IRL Press at Oxford University Press, Oxford. 1989. £29 (spiral bound)/£19 (paper) ISBN 0-19-963058-5/963059-3. Biochem Educ 18(1):1–60
8. Noble JE, Bailey MJ (2009) Quantitation of protein. Methods Enzymol 463:73–95. https://doi.org/10.1016/s0076-6879(09)63008-1
9. Gao Y, Lui WY, Lee WM, Cheng CY (2016) Polarity protein Crumbs homolog-3 (CRB3) regulates ectoplasmic specialization dynamics through its action on F-actin organization in Sertoli cells. Sci Rep 6:28589. https://doi.org/10.1038/srep28589
10. Xiao X, Cheng CY, Mruk DD (2012) Intercellular adhesion molecule-1 is a regulator of blood-testis barrier function. J Cell Sci 125(Pt 23):5677–5689. https://doi.org/10.1242/jcs.107987
11. Xiao X, Cheng CY, Mruk DD (2013) Intercellular adhesion molecule-2 is involved in apical ectoplasmic specialization dynamics during spermatogenesis in the rat. J Endocrinol 216(1):73–86. https://doi.org/10.1530/JOE-12-0434
12. Goldberg S (2015) Mechanical/physical methods of cell distribution and tissue homogenization. Methods Mol Biol 1295:1–20. https://doi.org/10.1007/978-1-4939-2550-6_1
13. Hiromi Tissera MK, Stochaj U (2010) Nuclear envelopes show cell-type specific sensitivity for the permeabilization with digitonin. Protocol Exchange. https://doi.org/10.1038/protex.2010.211

Chapter 7

Profiling Signaling Proteins in Sertoli Cells by Co-immunoprecipitation

Maria João Freitas and Margarida Fardilha

Abstract

Sertoli cells are crucial for germ cell support, create a suitable environment for spermatogenesis, and integrate information from the nervous system and germ cell line. To fully understand the role of Sertoli cells, it is necessary to characterize the protein-protein interactions. Identifying the interactome of a given protein may provide leads about the role and molecular mechanism of such protein in Sertoli cells. One of the techniques to characterize protein interactomes consists of co-immunoprecipitation followed by mass spectrometry or Western blot. Co-immunoprecipitation enables the isolation of a protein target and interactome under physiological conditions. In this chapter, we described how to perform an interactomic study using the co-immunoprecipitation technique in Sertoli cells. Moreover, we will focus on how to analyze and interpret the results of a co-immunoprecipitation before mass spectrometry analysis.

Key words Lysis buffer, Protein quantification, Co-immunoprecipitation, Western blot, Mass spectrometry

1 Introduction

Signaling pathways are defined as a series of molecular circuits, typically executed by proteins, that integrate external and internal signals to generate the appropriate response [1]. Sertoli cells need to receive and integrate information from the nervous system and germ cell line; supply germ cells with the factors they need for their division, differentiation, and metabolism; and create a unique and isolated microenvironment for the germ cell line (blood-testis barrier) [2, 3].

It is crucial to understand the signaling events occurring in Sertoli cells to ultimately identify key molecules that can be used for diagnosis and/or pharmacological intervention in pathological conditions. To identify signaling components in Sertoli cells, a proteomic or an interactomic approach may be used. In one hand, proteomic studies allow us to take a snapshot of the protein profile of a given cell [4]. In the other hand, interactomics allows to identify protein-protein interactions (PPIs) on cells [5].

Marco G. Alves and Pedro F. Oliveira (eds.), *Sertoli Cells: Methods and Protocols*, Methods in Molecular Biology, vol. 1748, https://doi.org/10.1007/978-1-4939-7698-0_7,

Both approaches provide complementary information and can elucidate about signaling events on Sertoli cells. So far proteomic and interactomic approaches to human Sertoli cells are limited. In other mammals, a few efforts have been done, specifically in bovine [6], mouse, and ram [7].

Co-IP followed by mass spectrometry is one of the techniques available to identify and characterize a protein-specific interactome in Sertoli cells. It has been used mostly in mouse isolated Sertoli cells [8, 9]. Co-IP is a technique in which a protein and its interactors are isolated (in either cells or tissues) by binding specifically to an antibody, which in turn is attached to a solid matrix. This is only possible because co-IP is always performed in non-denaturing condition. The biggest advantages of co-IP are the fact that physiological conditions are kept, it is very specific, and it is compatible with several downstream analysis methods. Nevertheless, it is necessary to consider that it does not prove direct interaction, since protein complexes are often identified with this technique. Briefly, co-IP consists in (1) solubilizing protein extract without breaking protein-protein interactions; (2) coupling specific antibodies to a solid matrix, typically beads; (3) isolating of the protein complex; and (4) finally analyzing of the protein complexes. Figure 1 is a scheme of a co-IP protocol.

In the next section, an indirect co-IP protocol will be described in detail, as well as the main features, advantages, and disadvantages of some materials/reagents. We advise to read the notes section before performing the protocol.

2 Materials

1. Magnetic protein A- or G-coupled beads.
2. Lysis buffer suitable for co-IP (please *see* Chapter 6).
3. Antibody for a specific protein of interest and antibody for the negative control.
4. Bovine serum albumin (BSA).
5. Magnet.
6. Rotating wheel.
7. Ice-cold PBS1× (137 mM NaCl; 2.7 mM KCl; 10 mM Na_2HPO_4; 1.8 mM KH_2PO_4).
8. Wash buffer: 1×PBS (137 mM NaCl; 2.7 mM KCl; 10 mM Na_2HPO_4; 1.8 mM KH_2PO_4); TBST (20 mM Tris; 150 mM NaCl, 0.05% Tween-20); lysis buffer suitable for co-IP.
9. 1% SDS.
10. Elution buffer: 1× Laemmli buffer (10% glycerol; 63 mM Tris–HCl pH 6.8; 2% SDS; 0.1% 2-mercaptoethanol or DTT; 0.0005% bromophenol blue), 1% SDS, 50 mM glycine, pH 2.5.

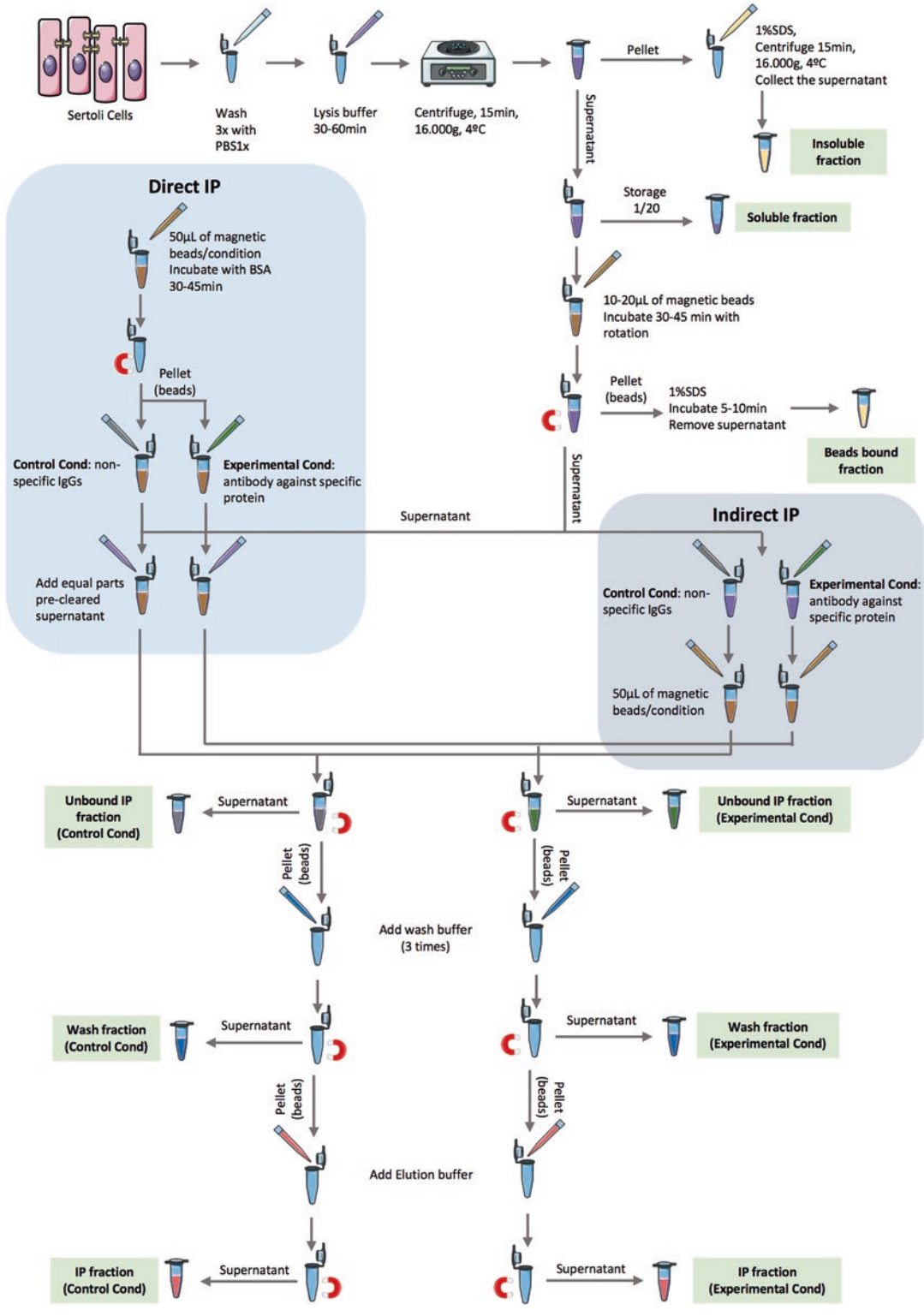

Fig. 1 Co-IP protocol. Two approaches to co-IP are represented: direct and indirect co-IP. The co-IP protocol described uses magnetic beads to separate the immunogen and its interactors. Nevertheless, other methods can be used such as agarose beads. In that case, instead of using a magnet to separate the beads from supernatant, agarose beads are centrifuged, and the supernatant is removed without disturbing the bead pellet

3 Methods

3.1 Sertoli Cell Lysis

1. Please *see* Chapter 6. Please note that protein-protein interactions must be kept.

3.2 Preclearance

1. Prepare 10–20 μL of magnetic beads according to the manufacturer's instructions (*see* **Note 1**).
2. Add the magnetic beads to the Sertoli cell lysate.
3. Incubate 30–45 min with rotation at 4 °C (*see* **Note 1**).
4. Place the tube on the magnet to separate the beads from the Sertoli cell lysate.
5. Recover the supernatant and set aside on ice.
6. To the beads add 10–20 μL of 1% SDS.
7. Remove the beads from the magnet and incubate the beads with 1% SDS for 5–10 min.
8. Place the tube on the magnet to separate the beads from the 1% SDS. Remove and store the supernatant at −20 °C (*beads-bound fraction*).

3.3 Antibody Binding

1. Divide the supernatant of **step 5** into the number of conditions plus the number of negative controls (*see* **Note 2**).
2. To each supernatant add one of the following:
   (a) Co-IP of a specific protein of interest:
   - 1–5 μg of purified monoclonal or polyclonal antibody.
   - 1–5 μL polyclonal antiserum.
   - 0.2–1 μL ascitic fluid containing monoclonal antibody.

   (b) Negative control: IgGs of the same species and same type of the antibody used in the co-IP. Use the same amount used in the co-IP.
3. Incubate from 1 h to overnight at 4 °C with rotation (*see* **Note 3**).

3.4 Capture of Protein Complexes

1. Prepare 50 μL of magnetic beads per condition.
2. Block the beads with 1–5% BSA in lysis buffer for 45 min (*see* **Note 4**).
3. Place the tubes on the magnet and remove the BSA.
4. Add the beads to the supernatant of each condition. Incubate 1–2 h at 4 °C with rotation.
5. Place the tubes on the magnet and remove the supernatant. Store each supernatant (*co-IP unbound fraction*).
6. Add 300–500 μL of wash buffer to the tubes. Incubate 5 min, 4 °C with rotation.

7. Place the tube in the magnet and remove the supernatant. Store the supernatant at −20 °C (*wash fraction*).
8. Repeat **steps 6** and **7** at least three more times (without saving the supernatant).
9. Add elution buffer and incubate 5–10 min, 4 °C with rotation. If a harsh elution is required, boil the beads at 95 °C for 3 min. If 50 mM of glycine pH 2.5 is used, neutralize with Tris pH 10 (1/20 of the volume) (*see* **Note 5–13**).
10. Place the tube in the magnet and remove the supernatant. Store the supernatant at −20 °C (co-IP fraction). This supernatant contains your protein of interest and its interactors.

3.5 Analysis of Co-IP Results by Western Blot

The co-IP protocol described previously only allows to isolate the interactors of a specific protein in Sertoli cells. The identity of the interactors is still unknown. Western blot allows the researcher to identify a specific interactor of the protein immunoprecipitated using an antibody that specifically recognizes the interactor. The detection or not by Western blot of the immunoprecipitated protein or a known interactor will help to decipher what happened during the co-IP and, more importantly, determine if the co-IP worked and confirm a protein-protein interaction. Table 1 presents the expected results and troubleshooting of co-IP followed by Western blot.

Figure 2 shows an example of an analysis of co-IP result by Western blot from Sertoli cells.

The immunoprecipitated protein, phosphoprotein phosphatase 1 catalytic subunit C, was immunodetected in the IP fraction proving that the immunoprecipitation worked. Moreover, in the negative control (co-IP with IgGs), no PPP1CC was detected, proving the specificity of the antibody used. To check if the co-IP worked, immunoblot of protein phosphatase 1 regulatory subunit 15A (PPP1R15A) a well-known PPP1 interactor was performed [10, 11]. The results show that PPP1CC interacts with PPP1R15A in Sertoli cells, since the latest appear in the co-IP fraction proving that isolation of PPP1CC interactors in Sertoli cell by co-IP worked.

The fact that neither PPP1CC nor PPP1R15A did not show up in the soluble fraction may be a concern. However, we believe this is only a consequence of loading a small fraction of the Sertoli cell lysate (2% of the total lysate).

Regarding the IgGs, heavy chains and light chains were detected in the co-IP fraction, showing that the antibody bonds to the beads.

3.6 Analysis of Co-IP Results by Mass Spectrometry

Opposite to the Western blot, mass spectrometry is a high-throughput technique that can identify thousands of interactors after a co-IP. The major advantages of mass spectrometry are the

Table 1
Expected results and troubleshooting of co-IP followed by Western blot

		Protein of interest and known interactor	
Fraction	**Content**	**Expected results**	**Troubleshooting**
Soluble fraction	All solubilized proteins	Must be present. It proves that the protein of interest and the interactor exist in the cells and were solubilized	If not present – Increase the strength of lysis buffer – Check with a different technique if the protein exists in the cells
Insoluble fraction	All proteins that the lysis buffer did not solubilize	May or may not be present	If exclusively present – Increase the strength of the lysis buffer. Keep in mind that increasing the strength affects protein-protein interactions
Beads-bound fraction	All protein that bound nonspecifically to the solid-phase matrix	Low to no presence	If in high quantities or exclusively present – Change the type of solid-phase matrix – Block the beads (1%–5% BSA)
Co-IP unbound fraction	All free proteins, free, antibody, protein-antibody, protein-interactor, and antibody-protein-interactor that did not bind to the solid-phase matrix	Low to no presence	If in high quantities or exclusively present – Check if the solid-phase matrix chosen is suitable for the antibody used – Change the antibody for the protein of interest – Cross-link the proteins previously to do co-IP – Protein of interest and putative interactor do not interact – If the antibody used in the co-IP is detected in high quantities, it does not bind to the solid-phase matrix. Change the antibody or beads
Wash fraction	All proteins that the wash buffer eluted from the solid-phase matrix	Low to no presence	If in high quantities or exclusively present – Change to a weaker wash buffer – Cross-link the proteins previously to do co-IP
Co-IP fraction	All proteins that the elution buffer extracted from the solid-phase matrix	Must be present. It proves that the protein of interest was immunoprecipitated and that protein-protein interactions were conserved	If not present or in very low amounts – Increase the amount of initial protein (cells) – Increase the amount of antibody – Change the antibody – Cross-link the proteins previously to do co-IP

(continued)

Table 1
(continued)

		Protein of interest and known interactor	
Fraction	**Content**	**Expected results**	**Troubleshooting**
Co-IP fraction of the negative control		Low to no presence	If in high quantities or exclusively present – The nonspecific antibody binds to the protein of interest and/or interactor – Change the nonspecific antibody – Change the type of solid-phase matrix – Block the beads (1%–5% BSA) – If the antibody used in the co-IP is not detected, it does not bind to the solid-phase matrix. Change the antibody or beads

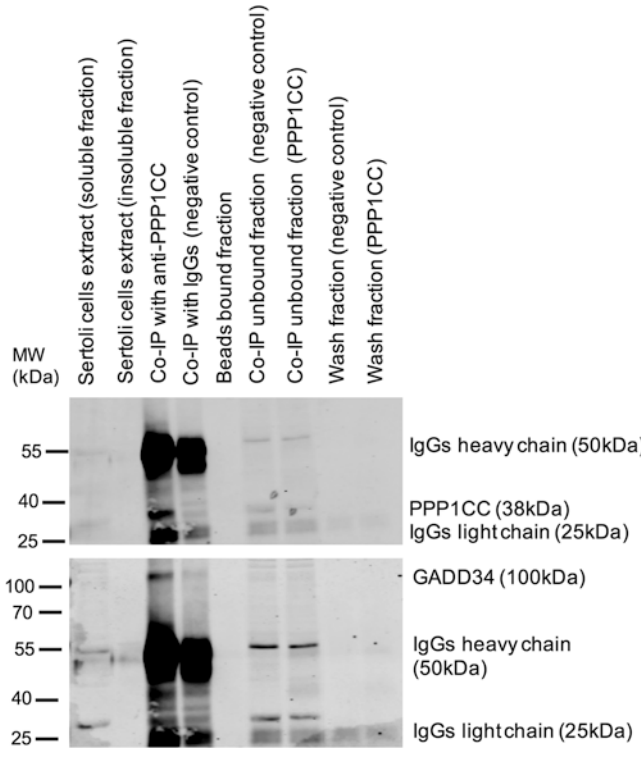

Fig. 2 Western blot analysis of co-IP of PPP1CC from primary culture of human Sertoli cells. After performing the protocol of co-IP, the proteins were separated by SDS-PAGE, and PPP1CC and PPP1R15A were detected by immunoblotting. Note that, apart from the co-IP fractions, all fractions correspond to 1/10 of the initial protein concentration. The blue color indicates an overexposed signal

sensitivity (small quantities of protein are detected) and it identifies hundreds of proteins in a single run and identifies the peptide sequence of the interactors. However, the high cost and challenging optimization can be a setback of mass spectrometry.

The fact that mass spectrometry provides the researcher with a great amount of information can be overwhelming. We believe that a bioinformatics analysis of the data is the best option to extract biological relevance and meaningful information. This type of analysis is outside of the scope of this chapter. To an in-depth training on how to analyze mass spectrometry data, we suggest checking the EMBL-EBI online training (http://www.ebi.ac.uk/training/online/). There is basic training such as "Bioinformatics for the terrified" and more advanced training such as building protein networks from your data.

4 Notes

1. The amount of beads and time of incubation for the preclearance are rough estimates based on the manufacturer's instructions and previous experience. Quantities and time can be adjusted.
2. Until this point the researcher can process the Sertoli cell protein lysate all together regardless of the antibodies used.
3. The incubation time for the antibody-antigen binding must be optimized. This will depend mostly on the quality of the antibody and expression of the antigen in Sertoli cells.
4. Adding bovine serum albumin (BSA) to the beads prior antibody-antigen incubation blocks nonspecific protein binding to the beads. This step can be ignored when preclearance is performed. In the case of the protocol presented, both preclearance of the Sertoli cell lysate and blocking of the beads were performed to significantly decrease unspecific binding to the beads.
5. The volume of elution buffer can vary. The least volume used, the more concentrated the proteins (interactors) will be. For most future analysis techniques, higher protein concentrations are preferable than low. Thus, small volumes can be used (50–100 μL). However, the researcher must keep in mind that the beads (or other solid-phase matrices) must be covered with elution buffer and incubation with rotation must be possible.
6. *Sertoli cell lysis:* Maybe the most important step of a co-IP is cell lysis. Cell lysis must be strong enough to disrupt the cell membrane, organelle membranes (mitochondria, nucleus, etc.), and cytoskeletal structures in order to solubilize all proteins, without disrupting protein-protein interactions. To better choose the most suitable lysis buffer, please *see* Chapter 6).

7. *Types of beads (solid-phase matrix)*: The solid-phase matrix corresponds to the support where the specific antibody will be attached. This physical support allows the capture of the complexes antibody-protein-interactors. Typically, in co-IPs the solid-phase matrices are small beads or slurries covalently bonded to one or both proteins A and G. The most commonly used beads are agarose (and derivatives, such as Sepharose) and magnetic beads. Nowadays, magnetic beads are widely used, while agarose beads are losing their popularity. Theoretically agarose beads have a higher binding capacity for antibody. However, antibodies captured within the agarose porous aren't always accessible to the target proteins. Moreover, since agarose beads have a large surface-area-to-volume ratio, the amount of antibody to saturate the binding capacity of the agarose is high and most of the times unnecessary and unachieved.

   Regardless of the chosen beads, unspecific protein binding to the beads is a problem that the researcher will always face. Trinkle-Mulcahy et al. identified, by mass spectrometry, the proteins that bind nonspecifically to agarose, Sepharose, and magnetic beads [12]. This can help the researcher to critically analyze its own results. To minimize the interference of nonspecifically bound proteins, we recommend a preclearance step. Please note that if your protein of interest binds nonspecifically to the beads, you may need to change the type of beads used.

8. *Protein A or protein G*? The solid-phase matrix provides the physical support for antibody binding. However, antibodies do not bind agarose or magnetic materials. Typically, beads are covered with either protein A, protein G, or both. The high capacity of proteins A and G of binding (up to 8 μg of human IgGs per mg of beads) and the wide range of immunoglobulin affinity make these two proteins the best option for co-IP. Nevertheless, the researcher must choose from beads coated with protein A and/or protein G. The binding strength and affinity between protein A or G and antibody are determined by the species and the properties of the antibody. This information can be consulted in beads datasheet.

9. *Antibodies, how to choose and how much to use*: The success of the co-IP depends on the binding of the antibody to the protein of interest. Frequently, the researcher must choose between a polyclonal and monoclonal antibody.

   Polyclonal antibodies recognize multiple epitopes of the target protein. Consequently, the chance of at least one being exposed is higher and therefore available for interaction with the antibodies. Therefore, the biggest advantage of polyclonal antibodies is the likelihood of success of the co-IP. Nevertheless,

the major advantage can become the main disadvantage. The high probability of cross-reactivity with epitopes of other proteins produces high backgrounds and misidentification of antigens.

Monoclonal antibodies offer specificity. However, monoclonal antibodies present less affinity than polyclonal. So, when choosing between monoclonal and polyclonal antibodies, the researcher must balance what is more critical: robustness or specificity.

Commercially available antibodies typically are tested for immunoprecipitation application. If possible we recommend the researcher to use these antibodies (and use the recommended dilution). If not possible, several conditions must be tested, particularly the amount of antibody to use. In the case that a range of antibody cannot be tested, we suggest a 1:100 dilution. Between different conditions, the same amount of antibody must be used.

10. *Cross-linking*, *to do or not to do*: Cross-linking refers to the process of chemically linking two or more molecules by a covalent bond. Typically, in co-IP, cross-linking is used to either stabilize weak protein-protein interaction or immobilize the antibody to the solid-phase matrix (beads).

    Weak transient protein-protein interactions can be lost even by using a mild cell lysis. Cross-linking reagents can be used to freeze these interactions in vivo and therefore insure that no interactions are lost. Cross-linking weak protein-protein interactions must be done prior to starting the co-IP.

    During co-IP, specifically elution, binding between antibody and beads is lost. Consequently, the antibody is eluted together with protein complexes. This represents a setback when analyzing the results of the co-IP by Western blot and mass spectrometry. Since the heavy chain and light chain of the antibody present a molecular weight of 50 kDa and 25 kDa, detecting proteins in this area is only possible when using primary antibody of a different species or if during the co-IP the antibody is cross-linked to the beads. This will reduce the amount of heavy and light chains and allows detection of the protein.

    If after co-IP the results will be analyzed by mass spectrometry, cross-linking the antibody to the beads can be an advantage. The presence of high quantities of antibody can mask and interfere with the detection and identification of less abundant proteins. Therefore, the elution of antibody must be minimized.

11. *Nonspecific controls*: Nonspecific controls or negative controls must be included in order to correctly interpret results of the co-IP. One type of control consists in performing a

co-IP with an irrelevant antibody (an antibody that does not recognize specifically any protein). Although antibodies are produced to only bind one specific protein, they are not completely inert molecules. Thus, there is always unspecific binding of proteins present in the cell lysate to the antibodies. By performing a co-IP with this antibody, all proteins that bind nonspecifically to the antibody will be identified. The best negative control that the research can use is an antibody from the same species and same antibody type as the one used in the co-IP.

12. *Choosing the buffers*, *washing and elution*: Besides the lysis buffer (*see* Chapter 6), during the co-IP the researcher will use two additional more buffers: the washing buffer to remove nonspecific binding of protein to the antibody or protein-protein interactions and the elution buffer to remove the protein-protein complexes from the antibody/bead matrix. Both buffers can be harsh, mild, or weak.

    Regarding the wash buffer, PBS 1× is weak. Consequently, there is an increased probability of detecting false positives. TBST and PBST are considered mild wash buffers. They contain 0.05% of Tween-20, which results in disruption of very weak interactions (normally formed by nonspecific interactions). Finally, the lysis buffer used for disrupting the Sertoli cells can be used as harsh wash buffer.

    The perfect elution would remove all the protein bound to the antibody, without breaking the bond between antibody and the solid-phase matrix. However, this is very difficult to achieve. If the antibody can be eluted together with the protein-protein complexes, we advise to use 1% SDS. Alternatively, in some applications, such as mass spectrometry, the presence of the antibody must be minimized. 50 mM of glycine pH 2.5 can be a good option to decrease the presence of antibody.

13. *Direct co-IP vs indirect co-IP*: In the co-IP protocol described in this chapter, the free antibody is first added to the Sertoli cell lysate, and the antigen-antibody complex is collected by the solid-phase matrix (indirect co-IP). However, the order of stages can be modified. The antibody can be first pre-bound to the solid matrix phase and then added to the cell lysate containing the antigen (direct co-IP). Both approaches have advantages, and the researcher may want to compare both protocols (Fig. 1).

    The direct co-IP allows the removal of unbound antibodies and to perform cross-linking. The indirect co-IP works better when the quality of the antibody used is not outstanding because it increases the number of antibody-antigen complexes.

Acknowledgments

This work was supported by FEDER funds through the "Programa Operacional Competitividade e Internacionalização (COMPETE 2020)" and by national funds through the FCT (Fundação para a Ciência e Tecnologia), Projects PTDB/BBB-BQB/3804/2014 and PTDC/DTP-DES/6077/2014. We are thankful to the Institute for Biomedicine (iBiMED) (UID/BIM/04501/2013) for supporting this project. iBiMED is supported by the Portuguese Foundation for Science and Technology (FCT), COMPETE 2020, and FEDER fund. This work was also supported by an individual grant from FCT of the Portuguese Ministry of Science and Higher Education to M.J.F. (SFRH/BD/84876/2012).

References

1. Berg JM, Tymoczko J, Stryer L (2002) Chapter 15, signal-transduction pathways: an introduction to information metabolism. In: Berg JM, Tymoczko J, Stryer L (eds) Biochemistry. W H Freeman, New York
2. Alves MG, Rato L, Moreira A, Oliveira P (2015) Célula se Sertoli: fisiologia, estrutura e função. In: Fardilha MV, Silva JV, Conde M (eds) Reprodução Humana Masculina Princípios Fundamentais. ARC Publishing, Aveiro, pp 45–55
3. Cheng CY, Wong EW, Yan HH, Mruk DD (2010) Regulation of spermatogenesis in the microenvironment of the seminiferous epithelium: new insights and advances. Mol Cell Endocrinol 315(1–2):49–56. https://doi.org/10.1016/j.mce.2009.08.004
4. Dhingra V, Gupta M, Andacht T, Fu ZF (2005) New frontiers in proteomics research: a perspective. Int J Pharm 299(1–2):1–18. https://doi.org/10.1016/j.ijpharm.2005.04.010
5. Bonetta L (2010) Protein-protein interactions: interactome under construction. Nature 468(7325):851–854. https://doi.org/10.1038/468851a
6. Tripathi UK, Aslam MK, Pandey S, Nayak S, Chhillar S, Srinivasan A, Mohanty TK, Kadam PH, Chauhan MS, Yadav S, Kumaresan A (2014) Differential proteomic profile of spermatogenic and Sertoli cells from peri-pubertal testes of three different bovine breeds. Front Cell Dev Biol 2:24. https://doi.org/10.3389/fcell.2014.00024
7. Chalmel F, Com E, Lavigne R, Hernio N, Teixeira-Gomes AP, Dacheux JL, Pineau C (2014) An integrative omics strategy to assess the germ cell secretome and to decipher sertoli-germ cell crosstalk in the Mammalian testis. PLoS One 9(8):e104418. https://doi.org/10.1371/journal.pone.0104418
8. Gao Y, Lui WY, Lee WM, Cheng CY (2016) Polarity protein Crumbs homolog-3 (CRB3) regulates ectoplasmic specialization dynamics through its action on F-actin organization in Sertoli cells. Sci Rep 6:28589. https://doi.org/10.1038/srep28589
9. Gungor-Ordueri NE, Tang EI, Celik-Ozenci C, Cheng CY (2014) Ezrin is an actin binding protein that regulates sertoli cell and spermatid adhesion during spermatogenesis. Endocrinology 155(10):3981–3995. https://doi.org/10.1210/en.2014-1163
10. Brush MH, Guardiola A, Connor JH, Yao TP, Shenolikar S (2004) Deactylase inhibitors disrupt cellular complexes containing protein phosphatases and deacetylases. J Biol Chem 279(9):7685–7691. https://doi.org/10.1074/jbc.M310997200
11. Wu DY, Tkachuck DC, Roberson RS, Schubach WH (2002) The human SNF5/INI1 protein facilitates the function of the growth arrest and DNA damage-inducible protein (GADD34) and modulates GADD34-bound protein phosphatase-1 activity. J Biol Chem 277(31):27706–27715. https://doi.org/10.1074/jbc.M200955200
12. Trinkle-Mulcahy L, Boulon S, Lam YW, Urcia R, Boisvert FM, Vandermoere F, Morrice NA, Swift S, Rothbauer U, Leonhardt H, Lamond A (2008) Identifying specific protein interaction partners using quantitative mass spectrometry and bead proteomes. J Cell Biol 183(2):223–239. https://doi.org/10.1083/jcb.200805092

Chapter 8

Phagocytosis by Sertoli Cells: Analysis of Main Phagocytosis Steps by Confocal and Electron Microscopy

Marina G. Yefimova, Nadia Messaddeq, Annie-Claire Meunier, Anne Cantereau, Bernard Jegou, and Nicolas Bourmeyster

Abstract

Sertoli cells were discovered in the seminiferous tubules by Enrico Sertoli in 1865 (Morgagni 7:31–33, 1865). Intense phagocytosis is, in the context of spermatogenesis cycle, morphologically the most noticeable function of Sertoli cells. In this chapter the major principles of phagocytosis machinery and its specificities in the seminiferous tubules will be briefly reviewed, guidelines of analysis of main phagocytosis steps by confocal and transmission electron microscopy will be described, and a simplified method to assess phagocytosis rate in routine experiments will be given.

Key words Apoptotic-like membranes, Homeostatic phagocytosis, Nonprofessional phagocytes, Phagocytosis steps, Residual bodies, Sertoli cells

1 Introduction

Somatic Sertoli cells from the seminiferous tubules, also called "nurse" cells, play a key role in sustaining male fertility [1]. Multiple activities operated by Sertoli cells provide a metabolic support for developing germ cells and create a specific microenvironment, which protects them from autoantigens. The latter is established through the cleaning of tubules from apoptotic substrates in phagocytosis cycle. Intense phagocytosis is the most noticeable function of Sertoli cells manifested by the emergence of lipid droplets in cell cytoplasm, known as Sertoli cell "lipid cycle" [1, 2].

Nonetheless, up to date this fundamental process is poorly studied. One of the hampering factors is the absence of routine methods to assess the rate of phagocytosis by the Sertoli cells. It is partly due to the significant peculiarities, which make phagocytosis in the seminiferous tubules different from phagocytosis performed by immune cells. Therefore, before exposition of technical part, some fundamental definitions regarding phagocytosis process and its counterpart in the seminiferous tubules will be given.

Marco G. Alves and Pedro F. Oliveira (eds.), *Sertoli Cells: Methods and Protocols*, Methods in Molecular Biology, vol. 1748, https://doi.org/10.1007/978-1-4939-7698-0_8,

1.1 Phagocytosis by Professional and Nonprofessional Phagocytes

By definition, phagocytosis is "the engulfment by cells of large particles (≥0.5 μm)" in order to degrade them [3]. It is realized by specialized cells, called phagocytes. Depending on their origin (hematopoietic or not), phagocytes are considered as *professional or nonprofessional*, respectively [4]. Freely circulating professional phagocytes constitute a critical component of the innate immune response to pathogens [5]. They destroy invading microbes by generating NADPH oxidase-mediated reactive oxygen species (ROS). Detection of ROS by luminol or tetrazolium salt assays [6–8] is used for the routine assessment of professional phagocyte activity.

In normal situation, professional phagocytes cannot infiltrate into the blood-separated tissues. In this case, resident cells of epithelial origin act as nonprofessional phagocytes, providing the clearance of *tissue-specific substrates*. This contributes to tissue homeostasis; therefore, such type of phagocytosis is termed as *homeostatic phagocytosis* [9]. As usual, phagocytosis by non-motile tissue-immerged phagocytes does not result in the generation of ROS, because they would cause oxidative lesions to neighboring cells [10, 11]. Therefore, other experimental approaches are needed to assess the rate of homeostatic phagocytosis.

Phagocytosis is a complex, tightly regulated process, which consists of three principal *steps*: the recognition and binding of the substrate (step 1), followed by its internalization (step 2), and completed by its degradation (step 3) [12]. Each phagocytosis step is an individually regulated event, so that the binding of phagocytosis substrate does not automatically trigger its ingestion; moreover ingested substrate could not be directly addressed for degradation, but can accumulate in cell cytoplasm. Degradation of ingested substrate is generally heralded by the formation of lipid droplets in the cytoplasm of phagocyte.

1.2 Phagocytosis in the Seminiferous Tubules: Cyclical Progression

Lipid droplets cyclically appear in the cytoplasm of the Sertoli cells [2]. Sertoli cell "lipid cycle" [2] coincides with the progression of *spermatogenesis*—a fundamental biological process leading to the production of male gametes. Spermatogenesis also progresses in cyclical manner, known as the cycle of the seminiferous epithelium [13–15]. It consists of series of individual cellular divisions (from spermatogonia to early spermatid) and differentiation steps (from round spermatid to streamlined spermatozoa) [16]. Spermatogenesis is divided into a species-specific number of *stages* or cell associations (stages XII and XIV in mouse and rat, respectively) at one location along a seminiferous tubule [13–15].

The massive emergence of lipid droplets in the cytoplasm of the Sertoli cells results from the degradation of residual bodies (RBs) which are the fragments of membranes which separate from the most differentiated spermatids at the time of spermiation, the latter corresponding to the shedding of spermatozoa in the lumen of the seminiferous tubules. Spermiation occurs at stages VII–VIII

of the seminiferous tubule cycle in the rat [17]. While detached from living cells, RBs are *apoptotic-like membranes*, because they manifest a strong immunostaining with apoptotic membrane marker, annexin V, and with anti-caspase-1 antibodies [18].

RBs are *tissue-specific phagocytosis substrates* in the testis. Phagocytosis of RBs exhibits the classical pattern, in which each individual *step* is clearly distinguished in the seminiferous tubule sections. It starts at the apical side of Sertoli cell, where RBs are detached from the elongated spermatids. RBs are immediately ingested by Sertoli cells and then fused with lysosomes. Whether in vivo phagocytosis operates through type I (membrane protrusions) or II (invagination) is currently unknown. After ingestion, RBs migrate toward the basal part of the Sertoli cells for degradation. In the rat where it has been very precisely studied, the latter completes within about 29 h after the release of RBs, as manifested by the emergence of lipid droplets [17, 19].

1.3 Phagocytosis by the Sertoli Cells: Assessment In Vitro

Phagocytosis by Sertoli cells can be studied in vitro using cultured primary Sertoli cells or Sertoli cell lines and purified fraction of RBs as tissue-specific substrate (*see* **Note 1**). Several protocols have been reported [20–26], but usually these protocols have to be adapted and further optimized to avoid the misinterpretation of experimental data.

Because each phagocytosis step is an individually regulated event, step-by-step analysis is needed to characterize the process in its integrity. This is of particular importance when the failure, modulation, or comparative analysis of phagocytosis rates in different experimental systems is explored. The most delicate trial is to distinguish between phagocytosis steps 1 and 2. Because of the transparency of the plasma membrane, it is often problematic to discern by light microscopy the substrates bound to plasma membrane and/or ingested by the Sertoli cells. Confocal microscopy resolution is rather substantial to distinguish phagocytosis step 1 from step 2, but confocal analysis of individual cells is an expensive and time-consuming procedure, which is not suitable for routine measurements. In this chapter, we describe first the protocols for step-by-step analysis of phagocytosis by light, confocal, and transmission electron microscopy and in a second time a simplified approach to analyze step-by-step phagocytosis by Sertoli cells for routine experiments.

2 Materials

2.1 Antibodies

1. Anti-activated GTP-Rac1 antibodies; 1:250 dilution in 2%BSA/PBS for IF.
2. Anti-phospho-MERTK antibodies; 1:1000 dilution in 0.5% milk/PBS for WB, 1:250 dilution in 2%BSA/PBS for IF.

3. Anti-non-muscle heavy chain myosin; 1:250 dilution in 2%BSA/PBS for IF.
4. Anti-Rac1 antibody (23C8 Millipore); 1:250 dilution in 2%BSA/PBS for IF, 1: 1000 in 0.5% milk/PBS for WB.

2.2 Cell Culture

1. TM4 mouse Sertoli cells line.
2. Primary Sertoli cell isolation medium (medium A): Leibovitz's L15 containing 1% penicillin/streptomycin and 2.5 μg/mL Fungizone.
3. Primary Sertoli cell culture medium (medium B): Dulbecco's Modified Eagle's Medium (DMEM) containing 1% penicillin/streptomycin, 2 mM L-glutamine, 50 ng/mL retinol, 200 ng/mL α-tocopherol, 2 μg/mL bovine insulin, and 2.5 μg/mL Fungizone.
4. TM4 Sertoli cell culture medium: DMEM/F12 containing 10% FCS and 1% penicillin/streptomycin.
5. Phosphate-buffered saline, powder.
6. 17–19-day-old and 3–5-month-old Wistar rats.

2.3 Biochemical Reagents

1. Acrylamide/bis-acrylamide, 30%.
2. Ammonium chloride.
3. Annexin V.
4. Bafilomycin A1.
5. BCA protein kit.
6. Biotinamidocaproate N-hydroxysuccinimide ester.
7. Biotin-labeling buffer: 10 mM Na borate, 150 mM NaCl, pH 8.8.
8. Blebbistatin.
9. BODIPY® 493/503.
10. Bovine serum albumin.
11. Collagenase II-S.
12. Cresyl Violet Solution.
13. Cytochalasin D.
14. DMSO cell culture grade.
15. DNase.
16. ECL chemiluminescence system.
17. Ethanol.
18. Glutathione Sepharose beads.
19. Glutaraldehyde 25%.
20. Glycerol.

21. Glycine.
22. Lysis buffer for affinity binding assay: 50 mM Tris–HCl, 100 mM NaCl, 2 mM $MgCl_2$, 1% NP-40 (w/v), 10% glycerol, 1 mM PMSF, 20 mM leupeptin, 0.8 mM aprotinin, 10 mM pepstatin, pH 7.4.
23. Membrane for protein transfer, nitrocellulose 0.2 μm.
24. Methanol.
25. Nonfat dry milk.
26. Osmium tetroxide 1%.
27. Paraformaldehyde 20% (EM grade).
28. Phosphate-buffered saline (PBS).
29. PGEX-2 T vectors containing the cDNAs of PAK-CRIB (PAK-CD) domain (obtained from JG Collard, Netherlands Cancer Institute, Amsterdam, NL).
30. Polystyrene microparticles (1–2 μm Ø).
31. Protease and phosphatase inhibitor cocktails.
32. Pulldown buffer containing $MgCl_2$ (Tris–HCl pH 7.4 50 mM, NaCl 100 mM, NP40 1% (v/v), $MgCl_2$ 2 mM), pH 7.4.
33. Sample buffer (reduced condition): 125 mM Tris–HCl, pH 6.8, 4% sodium dodecyl sulfate (SDS), 10% glycerol, 0.02% bromophenol blue, 5% β-mercaptoethanol.
34. Soybean trypsin inhibitor.
35. TBS (Tris-buffered saline).
36. Tetramethyl-rhodamine isothiocyanate-avidin conjugates.
37. Towbin transfer buffer: 25 mM Tris-base, 192 mM glycine, and 20% methanol, pH 8.3.
38. Trizma base and Tris–HCl.
39. Trypsin.
40. Triton X-100.
41. Uranyl-acetate 4% aqueous solution, to prepare from a 98% EM grade solution.

2.4 Equipment

Biosafety level 2 cell culture facility:

1. μ-dish 35 mm, High Glass Bottom.
2. 8-well Lab-Teck™ chamber glass slide.
3. Cell culture incubator (37 °C, 5% CO_2 atmosphere).
4. Centrifuge Jouan CR312/T4 swing-out rotor.
5. Centrifuge Eppendorf 5415R/rotor F45-24-11 (fixed angle).
6. Confocal FV-1000 station installed on an inverted microscope IX-81 (Olympus, Japan).

7. Electrophoretic apparatus.
8. Fine mesh plastic grid (Mesh Direct).
9. Formvar carbon film on 2 × 1 mm oval slot copper.
10. Glass Pasteur pipette.
11. Gnome transilluminator (Ozyme) with Genesis software (Syngene) for WB densitometric analysis.
12. Laboratory silk filter cloth.
13. Electrophoretic blotting unit.
14. Nitrocellulose membrane, 0.2 μm.
15. Shaking water bath.
16. Teflon glass homogenizer (Tenbroeck tissue grinder – 2 mL).
17. Tissue culture plasticware: T25 cm^2, T75 cm^2 vented flasks.
18. Transmission electron microscope Morgagni 268D (FEI), images captured by MegaView III camera (Soft Imaging System).

3 Methods

3.1 Primary Culture of Rat Sertoli Cells [26]

1. Collect the testes from ten 17–19-day-old rats in complemented Leibovitz's medium (medium A) at room temperature.
2. After removal of the testes' tunica albuginea, dissociate the seminiferous tubules on the glass Petri dish by sterile forceps, and transfer them immediately into 25 mL of enzymatic solution, containing 62.5 mg of trypsin and 0.25 mg of DNase.
3. Incubate the preparation at 34 °C for 20–30 min in a shaking water bath at 80 oscillations (osc)/min.
4. Transfer the preparation into 25 mL measuring cylinder and allow settling for 2 min; then discard 12.5 mL of supernatant.
5. Add 62.5 mg of soybean trypsin inhibitor, and mix gently with Pasteur pipette.
6. Flow the preparation into 50 mL measuring cylinder through the fine mesh plastic grid to get rid of indigested tissues, and then adjust the volume to 50 mL with medium A; mix gently with Pasteur pipette and allow settling for 5 min.
7. Remove the supernatant; add 10 mL of medium A, and then dissociate the cells by passing the preparation ten times through Teflon glass homogenizer.
8. Transfer the cells into 50 mL plastic tube, and then centrifuge the cells for 5 min at 80 × *g* (Jouan CR312/T4 swing-out rotor).
9. Remove the supernatant, add 10 mL of medium A, disperse the cells with Pasteur pipette, and filtrate the cells through sterile laboratory silk.

10. Centrifuge the cells for 5 min at 80 × *g* (Jouan CR312/T4 swing-out rotor).
11. Get rid of supernatant and suspend the cells in medium B.
12. Count the cells and seed them at 8-well glass Lab-Teck chambers at the concentration 0.15×10^{-6} cells per well.

3.2 Isolation of RBs from Rat Testes (Method [18] Modified in [27])

1. Recover testis content from two to three adult (3–5-month-old) rats through the incision in the tunica albuginea, and suspend in 25 mL of PBS, containing collagenase II-S (12.5 mg in 25 mL of PBS).
2. Incubate the tubules for 10 min at 34 °C in a shaking water bath (150 rpm).
3. Transfer the preparation in 50 mL measuring cylinder, and allow to sediment dispersed seminiferous tubules for 3–4 min. Discard the supernatant and repeat this process three times.
4. Incubate the seminiferous tubules in 25 mL PBS containing 0.25 mg/mL trypsin for 20 min at 34 °C, and then disperse cells by gentle pipetting.
5. Filter the suspension through sterile laboratory silk and pellet it by centrifugation at 800 × *g* for 10 min, and then wash the suspension twice at the same conditions.
6. Resuspend the pellet in 40 mL of PBS, supplemented with 1% penicillin/streptomycin and 2.5 μg/mL Fungizone, and then centrifuge at 200 × *g* for 3 min. Collect the supernatant, and then wash the pellet twice. Pool all supernatants. Pooled supernatants contain RBs and germ cells.
7. Centrifuge resulting supernatant at 800 × *g* for 5 min (Jouan CR312/T4 swing-out rotor), and discard the pellet, containing germ cells.
8. Centrifuge the supernatant at 800 × *g* for 30 min (Jouan CR312/T4 swing-out rotor), discard the supernatant, and suspend the pellet in PBS supplemented with 1% penicillin/streptomycin and 2.5 μg/mL Fungizone (*see* **Note 2**).

3.3 Biotinylation of RBs [27, 28]

1. Prepare biotin stock solution as 10 mg/mL in DMSO.
2. Suspend RBs in the biotin-labeling buffer, and then add the biotin from the stock solution to a final concentration 50 μg/mL.
3. Incubate at room temperature in darkness for 15 min.
4. Stop the reaction with 10 mM ammonium chloride.
5. Centrifuge the preparation for 30 min at 800 × *g*, and discard the supernatant.
6. Wash twice biotin-labeled RBs with PBS, suspend in PBS, and count.

3.4 Step-by-Step Analysis of Phagocytosis by Sertoli Cells

The protocol described here is suitable for both the primary culture of rat Sertoli cells and mouse TM4 cell line.

3.4.1 Phagocytosis Step 1

Recognition, binding, and engulfment of RBs by Sertoli cells:

Likewise as other phagocytes, involved in apoptotic substrate cleaning, Sertoli cells recognize and bind to phosphatidylserine (PS) [29], which is the best characterized "eat-me" signal. PS is exposed on the surface of "apoptotic-like" vesicle RBs [18, 30] (*see* **Note 3**). Recognition and binding of PS are mediated by cooperated action of specific receptors on the surface of phagocyte, which induce cytoskeletal modifications leading to the formation and closure of a phagocytic cup. This results in the engulfment of PS-exposing substrate and the formation of a nascent phagosome. In vitro phagocytosis of RBs is realized through type I mechanism, which involves the protrusions of pseudopodia and activation of small GTPase Rac1 (binding to GTP, GTP-Rac1) to recruit actin to the phagocytic cup [20, 30].

Therefore to characterize primary phagocytosis reply of the Sertoli cells, we recommend assessing:

- Pseudopod formation by electron microscopy (type I phagocytosis)
- Small GTPase Rac1 activation
  - By the presence of activated form of Rac1 in the phagocytic cup: detection after immunolabeling with GTP-bound-Rac1-specific antibody by confocal microscopy
  - By Rac1 activation state measurement by pulldown assay

Setting Off RB Phagocytosis by the Sertoli Cells

1. 48 h after cell seeding, replace the culture media, and then add RBs to Sertoli cells at the ratio 10:1 (RB/Sertoli cell).
2. Incubate the RBs with the Sertoli cells for 2–4 h at 34 °C in a humidified atmosphere of 5% CO_2.
3. Carefully wash the cells with culture media to remove the unbound RBs, three times.
4. Wash the cells with PBS 1× to remove the traces of the culture media.

IF Analysis of Phagocytic Cup Formation

1. For IF analysis, fix the cells with 4% PAF/PBS solution for 5 min.
2. Wash the cells three times with PBS 1×, and then treat the cells with 0.5% of Triton-X100/PBS for 3 min.
3. Wash the cells five times with PBS, and then briefly incubate the cells with 2% BSA/PBS solution.

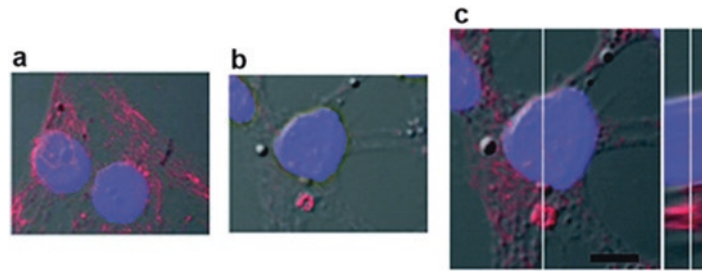

Fig. 1 RB engulfment by Sertoli cells is driven by small GTPase Rac1. In (**a**, **b**), immunostaining and confocal microscopy analysis of Rac1 activation (GTP-Rac1 staining) either in untreated Sertoli cells or in Sertoli cells exposed to RB with both DAPI staining (blue) and GTP-Rac1. In (**c**), confocal microscopy slicing of GTP-Rac1 staining of Sertoli cells exposed to RB. Scale bar, 5 μm. From [30]

4. Apply the antibody against activated Rac1 diluted in 2%BSA/PBS (1:250), and incubate the cells overnight at 4 °C in humidified atmosphere.
5. Next day, wash the preparations with PBS, and then add the secondary antibody conjugated with fluorophore marker (1:500 dilution in PBS), and incubate for 1 h at the room temperature.
6. After washing with PBS, incubate the preparations with DAPI (1:5000 dilution in PBS) for 1 min to stain the nucleus.
7. Mount the preparations with mounting media, and proceed for confocal microscopy slicing. 3D images are acquired with 0.2 μm z-steps simultaneously in fluorescence and transmission (interferential contrast-DIC) and analyzed with Imaris software (Bitplane, Switzerland).

Result to be obtained: activated Rac1 concentrates at the sites of contact with RBs, so that the top view shows the concentric circles around unstained RBs, while the side view shows the fine bands along color-free RBs (Fig. 1) (*see* **Note 4**). In some cases, Rac1 staining can be observed as a pronounced spot including the substrate, signing the closure of the phagocytic cup (*see* **Note 5**). To complete the study, Rac1 activation state should be checked on the substrate alone, which should normally be negative.

Rac1 Activation State Measurement

1. After 2 h of incubation with RBs, wash 10^7 cells with PBS, and then lyse in 1 mL of pulldown buffer. Total amount of protein in each lysate is measured and adjusted to 2 mg/mL.
2. PAK-CD domain in GST fusion is produced in bacteria using a pGEX-5X3 plasmid and then purified on Glutathione Sepharose beads.
3. Preserve a 50 μL aliquot of the cell lysate for determining the total cell content in GTPase by WB.

4. Incubate the remaining lysate with 50 μL of Glutathione Sepharose beads-linked PAK-CD domain corresponding to 5 μg of proteins. Add glycerol to a final concentration of 10%. Incubation is conducted at 4 °C during 1 h under agitation.
5. Realize a short centrifugation at 15,000 × *g* allowing pelleting the beads, and then wash four times in pulldown buffer.
6. Boil pelleted beads in 25 μL of Laëmmli buffer and load them onto a 13% SDS-PAGE in parallel with 25 μL of total lysate (also boiled in 25 μL Laëmmli buffer), and then transfer on nitrocellulose by Western blotting. Reveal the presence of Rac1 using anti-Rac1 antibody.
7. Densitometric analysis of the bands (on Genesys software after acquisition on Gnome transilluminator) allows comparing the amount of activated Rac1 (pulldown) against total Rac1 (cell lysate), measured as a ratio in %.

Electron Microscopy Analysis for Pseudopod's Presence

1. For EM examination, fix the cells by immersion overnight at 4 °C in 2.5% glutaraldehyde and 2.5% paraformaldehyde in cacodylate buffer (0.1 M, pH 7.4).
2. Next day wash the preparations in cacodylate buffer for further 30 min.
3. Postfix the cells in 1% osmium tetroxide for 1 h at 4 °C.
4. Dehydrate cells through graded ethanol series 70%/90%/100%.
5. Embed in Epon 812 resin, and incubate at 48–72 h at 60 °C.
6. Prepare ultrathin sections of 70 nm, and contrast them with uranyl acetate and lead citrate.
7. Examine at 70 kV with electron microscope.

Result to be obtained: pseudopodia protruded from Sertoli cell plasma membrane proceeding to the engulfment of RBs must be observed (Fig. 2).

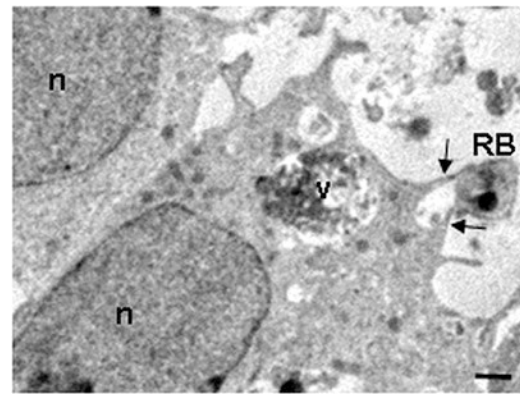

Fig. 2 Sertoli cells engulf RB via pseudopod protrusions. EM image showing engulfment of RB via pseudopod protrusions as indicated by the arrows. Abbreviations: *n* nucleus, *v* degradative vacuole. Scale bar, 1 μm. From [30]

3.4.2 Phagocytosis Step 2

Ingestion of RBs by Sertoli Cells

Cooperative action of several receptors including SCARB1/SR-BI, CD36, BAI I, and TAM tyrosine kinase receptors AXL, TYRO3, and MERTK contributes to the phagocytosis of RBs [22, 26, 30–35]. Studies from genetically modified animal models revealed the primary role of MERTK for phagocytosis of RBs by Sertoli cells [33–35]. Plasma membrane receptor MERTK mediates the ingestion of RBs [29]. In activated state phosphorylated MERTK transduces an external signal, leading to cytoskeleton rearrangement and molecular motor recruitment, which contributes to the ingestion of RBs. For MERTK-mediated ingestion, non-muscle myosin II has been shown to act as molecular motor molecule providing the movement of RBs in cell cytoplasm [30].

Therefore to characterize ingestion step, we recommend assessing the activation of MERTK, followed by the recruitment of myosin II molecular motor (*see* **Note 6**).

A negative control consists in polystyrene microparticles phagocytosis experiment, in which they are efficiently ingested, while no MERTK phosphorylation is observed.

3.4.3 WB, Confocal Studies, and EM Examination

WB Analysis of MERTK Activation

1. Incubate 300,000 Sertoli cells with the RBs (at the same ratio as above) for 0, 30, 60, and 120 min.
2. After washing with PBS, lyse the cells in Laëmmli sample buffer. Add 50 μL of 2× Laëmmli buffer to 300,000 cells, and then scrub preparations on ice bath using policeman rod.
3. Incubate cell lysates 1 h at 37 °C in the presence of protease and phosphatase inhibitor cocktails.
4. Separate the proteins on 8% SDS-polyacrylamide gels, and then transfer them (2 h, 70 V) to nitrocellulose membranes.
5. Block blots for 2 h in TBS-Tween containing 5% of nonfat dry milk.
6. Incubate blots with anti-phospho-MERTK antibodies (1:1000) overnight at 4 °C, and then proceed according to standard WB protocol using ECL chemiluminescence system.

Result to be obtained: phagocytosis of RBs results in phosphorylation of MERTK that starts after 30 min of incubation and decreases by 120 min. Negative control: phagocytosis of polystyrene microparticles does not result in MERTK phosphorylation.

IF Analysis of Cell Surface Changes Induced by Phagocytosis of RBs

1. Incubate the Sertoli cells with RBs for 2 h. Incubate control preparations of Sertoli cells (free of RBs) at the same conditions. Treat the cells as described above.
2. Incubate the cells overnight at 4 °C in humidified chamber with antibodies against phosphorylated MERTK (1:250) and myosin II (1:250) diluted in 2%BSA/PBS.
3. Next day wash the preparations with PBS, and then add the secondary antibodies conjugated with fluorophore marker

(1:500 dilution in PBS), and incubate for 1 h at the room temperature.

4. Then treat the preparations likewise as above (*see* Subheading "IF Analysis of Phagocytic Cup Formation").

Result to be obtained: in control condition, phospho-MERTK immunostaining appears as a uniform punctate pattern throughout the cell, while myosin II is distributed commonly in the cytoplasm and within cell boundaries. Phagocytosis induces clustering of phospho-MERTK and clumping of myosin II, which co-localize on the sites of contact with RBs (*see* **Note 7**).

EM Analysis of the Presence of RBs in Sertoli Cell Cytoplasm

1. Incubate the Sertoli cells with RBs for 4–6 h. Incubate control preparations of Sertoli cells (free of RBs) at the same conditions.
2. After washing with PBS, treat the cells as described above.

Result to be obtained: after ingestion, RBs are progressively addressed inward the cytoplasm of Sertoli cell. Partly degraded RBs can be also observed after fusion with lysosomes.

3.4.4 Phagocytosis Step 3

Degradation of RBs by the Sertoli Cells

Degradation of RBs results in the formation of lipid droplets in the cytoplasm of Sertoli cells. We recommend assessing phagocytosis step 3 by quantification of lipid droplet area in Sertoli cell cytoplasm, using BODIPY fluorescent probe, which detects neutral lipids. The probe functions in both live and fixed cells.

IF Analysis of Lipid Droplet Formation

1. Incubate the Sertoli cells with RBs for 24–30 h. Incubate control preparations of Sertoli cells (free of RBs) at the same conditions.
2. After washing living or fixed cells with PBS 1× to remove the traces of culture media or PAF, add BODIPY ($1{:}10^7$ dilution of stock solution in EtOH) and incubate the cells for 15 min at room temperature.
3. Wash with PBS, and then incubate the preparations with DAPI (1:5000 dilution in PBS) for 1 min to stain the nuclei.
4. After washing with PBS, mount the preparations with mounting media, and proceed for IF microscopy.
5. Count lipid droplet area and nuclei number using ImageJ software, and then calculate lipid droplet area/nuclei ratio. Because of the variability of lipid droplet size, quantification of lipid droplet area over lipid droplet number is recommended.

Result to be obtained: lipid droplet area/nuclei ratio increases in RB-treated cells, compared to control preparations (*see* **Note 8**).

EM Analysis of the Presence of Lipid Droplets in Sertoli Cell Cytoplasm

1. Incubate the Sertoli cells with RBs for 24–30 h. Incubate control preparations of Sertoli cells (free of RBs) at the same conditions.
2. After washing with PBS, treat the cells as described above.

Result to be obtained: the relative increase of the content of lipid droplets (which are heterogenous in size) in the cytoplasm of Sertoli cells exposed to RBs, compared with control.

3.4.5 Simplified Method to Assess Step-by-Step Phagocytosis by Sertoli Cells for Routine Experiments

The test allows discriminating between RBs bound to plasma membrane and ingested by the Sertoli cells. Test uses biotinylated RBs, which are further visualized after the staining with avidin-TRITC.

1. Seed the cells in 8-well Lab-Teck chamber at the concentration 1.5×10^5 cells per well.
2. Incubate the cells with 1.5×10^6 biotinylated RBs for 2, 4, 6, or 24 h at 34 °C in a humidified atmosphere of 5% CO_2.
3. Wash away unbound RBs with culture media, and then fix the cells for 5 min with 4% PAF/PBS (pH 7.4).
4. To distinguish ingested and plasma membrane-bound RBs, divide samples into two groups, each in duplicate wells. Permeabilize group 1 (total substrates) with 0.5% Triton X-100 for 5 min, while group 2 (bound-only substrates) remained unpermeabilized.
5. Add avidin-TRITC solution (dilution 1:100 in PBS), and incubate for 1 h at 25 °C.
6. After washing with PBS, stain the nuclei with DAPI (1:5000 dilution in PBS) for 1 min, and then wash again with PBs, mount in mounting medium, and proceed for IF (Fig. 3).
7. The total area of RBs (plasma membrane bound + ingested) is obtained from group 1, and the area of plasma membrane-bound RBs is obtained from group 2.
8. The area of ingested RBs is obtained by subtracting plasma membrane-bound RB's area from total RB's area.
9. Count RB's area and nuclei number using ImageJ software, and then calculate *phagocytosis index* as the ratio RB's area/nuclei in each well.
10. Cells from unpermeabilized group 2 can be also proceeded with BODIPY fluorescent probe as described above (*see* Subheading "IF Analysis of Lipid Droplet Formation") for degradation assessment.

Result to be obtained: progressive increase of total number of RBs (bound + ingested) associated with the Sertoli cells; prevalence of bound RBs over ingested RBs during 2–8 h of incubation; progressive increase of lipid droplets in Sertoli cell cytoplasm, which reaches its plateau by 24 h of incubation.

Quantification of Bound and Total (Bound + Ingested) RBs Using ImageJ Software

TRITC-stained RB is quantified from raw format images (*.oib* or *.tif*). To open this format, LOCI plug-in is copied in the plug-in folder of ImageJ (or is already present in Fiji software). With this proprietary format, ImageJ is able to read calibration pixel from

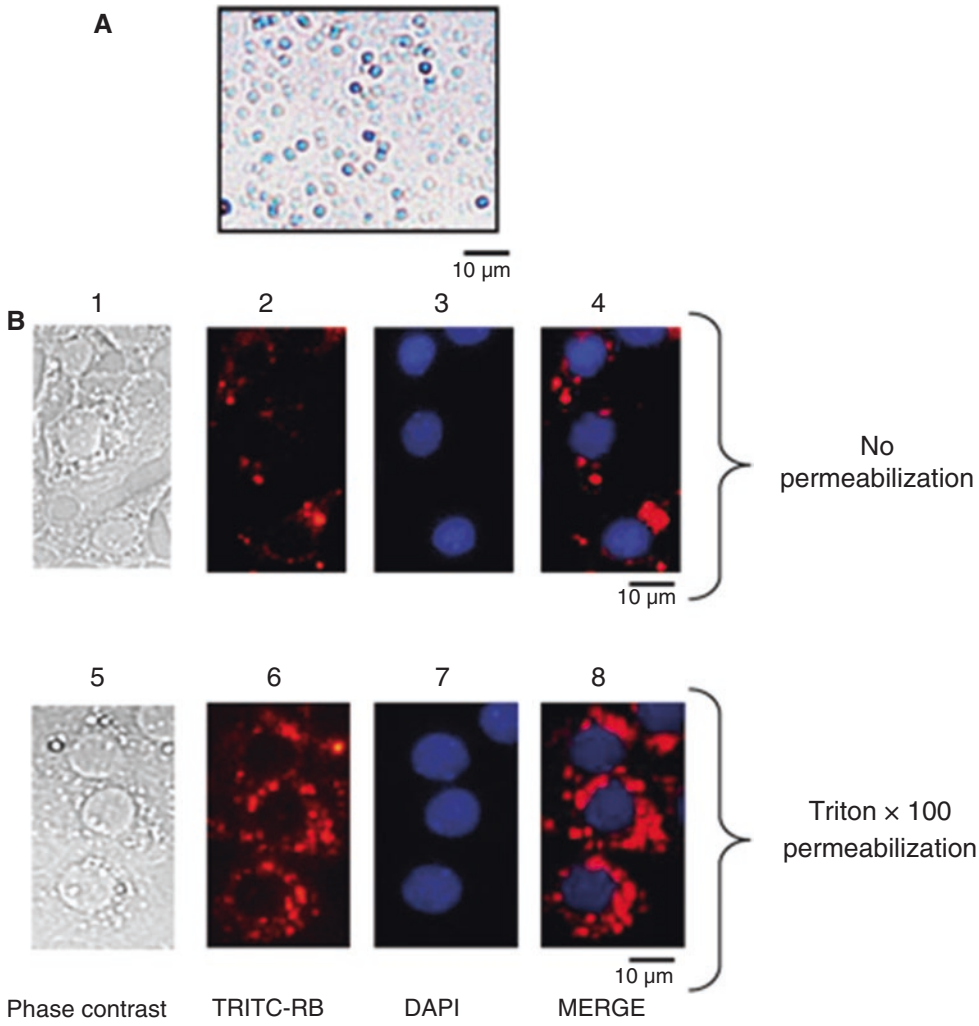

Fig. 3 Simplified method to discern bound and ingested substrates phagocyted by Sertoli cells. (**a**) A representative phase-contrast micrograph of RBs after the purification procedure. RBs are stained with cresyl violet. (**b**) Representative pictures of RB phagocytosis by Sertoli cells. Sertoli cells in culture were incubated with biotinylated RB for 24 h and then were treated with avidin-TRITC conjugate (red staining). Sertoli cell membranes were permeabilized or not, as indicated. Cells were counterstained with DAPI (blue). From [27]

metadata associated with the OIB images. Calibration can be checked in the properties (Image onglet). Quantification is normalized to the number of nuclei stained with DAPI.

Double fluorescence images (TRITC, DAPI) are separated using split channel function (Image onglet, color) and analyzed separately with the *analyze particle* procedure (Analyze onglet). A blue image for DAPI (nuclei) and a red image for RBs are generated simultaneously:

1. Image onglet > Adjust > Threshold. Select an algorithm and adjust the minimum value to a level that fits best the objects of interest (RB) with *dark background* selected. No need to apply.
2. Analyze onglet > Set measurements. Select the parameters needed as *area* and *limit to threshold*.
3. Analyze onglet > Analyze particles. Default value for size (0 to infinity) and circularity (0.00–1.00) shows outlines or masks. Summary will give the total area of RB.
4. For measuring the number of nuclei in the image, the same procedure is applied.

4 Notes

1. As accepted, Sertoli cells also eliminate apoptotic germ cells [31] at different stages of their differentiation, which form during spermatogenesis. Nevertheless, the mechanism by which Sertoli cells provide the cleaning of seminiferous tubules from apoptotic germ cells does not seem to be described in terms of three-step-progressing classical phagocytosis process. Therefore, the issue on the fate of apoptotic germ cells is not of the scope of this chapter, devoted to the assessment of classical phagocytosis process in the seminiferous tubules.
2. We recommend checking for the quality of RB preparation by microscopy observation after cresyl violet staining. To this end, smear the suspension of RBs on gelatin-coated glass slide, dry it at 37 °C for 48 h, then proceed by cresyl violet staining.
3. Phagocytosis step 1 can be partly inhibited [30] by the pretreatment of RBs with annexin V, which specifically bind to externalized PS.
4. Absence of concentric Rac1 staining around substrates questions about the reality of future engulfment of substrates or about the type I phagocytosis response and should imply supplementary experiments including RhoA activation state measurement by pulldown or by confocal microscopy and assessment of step 2 (ingestion; *see* Subheading 3.4.2).
5. It should be noted that Rac1 activation is coupled with the binding of substrate to the phagocytic cup, but is as well necessary for triggering the ingestion of the substrate, and then participates also to step 2.
6. Cytochalasin D (actin polymerization inhibitor) and blebbistatin (myosin II inhibitor) are well-described phagocytosis ingestion step blockers.
7. Negative control by inhibiting actin polymerization or myosin II activation by cytochalasin D or blebbistatin should be realized. To this end before exposure to RBs, preincubate the

Sertoli cells with either cytochalasin D (final concentration 10 μM) or blebbistatin (final concentration 12.5 μM).

8. Lipid droplet production can be inhibited by bafilomycin A_1 treatment (final concentration 100 nM). Bafilomycin inhibits the fusion of lysosomes with phagosomes.

Acknowledgments

We specially thank Drs Michel Blanc (Ret.), Jean-Louis Dacheux (Ret.), and Rustem Uzbekov (Plateforme IBiSA de Microscopie Electronique, Université François Rabelais and CHU de Tours, France) for the help in setting on simplified methods of phagocytosis rate analysis in routine experiments. We thank Image-UP platform from Poitiers University and Imaging & Microscopy Technology Platform from IGBMC, Strasbourg.

References

1. Jégou B (1993) The Sertoli-germ cell communication network in mammals. Int Rev Cytol 147:25–96
2. Lacy D (1960) Light and electron microscopy, and its use in the study of factors influencing spermatogenesis in the rat. J R Microsc Soc 79:209–225
3. Maderna P, Godson C (2003) Phagocytosis of apoptotic cells and the resolution of inflammation. Biochim Biophys Acta 1639:141–151
4. Rabinovitch M (1995) Professional and non-professional phagocytes: an introduction. Trends Cell Biol 5:85–87
5. Metchnikoff E (1887) Sur la lutte des cellules de l'organisme contre l'invasion des microbes. Ann Inst Pasteur 1:321–345
6. Nydegger UE, Miescher A, Anner RM et al (1973) Serum and cellular factor involvement in nitroblue tetrazolium (NBT) reduction by human neutrophils. Klin Wochenschr 51:377–382
7. Albrecht D, Jungi TW (1993) Luminol-enhanced chemiluminescence induced in peripheral blood-derived human phagocytes: obligatory requirement of myeloperoxidase exocytosis by monocytes. J Leukoc Biol 54:300–306
8. Kampen AH, Tollersrud T, Larsen S et al (2004) Repeatability of flow cytometric and classical measurement of phagocytosis and respiratory burst in bovine polymorphonuclear leucocytes. Vet Immunol Immunopathol 97:105–114
9. Lemke G, Rothlin CV (2008) Immunobiology of the TAM receptors. Nat Rev Immunol 8(5):327–336
10. Irschik EU, Sgonc R, Böck G et al (2004) Retinal pigment epithelial phagocytosis and metabolism differ from those of macrophage. Ophthalmic Res 36:200–210
11. Shiratsuchi A, Osada Y, Nakanishi Y (2013) Differences in the mode of phagocytosis of bacteria between macrophages and testicular Sertoli cells. Drug Discov Ther 7(2):73–77
12. Kevany BM, Palczewsky K (2010) Phagocytosis of retinal rod and cone photoreceptors. Physiology 25:8–15
13. Leblond CP, Clermont Y (1952) Definition of the stages of the cycle of the seminiferous epithelium in the rat. Ann N Y Acad Sci 55(4):548–573
14. Oakberg EF (1956) Duration of spermatogenesis in the mouse and timing of stages of the cycle of the seminiferous epithelium. Am J Anat 99(3):507–516
15. Clermont Y (1963) The cycle of the seminiferous epithelium in man. Am J Anat 112:35–51
16. Clermont Y (1972) Kinetics of spermatogenesis in mammals: seminiferous epithelium cycle and spermatogonial renewal. Physiol Rev 52(1):198–236
17. Chemes H (1986) The phagocytic function of Sertoli cells: a morphological, biochemical and endocrinological study of lysosomes and acid phosphatase localization in the rat testis. Endocrinology 119(4):1673–1681

18. Blanco-Rodriguez J, Martinez-Garcia C (1999) Apoptosis is physiologically restricted to a specialized cytoplasmic compartment in rat spermatids. Biol Reprod 61:1541–1547
19. Russell LD, Ettlin RA, Hikim APS, Clegg ED (1990) Histological and histopathological evaluation of the testis. Cache River Press, St. Louis
20. Pineau C, Le Magueresse B, Courtens JL, Jégou B (1991) Study in vitro of the phagocytic function of Sertoli cells in the rat. Cell Tissue Res 264(3):589–598
21. Grandjean V, Sage J, Ranc F et al (1997) Stage-specific signals in germ line differentiation: control of Sertoli cell phagocytic activity by spermatogenic cells. Dev Biol 184:165–174
22. Gillot I, Jehi-Petri C, Gounon P et al (2005) Germ cells and fatty acids induce translocation of CD36 scavenger receptor to the plasma membrane of Sertoli cells. J Cell Sci 118:3027–3035
23. Yamada H, Ohashi E, Abe T et al (2007) Amphiphysin 1 is important for actin polymerization during phagocytosis. Mol Biol Cell 18(11):4669–4680
24. Otsuka A, Abe T, Watanabe M et al (2009) Dynamin 2 is required for actin assembly in phagocytosis in Sertoli cells. Biochem Biophys Res Commun 378:478–482
25. Hu W, Wang H, Xiong W et al (2006) Evaluation on the phagocytosis of apoptotic spermatogenic cells by Sertoli cells *in vitro* through detecting lipid droplet formation by Oil Red O staining. Reproduction 132:485–492
26. Eliott MR, Zheng S, Park D et al (2010) Unexpected requirement for ELMO1 in clearance of apoptotic germ cells *in vivo*. Nature 467:333–339
27. Yefimova MG, Sow A, Fontaine I et al (2008) Dimeric transferrin inhibits phagocytosis of residual bodies by testicular rat Sertoli cells. Biol Reprod 78(4):697–704
28. Meier T, Arni S, Malarkannan S et al (1992) Immunodetection of biotinylated lymphocyte-surface proteins by enhanced chemiluminescence: a nonradioactive method for cell-surface protein analysis. Anal Biochem 204:220–226
29. Shiratsuchi A, Umeda M, Ohba Y, Nakanishi Y (1997) Recognition of phosphatidylserine on the surface of apoptotic spermatogenic cells and subsequent phagocytosis by Sertoli cells of the rat. J Biol Chem 272(4):2354–2358
30. Yefimova MG, Messaddeq N, Harnois T et al (2013) A chimerical phagocytosis model reveals the recruitment by Sertoli cells of autophagy for the degradation of ingested illegitimate substrates. Autophagy 9(5): 653–666
31. Shiratsuchi A, Kawasaki Y, Ikemoto M et al (1999) Role of class B scavenger receptor type I in phagocytosis of apoptotic rat spermatogenic cells by Sertoli cells. J Biol Chem 274(9):5901–5908
32. Kawasaki Y, Nakagawa A, Nagaosa K et al (2002) Phosphatidylserine binding of class B scavenger receptor type I, a phagocytosis receptor of testicular Sertoli cells. J Biol Chem 277:27559–27566
33. Lu Q, Gore M, Zhang Q et al (1999) Tyro-3 family receptors are essential regulators of mammalian spermatogenesis. Nature 398:723–728
34. Xiong W, Chen Y, Wang H et al (2008) Gas6 and the Tyro 3 receptor tyrosine kinase subfamily regulate the phagocytic function of Sertoli cells. Reproduction 135:77–87
35. Chen Y, Wang H, Qi N et al (2009) Functions of TAM RTKs in regulating spermatogenesis and male fertility in mice. Reproduction 138:655–666

Chapter 9

A Method for In Vivo Induction and Ultrastructural Detection of Mitophagy in Sertoli Cells

Nabil Eid, Yuko Ito, Akio Horibe, Hitomi Hamaoka, and Yoichi Kondo

Abstract

An emerging body of evidences based on in vitro studies indicate that mitophagy (selective autophagic clearance of damaged mitochondria) is a prosurvival mechanism, specifically under exposure to various stressors. Sertoli cells (SCs) play essential roles in maintenance of spermatogenesis via paracrine interactions with germ cells and other somatic cells in the testis; however, studies investigating mitophagy in SCs are still very few. In this chapter, we give a brief review of mechanisms and detection methods of mitophagy in SCs based on our recent publications on animal models of ethanol toxicity and current literature. In addition, we provide a method for induction and ultrastructural identification of mitophagy in SCs of adult Wistar rats using a single intraperitoneal injection (5 g/kg) of ethanol. Proper understanding of mitophagy features and mechanisms in SCs may have therapeutic implications for infertility associated with alcoholism and other diseases characterized by mitochondrial dysfunction.

Key words Autophagy, Ethanol, Mitophagy, Sertoli cell, TEM

1 Introduction

Autophagy is a prosurvival pathway for clearance of cellular components following multiple forms of stress such as oxidative stress, DNA damage, and lipid overload. Autophagy is characterized by the formation of Beclin1-mediated isolation membranes, which engulf a region of the cell forming autophagosomes via microtubule-associated protein light chain 3 (LC3). The autophagosomes then fuse with lysosomes via lysosomal-associated membrane protein 2 (LAMP-2), forming autolysosomes, where the contents of the cargo are digested by lysosomal cathepsins [1–4]. Based on in vitro studies, a growing body of evidences indicates that selective autophagic elimination of damaged mitochondria, referred to as mitophagy, is a prosurvival mechanism upon cellular exposure to various damaging agents [5–7]. In mammals, different mitophagy mechanisms, including the mitophagy receptors NIX, BNIP3, and FUNDC1 and the PINK1-Parkin pathway, participate in the

Marco G. Alves and Pedro F. Oliveira (eds.), *Sertoli Cells: Methods and Protocols*, Methods in Molecular Biology, vol. 1748, https://doi.org/10.1007/978-1-4939-7698-0_9,

selective clearance of damaged pro-apoptotic mitochondria. In response to damaging agents, PINK1 accumulates on the outer mitochondrial membrane (OMM), resulting in Parkin mitochondrial translocation, and subsequent ubiquitination of various proteins at the OMM. PINK1-Parkin accumulation on the surface of damaged mitochondria is a signal for recognition and clearance by autophagic machinery through the formation of LC3-mediated mitophagosomes, which fuse with lysosomes forming mitophagolysosomes [8–10]. Excessive alcohol consumption in humans and experimental animals has been reported to induce hepatic damage via mechanisms such as oxidative stress, DNA damage, and mitochondrial dysfunction [2–4]. A few studies including ours and others reported the involvement of PINK1-Parkin pathway in hepatocyte mitophagy in an animal model of binge ethanol exposure [11–13]. In these studies, we used various techniques indicating enhanced mitophagy in hepatocytes of ethanol-treated rats (ETRs) such as transmission electron microscopy (TEM), immunoelectron microscopy (IEM) of mitophagy proteins, and double labeling immunofluorescence (IF) of mitochondrial markers and mitophagy proteins. In addition, we reported in previous studies in an animal model of chronic alcoholism that mitophagy was upregulated in hepatocytes and SCs, possibly as protective mechanism reflecting ethanol toxicity [2, 14]. A schema showing mitophagy pathway in SCs and detection methods in brief is shown in Fig. 1. Although SCs play a major role in germ cells survival, and their death may result in marked germ cell loss and infertility [15, 16], studies investigating mitophagy in SCs in animal models are still very few [17]. Here we use an animal model of binge ethanol exposure for the induction of mitophagy in SCs as recently reported in hepatocytes and thymic macrophages [12, 13, 18]. Mitophagy in SCs of acute ethanol-treated rats (ETRs) is investigated using TEM, which is seen as the gold standard for autophagy and mitophagy identification [13, 19, 20].

2 Materials

1. Adult male Wistar rats (12 weeks old) (Shizuoka, Japan). Their body weight is around 250–300 g.
2. Buffer 0.1 M phosphate buffer (PB) (1 litre) (pH 7.4), prepared by mixture of the following reagents: 2.97 g $NaH_2PO_4 \cdot 2H_2O$, 29 g $Na_2H\ PO_4 \cdot 12H_2O$. The pH should be adjusted to 7.4 as any decrease or increase of this pH may hamper the fixation process.
3. Primary fixative (pre-fixative): 2% (w/v) paraformaldehyde and 2.5% (v/v) glutaraldehyde in 0.1 M phosphate buffer (PB) (pH 7.4).

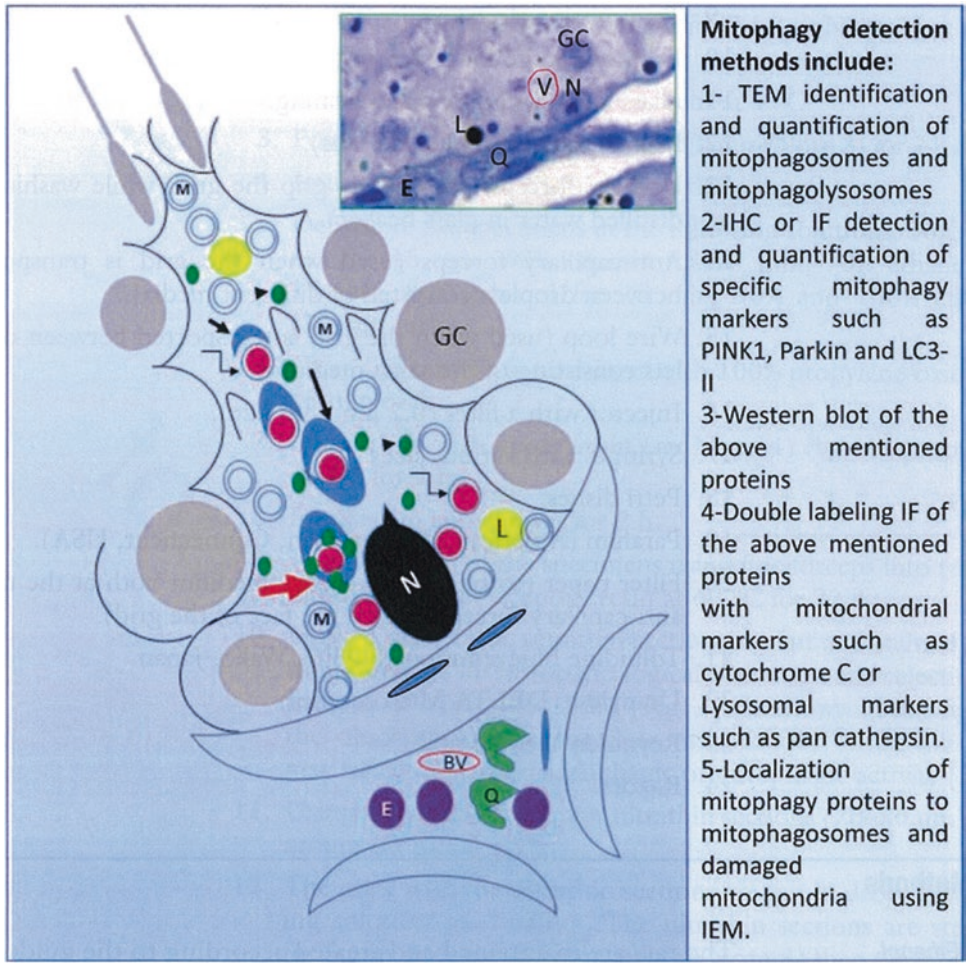

Fig. 1 A schema showing mitophagy in Sertoli cells based on animal models of alcoholism. Damaged mitochondria (broken arrows) are recognized by autophagic machinery and subsequently engulfed by isolation membranes (short black arrow) forming LC3-mediated mitophagosomes (long black arrow). The mitophagosomes then fuse with lysosomes (arrow heads) via LAMP-2 forming mitophagolysosomes (red arrow), where the contents of the cargo are lysed by cathepsins as prosurvival mechanism. The framed microphotograph is toluidine blue-stained semithin section for understanding the schema. The framed column on the right side of the schema summarizes the main methods for mitophagy detection. *N* nucleus of Sertoli cell, *M* mitochondria, *L* lipid droplet, *Q* macrophage, *E* cell of Leydig, *BV* blood vessel, *GC* germ cell, *V* vacuole

4. Secondary fixative (post-fixative): 1% (w/v) osmium tetroxide in 0.1 M PB (pH 7.4).
5. A series of graded ethanol solution: 30%, 50%, 70%, 80%, 90%, 99.5% (v/v in dH_2O), absolute ethanol.
6. Propylene oxide (C_3H_6O).
7. Embedding resin: Epoxy resin (total volume: 20.4 mL).

Mix 9.41 ml of Epon 812 with 5.65 ml methyl nadic anhydride (MNA), 4.95 of dodecenyl succinic anhydride (DDSA), and 0.4 ml of 2,4,6-dimethylaminomethyl phenol (DMP-30).

8. Ultramicrotome (RMC Power Tome-XL, USA).
9. Transmission electron microscope (Hitachi-7650, Tokyo, Japan).
10. Diamond knife for ultrathin sectioning (Diatome).
11. Glass knife for semithin sectioning.
12. Nickel grids (150–300 meshes).
13. Locking forceps (to securely grip the grid, while washing in distilled water in glass beaker).
14. Anti-capillary forceps (used when the grid is transported between droplets consisted of different media).
15. Wire loop (used when the grid is transported between droplets consisting of the same medium).
16. Injector with a filter (0.2 μm pore size).
17. Syringes with various sizes.
18. Petri dishes.
19. Parafilm (American National Can, Connecticut, USA).
20. Filter paper (to blot the excessive medium both at the tip of anti-capillary forceps and on the face of the grid).
21. Toluidine blue solution (0.05%), Wako, Japan.
22. Uranyless (DELTA Microscopies).
23. Reynolds' lead citrate.
24. Razors.

3 Methods

3.1 Ethanol Administration

The rats are maintained and treated according to the guidelines set by the Experimental Animal Research Committee of Osaka Medical College (*see* **Note 1**). The animals receive a single 5 g/kg intraperitoneal dose of ethanol (40% v/v) consistent with animal models of binge ethanol exposure [12, 18, 21–24]. A control group receive the same volume of physiological saline. For the time-course study, animals are sacrificed, and testicular samples are taken at 0, 3, 6, and 24 h after ethanol administration. The experiments were performed in accordance with the 3R's principle – reduction, refinement, and replacement. The time period 24 h is selected in this study for mitophagy detection as it showed the highest autophagic activity as previously reported [18].

3.2 Preparation of Testicular Samples for Light and Electron Microscopic Studies

1. After short exposure to inhalational anesthesia, the animals are killed by cervical dislocation, and testes are quickly removed and cut longitudinally into two halves with rinse in ice-cold physiological saline (4 °C) (10–20 ml). Testes are then cut into small pieces (2–4 mm^3) using clean razors and immersed in the primary fixative for 2 h (*see* **Note 2**) at room temperature (RT).
2. Rinse and immerse in PB overnight at 4 °C.
3. Postfix with osmium tetroxide (OsO_4) (*see* **Note 3**) for 2 h at RT.
4. Immerse in 0.1 M PB for 5 min, three times.
5. Dehydrate the specimens in the following solutions: 30% ethanol for 15 min, 50% ethanol for 15 min, 70% ethanol for 15 min, 80% ethanol for 15 min, 90% and 100% ethanol (30 min each).
6. Clear and rehydrate two times with 100% propylene oxide for 15 min each.
7. Immerse in 50% epoxy resin (*see* **Note 4**) (v/v in propylene oxide) for 2 h.
8. Immerse in epoxy resin for 2 h.
9. Transfer tissue of the specimens using fine forceps into rubber molds and cover in epoxy resin at 60 °C for 72 h.
10. Using a glass knife, semithin sections are cut and stained with toluidine blue for histopathological evaluation and selection of the area of interest for TEM (Fig. 2). As shown in this figure, the observation of perinuclear vacuolization in Sertoli cells may reflect enhanced autophagic or mitophagic activity [25].
11. Using a diamond knife, cut ultrathin sections (70–80 nm) and mount on nickel grids.
12. The grids with the ultrathin sections are put in drops of staining solution on Parafilm. The ultrathin sections are stained for 5 min in drops of Uranyless (*see* **Note 5**) then for 5 min in 1% lead citrate. The staining step is performed in covered Petri dishes.
13. The stained sections are stored in special grid box, examined and photographed (Fig. 3a–c) under Hitachi TEM.

3.3 Ultrastructural Definition of Mitochondria and Mitophagy in Sertoli Cells

Normal mitochondria in Sertoli cells are defined as structures with a smooth outer membrane and an inner membrane contiguous with vesicular type of cristae and containing a granular, moderately electron-dense internal matrix [14, 26, 27]. Mitophagy is characterized by presence of damaged mitochondria (isolated or clustered), often seen enclosed by isolation membranes or

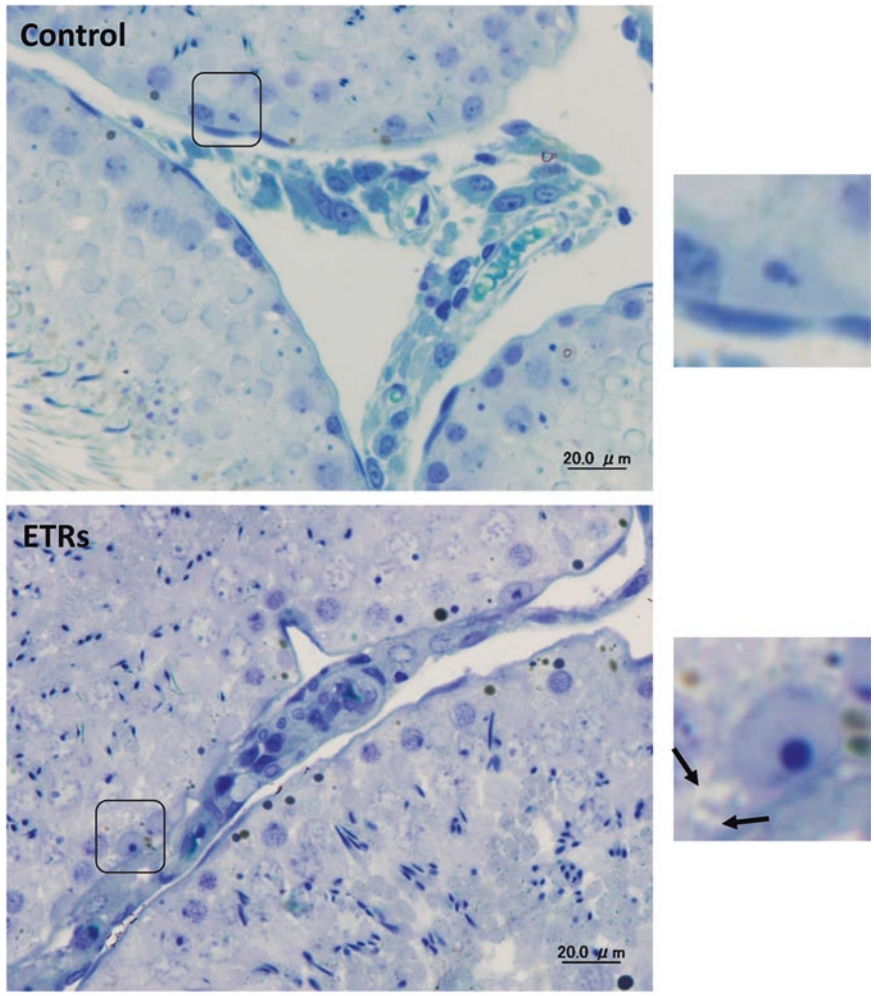

Fig. 2 Toluidine blue-stained semithin sections showing enhanced perinuclear vacuolization (arrows) in SCs of acute ETRs. The framed areas are magnified on the right

sequestrated inside mitophagosomes with double autophagosomal limiting membranes (*see* **Note 6**). These abnormal mitochondria have morphological alterations (such as rupture of mitochondrial membranes and injured or lost cristae) and usually are located at the perinuclear region [12, 14] (*see* **Note 7**). Mitophagolysosomes are defined by a single membrane that contains degenerating (and often unrecognizable) mitochondria associated with electron-dense material [12, 27]. As shown in Fig. 3, ethanol enhanced the formation of mitophagosomes and mitophagolysosomes, in SCs, consistent with the above mentioned ultrastructural definition of mitochondria and mitophagy.

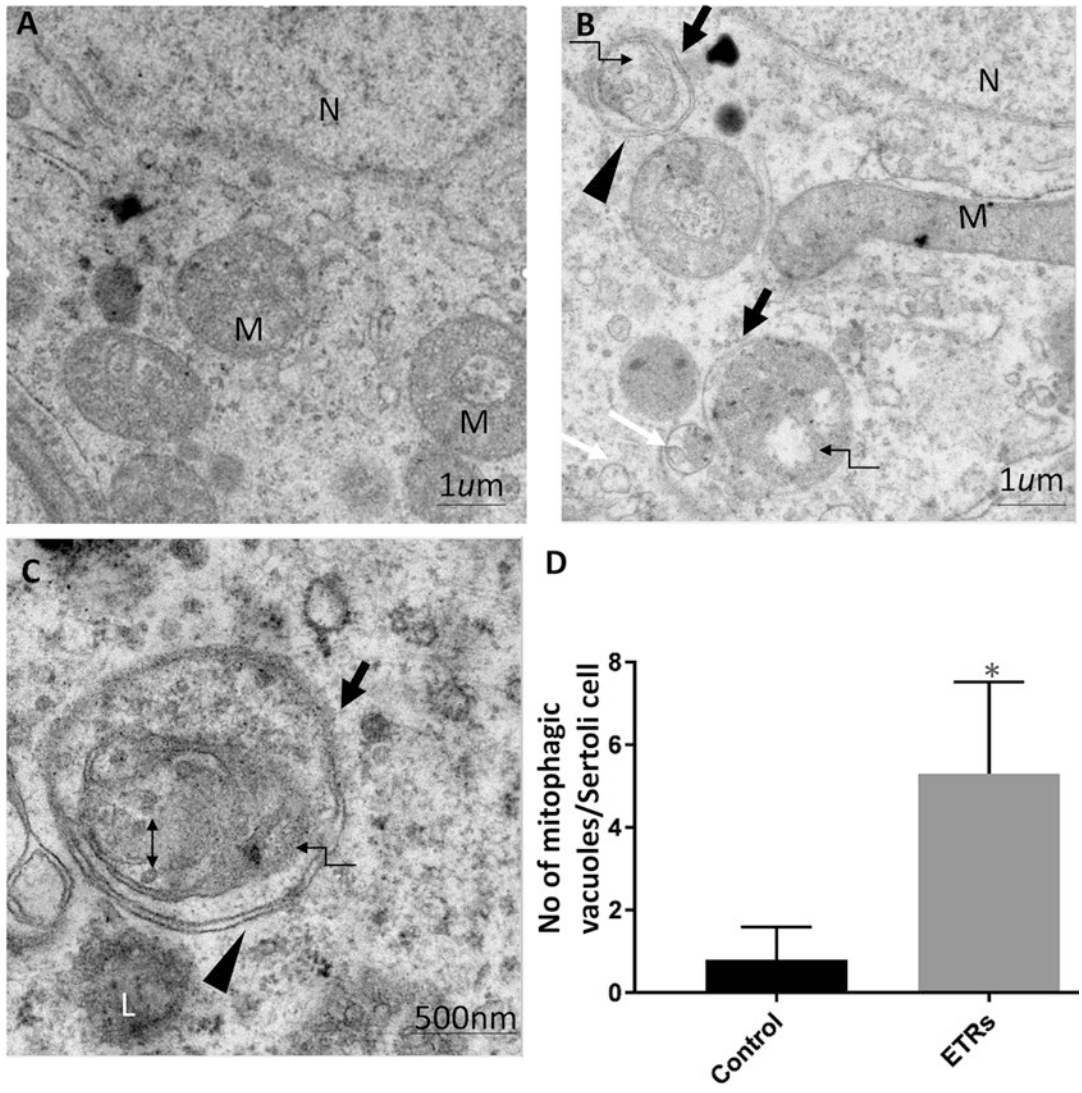

Fig. 3 Enhanced formation of mitophagic vacuoles (mitophagosomes and mitophagolysosomes) in SCs of acute ETRs. A, control; B, C, ETRs. The broken arrows indicate damaged mitochondria within mitophagosomes (black arrows) characterized by double-layer limiting membranes (arrow heads). The white arrows indicate mitophagolysosomes. The double head arrow in C marks remains of vesicular cristae in mitophagosome. *M* mitochondria, *N* nucleus of SC, *L* lysosome. The histogram (D) depicts quantification of mitophagic vacuoles in control and ETRs. $^{*}P < 0.05$

3.4 Quantification of Mitophagy in Sertoli Cells

For quantification of mitophagic vacuoles (mitophagosomes and mitophagolysosomes) in Sertoli cells (Fig. 3c), ten lower magnification photomicrographs from the testes of controls and ETRs (×2500–3000) are selected (each image containing at least one Sertoli cell nucleus) [14, 28]. Data are analyzed with the statistical software program PRISM 7. All data involving two groups (control and ETRs) are analyzed using Student's *t*-test.

In conclusion, TEM is the gold standard and confirmatory method for autophagy detection. SC mitophagy may be a prosurvival mechanism upon exposure to various toxicants, including ethanol. Ultrastructural identification of enhanced mitophagy in SCs of ETRs may help in understanding the various testicular pathologies associated with or induced by mitochondrial damage, inducing fertility problems.

4 Notes

1. Experiments involving live rodents must comply with the local regulations in research institutes. The rats were housed under controlled temperature (24 ± 1 °C), humidity (55 ± 5%), and lighting (lights on, 06:00–18:00). They have free access to standard rodent food and water. They are grouped and housed in standard cages.
2. Glutaraldehyde and paraformaldehyde are toxic, so it is better to wear mask during handling of these reagents.
3. Dissolve OsO_4 at 1–2 days before usage because it is difficult to dissolve it within a short time. Please note that OsO_4 is extremely toxic and should be handled with great care.
4. Epoxy resin is a carcinogen; therefore, it should be handled with gloves.
5. Uranyless stain (Delta Microscopy, France) is composed of lanthanides (La, Dy, Gd) and other compounds [29, 30]. It is less toxic than ordinary uranyl acetate, but the staining contrast may be weaker than commonly used and more toxic uranyl acetate.
6. The mitophagosomes, which are characterized by damaged mitochondria encircled with double autophagosomal membrane, should be differentiated from rough endoplasmic reticulum surrounding normal mitochondria and/or swollen mitochondria [19, 20].
7. The accumulation of mitophagosomes in the perinuclear area may indicate the activation of PINK1-Parkin pathway [2, 12].

Acknowledgments

This manuscript is partially supported by Grant-in-Aid for Scientific Research (Kakenhi) (No., 16K11073) from The Ministry of Education, Culture, Sports, Science and Technology, Japan. We thank Prof. Yoshinori Otsuki for critical advice and support of this study.

References

1. Kroemer G, Marino G, Levine B (2010) Autophagy and the integrated stress response. Mol Cell 40:280–293
2. Eid N, Ito Y, Maemura K et al (2013) Elevated autophagic sequestration of mitochondria and lipid droplets in steatotic hepatocytes of chronic ethanol treated rats: an immunohistochemical and electron microscopic study. J Mol Histol 44:311–326
3. Thomes PG, Ehlers RA, Trambly CS et al (2014) Multilevel regulation of autophagosome content by ethanol oxidation in HepG2 cells. Autophagy 9:63–73
4. Eid N, Ito Y, Otsuki Y (2013) The autophagic response to alcohol toxicity: the missing layer. J Hepatol 59:398
5. Sica V, Galluzzi L, Bravo-San Pedro JM et al (2015) Organelle-specific initiation of autophagy. Mol Cell 59:522–539
6. Kim I, Rodriguez-Enriquez S, Lemasters JJ (2007) Selective degradation of mitochondria by mitophagy. Arch Biochem Biophys 462:245–253
7. Youle RJ, Narendra DP (2011) Mechanisms of mitophagy. Nat Rev Mol Cell Biol 12:9–14
8. Zhu Y, Chen G, Chen L et al (2014) Monitoring mitophagy in mammalian cells. Methods Enzymol 547:39–55
9. Hamacher-Brady A, Brady NR (2016) Mitophagy programs: mechanisms and physiological implications of mitochondrial targeting by autophagy. Cell Mol Life Sci 73:775–795
10. Roberts RF, Tang MY, Fon EA, Durcan TM (2016) Defending the mitochondria: the pathways of mitophagy and mitochondrial-derived vesicles. Int J Biochem Cell Biol 79:427–436
11. Williams JA, Ni HM, Ding Y et al (2015) Parkin regulates mitophagy and mitochondrial function to protect against alcohol-induced liver injury and steatosis in mice. Am J Physiol Gastrointest Liver Physiol 309:324–340
12. Eid N, Ito Y, Horibe A et al (2016) Ethanol-induced mitophagy in liver is associated with activation of the PINK1-Parkin pathway triggered by oxidative DNA damage. Histol Histopathol 31:1143–1159
13. Eid N, Ito Y, Otsuki Y (2016) Triggering of Parkin mitochondrial translocation in mitophagy: implications for liver diseases. Front Pharmacol 7:100. https://doi.org/10.3389/fphar.2016.00100
14. Eid N, Ito Y, Otsuki Y (2012) Enhanced mitophagy in Sertoli cells of ethanol-treated rats: morphological evidence and clinical relevance. J Mol Histol 43:71–80
15. Rato L, Meneses MJ, Silva BM et al (2016) New insights on hormones and factors that modulate Sertoli cell metabolism. Histol Histopathol 31:499–513
16. Bao ZQ, Liao TT, Yang WR et al (2017) Heat stress-induced autophagy promotes lactate secretion in cultured immature boar Sertoli cells by inhibiting apoptosis and driving SLC2A3, LDHA, and SLC16A1 expression. Theriogenology 87:339–3348
17. Weckman A, Di Ieva A, Rotondo F et al (2014) Autophagy in the endocrine glands. J Mol Endocrinol 52:151–163
18. Betsuyaku T, Eid N, Ito Y et al (2017) Ethanol enhances thymocyte apoptosis and autophagy in macrophages of rat thymi. Histol Histopathol 32:963–975
19. Martinet W, Timmermans JP, De Meyer GR (2014) Methods to assess autophagy in situ-transmission electron microscopy versus immunohistochemistry. Methods Enzymol 543:89–114
20. Eskelinen EL (2008) To be or not to be? Examples of incorrect identification of autophagic compartments in conventional transmission electron microscopy of mammalian cells. Autophagy 4:257–260
21. D'Souza El-Guindy NB, Kovacs EJ, De Witte P et al (2010) Laboratory models available to study alcohol-induced organ damage and immune variations: choosing the appropriate model. Alcohol Clin Exp Res 3:1489–1511
22. Zhou Z, Wang L, Song Z, Lambert JC, McClain CJ, Kang YJ (2003) A critical involvement of oxidative stress in acute alcohol induced hepatic TNF-alpha production. Am J Pathol 163:1137–1146
23. Chen YY, Zhang CL, Zhao XL et al (2014) Inhibition of cytochrome P4502E1 by chlormethiazole attenuated acute ethanol-induced fatty liver. Chem Biol Interact 222:18–26
24. Nogales F, Rua RM, Ojeda ML et al (2014) Oral or intraperitoneal binge drinking and oxidative balance in adolescent rats. Chem Res Toxicol 27:1926–1933
25. Skuk D, Goulet M, Paradis M et al (2013) Myopathy in a rhesus monkey with biopsy findings similar to human sporadic inclusion body myositis. Neuromuscul Disord 23:155–159
26. Kaya M, Harrison RG (1976) The ultrastructural relationships between Sertoli cells and spermatogenic cells in the rat. J Anat 121: 279–290
27. Teckman JH, An JK, Blomenkamp K et al (2004) Mitochondrial autophagy and injury in the liver

in alpha1-antitrypsin deficiency. Am J Physiol Gastrointest Liver Physiol 286:851–862

28. Watanabe E, Muenzer JT, Hawkins WG et al (2009) Sepsis induces extensive autophagic vacuolization in hepatocytes: a clinical and laboratory-based study. Lab Investig 89:549–561
29. Benmeradi N, Payre B, Goodman SL (2015) Easier and safer biological staining: high contrast uranyless staining of TEM grids using mPrep/g capsules. Microsc Microanal 21(Suppl 3):721–722. https://doi.org/10.1017/S1431927615004407
30. Floriot S, Vesque C, Rodriguez S, Bourgain-Guglielmetti F et al (2015) C-Nap1 mutation affects centriole cohesion and is associated with a Seckel-like syndrome in cattle. Nat Commun 23: 6894. https://doi.org/10.1038/ncomms7894

Chapter 10

Assessing Autophagy in Sertoli Cells

Chao Liu, Jehangir Khan, and Wei Li

Abstract

Autophagy is an important cellular homeostatic process, it degrades most long-lived proteins and some organelles by lysosome to provide raw materials for the survival of the cells during nutrient or energy deprivation condition. Autophagy is active in Sertoli cells and involved in many cellular processes. However, the precise role of autophagy in Sertoli cells is still largely unknown. Thus, the assessment of autophagy in Sertoli cells should be helpful for investigating the functional roles of autophagy in Sertoli cells. This chapter describes some methods for assessing autophagy in Sertoli cells, including detection of LC3 maturation/aggregation, transmission electron microscopy, half-life assessments of long-lived proteins, immunofluorescence microscopy, and co-localization of autophagy-targeted proteins with autophagy components or lysosomal proteins.

Key words Autophagy, Sertoli cell, Transmission electron microscopy, LC3, Immunoblotting, Immunofluorescence

1 Introduction

Autophagy is an evolutionarily conserved membrane trafficking process that delivers cytoplasmic material such as long-lived proteins and organelles to the lysosome for degradation [1, 2]. Autophagy has been implicated in various physiological processes including cell growth, adaptation to stress conditions, anti-aging mechanisms, intracellular quality control, renovation during development and differentiation, and the biogenesis of organelles such as cilia and acrosome [3–6]. At least three types of autophagy have been defined, including macroautophagy, microautophagy, and chaperone-mediated autophagy [2, 7, 8]. Microautophagy involves direct engulfment of cytoplasmic cargos through the invagination and vesicle scission into the lysosomal lumen, which is the nonselective lysosomal degradative process [7]. The direct translocation of cytoplasmic proteins across the lysosomal membrane, which requires protein unfolding by chaperone proteins but not vesicle, is known as chaperone-mediated autophagy [8]. The most extensively investigated is macroautophagy, which is mediated by a special

Marco G. Alves and Pedro F. Oliveira (eds.), *Sertoli Cells: Methods and Protocols*, Methods in Molecular Biology, vol. 1748, https://doi.org/10.1007/978-1-4939-7698-0_10,

double-membrane organelle termed the autophagosome. The canonical macroautophagy is initiated from an isolated membrane and followed by the formation of a double-membrane autophagosome to engulf cytoplasmic cargos that then fuses with lysosomes for degradation, and then, the amino acids and other small molecules generated by autophagic degradation are delivered back to the cytoplasm for recycling or energy production [1, 2, 9].

Macroautophagy will be the focus of this chapter and referred to as autophagy hereafter. The process of autophagy includes the initiation, nucleation, expansion, maturation, and degradation [2, 9]. More than 40 autophagy-related (ATG) proteins have been characterized during autophagy, which consist of several functional units: ULK1 kinase complex, the PI3K complex, ATG9-ATG2-WIPI1/ATG18 complex, and two ubiquitin-like conjugation systems [6, 10, 11]. Nutrient, carbon, or nucleic acid starvation and some physiological stress stimuli could trigger the induction of autophagy in many organisms through intricate regulatory mechanisms via numerous kinases and signaling pathways with the Ser/Thr kinase TOR (target of rapamycin) at its center [2, 9, 10]. TOR could modulate the ULK1 complex undergoing a series of phosphorylation/dephosphorylation events and lead to the activation of this complex and the initiation of autophagy [12, 13]. After the induction of autophagy, the phagophore, a cup-shaped double-membrane structure, is gradually formed [12–14]. In mammalian cells, the nucleation of the phagophore membrane takes place at the omegasome through the recruitment of the ULK1 and PIK3C3 complexes to the nucleation site containing the transmembrane protein VMP1 [12, 14, 15]. The phosphatidylinositol 3-phosphate (PtdIns3P) produced by membrane-bound PIK3C3 complex at the nucleation site further enhances membrane bending and reinforce the localization of the ULK1 complex and other ATG proteins at the growing membrane [12, 14, 16]. And then, an ubiquitin-activating E1-like enzyme, ATG7, activates ATG12 and then facilitates ATG12-ATG5-ATG16L1 complex formation, which works as an E3 ligase for the second ubiquitin-like conjugation system, to promote LC3 conjugating to the growing membrane. As a scaffold protein, the LC3-lipid-containing membrane drives membrane expansion and vesicle completion to form an autophagosome [2, 10, 12, 14]. Once fused with a lysosome, the inner proteins of the autophagosome are eventually degraded in autolysosomes [10]. To investigate the mechanism and functional roles of autophagy, many routine methods have been developed to detect different stages of the autophagy pathway, such as early autophagosome, autolysosome, and autophagic degradation products [2, 17]. And these methods could also be used coordinately with each other to determine whether an increase in intermediates in the pathway represents a true increase in autophagic degradation or a block in the completion of the autophagic pathway [2, 17].

Sertoli cell is an important somatic cell in the seminiferous epithelium and plays key roles in the control of spermatogenesis [18, 19]. Autophagy is also active in Sertoli cells [20–23], where it is involved in the clearance of SHBG/ABP (sex hormone-binding globulin) that is selectively regulated by testosterone and ectoplasmic specialization assembly [20, 24]. However, the role of autophagy in Sertoli cells is still largely unknown. The assessment of autophagy in Sertoli cells should be helpful for further investigating the functional roles of autophagy in Sertoli cells. For instance, the transmission electron microscopy (TEM) is the most reliable and conventional technique to visualize autophagic vacuolization; biochemical methods and techniques could be designed to measure the aggregation of autophagosome markers (such as LC3 and SQSTM1/p62) and allow for the monitoring of autophagy in Sertoli cells. Here, we will provide an overview of routine methods for assessing autophagy in Sertoli cells.

2 Materials

2.1 Immunofluorescence Analysis of Autophagy Components

1. PBS (1×): 137 mM NaCl, 2.7 mM KCl, 4.3 mM Na_2HPO_4, 1.4 mM KH_2PO_4 in deionized water (dH_2O), adjust pH to 7.4 with 2 N NaOH.
2. 4% PFA: 4% paraformaldehyde in PBS, adjust pH to 7.4 with 2 N NaOH.
3. Sodium citrate buffer: 1.8 mM citric acid, 8.2 mM sodium citrate, adjust pH to 6.0 with citric acid.
4. 5% BSA: To PBS add 5% (w/v) bovine serum albumen (BSA) and store at 4 °C.
5. Primary antibody solution: predicted primary antibody of autophagy components, 1.5% (w/v) BSA in PBS.
6. Secondary antibody solution: predicted secondary antibody in PBS.
7. DAPI: Stock solution, 5 mg/mL in distilled water. Store in 40 mL aliquots at −20 °C in Eppendorf tubes in the dark. Working stain, 0.5 mg/mL in PBS in the dark.
8. Mounting medium.
9. 3-Aminopropyl-triethoxysilane (APES).

2.2 Immunoblotting Analysis of LC3

1. F12-DMEM: Dulbecco's Modified Eagle's Medium-Ham's Nutrient Mixture F-12.
2. Collagenase IV from *Clostridium histolyticum*, type IV.
3. DNase I from bovine pancreas, lyophilized.
4. Hyaluronidase type III.

5. Trypsin from bovine pancreas.
6. Sertoli cells culture medium: F12-DMEM containing 15% fetal calf serum and penicillin-streptomycin.
7. RIPA-like buffer: 25 mM Tris–HCl, pH 7.6, 150 mM NaCl, 1% Nonidet P-40, 1% sodium deoxycholate, 0.1% sodium dodecyl sulfate.
8. Phenylmethylsulfonyl fluoride (PMSF): 1 M stock solution in dimethyl sulfoxide (DMSO) to a final concentration of 1 mM.
9. Protease inhibitor cocktail.
10. 2× Loading buffer: 100 mM Tris–HCl, pH 6.8, 4% SDS, 20% glycerol, 200 mM dithiothreitol (DTT), and 0.2% bromophenol blue.
11. 15% Running gel: 2.3 mL of distilled water, 5.0 mL of 30% acrylamide solution, 2.5 mL of 1.5 M Tris–HCl, pH 8.8, 100 μL of 10% SDS, 100 μL of 10% APS, and 4 μL of TEMED.
12. Stacking gel: 2.7 mL of distilled water, 0.67 mL of 30% acrylamide solution, 0.5 mL of 1.0 M Tris–HCl, pH 6.8 [at 25 °C], 40 μL of 10% SDS, 40 μL of 10% APS, and 4 μL of TEMED.
13. Running buffer: 25 mM Tris, 192 mM glycine, and 0.1% (w/v) SDS. Store at room temperature.
14. Transfer buffer: 48 mM Tris, 39 mM glycine, 20% methanol (analytical grade).
15. Blocking buffer: 5% (w/v) nonfat dry milk in PBS.
16. Immunoblotting primary antibody solution: 1:1000 anti-LC3 (Sigma, L7543), 1% (w/v) BSA, 20 mM Tris–HCl, pH 7.5 at 25 °C, 0.1% NaN3, and 150 mM NaCl.
17. Immunoblotting secondary antibody solution: predicted secondary antibody in blocking buffer.

2.3 Transmission Electron Microscopy

1. 0.1 M cacodylate buffer: 5.35 g Na-cacodylic acid in 220 mL distilled water, adjust pH to 7.3 with 1 N HCl, and complete to 250 mL with distilled water.
2. 2.5% glutaraldehyde: 25% glutaraldehyde. Dilute to a final concentration of 2.5%.
3. 1.5% paraformaldehyde: 10% paraformaldehyde in distilled water, adjust pH to 7.3 with 2 N NaOH. Dilute to a final concentration of 1.5%.
4. 1% osmium tetroxide: dissolve 1 g osmium tetroxide (Sigma, 419494) in 100 mL distilled water. Store at 4 °C.
5. 2% uranyl acetate: dissolve 1 mL uranyl acetate (Zhong Jing Ke Yi, GS02625) in 49 mL distilled water. Store powder at RT. Radioactive.

6. Resin: SPI-Pon 812 Epoxy Embedding Kit (Spi Supplies, 02635-AB). Mix 13 mL SPI-Pon 812, 7 mL NMA, 8 mL DDSA, and 10–12 drops DMP-30. Store at 4 °C and keep dry.
7. Uranyl acetate for staining: dissolve 1 mL uranyl acetate in 99 mL of distilled water. Store in 10 mL Norm-Ject syringes with a 0.22 μm filter at the tip of the syringe. Light sensitive, cover syringe with aluminum foil. Stable for several months at 4 °C.
8. Lead citrate for staining of thin sections: Solution A: lead nitrate 1 M, i.e., 3.3 g in 10 mL water. Solution B: trisodic sodium citrate 1 M, i.e., 3.57 g in 10 mL water. Solution C: NaOH 1 N, i.e., 1 g in 25 mL water. To 16 mL of boiled distilled water, add 3 mL of solution B and mix gently with hand. Add 2 mL of solution A and mix gently with hand. A milky precipitate will form. Add, dropwise, 4 mL of solution C while mixing gently with hand. The precipitate must disappear completely. If not, discard and start over. Dispatch in 2 or 5 mL syringes with a 0.22 μm filter at the tip of the syringe. Stable for several months at 4 °C.

2.4 GFP-LC3 Lysosomal Delivery and Proteolysis

1. Opti-MEM: Opti-MEM reduced serum medium.
2. Lipofectamine 2000.

2.5 Turnover of Autophagic Substrate Proteins

1. Cycloheximide.
2. TAP buffer: 10% glycerol, 50 mM HEPES–KOH, pH 7.5, 100 mM KCl, 2 mM EDTA, 0.1% NP-40, 10 mM NaF, 0.25 mM Na_3VO_4, 50 mM β-glycerolphosphate, 2 mM DTT.
3. IP buffer: 20 mM Tris–HCl, pH 7.4, 2 mM EGTA, 1% NP-40.
4. Protein A-Sepharose.

2.6 Antibody

1. LC3 for immunofluorescence.
2. LAMP2 for immunofluorescence.
3. LC3 for immunoblotting.
4. SQSTM1/p62 for immunoblotting.
5. LC3 for immunoprecipitation.
6. Secondary antibodies for immunofluorescence: goat anti-rabbit FITC-conjugated secondary antibody, goat anti-mouse FITC-conjugated secondary antibody, goat anti-mouse TRITC-conjugated secondary antibody, goat anti-rabbit TRITC-conjugated secondary antibody, goat anti-rat TRITC-conjugated secondary antibody.
7. Secondary antibodies for immunoblotting: Alexa Fluor 680-conjugated goat anti-mouse and Alexa Fluor 680-conjugated goat anti-rabbit.

3 Methods

3.1 Immunofluorescence Analysis of Autophagy Components

As for the autophagic pathway, many molecules are very good marker proteins for the detection of autophagic membranes, such as ATG12-ATG5 and ATG16L which are specific markers for the isolation membrane and microtubule-associated protein 1A/1B-light chain 3 (LC3) which is a general marker for autophagosome membranes [2, 17, 25]. Their localizations are easily examined by the immunofluorescence analysis.

1. Kill adult male mice by cervical dislocation immediately. Lay each animal on its back; sterilize the ventral surface with 70% ethanol. Remove testes from the abdomen with a pair of surgical scissors. Wash testes with PBS immediately, and repeat twice. Fix testes in 4% paraformaldehyde (PFA) in PBS pH 7.4 at room temperature (RT) for up to 24 h, stored in 70% ethanol.
2. Embed testes in paraffin.
3. Cut 5-μm-thick testis sections and mount on 3-aminopropyl-triethoxysilane (APE) precoated glass slide.
4. Deparaffinize in xylene 3 × 10 min and hydrate in an ethanol series (3 × 5 min of 100%, 5 min each of 95%, 80%, 70%).
5. Rinse once in PBS and boil for 15 min in sodium citrate buffer for antigen retrieval. Chill the samples at RT.
6. Rinse 3 × 5 min in PBS at RT.
7. Incubate in 5% BSA in PBS (pH 7.4) at RT for 30 min.
8. Rinse 3 × 5 min in PBS at RT.
9. Incubate in primary antibody solution at 4 °C overnight (*see* **Note 1**).
10. Rinse 3 × 5 min in PBS at RT.
11. Incubate in secondary antibody solution at 37 °C for 60 min.
12. Rinse 3 × 5 min in PBS at RT.
13. Incubate in 1 × DAPI solution at RT for 5 min.
14. Rinse 2 × 5 min in PBS at RT.
15. Add one drop mounting medium on the samples. Put the slide facedown on the top of the cover slip, and then turn the slide over. Remove excess mounting medium and seal cover slip with nail polish to prevent drying. Store in dark at −20 °C or 4 °C.
16. Fluorescent images are obtained using a fluorescence microscope.

3.2 Immunoblotting Analysis of LC3

Microtubule-associated protein 1A/1B-light chain 3 (LC3) is an important autophagic marker protein. During autophagy, a cytosolic form of LC3 (LC3-I, approximately 18 kDa) is conjugated to phosphatidylethanolamine to form LC3-phosphatidylethanolamine

conjugate (LC3-II, approximately 16 kDa), which is recruited to autophagosomal membranes (Fig. 1). Thus, the detection of LC3 by immunoblotting has become a reliable method for monitoring autophagy and autophagy-related processes [2, 17, 25, 26].

3.2.1 Primary Sertoli Cell Isolation

1. Testes are dissected from mice at 18 to 22 days of age immediately after euthanasia. Wash testes with PBS immediately. Repeat twice.
2. Decapsulate the testes under the dissection microscope. Wash the seminiferous tubules with PBS three times.
3. Incubate with 2 mg/mL collagenase IV and 0.5 mg/mL DNase I in F12/DMEM medium for 30 min at 37 °C on a shaker at 85 rpm.
4. Wash twice with F12-DMEM medium.
5. Incubate with 2 mg/mL collagenase IV, 0.5 mg/mL DNase I, and 1 mg/mL hyaluronidase type III for 10 min at 37 °C on a shaker at 85 rpm.

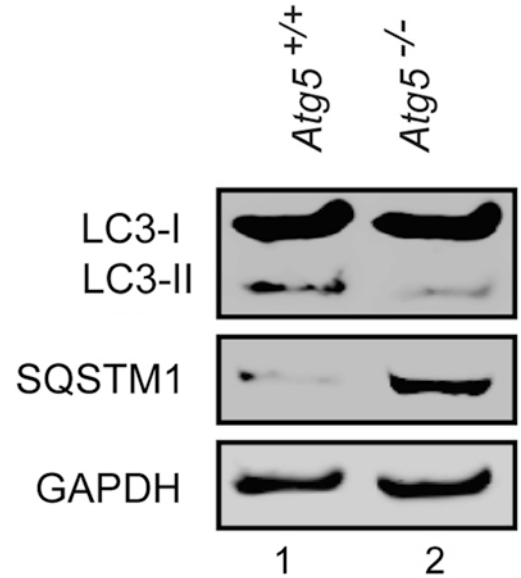

Fig. 1 Immunoblotting analysis of SQSTM1 and LC3 to monitor autophagic flux in Sertoli cells. LC3 is an important autophagic marker protein, and level of LC3-phosphatidylethanolamine conjugate (LC3-II) could indicate the activity of autophagy. In *Atg5*$^{+/+}$ Sertoli cells, LC3 II could be detected by immunoblotting (lane 1), suggesting autophagy is active in Sertoli cells. ATG5 is required for the initiation of autophagy. In *Atg5*$^{-/-}$ Sertoli cells, LC3B-II is reduced (lane 2), indicating the deficiency of autophagy initiation. The autophagic substrate SQSTM1/p62 is accumulated in *Atg5*-deficient Sertoli cells (lane 2), suggesting the autophagic flux is disrupted in *Atg5* knockout Sertoli cells. Thus, the immunoblotting analysis of SQSTM1 and LC3 could monitor autophagic flux in Sertoli cells

6. Centrifuge 500 × *g* for 1 min at RT and wash with F12-DMEM medium. Repeat twice.
7. Incubate with 2 mg/mL collagenase I, 0.5 mg/mL DNase I, 2 mg/mL hyaluronidase, and 1 mg/mL trypsin for 30 min at 37 °C on a shaker at 85 rpm (*see* **Note 2**).
8. Add equal volume of Sertoli cell culture medium. Using a pipette, gently pipette samples up and down to single cell suspension (*see* **Note 3**).
9. Filter the cell suspension through a 100 μm filter to remove any cell aggregates.
10. Centrifuge 1000 × *g* for 3 min at RT and wash with F12-DMEM medium. Repeat twice.
11. Place the dispersed cells into culture dishes, and incubate with Sertoli cell culture medium at 34 °C and 5% CO_2. Spermatogonia are unable to attach to the dish and removed during the medium change after 48 h.

3.2.2 Preparation of Sertoli Cell Lysates

1. Collect primary cultured Sertoli cells by trypsinization and wash once in cold (4 °C) PBS. Centrifuge at 4 °C, 500 × *g* for 5 min (*see* **Note 4**).
2. Discard supernatant, and resuspend the pellets by using 30–50 μL of RIPA-like buffer supplemented with 1 mM phenylmethylsulfonyl fluoride (PMSF) and a protein inhibitor cocktail. Incubate on ice for 30 min.
3. Centrifuge the homogenates at 4 °C, 13,523 × *g* for 15 min. Remove the supernatant to a new tube.
4. Determine the protein concentration of lysates by using the Bio-Rad DC Protein Assay (*see* **Note 5**).
5. Add equal volume of 2× loading buffer to proteins from each lysate, and then incubate for 15 min at 65 °C (*see* **Note 6**).
6. Chill the samples on ice and centrifuge at 4 °C, 13,523 × *g* for 10 min. Store at −20 °C or −80 °C.

3.2.3 SDS-PAGE

1. Prepare 15% running gel and pour into the space between the glass plates with1.0 mm thickness (*see* **Note 7**).
2. Gently overlay the solution with water to ensure a flat surface and exclude air (*see* **Note 8**).
3. After the polymerization (*see* **Note 9**), pour off water and gently wash the top of the gel with water.
4. Prepare the stacking gel and pour on top of the polymerized running gel. Insert the comb for the creation of wells.
5. After the polymerization, mount the gel into the SDS-PAGE electrophoresis chamber, and add running buffer.

6. Gently remove the comb and wash the wells with running buffer.
7. Load sample into the well. Run the gel by connecting the gel unit to power supply (*see* **Note 10**).

3.2.4 Immunoblotting

1. Incubate two sponges, four sheets of Whatman paper, and one nitrocellulose membrane of approximately the same size as the running gel in transfer buffer (1×) for 1–2 min at RT.
2. Disassemble the gel unit and discard the stacking gel.
3. Prepare the transfer "sandwich" by overlaying the following components: one sponge, two sheets of Whatman paper, the nitrocellulose membrane, the running gel, two sheets of Whatman paper, and one sponge.
4. Place the transfer "sandwich" in a transfer cassette and insert into the transfer apparatus. The transfer is accomplished at the constant voltage of 90 V for 2 h (*see* **Note 11**).
5. Once the transfer is complete, disassemble the transfer cassette. Incubate the nitrocellulose membrane in 10 mL of blocking buffer (45–40 min, RT) on a rocking platform.
6. Rinse the membrane with PBS twice, and incubate with the immunoblotting primary antibody solution at 4 °C overnight on the rocking platform.
7. Recover the immunoblotting primary antibody solution, and rinse the membrane 3 × 5 min in PBST on the rocking platform.
8. Incubate with the immunoblotting secondary antibody solution at RT for 1 h on the rocking platform.
9. Remove the secondary antibody solution and rinse the membrane 3 × 5 min in PBS on the rocking platform.
10. The membrane is scanned using an Odyssey infrared imager (9120, LI-COR Biosciences, Lincoln, NE).

3.3 Transmission Electron Microscopy

The transmission electron microscopy (TEM) is a reliable method to monitor autophagy [2, 17, 25, 27]. The fine structure of autophagic vacuoles could be identified by morphology such as the following: autophagosome is a double-membrane structure containing undigested cytoplasmic material including organelles, while the autolysosome is a single-membrane structure containing cytoplasmic components at various stages of degradation (Fig. 2).

3.3.1 Resin Flat Embedding of Aldehyde-Fixed Mouse Testes

1. Kill adult male mice by cervical dislocation immediately. Lay each animal on its back; sterilize the ventral surface with 70% ethanol. Remove testes from the abdomen with a pair of surgical scissors. Take the testis as soon as possible. Wash testes with PBS immediately. Repeat twice.

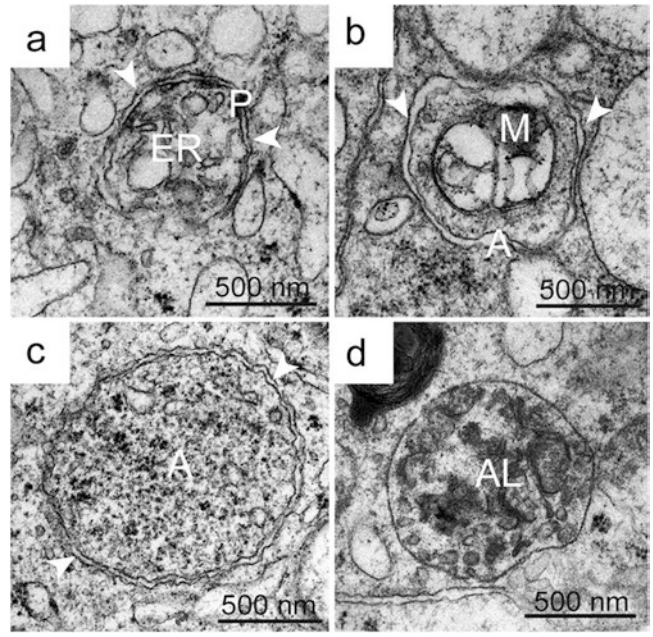

Fig. 2 Fine structure of phagophore, autophagosome, and autolysosome in Sertoli cells. (**a**) One putative phagophore seems to be in the process of wrapping around the endoplasmic reticulum (ER) with double membrane (arrow heads). P indicates phagophore. (**b**) The autophagosome contains a damaged mitochondrion. The limiting membrane (large arrowheads) is visible partially as a double membrane (arrow heads). M indicates mitochondrion, and A indicates autophagosome. (**c**) The autophagosome contains ER and ribosomes. The limiting membrane (large arrowheads) is visible as a double membrane (arrow heads). Ribosomes become more electron dense as the consequence of degradation. A indicates autophagosome. (**d**) One putative autolysosome seems to contain cytoplasmic components at various stages of degradation with a single-membrane structure. AL indicates autolysosome

2. Gently puncture testes in three to four areas with a 25G syringe needle and immersion fix in 2.5% (vol/vol) glutaraldehyde and 1.5% (vol/vol) paraformaldehyde in 0.1 M cacodylate buffer (pH 7.3) for 2 h at room temperature (RT) (*see* **Note 12**).
3. Cut testes into small pieces (1–2 mm cubes or pellets), and then fix the samples overnight at 4 °C.
4. Wash 5 × 15 min in 0.1 M cacodylate buffer (pH 7.3) at RT. It could be stored at 4 °C for up to some weeks.
5. Postfix in 1% osmium tetroxide in water for 1 h at 4 °C. As osmium is very toxic and volatile, use a good fume cupboard and gloves.
6. Wash 5 × 15 min in 0.1 M cacodylate buffer at RT.
7. Stain the cells in 2% uranyl acetate in water at RT, in the dark, for 1 h (*see* **Note 13**)

8. Wash 3 × 15 min in water at RT.
9. Dehydrate in a graded acetone series at RT (5 min each of 50%, 60%, 70%, 80%, 90%, 95% acetone in water). Incubate with 100% acetone 3 × 5 min in a new tube.
10. Incubate for 1.5 h in 3:1100% acetone and resin, followed by 1.5 h in 1:1100% acetone and resin at RT. And then incubate for 6 h in 1:3100% acetone and resin at RT.
11. Incubate for 3 × 12 h in pure resin at RT.
12. Embed the tissue in freshly made resin in a silicone mold (*see* **Note 14**). Polymerize the resin at 35 °C for 24 h, 45 °C for 24 h, and then at 65 °C for 24 h.

3.3.2 Sectioning and Collection on Grids

1. Cut 60 nm sections on an ultramicrotome and float on the water surface behind the diamond knife.
2. Collect sections on 100 mesh copper grids and stain the sections with uranyl acetate and lead citrate.
3. Image can be observed using a JEM-1400 transmission electron microscope (*see* **Note 15**).

3.4 GFP-LC3 Lysosomal Delivery and Proteolysis

GFP-LC3 is very useful to follow autophagy flux, as the LC3 part of the chimera is sensitive to degradation, whereas the GFP protein is relatively resistant to hydrolysis. The appearance of free GFP on western blots can be used to monitor lysis of the inner autophagosome membrane and breakdown of the cargo [2, 17].

1. Dilute 4 μg of GFP-LC3 plasmid in 100 μL Opti-MEM and 10 μL of lipofectamine 2000 in 100 μL Opti-MEM. After a first incubation of 5 min, gently mix the diluted plasmid solution and diluted lipofectamine 2000 solution, and incubate for another 20 min (*see* **Note 16**).
2. Add 200 μL of solution containing the lipofectamine 2000 and GFP-LC3 plasmid to 10^5 primary cultured Sertoli cells in 30 mm cell culture plates. Incubated at 34 °C, 5% CO_2 for 24 h.
3. Remove the medium and wash Sertoli cells with PBS.
4. Add fresh Sertoli cell culture medium and culture cell at 34 °C, 5% CO_2 for 24 h.
5. Collect primary cultured Sertoli cells by trypsinization, and perform the immunoblotting analysis of GFP as described in Subheading 3.2 (*see* **Note 17**).

3.5 Immunoblotting Analysis of SQSTM1/p62

The SQSTM1/p62 protein serves as a link between LC3 and ubiquitinated substrates, and it is incorporated into the completed autophagosome and degraded in autolysosomes. The inhibition of autophagy correlates with increased levels of SQSTM1 (Fig. 1),

suggesting that steady-state levels of this protein reflect the autophagic status [2, 17].

1. Isolate the primary Sertoli cell from mouse testes as described in Subheading 3.2.1.
2. Prepare Sertoli cell lysates as described in Subheading 3.2.2.
3. Perform the immunoblotting analysis of SQSTM1 as described in Subheadings 3.2.3 and 3.2.4.

3.6 Turnover of Autophagic Substrate Proteins

1. Isolate the primary Sertoli cell from mouse testes as described in Subheading 3.2.1.
2. Prepare Sertoli cell lysates as described in Subheading 3.2.2.
3. Perform the immunoblotting analysis of autophagic substrate proteins as described in Subheadings 3.2.3 and 3.2.4.

3.6.1 Immunoblotting Analysis of Autophagic Substrate Proteins

3.6.2 Immunofluorescence Analysis of Autophagic Substrate Proteins in Primary Sertoli Cells

1. Seed primary Sertoli cells in 6-well plates in which sterile cover slips have been previously deposited.
2. Culture Sertoli cells for 24 h. Remove growth medium and wash cells twice with PBS.
3. Fix Sertoli cells in 4% PFA for 5 min at RT (*see* **Note 18**).
4. Remove fixative solution and rinse Sertoli cells 3 × 5 min in PBS at RT.
5. Perform the immunofluorescence experiment as described in Subheading 3.1, **steps 7–14**.
6. Mount the cover slips with Sertoli cells onto slides using mounting medium, and seal cover slip with nail polish to prevent drying.
7. Fluorescent images are obtained using a fluorescence microscope.

3.6.3 Immunofluorescence Analysis of Autophagic Substrate Proteins in Apical Ectoplasmic Specialization Region of Sertoli Cells

1. Testes are dissected from adult mice after euthanasia. Wash testes with PBS immediately. Repeat twice.
2. Fix testis in 4% PFA at room temperature for 2 h.
3. Wash the testis with PBS twice and decapsulate it in PBS.
4. Mince the seminiferous tubules into small pieces using scalpels, and then gently aspirate the small pieces, first through an 18-gauge needle and then a 21-gauge needle to fragment the seminiferous epithelium.
5. Sediment for 5 min (*see* **Note 19**). Remove the supernatant fraction to a new tube and concentrate at 800 × *g* for 5 min.
6. Remove the supernatant fraction and resuspend the pellet in a small amount of PBS.
7. Place drops of the material on APE precoated slides for 10 min.

8. Remove excess fluid, and immediately submerge the samples in cold acetone (−20 °C) for 5 min and then air dry.
9. Perform the immunofluorescence experiment as described in Subheading 3.1, **steps 7–15**.

3.6.4 Cycloheximide Chase Assay for Autophagic Protein

1. Isolate the primary Sertoli cell from mouse testes as described in Subheading 3.2.1. Plate Sertoli cells 1 day before the experiment (*see* **Note 20**).
2. Add the cycloheximide to the culture at 100 μg/mL to block new protein synthesis.
3. Collect primary cultured Sertoli cells by trypsinization at different time points after the cycloheximide treatment.
4. Prepare Sertoli cell lysates as described in Subheading 3.2.2.
5. Perform the immunoblotting analysis of the targeted protein as described in Subheadings 3.2.3 and 3.2.4.

3.6.5 Co-immunoprecipitation of LC3 and Autophagic Substrate Proteins

1. Collect primary cultured Sertoli cells by trypsinization and wash once in cold (4 °C) PBS. Centrifuge at 4 °C, 500 × *g* for 5 min.
2. Discard supernatant, and resuspend the pellets by using 150–200 μL of TAP buffer supplemented with 1 mM PMSF and a protein inhibitor cocktail. Incubate on ice for 30 min.
3. Centrifuge the homogenates at 4 °C, 13,523 × *g* for 15 min. Remove the supernatant to a new tube.
4. Incubate cell lysates with primary antibody at 4 °C overnight.
5. Incubate samples with protein A-Sepharose at 4 °C for 2 h.
6. Centrifuge at 4 °C, 1500 × *g* for 2 min. Remove the supernatant.
7. Wash the precipitants twice with IP buffer.
8. Add 30 μL of 2× loading buffer to proteins from each lysate, and then incubate for 15 min at 65 °C.
9. Chill the samples on ice and centrifuge at 4 °C, 13,523 × *g* for 10 min.
10. Perform the immunoblotting analysis of the targeted protein as described in Subheadings 3.2.3 and 3.2.4.

4 Notes

1. As many autophagy marker proteins localize on the membranes, such as LC3-II which is recruited to autophagosomal membranes, it is important to consider the hydrophobicity of autophagy marker proteins and avoid adding Triton or some other detergent in the primary antibody solution.

2. In **step 3**, the testes should be sufficiently digested to the seminiferous tubules which showed filamentous dispersion. In **step 5**, the seminiferous tubules should be sufficiently digested to short fragments. In **step 7**, the seminiferous tubules should be sufficiently digested to small dots.
3. This final digestion step resulted in a cell suspension containing primarily Sertoli cells and type A spermatogonia.
4. To minimize proteolytic degradation, samples should be kept on ice until adding loading buffer and boiling or storage.
5. As protein quantification is performed by interpolating a calibration curve that is built from a serial dilution of BSA and BSA standards are rarely included in the kits for quantification, thus BSA standards should be prepared shortly before use from the BSA stock solution.
6. As LC3-II is recruited to autophagosomal membranes, it is important to consider the hydrophobicity of LC3-II.
7. The percentage of acrylamide directly influence its separation range and resolution determines. As a guideline, proteins with smaller proteins can be separated on gels containing 10–15% acrylamide.
8. Pouring should be performed quickly, while avoiding the formation of bubbles.
9. Polymerization time depends on acrylamide concentration, but usually 30 min is sufficient.
10. Before entry in the running gel, voltage should be set at 50–70 mV. Thereafter, voltage can be augmented to 140 mV. It should be kept in mind that higher voltages result in reduced migration time but also in lower resolution.
11. To control temperature, an ice block is placed next to the transfer cassette.
12. After being fixed for 30 min to 1 h, if the testis appears firm, it can be sliced in half and then fixed for the additional hour. Avoid undue pressure on the organ.
13. This step gives contrast to autophagosome membranes.
14. Wash the silicone mold clearly as soon as possible.
15. The defined autophagosomes are double-membrane vacuoles contained undegraded cytoplasmic cargos. In some case, the two membranes are often too close to see them as one lay membrane. However, sometimes the membrane may appear to contain multiple layers. Occasionally, it is possible to observe putative phagophores, a cup-shaped double-membrane structure, which seem to be engulfing portions of the cytoplasm. The cytoplasmic contents of autophagosomes include organelles, such as ER membranes, mitochondria, and ribosomes.

The diameter of autophagosome profiles varies between 300 and 400 nm and several micrometers. Autophagosomes are frequently observed in fusion profiles with endosomal or lysosomal vesicles. In the fusion event, the outer limiting membrane fuses with the endo/lysosome limiting membrane. The contents, still surrounded by the inner limiting membrane, are delivered to the endo/lysosome lumen. It should be noted that special attention must be paid when identifying autophagic vacuoles in transmission electron microscopy. There are several examples in the current literature of different organelles, including multilamellar or multivesicular endosomes, even mitochondria, being claimed as autophagic vacuoles. Only vacuoles containing cytoplasmic material, in most cases ribosomes, can be claimed as autophagic.

16. As the transfection rate of Sertoli cells is lower, the concentration of plasmid and lipofectamine 2000 should be excessive.
17. As slight non-autophagic degradation of GFP-LC3 may seriously influence this experiment, operations should be quick as soon as possible, and samples should be always kept on ice until adding loading buffer.
18. As Sertoli cells are much thinner than the testis, the fixed time should not exceed 5 min.
19. During this time, larger tubule fragments settled to the bottom of the tube, and smaller epithelial fragments containing mature spermatids with associated Sertoli cell apical processes remained suspended in solution.
20. To avoid the influence caused by the operations collecting samples in different time point, 30 mm cell culture plates, but not 6-well cell culture plates, are encouraged to be used in this experiment.

Acknowledgments

This work was supported by National Key R&D program of China (Grant No. 2016YFA0500901), and the National Nature Science of China (Grant No. 91519317, 91649202 and 31471277).

References

1. Levine B, Kroemer G (2008) Autophagy in the pathogenesis of disease. Cell 132(1): 27–42. https://doi.org/10.1016/j.cell.2007.12.018
2. Mizushima N, Yoshimori T, Levine B (2010) Methods in mammalian autophagy research. Cell 140(3):313–326. https://doi.org/10.1016/j.cell.2010.01.028
3. Wang H et al (2014) Atg7 is required for acrosome biogenesis during spermatogenesis in mice. Cell Res 24(7):852–869. https://doi.org/10.1038/cr.2014.70

4. Tang Z et al (2013) Autophagy promotes primary ciliogenesis by removing OFD1 from centriolar satellites. Nature 502(7470):254–257. https://doi.org/10.1038/nature12606
5. Mizushima N, Komatsu M (2011) Autophagy: renovation of cells and tissues. Cell 147(4):728–741. https://doi.org/10.1016/j.cell.2011.10.026
6. Mizushima N, Levine B (2010) Autophagy in mammalian development and differentiation. Nat Cell Biol 12(9):823–830. https://doi.org/10.1038/ncb0910-823
7. Li WW, Li J, Bao JK (2012) Microautophagy: lesser-known self-eating. Cell Mol Life Sci 69(7):1125–1136. https://doi.org/10.1007/s00018-011-0865-5
8. Cuervo AM, Wong E (2014) Chaperone-mediated autophagy: roles in disease and aging. Cell Res 24(1):92–104. https://doi.org/10.1038/cr.2013.153
9. Mizushima N (2007) Autophagy: process and function. Genes Dev 21(22):2861–2873. https://doi.org/10.1101/gad.1599207
10. Mizushima N, Yoshimori T, Ohsumi Y (2011) The role of Atg proteins in autophagosome formation. Annu Rev Cell Dev Biol 27:107–132. https://doi.org/10.1146/annurev-cellbio-092910-154005
11. Yang Z, Klionsky DJ (2009) An overview of the molecular mechanism of autophagy. Curr Top Microbiol Immunol 335:1–32. https://doi.org/10.1007/978-3-642-00302-8_1
12. Yu X, Long YC, Shen HM (2015) Differential regulatory functions of three classes of phosphatidylinositol and phosphoinositide 3-kinases in autophagy. Autophagy 11(10):1711–1728. https://doi.org/10.1080/15548627.2015.1043076
13. Nakatogawa H, Suzuki K, Kamada Y, Ohsumi Y (2009) Dynamics and diversity in autophagy mechanisms: lessons from yeast. Nat Rev Mol Cell Biol 10(7):458–467. https://doi.org/10.1038/nrm2708
14. Carlsson SR, Simonsen A (2015) Membrane dynamics in autophagosome biogenesis. J Cell Sci 128(2):193–205. https://doi.org/10.1242/jcs.141036
15. Itakura E, Mizushima N (2010) Characterization of autophagosome formation site by a hierarchical analysis of mammalian Atg proteins. Autophagy 6(6):764–776
16. Karanasios E, Stapleton E, Manifava M, Kaizuka T, Mizushima N, Walker SA, Ktistakis NT (2013) Dynamic association of the ULK1 complex with omegasomes during autophagy induction. J Cell Sci 126(Pt 22):5224–5238. https://doi.org/10.1242/jcs.132415
17. Klionsky DJ et al (2016) Guidelines for the use and interpretation of assays for monitoring autophagy (3rd edition). Autophagy 12(1):1–222. https://doi.org/10.1080/15548627.2015.1100356
18. Griswold MD (1998) The central role of Sertoli cells in spermatogenesis. Semin Cell Dev Biol 9(4):411–416. https://doi.org/10.1006/scdb.1998.0203
19. Hai Y, Hou J, Liu Y, Yang H, Li Z, He Z (2014) The roles and regulation of Sertoli cells in fate determinations of spermatogonial stem cells and spermatogenesis. Semin Cell Dev Biol 29:66–75. https://doi.org/10.1016/j.semcdb.2014.04.007
20. Ma Y, Yang HZ, Xu LM, Huang YR, Dai HL, Kang XN (2015) Testosterone regulates the autophagic clearance of androgen binding protein in rat Sertoli cells. Sci Rep 5:8894. https://doi.org/10.1038/srep08894
21. Yefimova MG et al (2013) A chimerical phagocytosis model reveals the recruitment by Sertoli cells of autophagy for the degradation of ingested illegitimate substrates. Autophagy 9(5):653–666. https://doi.org/10.4161/auto.23839
22. Chen Y, Zhou Y, Wang X, Qian W, Han X (2013) Microcystin-LR induces autophagy and apoptosis in rat Sertoli cells in vitro. Toxicon 76:84–93. https://doi.org/10.1016/j.toxicon.2013.09.005
23. Eid N, Ito Y, Otsuki Y (2012) Enhanced mitophagy in Sertoli cells of ethanol-treated rats: morphological evidence and clinical relevance. J Mol Histol 43(1):71–80. https://doi.org/10.1007/s10735-011-9372-0
24. Liu C et al (2016) Autophagy is required for ectoplasmic specialization assembly in sertoli cells. Autophagy 12(5):814–832. https://doi.org/10.1080/15548627.2016.1159377
25. Mizushima N (2004) Methods for monitoring autophagy. Int J Biochem Cell Biol 36(12):2491–2502. https://doi.org/10.1016/j.biocel.2004.02.005
26. Tanida I, Ueno T, Kominami E (2008) LC3 and autophagy. Methods Mol Biol 445:77–88. https://doi.org/10.1007/978-1-59745-157-4_4
27. Eskelinen EL (2008) Fine structure of the autophagosome. Methods Mol Biol 445:11–28. https://doi.org/10.1007/978-1-59745-157-4_2

Chapter 11

Molecular Mechanisms and Signaling Pathways Involved in the Nutritional Support of Spermatogenesis by Sertoli Cells

Luís Crisóstomo, Marco G. Alves, Agostina Gorga, Mário Sousa, María F. Riera, María N. Galardo, Silvina B. Meroni, and Pedro F. Oliveira

Abstract

Sertoli cells play a central role in spermatogenesis. They maintain the blood-testis barrier, an essential feature of seminiferous tubules which creates the proper environment for the occurrence of the spermatogenesis. However, this confinement renders germ cells almost exclusively dependent on Sertoli cells' nursing function and support. Throughout spermatogenesis, differentiating sperm cells become more specialized, and their biochemical machinery is insufficient to meet their metabolic demands. Although the needs are not the same at all differentiation stages, Sertoli cells are able to satisfy their needs. In order to maintain the seminiferous tubule energetic homeostasis, Sertoli cells react in response to several metabolic stimuli, through signaling cascades. The AMP-activated kinase, sensitive to the global energetic status; the hypoxia-inducible factors, sensitive to oxygen concentration; and the peroxisome proliferator-activated receptors, sensitive to fatty acid availability, are pathways already described in Sertoli cells. These cells' metabolism also reflects the whole-body metabolic dynamics. Metabolic diseases, including obesity and type II diabetes mellitus, induce changes that, both directly and indirectly, affect Sertoli cell function and, ultimately, (dys)function in male reproductive health. Insulin resistance, increased estrogen synthesis, vascular disease, and pubic fat accumulation are examples of metabolic-related conditions that affect male fertility potential. On the other hand, malnutrition can also induce negative effects on male sexual function. In this chapter, we review the molecular mechanisms associated with the nutritional state and male sexual (dys)function and the central role played by the Sertoli cells.

Key words Nutritional support, AMPK, PPAR, HIF, Metabolic (dys)function

1 Introduction

The reproductive system is the only system unnecessary for the survival of an individual of any species. Nevertheless, a considerable amount of energy is directed toward the reproductive functions. Under an evolutionary perspective, this fact is easy to understand, since (sexual) reproduction is the engine for any species to prevail, have success, and continue a permanent evolution.

Marco G. Alves and Pedro F. Oliveira (eds.), *Sertoli Cells: Methods and Protocols*, Methods in Molecular Biology, vol. 1748, https://doi.org/10.1007/978-1-4939-7698-0_11,

Known as "nurse cells" [1], the Sertoli cells (SCs) play a decisive role on the nutritional support of the male germline during the processes of differentiation, particularly to fulfill their energetic needs. To achieve this, SC metabolism is tightly regulated by a complex network of endocrine and paracrine stimuli, as well as by environmental cues. In addition, SCs' role is not restricted to the nutritional support of spermatogenesis; they also provide physical support for the differentiating germ cells, regulate and maintain the blood-testis barrier (BTB), and ensure the homeostasis of the tubular fluid in the seminiferous tubules' (SeT) lumen.

The SCs were firstly described by Enrico Sertoli in 1865, when he had just graduated in Medicine at the University of Pavia, Italy [2]. On his original work, Enrico Sertoli named his newly identified cells as "branched cells" due to their peculiar appearance, with many cytoplasmic projections surrounding germ cells [3]. Sertoli was able to notice with a regular optic microscope and a limited number of samples (check original again) several other histological details and cellular ultrastructure, such as the large nucleus [3]. SCs would only get their current designation 22 years later, by the Austrian histologist Victor von Ebner [4]. In spite of the immediate recognition of SC research potential, bibliography about them is scarce until the mid-1950s, when electronic microscopy and new biochemistry techniques, such as immunohistochemistry and immunocytochemistry, became available and after the discovery of DNA and RNA structure [5]. Since then, the number of journal articles has been steadily increasing, to the present 400 articles per year.

This chapter focuses on the molecular mechanisms and the signaling pathways responsible for SC metabolic regulation and, thus, regulation of the environment for proper germ cell development and differentiation.

2 Relevance of Sertoli Cells to Spermatogenesis

There is still some debate concerning the specific roles for SCs, but they are usually reported as the main supporters of spermatogenesis [1, 2, 6]. This evidence is supported by three experimental premises. Firstly, SCs are always present in the testis, whereas there is the SC-only condition where the testis does not present any germ cells [7]. When SC population suffers significant loss by any cause, germ cells are quickly lost, too [7]. This observation is further confirmed in vitro, where germ cells struggle to develop and thrive in the absence of SCs, and spermatogenesis has not been fully achieved in culture, while the closest attempts to mimic it are always based on co-cultures with SCs [2, 5, 8–10].

Secondly, there is evidence that the number of germ cells supported by a single SC is limited and species-dependent; hence, the

number of germ cells is directly proportional to the number of SCs [2, 5, 11, 12]. Experimental evidence comes from studies where the number of SCs was controlled and the spermatogenic output quantified [2, 11, 13–15]. When SC numbers were restricted by inhibition of proliferation during testicular development, either by hormonal or chemical action, spermatogenic output and testicular volume decreased, also illustrating that the number of SCs significantly contributes to a normal testicular volume [13]. When the procedure was hemicastration (ablation of a testis) during the development phase, the remaining testis had bigger volume and spermatogenic output [14, 15]. However, in both experimental approaches, the SC-spermatid ratio remains constant [2]. The direct relation between spermatogenic output and SC number is further supported by evidence that, in some species, adult SC proliferation occurs at the breeding season to increase their spermatogenic output, but, in humans, SCs have limited mitotic capacity in vivo [11].

Lastly, it is observed that spermatogenesis is highly dependent upon hormonal regulation from testosterone and FSH, and those hormones only exert their action directly over SCs, not germ cells [2, 5]. Experimental evidence relies in several in vitro and in vivo models. Follicle-stimulating hormone (FSH) and thyroid hormone mediate SC proliferation during testis development, thus affecting testis size, weight, and spermatogenic output [12]. In addition, there were several gene mutations identified in SC FSH receptor subunit, which resulted in dysfunctional protein and infertility in men [12, 16]. The affected individuals presented small testicular size and azoospermia [12, 16]. It is evidenced in vivo that the expansion of germ cell reserve is FSH-dependent rather than androgen-dependent but always primarily mediated by SC action [2, 17]. Furthermore, differentiation from germ cells to round spermatids by FSH stimulation is possible, but its yield is only about 5% of the normal, SC-mediated, yield [12].

The advances on SC research now elicit that their critical role on spermatogenesis is related, but not limited, to germ cell physical support, environmental control, BTB maintenance and modulation, tubular fluid dynamics, endocrine and paracrine regulation, biochemical stimulation, and germ cell nutritional support [1, 2, 6, 18–21].

SCs ensure the physical support to male germline cells due to a very distinguishable feature: long and thin cytoplasmic arms, similar to branches (as observed by Enrico Sertoli) [3]. These elongations create a cuplike form to hold germ cells, dramatically increasing the membrane surface area and creating stage-specific microenvironments for germ cells throughout their differentiation [5]. However, germ cells are not only stabilized by it but also gain protection and other important features. Another significant and singular characteristic is the apical ectoplasmic specialization, a

cell-cell adherent junction based on actin filaments, responsible for the germ cell movement and docking along the SC's membrane [5]. In a larger extent, Sertoli cells are the very nature of the seminiferous tubule epithelium, since their polarization and side-by-side placement create a tubular structure and two distinct mediums [22].

SCs are responsible for the maintenance of the two-compartment system found in the testis, which is a critical condition for spermatogenesis [6]. The BTB separates the interstitial fluid, which surrounds peripheral cells, and the tubular fluid, which fills the lumen of the seminiferous tubules [6]. In vitro studies have demonstrated that human stem cells are able to differentiate into spermatogonia in a SC-conditioned culture medium [9, 23], a strong evidence of the environment importance for spermatogenesis but also of a significant contribution from SCs, rather than from germ cells, in this process. The Sertoli cells maintain tubular fluid homeostasis by guaranteeing the integrity of BTB and regulating its composition [1, 24–26]. Due to the fact that Sertoli cell is highly polarized, SCs are the most important structure of BTB, since its basal membrane is directed toward the interstitial fluid, while its apical membrane is directed toward the seminiferous tubule lumen [27]. Tubulobulbar complexes are another SC peculiar feature. They are another anchoring system between cells at the BTB that works similarly to a puzzle: cytoplasmic elongations of a SC, ending on a spherical structure containing a cistern-like complex related to the endoplasmic reticulum, fit into corresponding invaginations on the adjacent cell [5, 28]. This cell junction is further reinforced by the action of other anchoring systems present in these cells [22, 29]. The tubular complexes at the basal region, tight junctions, gap junctions, and desmosome-like junctions, between SCs are responsible for making this blood-tissue barrier even more impermeable [22, 29]. SCs dock themselves through hemidesmosomes to the basal lamina, the physical border of seminiferous tubules consisting in the basement membrane, a collagen network, and a layer of peritubular myoid cells (MCs) [1, 6]. The apical Tubulobulbar complexes mainly promote interaction with germ cells, in late maturation stages (spermatid), and are thought to be crucial for spermiation, being involved in the cytoplasmic reduction and the release of mature spermatozoa [22].

The most important endocrine mechanism mediated by SCs is its role on the reproductive axis which is the central regulator for the reproductive function. It starts at the beginning of puberty, with the pulsatile release of gonadotropin-releasing hormone (GnRH). GnRH neurons secreting GnRH are derived from the nasal placode and migrate into the brain during prenatal development. Once within the brain, GnRH neurons become integral components of the hypothalamic-pituitary-gonadal axis, essential for reproductive maturation and maintenance of reproductive

function in adults. GnRH induces adenohypophysis production and release of gonadotropins, FSH, and luteinizing hormone (LH). In male reproductive system, LH stimulates steroidogenesis in Leydig cells, namely, androgens such as testosterone, while FSH stimulates SC activity, metabolism, and endocrine function, as inhibin source. The axis is under negative feedback control; therefore, inhibin and androgens inhibit GnRH and gonadotropin release when their bloodstream concentration overcomes its feedback threshold [12, 30, 31]. In males, this cycle lasts for life but can be disrupted by any abnormality in any of the players. When it happens, spermatogenesis might be seriously affected [30–32]. Spermatogenesis depends on paracrine regulation from SCs too, as they provide several differentiation factors [21, 30]. Nevertheless, SC endocrine and paracrine roles on spermatogenesis may also be indirect. Leydig cells, the most important steroidogenic cell of the testis and the main testosterone source, suffer dramatic population losses, and peritubular MCs, BTB is responsible for the immune-privilege, also suffer a significant drop in their activity in the absence of SCs [7].

The critical role of SCs in spermatogenesis begins long before sexual maturation and at the beginning of regular spermatogenesis. Their influence starts as soon as on testicular embryonic development [5, 7]. In addition to their stimulation by FSH to a normal testis development, SCs also secrete the anti-Mullerian hormone, a critical endocrine modulator involved on the correct development of the primary sexual characteristics [2, 6, 30]. Thus, these cells are involved in virtually all steps required for a normal spermatogenesis.

3 Germ Cell Dependence of Sertoli Cell Metabolism

Germ cells cross several differentiation stages during spermatogenesis. Their reliance on SCs are not the same at all stages, but it is a pivotal feature at all steps [6]. The least differentiated cells in this line are the spermatogonia, diploid germ cells that constitute the germline reserve. Within spermatogonia there is a low differentiation degree between those which are committed to mitotic division for germ cell reserve preservation (type A) and those which are committed to meiotic division and undergo spermatogenesis (type B) [2, 6, 12]. Spermatogenesis stage nomenclature differs from author to author, but here we will consider the following: spermatogonium (2n), primary spermatocyte (4n), secondary spermatocyte (n), round spermatid (n), elongated spermatid (n), and spermatozoon (n).

As mentioned, the two-compartment system, delimitating two distinctive environments, the interstitial fluid and the tubular fluid, is of the utmost importance for germ cell survival and differentiation

[12, 22]. SC metabolism controls the metabolic microenvironment needed for each stage of germ cell differentiation. This is evident on the onset of the first meiotic division, when a type B spermatogonium enters phase S on its cell cycle and doubles its genetic charge (4n). Some authors define this phase as two distinct stages, the preleptotene and leptotene spermatocyte [5, 12]. However, the interstitial environment is not suitable for meiosis, and in order to complete the first meiotic division, the cell crosses the BTB into the adluminal environment, where it readies meiosis (primary spermatocyte stage) and finally completes the first division to originate two secondary spermatocytes. The conversion of type A to type B spermatogonium seems to be modulated by retinoic acid (RA), a vitamin A derivate that cannot pass the BTB and is locally secreted by SCs, so it acts as a signal for meiosis initiation and thus spermatogenesis [33].

Overall, testes are oxygen-deprived organs; hence, germ cells, independently from its maturation stage, mainly rely on glycolytic metabolism to obtain energy [30, 34]. The importance of glycolytic pathways is such that germ cells present, while undergoing spermatogenesis, unique enzyme isoforms related to it [20]. Glycolytic potential decreases along the differentiation stages of spermatogenesis. Spermatozoon is the illustrious exception. It is even the most glycolytic cell of the male germline family, but has the lowest tricarboxylic acid (TCA) cycle activity, and relies almost exclusively on hexoses as substrate [1, 35]. Lactate and pyruvate resulting from SC metabolism is an important energy substrate for germ cells [18]. SCs export both to the tubular fluid via monocarboxylate transporter (MCT) membrane transporter family members, while germ cells also import those substrates via MCTs [18, 36, 37]. Therefore, lactate availability for germ cells depends on its production and release rate from SCs, which in turn is dependent upon MCT protein expression and glycolytic flux [1, 20]. Nevertheless, SCs' glycolytic activity depends on substrate availability, i.e., glucose import from the extracellular, interstitial environment, mediated by glucose transporter (GLUT) family member [1, 20]. Summarily, germ cell substrate availability is intimately related to SCs' own substrate availability and metabolic rate. Fortunately for germ cells, albeit oxygen deprivation promotes the glycolytic metabolism rather than more oxidative metabolic pathways, SCs are competent metabolic "factories" able to metabolize a large spectra of substrates, including fatty acids and amino acids, in order to sustain the production of lactate and pyruvate [1, 6]. SCs direct three quarters of all their own pyruvate production to germ cells, either as lactate or pyruvate, whereas β-oxidation is suggested to be used only to satisfy their own energy needs [38]. Interestingly, SC metabolism resembles a cancer cell metabolism, heavily relying on glycolytic metabolism and glutaminolysis; however, contrarily to cancer cells which direct such energy for cell

proliferation, SCs seem to direct it for production of substrates for developing germ cells [20, 30].

Besides being the preferred energy substrate, a novel evidence for a role of lactate as a signaling molecule in the seminiferous tubule has been provided, and lactate might be considered a paracrine factor secreted by SCs. In this context, lactate, taken up by germ cells, becomes oxidized to pyruvate with the resultant increase in reactive oxygen species (ROS) which act as second messengers regulating signal transduction pathways and gene expression [39]. In addition, lactate has also anti-apoptotic properties on germ cells and promotes RNA and protein synthesis on spermatids, by promoting NADPH oxidation for pentose phosphate pathway (PPP) and ATP production for protein synthesis [40]. On the other hand, SCs are relevant for germ cell apoptosis through other mechanisms [41]. The division rate of spermatogonia is higher than the spermatozoa release rate. In mammals, germ cell death is conspicuous during spermatogenesis and occurs spontaneously at various phases of germ cell development such that seminiferous epithelium yields fewer spermatozoa than might be anticipated from spermatogonial proliferations. Although most of the apoptotic cells are type B spermatogonia and primary spermatocytes, programmed cell death can occur at any differentiation stage [41]. SCs quickly absorb their apoptotic bodies by phagocytosis, because they express class B scavenger receptor type I (SR-BI), a receptor sensitive to the apoptosis-marker phospholipid phosphatidylserine [41]. Thus, apoptotic cells are rarely spotted on histological preparations [41]. Notably, SCs are reported to even use the apoptotic bodies as energy source [42] illustrating their high metabolic capacity to metabolize substrates and convert them into relevant metabolites for spermatogenesis.

SCs are responsible for ionic balance and pH control in tubular fluid, due to their metabolic and secretory activity [24–26]. The hydrocarbonate ion plays a decisive role on pH balance, and its concentration depends on SC protein expression of cystic fibrosis transmembrane conductance regulator (CFTR) [24, 25]. Another SC-related pH regulation mechanism is the solute carrier 9 family members (SLC9) Na^+/H^+ exchangers [26]. Aquaporins (AQPs) expressed by SCs are another important transporter family for tubular fluid homeostasis and are reported to be co-expressed with CFTR [43, 44]. Germ cells heavily rely on this regulation, as they are very fragile against environmental aggression. Indeed, oxidative stress is a major external aggression for germ cells, as they lack antioxidant mechanisms. Oxidative stress induces germ cell apoptosis due to lipid peroxidation of the germ cell membrane's lipids [1]. The physical supportive role of SCs is a key factor for germ cell survival as shown before the end of spermiation when a premature germ cell detachment causes apoptosis on detached germ cells [29]. In the occurrence of SC death, the previously nursed germ

cells, which became freely suspended in the lumen, rapidly engage programmed cell death [29]. This might be caused by the germ cell stage-specific environmental needs, only maintainable at the microenvironments created by the SC's membrane invaginations and by the necessity of growth factors synthesized by these cells [28, 29]. Figure 1 summarily illustrates the most important roles of SCs in the testicular tissue.

Within paracrine mediators and growth factors in the cross talk between SCs and germ cells, perhaps the most described players are basic fibroblast growth factor (bFGF) and interleukin-1 (IL-1). bFGF is expressed by Sertoli and germ cells, but only SCs express its receptor, where it acts as a major metabolic modulator. It modulates transferrin, 17β-estradiol (E_2) and lactate secretion, glucose uptake, and FSH receptor expression [30]. Transferrin is an iron-binding plasmatic glycoprotein that, due to BTB impermeability, cannot transfer their ferric ions to the adluminal compartment where it is needed by the differentiating germ cells. Once again, SCs mediate the ferric ion transport from the interstitial fluid to the tubular fluid. Many proteins have been demonstrated to be implicated in iron transport to germ cells. Iron import to the seminiferous tubule by transferrin was demonstrated, and it was hypothesized that SC could import iron basolaterally, transport it across the BTB, and supply iron to the developing male germ cells. In this way, the entry of iron to the germ cells is thought to be mediated by transferrin secreted by SC [2]. Furthermore, ferroportin transcript levels were detected in SC and can contribute with this

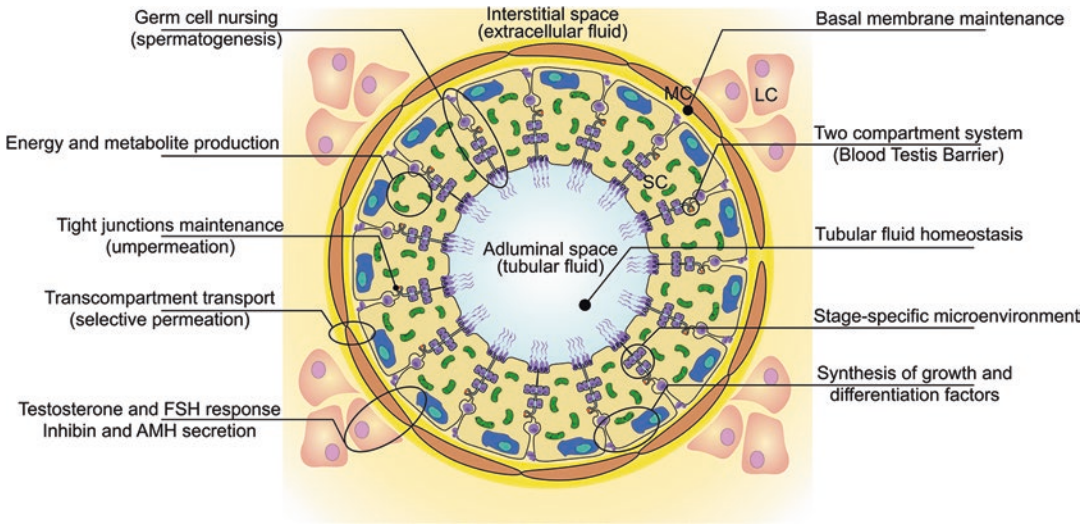

Fig. 1 The central role of Sertoli cells in testicular tissue environment and organization. Sertoli cells play several roles in testicular tissue's physiology. Besides their critical role on spermatogenesis, granting physical and nutritional support to developing germ cells, they also show paracrine and endocrine properties and are the main component of the blood-testis barrier, one of the tightest blood-tissue barriers of the human body

transport. In addition to transferrin and TfR1(Transferrin receptor 1), other proteins involved in iron transport, such as DMT1 and glycosyl phosphatidylinositol-anchored ceruloplasmin and iron storage, such as cytosolic and mitochondrial ferritin, were found in the testis. IL-1 is a multifunctional cytokine, having two isoforms: IL-1α and IL-1β. In the testis, IL-1α is produced by SCs and germ cells, while IL-1β is produced by Leydig cells and interstitial macrophages [21]. Surprisingly, IL-1α causes antispermatogenic effects over SCs, while IL-1β promotes pro-spermatogenic responses from them [30]. On the other hand, IL-1 is specially involved in meiosis initiation, promoting DNA synthesis and differentiation of type B spermatogonium into preleptotene spermatocytes [30]. Nevertheless, we have to take into account that the majority of the studies of paracrine and growth factor regulation of spermatogenesis were performed in vitro; hence, differences in in vivo behavior must be considered [30].

4 Maintaining Seminiferous Tubule Energetic Homeostasis: Role of the AMP-Activated Protein Kinase (AMPK)

It is widely known that SCs assume the responsibility for maintaining energy balance in germ cells situated beyond BTB. Thus, it is expectable that a signaling pathway might be activated by any energy deprivation signal arising from the seminiferous tubules.

AMPK is a key regulator of cellular energy homeostasis [45]. It is a heterotrimeric enzyme consisting of a catalytic α-subunit and regulatory β and γ subunits. In vertebrates, each subunit exists as multiple isoforms encoded by distinct genes. In mammals, *Prkaa1* and *Prkaa2* encode for α1AMPK and α2AMPK subunits, *Prkab1* and *Prkab2* encode for β1AMPK and β2AMPK isoforms, and *Prkag1*, *Prkag2*, and *Prkag3* encode for γ1AMPK, γ2AMPK, and γ3AMPK subunits, respectively [46–48]. These seven subunit isoforms could potentially give rise to 12 heterotrimeric combinations. The question of whether these distinct heterotrimeric combinations have different functions has not received much attention, although interesting new evidence is beginning to emerge.

AMPK is activated by an increase in the AMP:ATP ratio, and its activation involves several mechanisms:

1. The AMPK ability to sensitively respond to subtle changes in the AMP:ATP ratio is given by two binding sites for AMP, known as Bateman domains, in γ subunit. When AMP levels are increased, the nucleotide competitively displaces the ATP bound to the enzyme; and now, the bound AMP induces a conformational change that makes the protein a better substrate for the phosphorylation of the α-subunit at a specific threonine residue—Thr 172—by upstream kinases, AMPKK.

2. Phosphorylation by AMPKK constitutes the primary mechanism for the stimulation of AMPK activity.
3. The conformational modification of the protein induced by AMP binding also provokes a decrease in dephosphorylation by phosphatases and contributes to a sustained activation of the enzyme [49].

Altogether, these mechanisms make the AMPK system ultrasensitive to energy changes, an important fact for the ability of the enzyme to maintain the energy status of the cell within narrow limits.

Several reviews have dealt with the downstream targets and processes regulated by AMPK [50–53]. In general, activation of AMPK downregulates biosynthetic pathways such as fatty acid and cholesterol biosynthesis yet switches on catabolic pathways that generate ATP, such as fatty acid oxidation, glucose uptake, and glucose oxidation. AMPK regulates the above mentioned phenomena not only through direct phosphorylation of metabolic enzymes but also through effects on the expression of genes that are important to these metabolic pathways. Although protein expression, as a whole, is downregulated following AMPK activation, specific proteins, which are essential for metabolic adaptation, will bypass the condition of energy saving associated with the activation of this kinase and will increase their expression [54].

The expression of AMPK in the testis was demonstrated by Cheung and collaborators in 2000 [46]. These authors have also shown that the 75% of AMPK activity in the whole testis is attributed to α1AMPK and the remaining 25% to α2AMPK. However, it was not until 2007 that the role of AMPK in SC nutritional function gained increasing relevance.

AMPK activation leads to metabolic changes responsible for obtaining a maximum energy yield of glucose oxidation with a reduction in lactate production [55–57]. In this context, Faubert and collaborators [58] have recently demonstrated that AMPK is a negative regulator of Warburg effect in cancer cells. Surprisingly, the activation of AMPK in SCs leads to an increase in lactate production [59]. The latter piece of evidence suggested that under those conditions when there is an increase in the AMP:ATP ratio, indicative of low energy levels, SCs privilege lactate secretion in order to maintain the energy supply to germ cells. This asseveration was supported by the findings of Riera and collaborators [60]. The researchers have demonstrated that SCs adapt to conditions of glucose deprivation by AMPK activation to ensure an adequate lactate concentration in the microenvironment where germ cell development occurs. It is worth mentioning that α1AMPK-deficient male mice present decreased fertility and altered sperm morphology; meanwhile knockout mice for α2AMPK do not show

any anomaly in fertility or sperm morphology [61]. Further research has shown that specific deletion of the α1AMPK gene in mouse SCs results in a 25% reduction in male fertility associated with a deregulation in energy metabolism in SCs and thin-shaped sperm heads [62]. In agreement with the results obtained by Galardo and collaborators [59], these authors also suggest that AMPK is a positive regulator of Warburg effect in SCs. Considering that AMPK activation leads to an increase in aerobic glycolytic pathway, it is tempting to speculate that one of the mechanisms underlying low fertility rate in the above mentioned animal model may be related to the inability to produce sufficient amounts of lactate to maintain germ cell development.

As previously mentioned, several biochemical mechanisms may contribute to an increase in SC lactate secretion. The rise in lactate by AMPK activation in SCs is accompanied by an increase in glucose uptake (explained by GLUT1 expression augmentation), a downregulation of MCT1 mRNA levels, and a rise in MCT4 expression [59, 60]. The manner in which MCT1, specialized in lactate import, and MCT4, specialized in lactate export, are regulated in SCs by AMPK activation may reflect a situation of increased lactate export and decreased lactate recapture from the extracellular milieu leading to adequate lactate levels at the disposal of germ cells.

Taking into account that lactate is the main energy source for spermatocytes and spermatids and its production is tightly regulated [63–69], it is quite probable that hormones are not the only regulators of lactate production in SCs. Factors of nonprotein nature secreted by germ cells, which indicate a disbalance in energy levels in this cell type, should be considered. Regarding the signaling pathways that might be triggered in SCs by the latter factors released by germ cells, AMPK was postulated as the main candidate involved in restoring ATP levels in seminiferous tubule.

Many years ago, Monaco and Conti [70] postulated that adenosine resulting from ATP dephosphorylation in germ cells adequates SC function in order to promote energy balance reestablishment in germ cells. In support of the hypothesis that adenosine is secreted by germ cells, it is worth mentioning that Gelain and collaborators [71] showed that germ cells in culture release measurable adenosine levels to the extracellular milieu. Even more, the cellular production of adenosine is triggered by an increase in energy consumption or by hypoxia [72].

Most of the adenosine actions demonstrated in a variety of tissues have been studied by treatment with non-metabolizable nucleoside derivatives which bind to purinergic receptors coupled to specific signal transduction pathways [73]. The studies carried out in SCs incubated with nucleoside derivatives enabled to understand that the observed effects were mediated by type A1 purinergic

receptor coupled to Gi protein, which activation leads to a decrease in cAMP levels [74–77]. In addition to binding to purinergic receptors, adenosine can traverse cell membranes through nucleoside transporters—concentrative (CNT) and equilibrative (ENT) nucleoside transporters—which have been described in testicular cells [78].

It was shown that in SCs, adenosine increases lactate production regulating the expression of GLUT1, LDHA, and MCT4. Even more, the adenosine effects differ from those by N6-cyclohexyladenosine, a type A1 purinergic receptor agonist fully resistant to cellular uptake. These authors have also demonstrated that adenosine, after entering to SC and being converted into AMP by adenosine kinase, activates AMPK and that the augmentation in lactate production, induced by the nucleoside, depends on AMPK activation [79]. Figure 2 depicts the molecular mechanism involved in the regulation of lactate production regulated by adenosine in the seminiferous tubule.

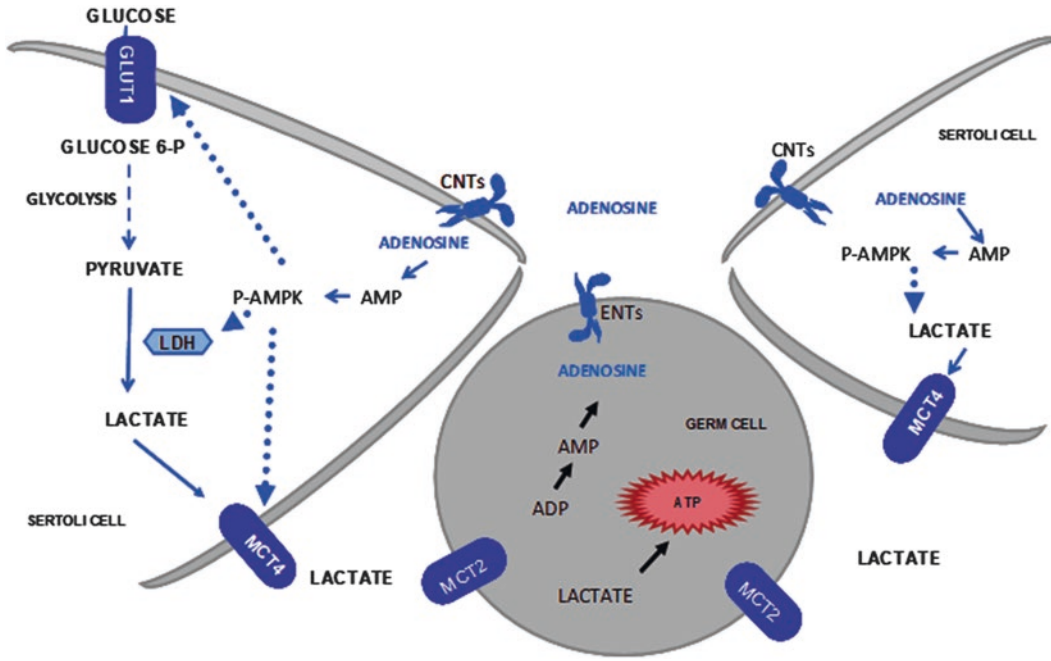

Fig. 2 Molecular mechanism involved in the regulation of lactate production by adenosine in the seminiferous tubule. Adenosine acts as a paracrine regulator between germ cells and Sertoli cells. Adenosine is secreted by germ cell through equilibrative nucleoside transporters (ENTs) and is later imported by Sertoli cells through concentrative nucleoside transporters (CNTs). There, it promotes GLUT1, LDHA and MCT4 expression and increases glucose uptake and LDH activity, resulting in lactate production augmentation. This lactate is exported to germ cells, which use it as nutritional source. Resulting ATP is used by germ cells, inevitably leading to ADP, later converted to AMP, and, finally, adenosine, reinitiating this cycle

5 Involvement of Hypoxia-Inducible Factors (HIFs) in Sertoli Cell Nutritional Function

The hypoxia-inducible factor (HIF) plays a central role in the regulation of mammalian metabolism. Active HIF is a heterodimer consisting of an oxygen-dependent HIFα subunit and a constitutively expressed HIFβ subunit. Under normoxic conditions, HIFα subunit is rapidly degraded via a mechanism that involves its hydroxylation by oxygen-dependent prolyl-hydroxylases. Prolyl-hydroxylase inhibition by low oxygen tension or transition metals like cobalt^{2+} (Co^{2+}) [80, 81] leads to HIFα subunit stabilization, which enables HIFα and HIFβ subunits to associate and form active HIF. Active HIF interacts with a consensus hypoxia response element (HRE) in the promoter region of target genes in order to stimulate transcription. Three isoforms of HIFα subunit (HIF1α, HIF2α, and HIF3α) have been characterized [82]. The association of each HIFα subunit with HIFβ subunit constitutes three active transcription factors: HIF1, HIF2, and HIF3 [83].

Classically HIF transcriptional activity has been associated with hypoxic conditions. However, some years ago, regulation by hormones of HIF transcriptional activity under normoxic conditions was demonstrated [84–86]. The physiological roles of HIFs are multifarious. While HIF1 and HIF2 regulate the expression of many genes in common, HIF1 preferentially induces genes involved in the glycolytic pathway [87–89], and HIF2 induces genes important for cell cycle progression like c-Myc [90] and cyclin D1 [91].

The expression of HIF1α and HIF2α in SCs was observed [92, 93], and in rather elegant experiments, a role of HIF2 in blood-testis barrier integrity was demonstrated [94].

Regarding SC nutritional function, the participation of HIFs in the regulation of lactate production was recently evidenced under normoxic conditions [95]. Authors have also shown that HIF transcriptional activity is modulated by FSH through the increase of HIF1α and HIF2α expression. Even more, FSH-stimulated lactate production depends on HIF transcriptional activity. The experimental strategy utilized by these authors to evaluate HIF participation in the regulation of lactate production by FSH does not enable to discern which hypoxia-inducible factor, HIF1 and/or HIF2, is involved. Considering that HIF1 is the master regulator of glycolysis, HIF1 may be predicted as the hypoxia-inducible factor that mostly contributes to the regulation of lactate production by FSH. The genes induced by FSH in a HIF-dependent manner, which explain the increase in lactate production, are GLUT1, PKM2, and LDHA [96]. Precisely, the latter genes present HRE sequences in their promoters [97, 98].

The mechanisms that regulate SC metabolism are essential for the maintenance of spermatogenesis and male fertility and deserve deep study. The relevant role of HIFs in modulating SC nutritional function has been elucidated. In addition, HIFs are key components of the intricate pathways utilized by FSH to regulate the provision of lactate for germ cells. Considering that FSH is the master endocrine regulator of SCs, it is not surprising that this hormone may employ several regulatory mechanisms to fulfill the nourishing functions of this cell type and to create the microenvironment where germ cell development takes place.

6 Regulation of Sertoli Cell Energy Metabolism: Participation of Peroxisome Proliferator-Activated Receptors (PPARs)

As described in previous paragraphs, there are a vast number of studies sought to clarify the molecular mechanisms involved in the maintenance of energy homeostasis of germ cells through SC function modulation. However, the molecular mechanisms that participate in the regulation of ATP levels in SCs have been neglected for many years.

As mentioned before, SC metabolism presents unique characteristics. Glucose is not an important source of energy for SCs; actually it has been shown that this cell type can survive in culture for at least 48 h in the absence of glucose [60]. Glucose is metabolized to lactate since germ cells situated beyond the blood-testis barrier rely on SC production of this hydroxy acid to obtain energy. In this metabolic scenario, it was observed that palmitate could be oxidized to CO_2, and it was suggested that the oxidation of fatty acids (FA) might yield much of the energy required by SC [99]. More recently, it has been demonstrated that FA must be readily available to sustain SC energy status [42]. The presence of numerous lipid droplets (LD) is characteristic in SC, and it may be assumed that these LD constitute the storage of FA. The possible regulation of FA utilization and storage, which would ensure FA availability for SC energetic requirements, by receptors that sense lipid status can be imagined.

Peroxisome proliferator-activated receptors (PPARs), α (NR1C1), β/δ (NR1C2), and γ (NR1C3), are ligand-activated transcription factors that are members of the nuclear-hormone receptor superfamily [100, 101]. All PPARs function as sensors of fatty acids and fatty acid derivatives and thus control metabolic pathways involved in lipid and energy metabolism [102, 103]. It has been well documented that PPARγ mainly mediates lipid anabolism, while PPARα and PPARβ/δ are regulators of lipid catabolism [104–108]. The expression of PPARs varies in different tissues [109]. In adult SCs, PPARα, PPARβ, and PPARγ seem to be

expressed at variable degrees [110]. Additionally, a developmental pattern of PPAR gene expression in SCs during spermatogenesis, probably reflecting an important physiological role of these nuclear receptors in germ cell development, has been demonstrated [111]. Considering the important role of FA utilization and storage for SC metabolic activity, a central role of PPARs in the regulation of SC energetic metabolism could be envisaged. In this context, the role of catabolic PPARs was highlighted by a study carried out in 2014 by Regueira and collaborators [112]. These authors have shown that pharmacological PPARα and PPARβ/δ activation regulates the expression of genes involved in FA catabolism such as Fat/CD36, carnitine palmitoyltransferase 1 (CPT1), and long- and medium-chain 3-hydroxyacyl-CoA dehydrogenases (LCAD and MCAD) in SC [112]. They have also observed that PPARβ/δ activation can simultaneously regulate FA oxidation and lactate production, and these results have been interpreted as a coordinated mechanism that will ensure the concurrent provision of energy to SC and germ cells.

Regarding PPARγ role in SC metabolism, it is tempting to speculate that activation of this anabolic PPAR exerts effects related with lipid synthesis and storage. Recent evidence shows the participation of PPARγ in the regulation of triacylglycerol synthesis and lipid droplet formation in SCs [113]. The authors show that the increase in TAG and lipid droplet levels was accompanied by a rise in the expression of genes that are involved in fatty acid storage such as the fatty acid transporter FAT/CD36, the glycerol-3-phosphate-acyltransferase 1 (GPAT1), and perilipins 1, 2, and 3, proteins that participate in lipid droplet formation and stabilization. On the other hand, PPARγ activation increased lactate production. This increase was accompanied by an augmentation in glucose uptake and Glut2 expression. Altogether, the results suggest that PPARγ activation in SCs participates in the regulation of lipid storage and lactate production ensuring simultaneously the energetic metabolism for Sertoli and germ cells.

In summary, PPAR activation in SC plays a central role in lipid and lactate utilization. On the one hand, PPARα and PPARβ/δ (PPARs with catabolic functions) regulate the expression of genes involved in fatty acid transport and catabolism, and on the other hand, PPARγ regulates anabolic lipid metabolism, increasing TAG and lipid droplet levels. Both PPARβ/δ and PPARγ also participate in the regulation of lactate production to provide energetic substrates for germ cell and positioning these PPARs as main players in the regulation of seminiferous tubule metabolism. Figure 3 shows how different PPAR isoform combinations shift SC metabolism toward specific pathways.

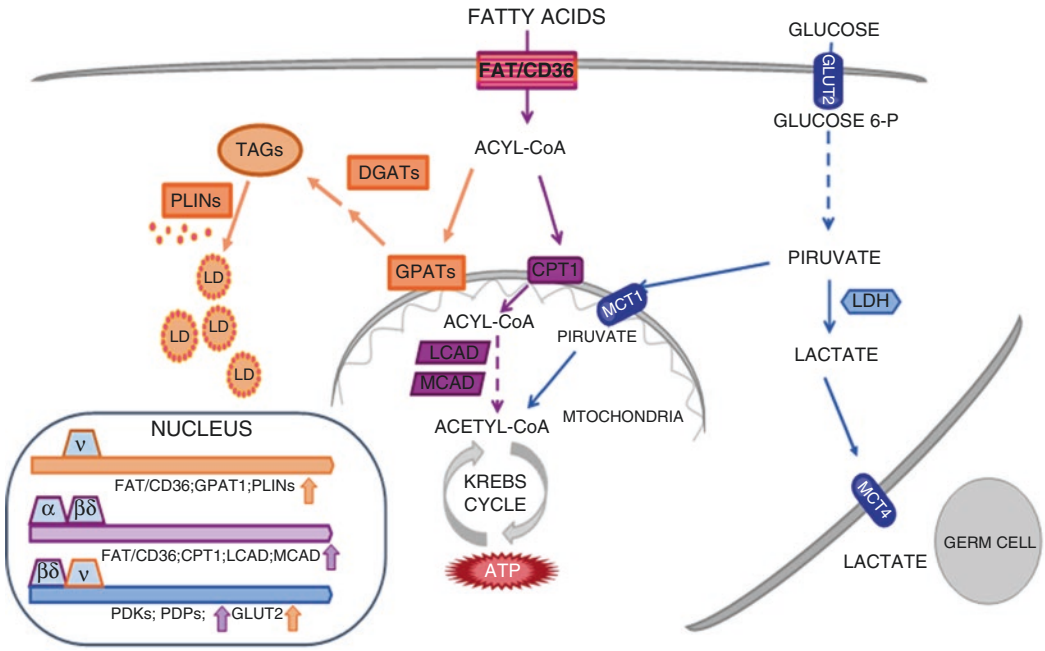

Fig. 3 Role of PPARs in the regulation of fatty acid metabolism and lactate production in Sertoli cells. Each isoform of peroxisome proliferator-activated receptor (PPAR) promotes different metabolic pathways in Sertoli cells. When PPARγ is activated, the expression of FAT/CD36, GPAT1 and PLINs is promoted, causing a shift toward lipogenesis. On the other hand, when PPARα and PPARβ/δ are activated, Sertoli cell metabolism moves toward full free fatty acid oxidation, due to an increase in FAT/CD36, CPT1, LCAD, and MCAD expression resulting in ATP augmentation. Simultaneously, activation of PPARγ and PPARβ/δ stimulates the glycolytic pathway, through the increase in GLUT2, PDKs and PDPs expression. In this scenario, lactate production and export to germ cells is also promoted, while a smaller portion of pyruvate is used to obtain ATP

7 Impact of Whole-Body Metabolic Dysfunction in Sertoli Cell Metabolism and Spermatogenesis

In the last decades, we have been witnessing a steady increase in male fertility dysfunction and a decrease on fertility rates worldwide but particularly significant on high HDI countries [114]. Simultaneously, the incidence of metabolic disorders, particularly obesity and type 2 diabetes (T2D), significantly increased worldwide and again with special impact in developed countries [115]. The overlapping nature of both premises led to the hypothesis that a relation between metabolic dysfunction and male infertility may occur [116]. In fact, clinical studies seem to confirm this association: obese and overweight men have poorer fertility outcomes than lean men, and thus, couples with an overweight or obese man will have problems to conceive [116]. Although some causes for those fertility problems were not difficult to associate to excess of weight, the same is not true for other metabolic disorders such as T2D. Obese and overweight men often have their fertility

compromised by mechanic factors, such as testicular overheat due to adipose tissue accumulation or even coitus difficulties and erectile dysfunction linked to cardiovascular complications [117]. Diabetic men also present fertility dysfunction linked to microvascular disease, reflected as lower tubule diameter, abnormal testicular capillary and lymphatic endothelia, SC-only tubules, and ultrastructural damage in SC apical cytoplasm [118]. It is also reported that microvascular disease increases vascular density and cellular matrix thickening, simultaneously promoting germ cell apoptosis due to increased scrotal temperature and hypoxia-induced cellular damage [32, 118, 119]. Moreover, T2D patients often present ejaculatory defects, such as erectile dysfunction and retrograde ejaculation [118]. But those factors do not reflect most of infertility's etiology.

One of the first molecular mechanisms explaining male infertility due to obesity was based on the steroidogenic potential of adipocytes [120]. Obese men present higher E_2 levels than the average male population, because they have more fat cells, and those cells present p450 aromatase, an enzyme that converts testosterone to E_2 [121]. Estrogens in men have similar effects over the pituitary as in women, exerting a negative feedback over LH and FSH release [31] and a consequent decrease of testosterone secretion and SC activity. Ultimately, the reproductive axis disruption leads to spermatogenesis defects or even arrest [30, 31, 122]. Furthermore, E_2 impairs ionic transport via CFTR on SCs, resulting in less ionic exchanges between lumen and intracellular environment, cytoplasmic acidification, and possibly spermatogenic defects [24, 25]. On the opposite side, fasting suppresses GnRH pulses, thus perturbing reproductive axis, first by inhibiting LH release, which in turn inhibits the release of gonadotropins, and lastly by decreasing androgen secretion by Leydig cells and Sertoli activity [1, 123].

The SC is the central target of environmental toxicants responsible to male reproductive defects, as evidenced by in vitro and in vivo models [124]. The first compromising action of those toxicants is the negative effect on cell junctions between SCs and Sertoli-germ cells [124]. Chemotherapeutic drugs [125], gossypol [126], glycerol [127], alkylphenols [128], pesticides [129], and heavy metals [130] are just examples of compounds known for interfering with cells' adhesion. Furthermore, some pesticides, phthalates, and obesogens can also work as endocrine disruptors, since their chemical structure is either similar to steroid hormones or competitively inhibits gonadotropin's receptors in SCs [31, 124]. Those compounds are known as endocrine disruptors because their action causes imbalances on the tightly balanced reproductive axis, disrupting the expected negative feedback mechanisms between the hypothalamus and hypophysis complex and the gonads [31, 124]. Obesogens aggravate their disrupting effect by promoting adipose tissue accumulation, which causes

(1) increasing storage of environmental toxicants, since most of them are fat-soluble, and (2) a self-endocrine disruptor, since adipocytes present significant activity levels of aromatase, an enzyme that converts testosterone to E_2 [31].

However, the nefarious effects of metabolic disorders are not restricted to systemic defects; they are also reflected *in loco*. Metabolic hormones affect whole-body cell metabolism, and testes are no exception [1, 37, 123, 131–133]. One of the main metabolites secreted by SC is acetate, which is suggested to be involved in germ cell membrane remodeling. Interestingly, in the absence of insulin, SCs totally inhibit acetate production [18], illustrating that insulin dysfunction may cause serious defects on the metabolic support of spermatogenesis by SCs. The close metabolic cooperation between Sertoli and germ cells is based on their proximity, maintained by the numerous cell junctions, which are threatened by changes on environment composition, and metabolic by-products capable to disrupt those junctions [124]. Glycerol is a suitable example. Its antispermatogenic properties when directly injected in testes, at high concentrations, are caused by BTB disassembly due to tight junctions' cleavage and overall SeT disorganization [127, 134]. There are several examples of hormones linked to whole-body metabolic status that also exert direct and indirect effects on SC metabolism [1, 21, 37, 123, 131, 132].

Leptin increases fat mobilization from adipocytes so it can be used as fuel by cells. Liver is the main destiny of adipocyte-derived triacylglycerols, where they suffer lipolysis. The resulting fatty acids are used for energy production, mainly through β-oxidation [135]. Resulting glycerol is phosphorylated into glycerol-3-phosphate (G3P) and enters the G3P shuttle, a cyclic reaction group that links lipidic and carbohydrate metabolism, TCA cycle, and electron transport chain (ETC) [136]. Obese and diabetic men present higher serum glycerol concentrations resulting from triacylglycerol breakdown [137]. The combination of insulin and leptin also promotes lipid mobilization in SCs for energy production, and they express several aquaglyceroporins (AQGPs), a AQP subfamily capable of transporting small solutes such as glycerol, in addition to water [44, 135, 138]. However, glycerol has antispermatogenic properties, since it destabilizes the actin filaments that allow the BTB and the germ cell attachment to SCs [127]. Leptin also promotes GLUT expression and lactate dehydrogenase (LDH) activity in SCs but decreases acetate production [132].

Ghrelin is another metabolic hormone whose receptor is present in SCs. Its whole-body metabolic effect is glucose blood and interstitial concentration decrease, due to increased insulin sensitivity of the cells [139]. Ghrelin concentration is inversely proportional to nutritional state, so obese individuals show the lowest blood concentration (and higher insulin resistance), while undernourished present the highest blood concentration (and lowest insulin resistance) [133]. In cultured SCs, ghrelin media concentration seems

to be inversely proportional to lactate production [133], which indicates that fasting may be worse than overeating in what concerns the effects of ghrelin on the nutritional support of spermatogenesis by SCs. However, the ghrelin concentration corresponding to the average in lean man increases the efficiency of glycolytic metabolism, i.e., redirects the cell metabolism to obtain a better lactate-to-glucose ratio, increasing LDH activity while decreasing glucose consumption [133]. Since reproductive function requires a proper nutritional state, and according to ghrelin concentration variation in function of the nutritional state of the individual, it is legitimate to declare that ghrelin acts as a nutritional state sensor [140]. Ghrelin inhibits LH release by pituitary in dose-dependent manner. This is especially important for puberty onset, as it needs proper energy store, although this has only been observed in males [140]. Yet, this effect is valid for adulthood as well; thus, ghrelin may impair the reproductive axis due to LH release inhibition and consequent decrease in testosterone [140]. In Fig. 4, all the hormonal mechanisms which influence Sertoli cell function mentioned in this chapter are depicted.

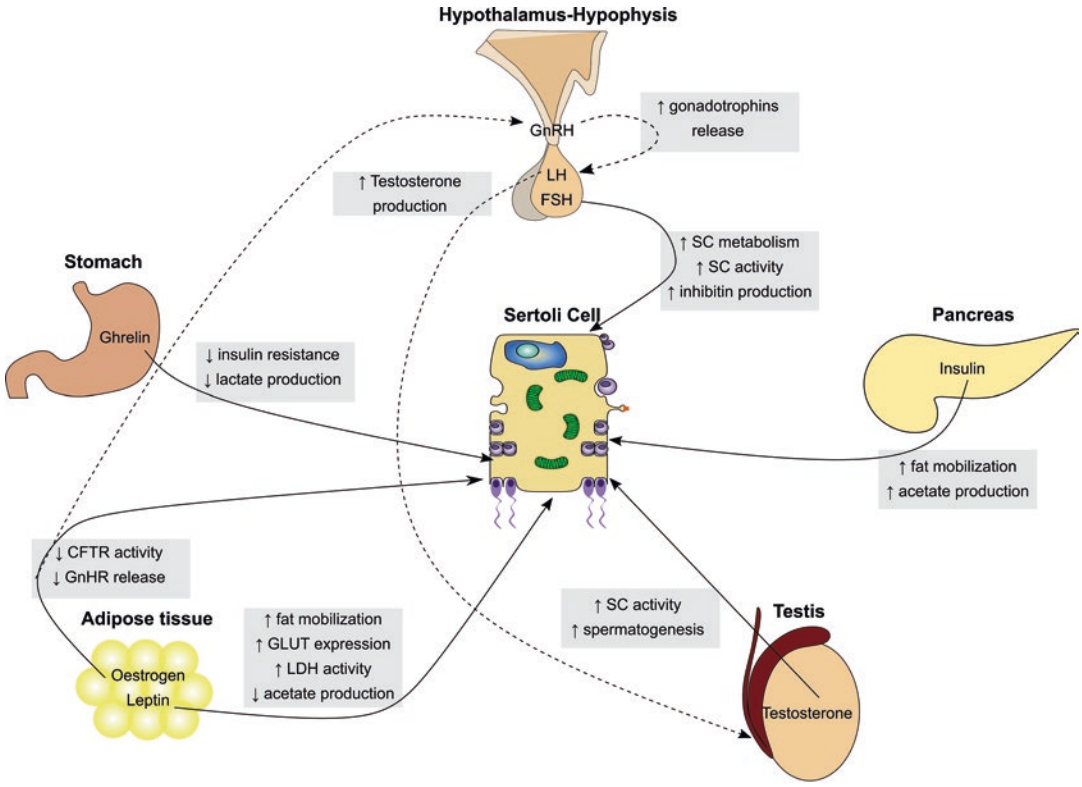

Fig. 4 Hormonal regulation of Sertoli cells. Sertoli cells are directly targeted and react to several hormones. Due to their central role on testicular physiology, those responses potentially affect spermatogenesis outcomes, either positively or negatively. Moreover, the tightly regulated hormonal circuits mean that there are hormones that can indirectly affect Sertoli cell function

8 Conclusions

The importance of SCs in spermatogenesis is undeniable. They are extremely specialized cells and had developed unique characteristics to accomplish their function effectively. We must not forget that germ cells are also unique cells in the human body, thus requiring unparalleled conditions. SCs reflect their unique needs and are responsible for creating the suitable environment for germ cell differentiation and survival throughout spermatogenesis, acting as an interface between them and the extracellular environment. Knowing this principle, it becomes easier to understand all the actions promoted by SCs to achieve a successful spermatogenesis. They create the BTB, by the tight junctions, hemidesmosomes and tubulobulbar complexes between SCs, creating the two-compartment system. This barrier impermeates the adluminal space, where germ cells differentiate, while granting it immunological immunity; otherwise, germ cells would be regarded as targets of the immune system. However, this isolation makes difficult the diffusion of substrates for germ cells. Once more, SCs mediate their diffusion, importing the substrates from the extracellular medium and then providing them to the germ cells or exporting them to the tubular fluid while maintaining the right pH and ionic balance of this fluid.

The regulation of the abovementioned functions is complex. SCs must respond to tubular fluid and extracellular medium composition, to the cooperation of the neighboring cells, and to hormonal regulation. In this chapter, we had shed light over the molecular mechanisms which regulate SC response to the various stimuli. Understanding those processes is pivotal on male fertility research. Any alteration of the metabolites, hormones, and messengers on these processes can deeply impact male fertility. Although there are already plenty bibliographies on the subject, many questions arise from the actual knowledge. The molecular mechanisms which regulate SC is a fertile research ground. Hopefully, advances on the research on this subject may lead us to new therapeutical approaches against the ever-increasing number of male infertility cases.

Acknowledgments

This work was supported by the “Fundação para a Ciência e a Tecnologia” (FCT) and co-funded by Fundo Europeu de Desenvolvimento Regional (FEDER) via Programa Operacional Factores de Competitividade COMPETE/QREN to UMIB (Pest OE/SAU/UI0215/2014); POCI—COMPETE 2020—Operational Programme Competitiveness and Internationalization in Axis I (Strengthening research, technological development and

innovation) (Project No. 007491); and National Funds of FCT (Foundation for Science and Technology): PF Oliveira (PTDC/BBB-BQB/1368/2014 and IFCT2015) and MG Alves (PTDC/BIM-MET/4712/2014 and IFCT2015). L Crisóstomo was funded by the fellowship "Bolsa Nuno Castel-Branco" from the Portuguese Society of Diabetology. This work was also supported by grants from the Agencia Nacional de Promoción Científica y Tecnológica (ANPCYT) (PICT 2014/945) and the Consejo Nacional de Investigaciones Científicas y Técnicas (CONICET) (PIP 2015/1827). M.F. Riera, M.N. Galardo, and S.B. Meroni are established investigators of CONICET. A. Gorga is a recipient of ANPCYT fellowship.

References

1. Rato L, Alves MG, Socorro S, Duarte AI, Cavaco JE, Oliveira PF (2012) Metabolic regulation is important for spermatogenesis. Nat Rev Urol 9(6):330–338. https://doi.org/10.1038/nrurol.2012.77
2. Griswold MD (1998) The central role of Sertoli cells in spermatogenesis. Semin Cell Dev Biol 9:411–416
3. Sertoli E (1865) Dell'esistenza di particolari cellule ramificate nei canalicoli seminiferi del testicolo umano. Il Morgagni 7:31–39
4. von Ebner V (1887) Zur spermatogenese bei den säugethieren. Arch Mikrosk Anat 31(1):236–292
5. França L, Hess R, Dufour J, Hofmann M, Griswold M (2016) The Sertoli cell: one hundred fifty years of beauty and plasticity. Andrology 4(2):182–212
6. Oliveira PF, Alves MG (2015) Sertoli cell metabolism and spermatogenesis, Springer briefs in cell biology, 1st edn. Springer International Publishing, New York. https://doi.org/10.1007/978-3-319-19791-3
7. Rebourcet D, O'Shaughnessy PJ, Monteiro A, Milne L, Cruickshanks L, Jeffrey N, Guillou F, Freeman TC, Mitchell RT, Smith LB (2014) Sertoli cells maintain Leydig cell number and peritubular myoid cell activity in the adult mouse testis. PLoS One 9(8):e105687
8. Nagano M, Avarbock MR, Leonida EB, Brinster CJ, Brinster RL (1998) Culture of mouse spermatogonial stem cells. Tissue Cell 30(4):389–397
9. Xie L, Lin L, Tang Q, Li W, Huang T, Huo X, Liu X, Jiang J, He G, Ma L (2015) Sertoli cell-mediated differentiation of male germ cell-like cells from human umbilical cord Wharton's jelly-derived mesenchymal stem cells in an in vitro co-culture system. Eur J Med Res 20(1):9–19
10. Zanganeh BM, Rastegar T, Roudkenar MH, Kashani IR, Amidi F, Abolhasani F, Barbarestani M (2013) Co-culture of spermatogonial stem cells with sertoli cells in the presence of testosterone and FSH improved differentiation via up-regulation of post meiotic genes. Acta Med Iran 51(1):1–11
11. Johnson L, Thompson DL, Varner DD (2008) Role of Sertoli cell number and function on regulation of spermatogenesis. Anim Reprod Sci 105(1):23–51
12. Schlatt S, Ehmcke J (2014) Regulation of spermatogenesis: an evolutionary biologist's perspective. Semin Cell Dev Biol 29:2–16
13. Orth JM, Gunsalus GL, Lamperti AA (1988) Evidence from Sertoli cell-depleted rats indicates that spermatid number in adults depends on numbers of Sertoli cells produced during perinatal development. Endocrinology 122(3):787–794
14. Orth JM, Higginbotham C, Salisbury R (1984) Hemicastration causes and testosterone prevents enhanced uptake of [3H] thymidine by Sertoli cells in testes of immature rats. Biol Reprod 30(1):263–270
15. Simorangkir D, De Kretser D, Wreford N (1995) Increased numbers of Sertoli and germ cells in adult rat testes induced by synergistic action of transient neonatal hypothyroidism and neonatal hemicastration. J Reprod Fertil 104(2):207–213
16. Layman LC, Porto AL, Xie J, Da Motta LACR, Da Motta LDC, Weiser W, Sluss PM (2002) FSHβ gene mutations in a female with partial breast development and a male sibling with normal puberty and azoospermia. J Clin Endocrinol Metab 87(8):3702–3707
17. Arslan M, Zaidi P, Akhtar FB, Amin S, Rana T, Qazi M (1981) Effects of gonadotrophin treatment in vivo on testicular function in

immature rhesus monkeys (Macaca mulatta). Int J Androl 4(1–6):462–474
18. Alves MG, Martins AD, Rato L, Moreira PI, Socorro S, Oliveira PF (2013) Molecular mechanisms beyond glucose transport in diabetes-related male infertility. Biochim Biophys Acta 1832(5):626–635. https://doi.org/10.1016/j.bbadis.2013.01.011
19. Dimitriadis F, Tsiampali C, Chaliasos N, Tsounapi P, Takenaka A, Sofikitis N (2015) The Sertoli cell as the orchestra conductor of spermatogenesis: spermatogenic cells dance to the tune of testosterone. Hormones 14(4):479–503
20. Oliveira PF, Martins AD, Moreira AC, Cheng CY, Alves MG (2015) The Warburg effect revisited—lesson from the Sertoli cell. Med Res Rev 35(1):126–151
21. Rato L, Meneses MJ, Silva BM, Sousa M, Alves MG, Oliveira PF (2016) New insights on hormones and factors that modulate Sertoli cell metabolism. Histol Histopathol 31(5):499–513
22. Wong CH, Cheng CY (2005) The blood-testis barrier: its biology, regulation, and physiological role in spermatogenesis. In: Schatten GP (ed) Current topics in developmental biology, vol 71, 1st edn. Elsevier Inc., Amsterdam, pp 263–296. https://doi.org/10.1016/S0070-2153(05)71008-5
23. Geens M, Sermon KD, Van de Velde H, Tournaye H (2011) Sertoli cell-conditioned medium induces germ cell differentiation in human embryonic stem cells. J Assist Reprod Genet 28(5):471–480
24. Bernardino RL, Costa AR, Martins AD, Silva J, Barros A, Sousa M, Sá R, Alves MG, Oliveira PF (2016) Estradiol modulates Na+−dependent HCO3− transporters altering intracellular pH and ion transport in human Sertoli cells: a role on male fertility? Biol Cell 108(7):179–188
25. Bernardino RL, Jesus TT, Martins AD, Sousa M, Barros A, Cavaco JE, Socorro S, Alves MG, Oliveira PF (2013) Molecular basis of bicarbonate membrane transport in the male reproductive tract. Curr Med Chem 20(32):4037–4049. https://doi.org/10.2174/15672050113109990200
26. Martins AD, Bernardino RL, Neuhaus-Oliveira A, Sousa M, Sá R, Alves MG, Oliveira PF (2014) Physiology of Na+/H+ exchangers in the male reproductive tract: relevance for male fertility. Biol Reprod 91(1):11–16
27. Janecki A, Steinberger A (1986) Polarized Sertoli cell functions in a new two-compartment culture system. J Androl 7(1):69–71
28. Vogl AW, Young J, Du M (2013) New insights into roles of tubulobulbar complexes in sperm release and turnover of blood-testis barrier. Int Rev Cell Mol Biol 303:319–355
29. Cheng CY, Mruk DD (2002) Cell junction dynamics in the testis: Sertoli-germ cell interactions and male contraceptive development. Physiol Rev 82(4):825–874
30. Alves MG, Rato L, Carvalho RA, Moreira PI, Socorro S, Oliveira PF (2013) Hormonal control of Sertoli cell metabolism regulates spermatogenesis. Cell Mol Life Sci 70(5):777–793. https://doi.org/10.1007/s00018-012-1079-1
31. Cardoso AM, Alves MG, Mathur PP, Oliveira PF, Cavaco JE, Rato L (2017) Obesogens and male fertility. Obes Rev 18(1):109–125
32. Anderson JE, Thliveris JA (1986) Testicular histology in streptozotocin-induced diabetes. Anat Rec (Hoboken) 214(4):378–382. https://doi.org/10.1002/ar.1092140407
33. Whitmore LS, Ye P (2015) Dissecting germ cell metabolism through network modeling. PLoS One 10(9):e0137607
34. Boussouar F, Benahmed M (2004) Lactate and energy metabolism in male germ cells. Trends Endocrinol Metab 15(7):345–350
35. Miki K (2006) Energy metabolism and sperm function. Soc Reprod Fertil Suppl 65:309–325
36. Martins AD, Alves MG, Simões VL, Dias TR, Rato L, Moreira PI, Socorro S, Cavaco JE, Oliveira PF (2013) Control of Sertoli cell metabolism by sex steroid hormones is mediated through modulation in glycolysis-related transporters and enzymes. Cell Tissue Res 354(3):861–868
37. Oliveira PF, Alves MG, Rato L, Laurentino S, Silva J, Sá R, Barros A, Sousa M, Carvalho RA, Cavaco JE (2012) Effect of insulin deprivation on metabolism and metabolism-associated gene transcript levels of in vitro cultured human Sertoli cells. Biochim Biophys Acta 1820(2):84–89
38. Grootegoed J, Oonk R, Jansen R, Van der Molen H (1986) Metabolism of radiolabelled energy-yielding substrates by rat Sertoli cells. J Reprod Fertil 77(1):109–118
39. Galardo MN, Regueira M, Riera MF, Pellizzari EH, Cigorraga SB, Meroni SB (2014) Lactate regulates rat male germ cell function through reactive oxygen species. PLoS One 9(1):e88024
40. Erkkilä K, Aito H, Aalto K, Pentikäinen V, Dunkel L (2002) Lactate inhibits germ cell apoptosis in the human testis. Mol Hum Reprod 8(2):109–117
41. Murphy CJ, Richburg JH (2014) Implications of Sertoli cell induced germ cell apoptosis

to testicular pathology. Spermatogenesis 4(2):e979110
42. Xiong W, Wang H, Wu H, Chen Y, Han D (2009) Apoptotic spermatogenic cells can be energy sources for Sertoli cells. Reproduction 137(3):469–479
43. Jesus TT, Bernardino RL, Martins AD, Sá R, Sousa M, Alves MG, Oliveira PF (2014) Aquaporin-4 as a molecular partner of cystic fibrosis transmembrane conductance regulator in rat Sertoli cells. Biochem Biophys Res Commun 446(4):1017–1021
44. Jesus TT, Bernardino RL, Martins AD, Sá R, Sousa M, Alves MG, Oliveira PF (2014) Aquaporin-9 is expressed in rat Sertoli cells and interacts with the cystic fibrosis transmembrane conductance regulator. IUBMB Life 66(9):639–644. https://doi.org/10.1002/iub.1312
45. Hardie DG (2003) Minireview: the AMP-activated protein kinase cascade: the key sensor of cellular energy status. Endocrinology 144(12):5179–5183
46. Cheung PC, Davies SP, Hardie DG, Carling D (2000) Characterization of AMP-activated protein kinase γ-subunit isoforms and their role in AMP binding. Biochem J 346(3):659–669
47. Stapleton D, Mitchelhill KI, Gao G, Widmer J, Michell BJ, Teh T, House CM, Fernandez CS, Cox T, Witters LA (1996) Mammalian AMP-activated protein kinase subfamily. J Biol Chem 271(2):611–614
48. Thornton C, Snowden MA, Carling D (1998) Identification of a novel AMP-activated protein kinase β subunit isoform that is highly expressed in skeletal muscle. J Biol Chem 273(20):12443–12450
49. Hardie DG (2004) The AMP-activated protein kinase pathway–new players upstream and downstream. J Cell Sci 117(23):5479–5487
50. Hardie DG (2005) New roles for the LKB1 → AMPK pathway. Curr Opin Cell Biol 17(2):167–173
51. Hardie DG, Ashford ML (2014) AMPK: regulating energy balance at the cellular and whole body levels. Physiology 29(2):99–107
52. Hardie DG, Pan D (2002) Regulation of fatty acid synthesis and oxidation by the AMP-activated protein kinase. Biochem Soc Trans 30(6):1064–1070
53. Hardie DG, Sakamoto K (2006) AMPK: a key sensor of fuel and energy status in skeletal muscle. Physiology 21(1):48–60
54. Hardie DG, Hawley SA (2001) AMP-activated protein kinase: the energy charge hypothesis revisited. BioEssays 23(12):1112–1119
55. Ceddia RB, Sweeney G (2004) Creatine supplementation increases glucose oxidation and AMPK phosphorylation and reduces lactate production in L6 rat skeletal muscle cells. J Physiol 555(2):409–421
56. Putman CT, Kiricsi M, Pearcey J, MacLean IM, Bamford JA, Murdoch GK, Dixon WT, Pette D (2003) AMPK activation increases uncoupling protein-3 expression and mitochondrial enzyme activities in rat muscle without fibre type transitions. J Physiol 551(1):169–178
57. Smith AC, Bruce CR, Dyck DJ (2005) AMP kinase activation with AICAR simultaneously increases fatty acid and glucose oxidation in resting rat soleus muscle. J Physiol 565(2):537–546
58. Faubert B, Boily G, Izreig S, Griss T, Samborska B, Dong Z, Dupuy F, Chambers C, Fuerth BJ, Viollet B (2013) AMPK is a negative regulator of the Warburg effect and suppresses tumor growth in vivo. Cell Metab 17(1):113–124
59. Galardo MN, Riera MF, Pellizzari EH, Cigorraga SB, Meroni SB (2007) The AMP-activated protein kinase activator, 5-aminoimidazole-4-carboxamide-1-bD-ribonucleoside, regulates lactate production in rat Sertoli cells. J Mol Endocrinol 39(4):279–288
60. Riera MF, Galardo MN, Pellizzari EH, Meroni SB, Cigorraga SB (2009) Molecular mechanisms involved in Sertoli cell adaptation to glucose deprivation. Am J Physiol Endocrinol Metab 297(4):E907–E914
61. Tartarin P, Guibert E, Touré A, Ouiste C, Leclerc J, Sanz N, Brière S, Dacheux J-L, Delaleu B, McNeilly JR (2012) Inactivation of AMPKα1 induces asthenozoospermia and alters spermatozoa morphology. Endocrinology 153(7):3468–3481
62. Bertoldo MJ, Guibert E, Faure M, Guillou F, Ramé C, Nadal-Desbarats L, Foretz M, Viollet B, Dupont J, Froment P (2016) Specific deletion of AMP-activated protein kinase (α1AMPK) in mouse Sertoli cells modifies germ cell quality. Mol Cell Endocrinol 423:96–112
63. Boussouar F, Benahmed M (1999) Epidermal growth factor regulates glucose metabolism through lactate dehydrogenase A messenger ribonucleic acid expression in cultured porcine Sertoli cells. Biol Reprod 61(4):1139–1145
64. Meroni S, Riera M, Pellizzari E, Cigorraga S (2002) Regulation of rat Sertoli cell function by FSH: possible role of phosphatidylinositol 3-kinase/protein kinase B pathway. J Endocrinol 174(2):195–204
65. Nehar D, Mauduit C, Boussouar F, Benahmed M (1998) Interleukin 1α stimulates lactate dehydrogenase A expression and lactate pro-

duction in cultured porcine Sertoli cells. Biol Reprod 59(6):1425–1432
66. Rato L, Alves MG, Socorro S, Carvalho RA, Cavaco JE, Oliveira PF (2012) Metabolic modulation induced by oestradiol and DHT in immature rat Sertoli cells cultured in vitro. Biosci Rep 32(1):61–69
67. Regueira M, Artagaveytia SL, Galardo MN, Pellizzari EH, Cigorraga SB, Meroni SB, Riera MF (2015) Novel molecular mechanisms involved in hormonal regulation of lactate production in Sertoli cells. Reproduction 150(4):311–321
68. Riera MF, Galardo MN, Pellizzari EH, Meroni SB, Cigorraga SB (2007) Participation of phosphatidyl inositol 3-kinase/protein kinase B and ERK1/2 pathways in interleukin-1β stimulation of lactate production in Sertoli cells. Reproduction 133(4):763–773
69. Rocha CS, Martins AD, Rato L, Silva BM, Oliveira PF, Alves MG (2014) Melatonin alters the glycolytic profile of Sertoli cells: implications for male fertility. Mol Hum Reprod 20(11):1067–1076
70. Monaco L, Conti M (1986) Localization of adenosine receptors in rat testicular cells. Biol Reprod 35(2):258–266
71. Gelain DP, De Souza LF, Bernard EA (2003) Extracellular purines from cells of seminiferous tubules. Mol Cell Biochem 245(1):1–9
72. Newby AC (1984) Adenosine and the concept of 'retaliatory metabolites'. Trends Biochem Sci 9(2):42–44
73. Bjelobaba I, Janjic MM, Stojilkovic SS (2015) Purinergic signaling pathways in endocrine system. Auton Neurosci 191:102–116
74. Conti M, Boitani C, Demanno D, Migliaccio S, Monaco L, Szymeczek C (1989) Characterization and function of adenosine receptors in the testisa. Ann N Y Acad Sci 564(1):39–47
75. Conti M, Culler MD, Negro-Vilar A (1988) Adenosine receptor-dependent modulation of inhibin secretion in cultured immature rat Sertoli cells. Mol Cell Endocrinol 59(3):255–259
76. Meroni S, Cánepa D, Pellizzari E, Schteingart H, Cigorraga S (1998) Effects of purinergic agonists on aromatase and gamma-glutamyl transpeptidase activities and on transferrin secretion in cultured Sertoli cells. J Endocrinol 157(2):275–283
77. Monaco L, Toscano M, Conti M (1984) Purine modulation of the hormonal response of the rat Sertoli cell in culture. Endocrinology 115(4):1616–1624
78. Kato R, Maeda T, Akaike T, Tamai I (2005) Nucleoside transport at the blood-testis barrier studied with primary-cultured sertoli cells. J Pharmacol Exp Ther 312(2):601–608
79. Galardo M, Riera M, Pellizzari E, Sobarzo C, Scarcelli R, Denduchis B, Lustig L, Cigorraga S, Meroni S (2010) Adenosine regulates Sertoli cell function by activating AMPK. Mol Cell Endocrinol 330(1):49–58
80. Biswas S, Mukherjee R, Tapryal N, Singh AK, Mukhopadhyay CK (2013) Insulin regulates hypoxia-inducible factor-1α transcription by reactive oxygen species sensitive activation of Sp1 in 3T3-L1 preadipocyte. PLoS One 8(4):e62128
81. Chan DA, Sutphin PD, Denko NC, Giaccia AJ (2002) Role of prolyl hydroxylation in oncogenically stabilized hypoxia-inducible factor-1α. J Biol Chem 277(42):40112–40117
82. Kietzmann T, Cornesse Y, Brechtel K, Modaressi S, Jungermann K (2001) Perivenous expression of the mRNA of the three hypoxia-inducible factor α-subunits, HIF1α, HIF2α and HIF3α, in rat liver. Biochem J 354(3):531–537
83. Wenger RH (2002) Cellular adaptation to hypoxia: O2-sensing protein hydroxylases, hypoxia-inducible transcription factors, and O2-regulated gene expression. FASEB J 16(10):1151–1162
84. Fukuda R, Hirota K, Fan F, Do Jung Y, Ellis LM, Semenza GL (2002) Insulin-like growth factor 1 induces hypoxia-inducible factor 1-mediated vascular endothelial growth factor expression, which is dependent on MAP kinase and phosphatidylinositol 3-kinase signaling in colon cancer cells. J Biol Chem 277(41):38205–38211
85. Laughner E, Taghavi P, Chiles K, Mahon PC, Semenza GL (2001) HER2 (neu) signaling increases the rate of hypoxia-inducible factor 1α (HIF-1α) synthesis: novel mechanism for HIF-1-mediated vascular endothelial growth factor expression. Mol Cell Biol 21(12):3995–4004
86. Treins C, Giorgetti-Peraldi S, Murdaca J, Semenza GL, Van Obberghen E (2002) Insulin stimulates hypoxia-inducible factor 1 through a phosphatidylinositol 3-kinase/target of rapamycin-dependent signaling pathway. J Biol Chem 277(31):27975–27981
87. Hu C-J, Sataur A, Wang L, Chen H, Simon MC (2007) The N-terminal transactivation domain confers target gene specificity of hypoxia-inducible factors HIF-1α and HIF-2α. Mol Biol Cell 18(11):4528–4542
88. Hu C-J, Wang L-Y, Chodosh LA, Keith B, Simon MC (2003) Differential roles of hypoxia-inducible factor 1α (HIF-1α) and HIF-2α in hypoxic gene regulation. Mol Cell Biol 23(24):9361–9374
89. Wang V, Davis DA, Haque M, Huang LE, Yarchoan R (2005) Differential gene up-regulation by hypoxia-inducible factor-1α and

hypoxia-inducible factor-2α in HEK293T cells. Cancer Res 65(8):3299–3306
90. Gordan JD, Bertout JA, C-J H, Diehl JA, Simon MC (2007) HIF-2α promotes hypoxic cell proliferation by enhancing c-myc transcriptional activity. Cancer Cell 11(4):335–347
91. Raval RR, Lau KW, Tran MG, Sowter HM, Mandriota SJ, Li J-L, Pugh CW, Maxwell PH, Harris AL, Ratcliffe PJ (2005) Contrasting properties of hypoxia-inducible factor 1 (HIF-1) and HIF-2 in von Hippel-Lindau-associated renal cell carcinoma. Mol Cell Biol 25(13):5675–5686
92. Gruber M, Mathew LK, Runge AC, Garcia JA, Simon MC (2010) EPAS1 is required for spermatogenesis in the postnatal mouse testis. Biol Reprod 82(6):1227–1236
93. Guven A, Ickin M, Uzun O, Bakar C, Gulec Balbay E, Balbay O (2014) Erdosteine protects rat testis tissue from hypoxic injury by reducing apoptotic cell death. Andrologia 46(1):50–58
94. Zimmermann C, Stévant I, Borel C, Conne B, Pitetti J-L, Calvel P, Kaessmann H, Jégou B, Chalmel F, Nef S (2015) Research resource: the dynamic transcriptional profile of sertoli cells during the progression of spermatogenesis. Mol Endocrinol 29(4):627–642
95. Galardo MN, Gorga A, Merlo JP, Regueira M, Pellizzari EH, Cigorraga SB, Riera MF, Meroni SB (2017) Participation of HIFs in the regulation of Sertoli cell lactate production. Biochimie 132:9–18
96. Firth JD, Ebert BL, Ratcliffe PJ (1995) Hypoxic regulation of lactate dehydrogenase A interaction between hypoxia-inducible factor 1 and cAMP response elements. J Biol Chem 270(36):21021–21027
97. Hayashi M, Sakata M, Takeda T, Yamamoto T, Okamoto Y, Sawada K, Kimura A, Minekawa R, Tahara M, Tasaka K (2004) Induction of glucose transporter 1 expression through hypoxia-inducible factor 1α under hypoxic conditions in trophoblast-derived cells. J Endocrinol 183(1):145–154
98. Luo W, Hu H, Chang R, Zhong J, Knabel M, O'Meally R, Cole RN, Pandey A, Semenza GL (2011) Pyruvate kinase M2 is a PHD3-stimulated coactivator for hypoxia-inducible factor 1. Cell 145(5):732–744
99. Jutte NH, Eikvar L, Levy F, Hansson V (1985) Metabolism of palmitate in cultured rat Sertoli cells. J Reprod Fertil 73(2):497–503
100. Issemann I, Green S (1990) Activation of a member of the steroid hormone receptor superfamily by peroxisome proliferators. Nature 347(6294):645–650
101. Michalik L, Auwerx J, Berger JP, Chatterjee VK, Glass CK, Gonzalez FJ, Grimaldi PA, Kadowaki T, Lazar MA, O'Rahilly S (2006) International Union of Pharmacology. LXI. Peroxisome proliferator-activated receptors. Pharmacol Rev 58(4):726–741
102. Green S, Wahli W (1994) Peroxisome proliferator-activated receptors: finding the orphan a home. Mol Cell Endocrinol 100(1):149–153
103. Krey G, Braissant O, L'Horset F, Kalkhoven E, Perroud M, Parker MG, Wahli W (1997) Fatty acids, eicosanoids, and hypolipidemic agents identified as ligands of peroxisome proliferator-activated receptors by coactivator-dependent receptor ligand assay. Mol Endocrinol 11(6):779–791
104. Burkart EM, Sambandam N, Han X, Gross RW, Courtois M, Gierasch CM, Shoghi K, Welch MJ, Kelly DP (2007) Nuclear receptors PPARβ/δ and PPARα direct distinct metabolic regulatory programs in the mouse heart. J Clin Invest 117(12):3930–3939
105. Chawla A, Schwarz EJ, Dimaculangan DD, Lazar MA (1994) Peroxisome proliferator-activated receptor (PPAR) gamma: adipose-predominant expression and induction early in adipocyte differentiation. Endocrinology 135(2):798–800
106. Jump DB, Botolin D, Wang Y, Xu J, Christian B, Demeure O (2005) Fatty acid regulation of hepatic gene transcription. J Nutr 135(11):2503–2506
107. Tontonoz P, Hu E, Spiegelman BM (1994) Stimulation of adipogenesis in fibroblasts by PPARγ2, a lipid-activated transcription factor. Cell 79(7):1147–1156
108. Wang Y-X, Lee C-H, Tiep S, Ruth TY, Ham J, Kang H, Evans RM (2003) Peroxisome-proliferator-activated receptor δ activates fat metabolism to prevent obesity. Cell 113(2):159–170
109. Kliewer SA, Xu HE, Lambert MH, Willson TM (2000) Peroxisome proliferator-activated receptors: from genes to physiology. Recent Prog Horm Res 56:239–263
110. Braissant O, Foufelle F, Scotto C, Dauça M, Wahli W (1996) Differential expression of peroxisome proliferator-activated receptors (PPARs): tissue distribution of PPAR-alpha,-beta, and-gamma in the adult rat. Endocrinology 137(1):354–366
111. Thomas K, Sung D, Chen X, Thompson W, Chen Y, McCarrey J, Walker W, Griswold M (2010) Developmental patterns of PPAR and RXR gene expression during spermatogenesis. Front Biosci (Elite Ed) 3:1209–1220
112. Regueira M, Riera MF, Galardo M, Pellizzari E, Cigorraga S, Meroni S (2014) Activation

of PPAR α and PPAR β/δ regulates Sertoli cell metabolism. Mol Cell Endocrinol 382(1):271–281
113. Gorga A, Rindone G, Regueira M, Pellizzari E, Cigorraga S, Riera MF, Meroni SB (2017) PPARγ activation regulates lipid droplet formation and lactate production in rat Sertoli cells. Cell Tissue Res. https://doi.org/10.1007/s00441-017-2615-y
114. Hamilton BE, Ventura SJ (2006) Fertility and abortion rates in the United States, 1960–2002. Int J Androl 29(1):34–45
115. World Health Organization (2000) Obesity: preventing and managing the global epidemic, WHO technical report series, vol vol 894. World Health Organization, Genève
116. Crisóstomo L, Sousa M, Alves MG, Oliveira PF (2017) The burden of metabolic diseases on male reproductive health. Int J Diabetol Vasc Dis Res 5(1e):1–2
117. Chambers T, Richard R (2015) The impact of obesity on male fertility. Hormones 14:563–568
118. Alves MG, Martins AD, Cavaco JE, Socorro S, Oliveira PF (2013) Diabetes, insulin-mediated glucose metabolism and Sertoli/blood-testis barrier function. Tissue barriers 1(2):e23992. https://doi.org/10.4161/tisb.23992
119. Cai L, Chen S, Evans T, Deng DX, Mukherjee K, Chakrabarti S (2000) Apoptotic germ-cell death and testicular damage in experimental diabetes: prevention by endothelin antagonism. Urol Res 28(5):342–347
120. Belanger C, Dupont P, Tchernof A (2002) Adipose tissue intracrinology: potential importance of local androgen/estrogen metabolism in the regulation of adiposity. Horm Metab Res 34(11/12):737–745
121. Roumaud P, Martin LJ (2015) Roles of leptin, adiponectin and resistin in the transcriptional regulation of steroidogenic genes contributing to decreased Leydig cells function in obesity. Horm Mol Biol Clin Investig 24(1):25–45. https://doi.org/10.1515/hmbci-2015-0046
122. Rato L, Alves MG, Duarte AI, Santos MS, Moreira PI, Cavaco JE, Oliveira PF (2015) Testosterone deficiency induced by progressive stages of diabetes mellitus impairs glucose metabolism and favors glycogenesis in mature rat Sertoli cells. Int J Biochem Cell Biol 66:1–10
123. Oliveira PF, Sousa M, Silva BM, Monteiro MP, Alves MG (2017) Obesity, energy balance and spermatogenesis. Reproduction 153(6):R173–R185. https://doi.org/10.1530/rep-17-0018
124. Reis M, Moreira AC, Sousa M, Mathur PP, Oliveira PF, Alves MG (2015) Sertoli cell as a model in male reproductive toxicology: advantages and disadvantages. J Appl Toxicol 35(8):870–883
125. Wallace WHB, Shalet SM, Crowne E, Morris-Jones P, Gattamaneni H, Price DA (1989) Gonadal dysfunction due to cis-platinum. Med Pediatr Oncol 17(5–6):409–413
126. Monsees T, Franz M, Gebhardt S, Winterstein U, Schill WB, Hayatpour J (2000) Sertoli cells as a target for reproductive hazards. Andrologia 32(4–5):239–246
127. Wiebe JP, Kowalik A, Gallardi RL, Egeler O, Clubb BH (2000) Glycerol disrupts tight junction-associated actin microfilaments, occludin, and microtubules in Sertoli cells. J Androl 21(5):625–635
128. Raychoudhury SS, Blake CA, Millette CF (1999) Toxic effects of octylphenol on cultured rat spermatogenic cells and Sertoli cells. Toxicol Appl Pharmacol 157(3):192–202
129. Alves MG, Neuhaus-Oliveira A, Moreira PI, Socorro S, Oliveira PF (2013) Exposure to 2,4-dichlorophenoxyacetic acid alters glucose metabolism in immature rat Sertoli cells. Reprod Toxicol 38:81–88. https://doi.org/10.1016/j.reprotox.2013.03.005
130. Bizarro P, Acevedo S, Niño-Cabrera G, Mussali-Galante P, Pasos F, Avila-Costa MR, Fortoul TI (2003) Ultrastructural modifications in the mitochondrion of mouse Sertoli cells after inhalation of lead, cadmium or lead–cadmium mixture. Reprod Toxicol 17(5):561–566
131. Alves MG, Jesus TT, Sousa M, Goldberg E, Silva BM, Oliveira PF (2016) Male fertility and obesity: are ghrelin, leptin and glucagon-like peptide-1 pharmacologically relevant? Curr Pharm Des 22(7):783–791. https://doi.org/10.2174/1381612822666151209151550
132. Martins AD, Moreira AC, Sá R, Monteiro MP, Sousa M, Carvalho RA, Silva BM, Oliveira PF, Alves MG (2015) Leptin modulates human Sertoli cells acetate production and glycolytic profile: a novel mechanism of obesity-induced male infertility? Biochim Biophys Acta 1852(9):1824–1832
133. Martins AD, Sá R, Monteiro MP, Barros A, Sousa M, Carvalho RA, Silva BM, Oliveira PF, Alves MG (2016) Ghrelin acts as energy status sensor of male reproduction by modulating Sertoli cells glycolytic metabolism and mitochondrial bioenergetics. Mol Cell Endocrinol 434:199–209
134. Wiebe JP, Barr KJ (1984) The control of male fertility by 1,2,3-trihydroxypropane (THP;glycerol): rapid arrest of spermato-

genesis without altering libido, accessory organs, gonadal steroidogenesis, and serum testosterone, LH and FSH. Contraception 29(3):291–302
135. Rodríguez A, Catalán V, Gómez-Ambrosi J, García-Navarro S, Rotellar F, Valentí V, Silva C, Gil MJ, Salvador J, Burrell MA (2011) Insulin-and leptin-mediated control of aquaglyceroporins in human adipocytes and hepatocytes is mediated via the PI3K/Akt/mTOR signaling cascade. J Clin Endocrinol Metab 96(4):E586–E597
136. Lin EC (1977) Glycerol utilization and its regulation in mammals. Annu Rev Biochem 46:765–795. https://doi.org/10.1146/annurev.bi.46.070177.004001
137. Hagstrom-Toft E, Enoksson S, Moberg E, Bolinder J, Arner P (1997) Absolute concentrations of glycerol and lactate in human skeletal muscle, adipose tissue, and blood. Am J Phys 273(3 Pt 1):E584–E592
138. Yeung CH, Callies C, Tuttelmann F, Kliesch S, Cooper TG (2010) Aquaporins in the human testis and spermatozoa - identification, involvement in sperm volume regulation and clinical relevance. Int J Androl 33(4):629–641. https://doi.org/10.1111/j.1365-2605.2009.00998.x
139. Vestergaard ET, Moller N, Jorgensen JO (2013) Acute peripheral tissue effects of ghrelin on interstitial levels of glucose, glycerol, and lactate: a microdialysis study in healthy human subjects. Am J Physiol Endocrinol Metab 304(12):E1273–E1280. https://doi.org/10.1152/ajpendo.00662.2012
140. Lorenzi T, Meli R, Marzioni D, Morroni M, Baragli A, Castellucci M, Gualillo O, Muccioli G (2009) Ghrelin: a metabolic signal affecting the reproductive system. Cytokine Growth Factor Rev 20(2):137–152

Chapter 12

Assessing Sertoli Cell Metabolic Activity

Ivana Jarak, Pedro F. Oliveira, Gustavo Rindone, Rui A. Carvalho, María N. Galardo, María F. Riera, Silvina B. Meroni, and Marco G. Alves

Abstract

Nuclear magnetic resonance (NMR)-based metabolomics is widely used in the research of metabolic conditions of complex biological systems under various conditions, and its use has been found in the field of male fertility. Here we describe the implementation of total and targeted NMR-based metabolomics in the research on Sertoli cell metabolism. Main principles and techniques of cell medium, cellular extracts, and intact cells are explained, as well as some classical experiments that can give complementary information on the Sertoli cell metabolism.

Key words Sertoli, Fertility, Metabolism, NMR, Intracellular, Extracellular, Metabolomics, Glucose uptake, Lipids

1 Introduction

Even though male infertility contributes to almost half of all infertility, its causes remain in many cases inconclusive. Recent development of novel techniques such as genomics, transcriptomics, proteomics, and metabolomics has opened novel possibilities at an integrated insight into the causes and mechanisms behind male infertility as well as in diagnostics and treatment [1, 2]. Metabolomics can be described as a comprehensive analysis of the total metabolic response of a complex system to an intervention, disease, or genetic modification. Several metabolomics-based studies based on chromatography/mass spectrometry or nuclear magnetic resonance (NMR) spectroscopy have focused on the discrimination between different forms of male infertility through the analysis of seminal fluid, spermatozoa, or testis [3–5]. On the other hand, targeted metabolomics focuses on the quantification of a defined set of known metabolites of interest and has also been successfully applied in the analysis of the intracellular (Fig. 1) and extracellular (Fig. 2) Sertoli cell metabolism [6, 7]. Cell cultures, being a closed isolated system, provide the means to observe the

Marco G. Alves and Pedro F. Oliveira (eds.), *Sertoli Cells: Methods and Protocols*, Methods in Molecular Biology, vol. 1748, https://doi.org/10.1007/978-1-4939-7698-0_12,

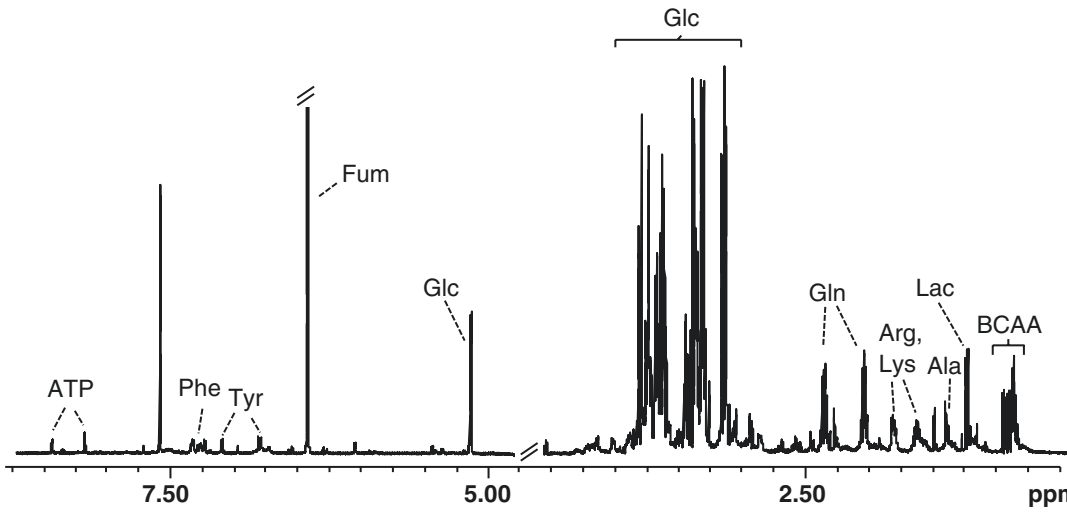

Fig. 1 ^{1}H-NMR spectrum of Sertoli cell polar extracts (δ 0.5–8.8 ppm). Assignments of major metabolites are indicated. Abbreviations: *Ala* alanine, *Arg* arginine, *ATP* adenosine triphosphate, *BCAA* branched-chain amino acids (valine, isoleucine, leucine), *Fum* fumarate (internal standard), *Glc* glucose, *Gln* glutamine, *Lac* lactate, *Lys* lysine, *Tyr* tyrosine, *Phe* phenylalanine

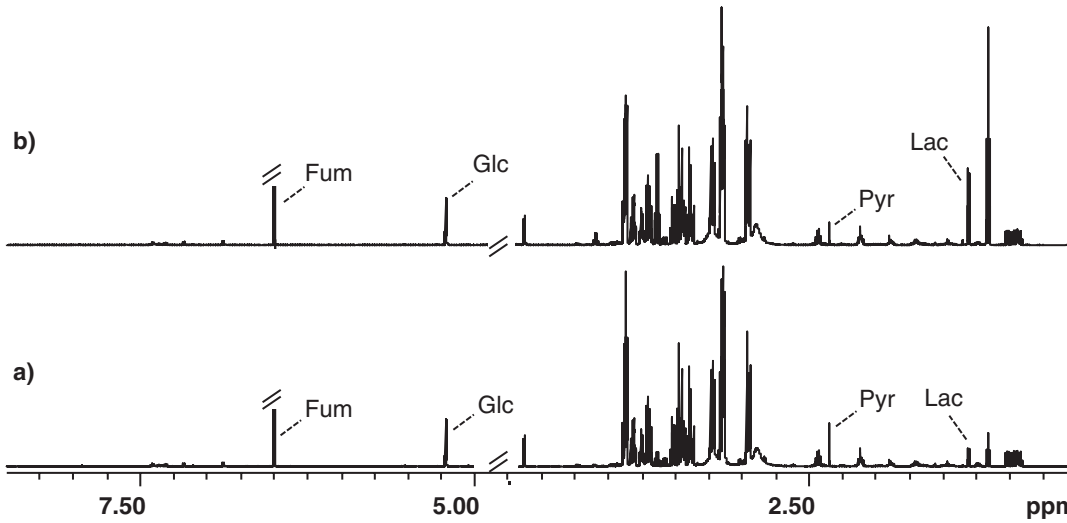

Fig. 2 ^{1}H-NMR spectrum of Sertoli cell medium (δ 0.5–8.5 ppm): (**a**) pure medium and (**b**) medium with cells. After 6 h of incubation, increased excretion of lactate levels and concomitant uptake of glucose and pyruvate were observed. Assignments of metabolites of interest are indicated. Abbreviations: *Fum* fumarate (internal standard), *Glc* glucose, *Lac* lactate, *Pyr* pyruvate

cells under strictly controlled conditions and allow the analysis of the metabolic content of the cell medium (exometabolome, "footprinting"), thus permitting the probing of the internal system functioning while manipulating external conditions [8]. It provides information on the metabolic needs of the cells by observing

what is taken up from the medium and also by monitoring what is excreted into it. It is an excellent complement to the intracellular metabolome ("fingerprinting"). Besides the analysis of total or targeted exometabolome, kinetic studies of metabolite uptake and excretion under given conditions are also pivotal for a more robust understanding of the metabolic interplay.

It is important to note that energetic metabolism of Sertoli cells has been considered to have features of its own. Studies of Sertoli cell glucose metabolism have shown that these cells actively metabolize glucose but that the vast majority is converted to lactate, which is an important source of energy for postmeiotic germ cells [9]. Furthermore, Sertoli cells can oxidize fatty acids to fulfill their own energy requirements. Fatty acids are stored as triacylglycerides within lipid droplets. In this context, information about lipid metabolism can be provided by classical biochemical experiments, such as colorimetric cellular triglyceride quantification assay, and by observation of cellular lipid droplets by oil red O (ORO) staining under light microscope [10, 11]. Complementary insight information into glucose metabolism to lactate can be obtained by measuring glucose transport, analyzing the uptake of the labeled nonmetabolizable glucose analog 2-deoxy-D-glucose (2-DOG), and LDH activity, utilizing a spectrophotometric assay, in Sertoli cell monolayers [12, 13].

2 Materials

2.1 NMR Analysis

2.1.1 Sample Collection (Culture Medium, Intact Cells) and Cell Culture Extraction

1. Methanol (anhydrous, ≥99.8%).
2. Chloroform (ACS, ≥99.8%).
3. Deionized water.
4. PBS (phosphate-buffered saline).
5. D_2O phosphate buffer (0.2 M, pH 7.4).
6. Microcentrifuge tubes.
7. Glass vials (LCMS type).
8. Glass beads for cell lysis (0.5 mm).
9. Cell scrapers.
10. Vortex mixer.
11. Centrifuge.
12. Pipettes.

2.1.2 Sample Preparation for NMR Analysis

1. D_2O phosphate buffer (0.2 M, pH 7.4).
2. Sodium fumarate.
3. D_2O phosphate buffer/fumarate (2 mM sodium fumarate solution in D_2O phosphate buffer).

4. D_2O phosphate buffer/fumarate (10 mM sodium fumarate solution in D_2O phosphate buffer).
5. Deuterated chloroform (with the addition of 0.03% of 3-(Trimethylsilyl)propionic-2,2,3,3-d4 acid sodium salt, TSP).
6. NMR spectrometer.
7. Liquid indirect detection 3 mm or 5 mm NMR probe.
8. HRMAS (high-resolution magic angle spinning) NMR probe.
9. NMR tubes (3 mm or 5 mm, depending on the probe diameter).
10. 4 mm zirconium oxide NMR rotor (for the HRMAS NMR analysis).
11. Pipettes.

2.2 Measuring Triacylglycerol (TAG) Levels

1. Tissue culture flasks (25 cm^2 growing surface) (*see* **Note 1**).
2. Type 1 ultrapure water (less than 18 MΩ cm at 25 °C) (*see* **Note 2**).
3. Phosphate-buffered saline (PBS): 137 mM NaCl, 2.7 mM KCl, 10 mM Na_2HPO_4, 2 mM KH_2PO_4, pH 7.4.
4. Cell detachment solution (CDS): trypsin from bovine pancreas 0.05% w/v and ethylenediaminetetraacetic acid disodium salt (EDTA) 0.02% w/v in PBS, pH 7.4.
5. Trypsin inhibitor (TI) solution: soybean trypsin inhibitor 0.3% w/v in PBS pH 7.4 (*see* **Note 3**).
6. TAG determination kit (TG Color, GPO/PAP AA; Wiener Lab, Rosario, Argentina) (*see* **Note 4**).
7. 1.5 mL microtubes.
8. Khan tubes.
9. UV spectrophotometer cuvettes.
10. Microtube centrifuge.
11. Ultrasonic cell disruptor.
12. CO_2 incubator set at 34 °C.
13. Water bath set at 37 °C.
14. UV spectrophotometer.
15. Contrast phase microscopy.

2.3 Evaluation of Lipid Droplet Number

1. 8-Well chamber Permanox slides (*see* **Note 5**).
2. Phosphate-buffered saline (PBS).
3. 10% v/v formalin.
4. Oil red O (ORO) saturated solution (*see* **Note 6**).
5. Deionized water.

6. Hematoxylin solution.
7. Coplin jars.
8. Light microscope with digital camera (*see* **Note 7**).

2.4 Measurement of Glucose Transport

1. Ultrapure water (resistivity of 18 MΩ cm at 25 °C) (*see* **Note 2**).
2. 24-Well plates (*see* **Note 8**).
3. [1,2-^{3}H(N)]-2-Deoxy-D-glucose (20 Ci/mmol; 740 GBq/mmol; PerkinElmer) (^{3}H-2-DOG).
4. 2-Deoxy-D-glucose (≥99%, crystalline, Sigma-Aldrich) (2-DOG).
5. Phosphate-buffered saline (PBS).
6. 1 M $CaCl_2$ and 1 M $MgCl_2$ solutions.
7. Solution of 0.4% w/v sodium deoxycholate in 0.5 N sodium hydroxide.
8. Liquid scintillation cocktail, Optiphase HiSafe 3 (PerkinElmer).
9. 4.5 mL plastic vials.
10. Liquid scintillation spectrophotometer.
11. CO_2 incubator set at 34 °C.

2.5 Measurement of LDH Activity

1. 24-Well plates (*see* **Note 8**).
2. Physiological saline solution (NaCl 0.9%).
3. Microcentrifuge tubes.
4. Khan tubes.
5. Ultrasonic cell disruptor.
6. Microcentrifuge.
7. Reagent for lactate dehydrogenase (LDH) assay (Roche Diagnostics).
8. Chemistry analyzer or UV spectrophotometer cuvettes and spectrophotometer.

3 Methods

3.1 NMR Analysis

3.1.1 Cell Culture Metabolite Extraction

1. Rinse the microcentrifuge tubes with methanol and dry.
2. Wash glass vials with water, rinse with distilled water, and dry.
3. Chill all the solvents overnight (methanol and chloroform can be kept in the freezer).
4. Keep the solvents on ice during the extraction procedure.
5. Weigh glass beads into the microcentrifuge tube (150 mg) (*see* **Note 9**).

6. Remove the medium and gently wash the cells with ice-cold PBS (2 × 1 mL) (*see* **Notes 10** and **11**).
7. Remove PBS with pipette after each washing.
8. Add ice-cold methanol (650 μL) so that it wets all the cells, and scrape the cells from the dish surface into methanol using a cell scraper.
9. Transfer the cell suspension into the microcentrifuge tube with glass beads. The transfer can be conducted in two or three stages and the supernatant methanol used to rinse any leftover cells into the suspension.
10. Vortex for 1 min.
11. Add ice-cold chloroform (260 μL) and vortex for 1 min.
12. Add another portion of chloroform (260 μL) and ice-cold water (220 μL) and vortex for another minute.
13. Keep the mixture on ice for 10 min and centrifuge for 15 min at 4 °C at 1000 × *g*. The upper aqueous layer (polar extracts) and lower organic solvent layer (nonpolar lipid extracts) will separate during centrifugation.
14. Carefully remove the upper layer and transfer it to the washed microcentrifuge tube. Transfer the lower layer to the clean glass vial. Lyophilize the aqueous fraction in vacuum concentrator. Use a stream of dry nitrogen to dry the organic fraction. Alternatively, it can be dried in the fume hood. Keep the middle layer precipitate (cell pellet) for protein quantification (if needed). Dry samples should be stored at −80 °C until analysis.

3.1.2 Cell Medium Collection

1. Centrifuge the collected medium to remove any remaining cells and cell debris (2000 × *g*, 5 min) (*see* **Note 12**).
2. Store the mediums at −80 °C until analysis.

3.1.3 Intact Cell Collection

1. Remove the medium and collect the cells by trypsinization or scraping in phosphate buffer.
2. Centrifuge at 1000 × *g* for 5 min.
3. Remove the supernatant and wash the cells in PBS (8 mL).
4. Centrifuge at 500 × *g* for 5 min, remove the supernatant, resuspend the cells in D_2O phosphate buffer (1.5 mL), and transfer into the microcentrifuge tube.
5. Centrifuge at 1000 × *g* for 5 min, remove the supernatant, and store the cells at −80 °C until analysis (*see* **Note 13**).

3.1.4 Sample Preparation for the NMR Analysis: Cell Extracts

1. Reconstitute the polar extracts in 600 μL of D_2O phosphate buffer/fumarate (or some other internal standard), and vortex until dissolved. Centrifuge the solution (5000 × *g*, 2 min), and transfer 550 μL to the 5 mm NMR tube (*see* **Notes 14** and **15**).

2. Reconstitute lipid extracts in 600 μL deuterated chloroform (containing TSP), and vortex until dissolved. After centrifugation (5000 × *g*, 2 min), transfer 550 μL to the 5 mm NMR tube (*see* **Note 16**).

3.1.5 Sample Preparation for the NMR Analysis: Cell Medium

1. Place 480 μL of the thawed medium in the microcentrifuge tube, and add 120 μL of PBS/D_2O/fumarate (final fumarate concentration is 2 mM).
2. Mix and transfer 550 μL to the 5 mm NMR tube.

3.1.6 Sample Preparation for the NMR Analysis: Intact Cells

1. At the time of the NMR analysis, thaw the cells, and transfer the cell pellet to the HRMAS rotor containing 10 μL of D_2O phosphate buffer/fumarate (or other internal standard or reference of choice). Alternatively, cell pellet can be mixed with some D_2O phosphate buffer/fumarate to facilitate the transfer (*see* **Note 17**).

3.1.7 Quantitative ^1H NMR Methodology for Small Metabolites

1. For the acquisition of quantitative NMR spectra of polar metabolites, a water presaturation NMR pulse sequence is used (zgpr in Bruker or preset from Varian experiment library). For the analysis of lipid extracts, a normal proton sequence (zg) is used.
2. In order to collect quantitative spectra, enough time has to be allowed for all the nuclei to completely relax. Since the repetition time (includes acquisition time and interpulse delay) should be at least five times the longest relaxation time in the metabolite mixture, the knowledge of the relaxation behavior is necessary. It is advisable to estimate these parameters at the beginning of each study.
3. The choice of the radiofrequency pulse duration has to consider the maximum T1 of all metabolites in the mixture. Typically, a 45° pulse is used to collect signal. 90° pulses are seldom used in quantitative spectra acquisition using simple 1D pulse sequences since they require much longer interpulse delays.
4. When the repetition times do not meet the full relaxation criteria, correction of saturation effects might be necessary [14]. Optimization of the pulse duration for each sample is advisable since it is affected by the composition of the biological matrix (e.g., salt content). Water saturation frequency should also be optimized.
5. Enough transients (scans) should be collected to achieve adequate S/N. For precise absolute metabolite quantitation (qNMR), S/N should be >100 for the smallest peak to be quantified.
6. Typically, ^1H NMR spectra are acquired using sweep width of at least 12 ppm (−1 to 11 ppm) and enough points to obtain the resolution of ≤0.25 Hz/point. Number of scans used will

depend on the size of the biological material disposable for the analysis (cell number or tissue sample) (*see* **Note 18**).

7. Liquid high-resolution ^{1}H NMR spectra are usually acquired at 25 °C.
8. Keeping the sample height constant by placing exact volumes of sample solution into the NMR tube can considerably speed up the analysis by avoiding much time being spent on field adjustment (shimming). Try to prevent air bubble formation in the NMR tube since it results in considerable sample heterogeneity and consequent line broadening.

3.1.8 ^{1}H NMR Metabolomics Methodology

1. When metabolomics analysis is considered the use of high field magnets, like 500 or 600 MHz, NMR spectrometers is preferred since the better resolution they provide helps in signal assignment and analysis.
2. Acquisition of comparable ^{1}H NMR spectra for metabolic profiling should be performed under identical conditions (temperature, sweep width, acquisition time, relaxation delay, number of scans, gain, pulse length, and water suppression frequency optimized for each sample).
3. Unlike in the case of qNMR where high S/N is needed, in metabolic profiling S/N of at least 10 for the smallest metabolite of interest is acceptable for relative quantification purposes [15].
4. Several NMR experiments are routinely used for metabolic profiling purposes. 1D experiments include NOESY-presaturation, CPMG (Carr-Purcell-Meiboom-Gill) spin-echo (eliminates broad resonances of proteins and lipids), and diffusion-edited (attenuates the signals of low-molecular-weight metabolites) pulse sequences. Simple pulse-acquire proton pulse sequences (zg) are used for the analysis of lipid extract $CDCl_3$ solutions. The use of 2D experiments such as ^{1}H-^{1}H total correlation (TOCSY), ^{1}H-^{13}C phase-sensitive heteronuclear single quantum coherence (HSQC), and J-resolved pulse sequences can greatly facilitate correct metabolite assignment and identification (*see* **Note 19**).
5. Sufficiently long repetition times (acquisition time plus interpulse delay) should be chosen not to cause significant signal saturation. We routinely use acquisition time of 3 s and interpulse delay of 4 s for liquid NMR experiments and 2.5 s acquisition time and 4 s interpulse delay for HRMAS. For NOESY experiments 128 scans are typically collected. For CPMG spectra a total of 256 scans are frequently averaged. Like in the case of absolute quantification (*see* Subheading 3.1.7), the number of scans will depend on the sample size and should be evaluated experimentally (*see* **Note 20**).

3.1.9 Small Guide for ^{1}H NMR Result Treatment

1. Spectra are processed using specialized packages (e.g., TopSpin, NUTS, ACD/Labs). Exponential multiplication with a Lorentzian function (lb = 0.3 Hz) is usually applied, followed by zero filling, Fourier transformation, and manual phase and baseline correction. While line broadening will improve S/N at the expense of the signal width, manipulating the size of zero filling can improve digital resolution. Proper phase and base correction is essential for the correct integration and subsequent metabolite quantification or metabolomics analysis.
2. In the case of quantitative analysis, peaks of interest are integrated (deconvolution or peak fitting can be used for overlapping peak multiplets) and the metabolites quantified according to the equation:

$$c(x) = c(\mathrm{Std}) * [I(x) * N(\mathrm{Std}) * V(x + \mathrm{Std})] / [(I(\mathrm{Std}) * N(x) * V(x)].$$

where c is concentration (mM), I intensity, N number of protons giving rise to the integrated multiplet, and V volume of the analyte (X) and the internal standard (Std), respectively. Obtained concentration values are normalized for the cell number or total protein concentration. Metabolite uptake or excretion (metabolites in the cell medium) is expressed as the difference between the amount (mol) of the metabolite present in the total volume of pure medium and the medium incubated with cells.

3. For the metabolomics analysis, processed spectra are binned, aligned if necessary, and normalized (e.g., total area, probabilistic quotient) before the multivariate analysis is applied. Principal component analysis (PCA) and partial least squares discriminant analysis (PLS-DA) are the most commonly used methods [16].

3.2 Measuring Triacylglycerol (TAG) Levels

1. Remove culture medium and wash the cell monolayers twice with 1 mL PBS at room temperature.
2. Add 0.8 mL of CDS to the cell monolayers and incubate for 1–2 min at 34 °C (*see* **Note 21**).
3. As soon as the cells are detached, stop trypsin action by the addition of 150 μL of TI solution.
4. Transfer the cell suspension to a microcentrifuge tube.
5. Wash the tissue culture flask with 0.4 mL PBS and add to the same microcentrifuge tube.
6. Centrifuge cells at 800 × *g* for 5 min.
7. Discard supernatant.
8. Resuspend cell pellet in 60 μL of PBS pH 7.4 (*see* **Note 22**).

9. Homogenize cell suspension by ultrasonic irradiation with three pulses of 5 s on ice (*see* **Note 23**).
10. Transfer 10 μL of cell lysate to a Kahn tube for TAG determination.
11. Add 1 mL of reaction buffer to each tube (*see* **Note 24**).
12. Incubate for 5 min in a water bath at 37 °C.
13. Read absorbance of each sample at 505 nm.
14. Calculate TAG levels according to the manufacturer instructions and express results as μg TAG/μg DNA.

3.3 Evaluation of Lipid Droplet Number

1. Remove culture medium and wash the cells twice with PBS at room temperature.
2. Fix cells with 10% v/v formalin for 1 h.
3. Stain slides with ORO saturated solution for 30 min in a Coplin jar.
4. Wash the cells with deionized water for 5 s.
5. Counterstain with hematoxylin (20 s; Fisher CS401-D) and rinse gently with water.
6. Mount the sections using aqueous mounting medium such as glycerol gelatin. Coverslip may be sealed with clear nail polish.
7. Visualize slides under light microscope.
8. Take photomicrographs of several representative fields.
9. Quantify LD (*see* **Note 25**).
10. Express the results as number of lipid droplets per cell (mean ± SD).

3.4 Measurement of Glucose Transport

1. Prepare PBS containing Ca^{2+} and Mg^{2+} (PBS-Ca-Mg). Add 1 μL of 1 M $CaCl_2$ and 1 μL of 1 M $MgCl_2$ solutions per mL of PBS. Warm up the PBS-Ca-Mg at 34 °C in incubator.
2. Prepare ^{3}H-2-DOG solution. Add 1 μL of ^{3}H-2-DOG to 1 mL of PBS-Ca-Mg. This solution contains 0.5 μCi/mL of ^{3}H-2-DOG (*see* **Note 26**).
3. Make non-specific uptake solution. Add to ^{3}H-2-DOG solution the unlabeled 2-DOG. Final concentration of unlabeled 2-DOG must be 100 mM.
4. Remove culture medium and wash cells cultured in 24-well plate twice with 1 mL of warmed PBS-Ca-Mg.
5. Add 0.5 mL of ^{3}H-2-DOG solution to each well and incubate for 30 min at 34 °C in CO_2 incubator. Run for triplicate each experimental condition.

6. To determine non-specific uptake for each experimental condition tested, add in one well 0.5 mL of non-specific uptake solution instead of ^{3}H-2-DOG solution. Also, incubate for 30 min at 34 °C in CO_2 incubator.
7. Put the plate on ice and remove ^{3}H-2-DOG solution or non-specific uptake solution. Wash the plate three times by filling the wells with 1 mL of cold PBS-Ca-Mg.
8. After washing, discard PBS-Ca-Mg, and add 0.5 mL of solution of 0.4% w/v sodium deoxycholate in 0.5 N NaOH to lyse the cells.
9. Pipette the lysate up and down several times to homogenize, and transfer it to a plastic vial.
10. Add 3 mL of liquid scintillation cocktail to each vial and vortex briefly.
11. Count on liquid scintillation spectrophotometer.
12. Calculate specific uptake as dpm of sample − dpm of non-specific uptake.
13. Express the results as specific uptake (dpm)/μg of DNA (*see* **Note 27**).

3.5 Determination of LDH Activity

1. Remove culture medium, and wash cells cultured in 24-well plate with 1 mL physiological saline solution at room temperature.
2. After washing, put the plate on ice, and add 0.2 mL of physiological saline solution to each well.
3. Disrupt cells by ultrasonic irradiation with three pulses of 5 s on ice.
4. Transfer the cell suspension to a microcentrifuge tube.
5. Wash the well plate with 0.1 mL physiological saline solution, and add to the same microcentrifuge tube.
6. Transfer 30 μL of cell lysate to a Kahn tube for DNA determination (*see* **Note 28**).
7. Centrifuge cells at 15,800 × *g* for 10 min.
8. Transfer supernatant to a clean microcentrifuge tube. Store at 4 °C (*see* **Note 29**).
9. Use supernatant for determination of LDH activity utilizing a commercial kit such as lactate dehydrogenase assay from Roche Diagnostics (*see* **Note 30**).
10. Calculate LDH activity according to the manufacturer instructions and express results as mIU/μg DNA.

4 Notes

1. Due to the low sensitivity of this commercial kit, a considerable number of cells are needed to detect TAG levels. For this reason, Sertoli cells are seeded at 5 μg DNA/cm^2 and cultured in 25 cm^2 tissue culture flasks. Cultures must be maintained for at least 48 h to obtain a suitable Sertoli cell monolayer.
2. The ultrapure water must be used for preparing tissue culture media and all other solutions required in the biochemical assays.
3. This solution should be freshly prepared upon use.
4. The commercial kit utilized for this assay is routinely used for clinical determination of serum TAG levels.
5. Cells must be seeded at a density of 4 μg DNA/cm^2 in 8-well chamber Permanox slides. Cultures must be maintained for at least 48 h to obtain a suitable Sertoli cell monolayer.
6. ORO saturated solution must be freshly prepared upon use. To prepare ORO saturated solution, dissolve 200 mg of ORO (Sigma) in 60 mL of isopropanol, and maintain this solution overnight at room temperature. Filter this solution through a paper filter and add 40 mL of deionized water. Keep this last solution overnight at 4 °C. Then, filter twice through a paper filter, and filter again twice through a 45 μm mixed acetate-cellulose membrane.
7. Eclipse 50i microscope with a DS-Fi1 digital camera.
8. Cells must be seeded at a density of 5 μg DNA/cm^2 in 24-well plates. Sertoli cells must be maintained for at least 48 h in culture to obtain a proper monolayer.
9. To extract the intracellular metabolites, cells can be disrupted by vortexing without glass beads. If the glass beads are used, prior to the use, they should be washed with concentrated HCl, thoroughly rinsed with distilled water, and dried at 150 °C.
10. The protocol for cell extraction was based on the use of 10 mL of growing medium.
11. After the removal of the cell medium, the cells should be carefully washed with PBS to avoid cross contamination of intracellular metabolites with the content of the medium.
12. When conducting kinetic studies, aliquots can be taken periodically (e.g., every 12 h) from the growing medium during the experiment. This will, however, reduce the nutrients available to the growing cell cultures. Depending on the experimental setup (medium volume, number of samplings and

experimental period, NMR probe), cell medium can be replenished taking into account the concentration change in the resulting medium when calculating metabolite consumption and excretion.

13. Integrity of cells can be severely compromised depending on the type of freezing. Both snap-freezing and gradual freezing, which are commonly used in storing intact cells for HRMAS NMR analysis, lead to complete lyses, which influence the lipid content of the metabolic profile. The use of freshly collected cells or gradually frozen cells in the presence of cryopreservative medium preserves the integrity of the cells [17].
14. Although fumarate can be used as an internal standard for the metabolite quantification and/or chemical shift reference in all types of biological samples (cell media, cell and tissue extracts, bodily fluids), other internal standards like 3-(trimethylsilyl)-1-propanesulfonic acid sodium salt (DSS) and 3-(trimethylsilyl)propionic acid-d4 sodium salt (TSP) are also widely used. However, both DSS and TSP bind with proteins, peptides, and lipids which influence their quantitative efficacy and application, especially in biological matrices rich in proteins and lipids such as bodily fluids or tissue biopsies. Although fumarate does not suffer from this drawback, it can potentially mask the fumarate excreted by the cells into the medium; however these are about two orders of magnitudes lower than the concentration of internal standard itself, and quantification errors are minimal [18]. 4,4-Dimethyl-4-silapentane-1-ammonium trifluoroacetate (DSA) is another alternative to TSP and DSS that does not interact with biomolecules [19].
15. In the case where 3 mm NMR tubes are used, polar extracts are reconstituted in 210 μL of fumarate (2 mM) containing PBS, and 200 μL are transferred to a 3 mm NMR tube. Lipid extracts are dissolved in 210 μL of deuterated chloroform, and 200 μL are transferred to the NMR tube. In the case of cell medium, 180 μL of medium is mixed with 45 μL of D_2O phosphate buffer/fumarate, and 200 μL are transferred to the NMR tube.
16. Lipid samples should be freshly prepared before the analysis to avoid solvent evaporation and biased quantification.
17. HRMAS can also be used for the analysis of intact tissue samples (biopsies).
18. Digital resolution and S/N can additionally be manipulated during data preprocessing (*see* Subheading 3.1.9).
19. Using cell medium product sheet can help in identifying medium metabolites.

20. Fan et al. [20] recommend at least 3 × T_1, which causes less than 10% of peak saturation for most crude extracts (e.g., 2 s acquisition time and 3 s interpulse delay).
21. Detachment of Sertoli cells from the tissue culture flask surface must be monitored by visualizing this process under a contrast phase microscopy.
22. The final volume of the cell suspension is 100 μL.
23. As the results are expressed per DNA content, 2 μL of Sertoli cell lysate is used for DNA determination. DNA is determined according to Labarca and Paigen [21].
24. Reaction buffer is provided with the TG Color, GPO/PAP AA kit. Final concentrations: GoDPod 50 mmol/L, pH 6.8; chlorophenol 2 mmol/L; lipoprotein lipase ≥800 U/L; glycerol kinase ≥500 U/L; glycerol phosphate oxidase ≥1500 U/L; peroxidase ≥900 U/L; ATP 2 mol/L; 4-aminophenazone 0.4 mmol/L.
25. Although 400× magnification is recommended, quantification can also be performed under 200×. Count at least 200 Sertoli cells in each experimental condition performed in quadruplicate. The ratio LD to cell nucleus is calculated.
26. We recommend preparing this solution in laminar flow cabinet to avoid contamination of ^{3}H-2-DOG stock solution.
27. As the results are expressed per DNA content, parallel cultures receiving identical treatments to those performed before the glucose uptake assay are destined to DNA determinations. DNA is assessed according to Labarca and Paigen [21].
28. Determine DNA content in this sample according to Labarca and Paigen [21].
29. Maintain samples at 4 °C until LDH activity determination. Do not freeze samples.
30. The commercial kit utilized for this assay is routinely used for clinical determination of serum LDH activity. Therefore, you can use any available commercial reagent. You can do measurement in automated chemistry analyzer or in manual form.

Acknowledgments

This work was supported by the Portuguese Foundation for Science and Technology (FCT) grant PTDC/BIM-MET/4712/2014 and by the Agencia Nacional de Promoción Científica y Tecnológica grants PICT 2014/945 and PICT2015/228 and by the Consejo Nacional de Investigaciones Científicas y Técnicas (CONICET) grant PIP 2015/127.

References

1. Kovac JR, Pastuszak AW, Lamb DJ (2013) The use of genomics, proteomics, and metabolomics in identifying biomarkers of male infertility. Fertil Steril 99(4):998–1007. https://doi.org/10.1016/j.fertnstert.2013.01.111
2. Bieniek JM, Drabovich AP, Lo KC (2016) Seminal biomarkers for the evaluation of male infertility. Asian J Androl 18(3):426–433. https://doi.org/10.4103/1008-682x.175781
3. Jayaraman V, Ghosh S, Sengupta A, Srivastava S, Sonawat HM, Narayan PK (2014) Identification of biochemical differences between different forms of male infertility by nuclear magnetic resonance (NMR) spectroscopy. J Assist Reprod Genet 31(9):1195–1204. https://doi.org/10.1007/s10815-014-0282-4
4. Aaronson DS, Iman R, Walsh TJ, Kurhanewicz J, Turek PJ (2010) A novel application of 1H magnetic resonance spectroscopy: non-invasive identification of spermatogenesis in men with non-obstructive azoospermia. Hum Reprod 25(4):847–852. https://doi.org/10.1093/humrep/dep475
5. Dias TR, Alves MG, Rato L, Casal S, Silva BM, Oliveira PF (2016) White tea intake prevents prediabetes-induced metabolic dysfunctions in testis and epididymis preserving sperm quality. J Nutr Biochem 37:83–93. https://doi.org/10.1016/j.jnutbio.2016.07.018
6. Rocha CS, Martins AD, Rato L, Silva BM, Oliveira PF, Alves MG (2014) Melatonin alters the glycolytic profile of Sertoli cells: implications for male fertility. Mol Hum Reprod 20(11):1067–1076. https://doi.org/10.1093/molehr/gau080
7. Rato L, Alves MG, Socorro S, Carvalho RA, Cavaco JE, Oliveira PF (2012) Metabolic modulation induced by oestradiol and DHT in immature rat Sertoli cells cultured in vitro. Biosci Rep 32(1):61–69. https://doi.org/10.1042/bsr20110030
8. Kell DB, Brown M, Davey HM, Dunn WB, Spasic I, Oliver SG (2005) Metabolic footprinting and systems biology: the medium is the message. Nat Rev Microbiol 3(7):557–565. https://doi.org/10.1038/nrmicro1177
9. Boussouar F, Benahmed M (2004) Lactate and energy metabolism in male germ cells. Trends Endocrinol Metabol 15(7):345–350
10. Regueira M, Riera MF, Galardo MN, Pellizzari EH, Cigorraga SB, Meroni SB (2014) Activation of PPAR α and PPAR β/δ regulates Sertoli cell metabolism. Mol Cell Endocrinol 382(1):271–281
11. Gorga A, Rindone GM, Regueira M, Pellizzari EH, Camberos MC, Cigorraga SB, Riera MF, Galardo MN, Meroni SB (2017) PPARγ activation regulates lipid droplet formation and lactate production in rat Sertoli cells. Cell Tissue Res 369(3):611–624
12. Riera M (2002) Regulation of lactate production and glucose transport as well as of glucose transporter 1 and lactate dehydrogenase A mRNA levels by basic fibroblast growth factor in rat Sertoli cells. J Endocrinol 173(2):335–343
13. Galardo MN, Gorga A, Merlo JP, Regueira M, Pellizzari EH, Cigorraga SB, Riera MF, Meroni SB (2017) Participation of HIFs in the regulation of Sertoli cell lactate production. Biochimie 132:9–18
14. Fan TW-M (1996) Metabolite profiling by one- and two-dimensional NMR analysis of complex mixtures. Prog Nucl Magn Reson Spectrosc 28:161–219. https://doi.org/10.1016/0079-6565(95)01017-3
15. Barding GA Jr, Salditos R, Larive CK (2012) Quantitative NMR for bioanalysis and metabolomics. Anal Bioanal Chem 404(4):1165–1179. https://doi.org/10.1007/s00216-012-6188-z
16. Carrola J et al (2016) Metabolomics of silver nanoparticles toxicity in HaCaT cells: structure-activity relationships and role of ionic silver and oxidative stress. Nanotoxicology 10(8):1105–1117. https://doi.org/10.1080/17435390.2016.1177744
17. Duarte IF et al (2009) Analytical approaches toward successful human cell metabolome studies by NMR spectroscopy. Anal Chem 81(12):5023–5032. https://doi.org/10.1021/ac900545q
18. Ritter JB, Wahl AS, Freund S, Genzel Y, Reichl U (2010) Metabolic effects of influenza virus infection in cultured animal cells: intra- and extracellular metabolite profiling. BMC Syst Biol 4:61. https://doi.org/10.1186/1752-0509-4-61
19. Nowick JS, Khakshoor O, Hashemzadeh M, Brower JO (2003) DSA: a new internal standard for NMR studies in aqueous solution. Org Lett 5(19):3511–3513. https://doi.org/10.1021/ol035347w
20. Fan TW-M, Lane AN (2008) Structure-based profiling of metabolites and isotopomers by NMR. Prog Nucl Magn Reson Spectrosc 42:69–117. https://doi.org/10.1016/j.pnmrs.2007.03.002
21. Labarca C, Paigen K (1980) A simple, rapid, and sensitive DNA assay procedure. Anal Biochem 102(2):344–352

Chapter 13

Proteome Profiling of Sertoli Cells Using a GeLC-MS/MS Strategy

Rita Ferreira, Fábio Trindade, and Rui Vitorino

Abstract

Proteomics is a technology that allows to decipher the molecular networks involved in the regulation of biological processes such as spermatogenesis. Sertoli cells (SCs) are key players in the paracrine control of this process. Envisioning to increase the knowledge on the molecular networks harbored in SCs, we propose a methodology based on GeLC-MS/MS for the characterization of these cells' proteome. Proteins are separated by SDS-PAGE hyphenated to HPLC and identified by mass spectrometry. The integration of data with bioinformatics tools such as ClueGO + CluePedia from Cytoscape allows the identification of the biological pathways more prevalent in SCs, and that might be modulated by pathophysiological conditions. Moreover, the proteome analysis with tools as SignalP/SecretomeP highlights the proteins more prone to be secreted and involved in the paracrine control of germ cells, which might also be deregulated by diseases.

Key words Proteomics, Spermatogenesis, MALDI-TOF/TOF, Network analysis, Sertoli cells

1 Introduction

Complex signaling networks are required for development and survival. So, considerable efforts have been made to elucidate these signaling networks in human cells [1]. Such events are by definition associated with protein changes [1]. Thus, the characterization of cells' proteome might improve our knowledge on the signaling networks involved in the regulation of biological processes such as spermatogenesis [2, 3]. In this biological process, Sertoli cells (SCs) are key players that coordinate the development of germ cells through the various phases of development [2, 4, 5]. Indeed, SCs orchestrate the paracrine control of spermatogenesis through the supply of factors required for division, differentiation, and metabolism of germ cells [4–7].

Electronic Supplementary Material: The online version of this chapter (https://doi.org/10.1007/978-1-4939-7698-0_13) contains supplementary material, which is available to authorized users.

Marco G. Alves and Pedro F. Oliveira (eds.), *Sertoli Cells: Methods and Protocols*, Methods in Molecular Biology, vol. 1748, https://doi.org/10.1007/978-1-4939-7698-0_13,

Proteomics allow the study of protein complement of cells, including identification, modification, quantification, and localization [8, 9]. Mass spectrometry (MS) is the most comprehensive and versatile tool in large-scale proteomics [8, 10]. Great efforts have been made to ensure reliable and accurate measurement of the absolute or relative protein abundance among different samples through MS-based technologies [8]. One of the main achievements in MS instrumentation was the introduction of soft ionization methods that allow the analysis of proteins and peptides [8]. The ionization methods most commonly used are matrix-assisted laser desorption ionization (MALDI) and electrospray ionization (ESI) [10]. In brief, the MS characterization of peptides comprises three main steps: (1) transformation of the peptides into gas-phase ions, (2) separation of ions on the basis of mass/charge (m/z) values in the presence of electric or magnetic fields in the mass analyzer, and (3) measurement of the separated ions and the amount of each species with a particular m/z value [10].

The successful application of MS-based proteomics is highly dependent on separation technologies that simplify complex biological samples prior to MS analysis. Indeed, accurate and sensitive MS experiments are highly reliant on efficient separation, which is the first step in any proteomic approach to a biological problem [8]. Two major separation strategies might be tracked in proteomics: gel-based and gel-free ones. Considering the complexity of biological systems as human cells, multidimensional separation approaches might be preferred, which combine the sequential application of gel-based and/or gel-free techniques. An important consideration in this separation strategy is the orthogonality of the separation method in each dimension, which relies on different (orthogonal) molecular properties as the basis for separation [8]. Sodium dodecyl sulfate-polyacrylamide gel electrophoresis (SDS-PAGE) followed by liquid chromatography (LC) separation of peptides, also known as GeLC, has been successfully applied to the proteome characterization of distinct biological samples as human cells, tissues, or bodily fluids [6, 11]. This approach was successfully applied to the characterization of testes' fluids [5]. Proteins are firstly separated according to their molecular weight and in-gel digested, and the resulting peptides are then extracted and desalted for subsequent LC separation according to their polarity, being then characterized by MS/MS analysis [10, 11]. The high-resolution power of MS, high scanning rates, and precise chromatogram alignment are essential conditions for the successful application of MS in proteomics [10]. With the introduction of high-throughput proteomics, it is possible to identify thousands of proteins, which biological relevance analysis is a challenge [12]. To support biological knowledge discovery, many bioinformatics databases and software tools have been developed. These organize and provide biological annotations for individual proteins to support functional analyses in the set of pathway, network, and systems biology [10, 12]. The UniProt Knowledgebase

(UniProtKB) is the predominant data store for functional information on proteins, and the UniProt web site (http://www.uniprot.org) is the primary access point [12]. Protein function databases maintain information about metabolic pathways, the intermolecular interactions, and regulatory pathway mechanisms underlying biological processes [12]. The KEGG, Ingenuity, Pathway Knowledgebase Reactome, and BioCarta are some of these databases [10]. Specific databases for signal transduction pathways include PANTHER and STRING [10].

Herein, we describe a methodology for the characterization of SCs proteome that combines GeLC separation of extracted proteins with MS identification followed by data analysis with the bioinformatics tools Cytoscape [13, 14] and SecretomeP/SignalP [15].

2 Materials

2.1 Preparation of Protein Extracts from Sertoli Cells

1. Sample buffer: PBS with 0.4% Triton X-100.

2.2 Determination of Protein Concentration

1. Reagent A: DC protein assay kit (Bio-Rad Laboratories, Berkeley, CA).
2. Reagent S: DC protein assay kit (Bio-Rad Laboratories, Berkeley, CA).
3. Reagent B: DC protein assay kit (Bio-Rad Laboratories, Berkeley, CA).
4. Bovine serum albumin (BSA) solution: dissolve 1.5 mg of BSA in 1 mL of water.

2.3 Sodium Dodecyl Sulfate-Polyacrylamide Gel Electrophoresis

1. Running buffer (10×): 0.25 M Tris, 1.92 M Glycine, 1% SDS pH 8.6 (*see* **Note 1**).
2. Buffer of the running gel (Buffer RG): 1.5 M Tris pH 8.8 (*see* **Note 2**).
3. Buffer of the stacking gel (Buffer SG): 0.5 M Tris pH 6.8 (*see* **Note 2**).
4. SDS: 10% (w/v) (*see* **Note 3**).
5. APS (ammonium persulfate) solution: 10% (w/v) (prepare fresh or prepare aliquots preserved at −20 °C).
6. TEMED: *N*,*N*,*N*′,*N*′-Tetramethylethylenediamine.
7. Acrylamide: 40%.
8. Bis: bis-acrylamide 2%.
9. Laemmli buffer: 4% SDS (40% (v/v) of SDS 10% (m/v)), 20% mercaptoethanol, 15% glycerol, 25% Buffer SG, and 10 mg bromophenol blue.

2.4 In-Gel Digestion

1. Wash solution: 0.1 M ammonium bicarbonate (NH_4HCO_3).
2. ACN: acetonitrile.
3. FA: 10% formic acid.
4. Reducing reagent: 10 mM dithiothreitol (DTT) in 0.1 M ammonium bicarbonate.
5. Alkylation reagent: 50 mM iodoacetamide in 0.1 M ammonium bicarbonate.
6. Trypsin (25 μg/2 mL, solubilized in 0.05 M ammonium bicarbonate).
7. Zip-Tip.

2.5 LC Separation of Digested Peptides

1. Nano-HPLC: ultimate 3000 (Dionex Corporation, Sunnyvale, CA).
2. Chromeleon (v.6.8, Dionex Corporation, Sunnyvale, CA).
3. Probot: (Dionex Corporation, Sunnyvale, CA).
4. TS2Mascot (v1.0, MatrixScience, UK).
5. Calmix 5 (Applied Biosystems).
6. Matrix: 3 mg/mL of α-Cyano-4-hydroxycinnamic acid, 0.1% trifluoroacetic acid (TFA), 15 fmol Glu-fib.
7. Eluent A: 95% H_2O, 5% ACN, 0.05% TFA.
8. Eluent B: 90% ACN, 10% H_2O, 0.045% TFA.
9. Solubilizing solution: 50% ACN, 50% H_2O, 0.1% TFA.

3 Methods

The methodologic strategy proposed in this chapter is suitable for proteome profiling of Sertoli cells. Proteins are separated by SDS-PAGE, and the annotated bands in-gel maps are subjected to trypsin digestion followed by nano-HPLC MALDI-TOF/TOF analysis. One should not forget that the quality of the data produced in any MS experiment is highly dependent on the quality of the sample analyzed. GeLC-MS/MS is expected to retrieve 100 to some thousands of identified proteins, which biological significance might be disclosed with bioinformatics tools freely available. Cytoscape (http://www.cytoscape.org/) is an open source software platform for the graphical interpretation of complex networks and integration of these with any type of data attributes. SecretomeP/SignalP server (http://www.cbs.dtu.dk/services/SecretomeP/) allows to predict the proteins potentially secreted by the classical pathway, which means in an endoplasmic reticulum/Golgi-dependent secretory pathway requiring the presence of a signal peptide, and the ones secreted via the nonclassical pathways, which means through membrane transporters or exosomes [15]. Figure 1 overviews the main steps and time course of the proposed methodology.

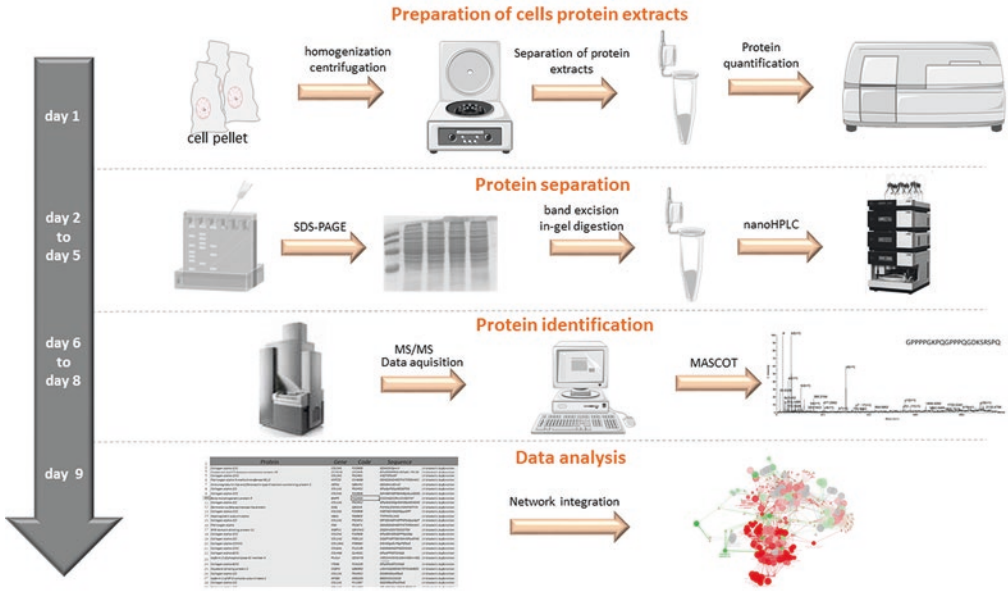

Fig. 1 Workflow and time course of the main experimental steps for GeLC-MS/MS analysis of SCs proteome. Figure was made with Servier Medical Art

3.1 Preparation of Cell Extracts

1. Suspend the Sertoli cells' pellet in sample buffer and incubate for 30 min at 4 °C (*see* **Note 4**).
2. Centrifuge samples at 13,200 × *g* for 30 min at 4 °C.
3. Collect the supernatants to an Eppendorf.
4. Determine protein concentration in cell extracts using DC protein assay kit according to the manufacturer's instructions (*see* **Note 5**).

3.2 SDS-PAGE

1. Prepare gel cassette assembly following the manufacturer instructions with 0.75 mm cassettes for 7 cm gels (*see* **Note 6**).
2. Cast the running gel with the appropriate acrylamide concentration prepared in accordance with Table 1 (*see* **Note 7**).
3. Allow the gel to polymerize.
4. Cast the stacking gel with 4% acrylamide concentration prepared according to Table 2.
5. Place the combs between the cassette glasses.
6. While waiting for gel polymerization, prepare 1× running buffer by diluting 100 mL of 10× buffer with 900 mL of deionized water.
7. Remove the combs, and wash the gel wells with running buffer to remove non-polymerized acrylamide.
8. Load molecular weight marker into one gel well (*see* **Note 8**).
9. Load a sample volume of 1:2 diluted sample in Laemmli buffer with 40 μg of protein (*see* **Note 9**).

Table 1

Guide for the preparation of running gels of different percentage of acrylamide/bis-acrylamide

Volumes (mL)	Running gel		
	10%	12.5%	15%
Acrylamide (40%)	2.43	3.04	3.65
Bis-acrylamide (2%)	1.34	1.68	2.01
Buffer RG	2.50	2.50	2.50
H_2O	2.18	1.24	0.29
SDS	0.10	0.10	0.10
APS[a]	0.05	0.05	0.05
TEMED[a]	0.005	0.005	0.005
Final volume	10.0	10.0	10.0

[a]Add just prior to pouring in the casting frames

Table 2

Guide for the preparation of 4% stacking gel

Volumes (mL)	Stacking gel
	4%
Acrylamide (40%)	0.97
Bis-acrylamide (2%)	0.54
Buffer SG	2.50
H_2O	4.44
SDS	0.10
APS[a]	0.05
TEMED[a]	0.005
Final volume	10.0

[a]Add just prior to pouring in the casting frames

10. Run the gels at 180 V for approximately 20 min at room temperature, until the dye front (bromophenol blue) reach one third of the gel length (*see* **Note 10**).
11. Open the gel assembly and remove the gels.
12. Stain the gel with BlueSafe™ for 15 min until the bands become visible (*see* **Note 11**).

13. Scan the gel using GelDoc XR+.
14. After gel scanning, import to the image analysis program, e.g., Quantity One, for band detection.
15. Crop images to only visualize the gel, and assure that all bands are visible in the image (*see* **Note 12**).
16. Identify the bands to be further analyzed by LC-MS/MS. For the analysis of all proteome, define six sections for each sample (which means gel lane).
17. Cut each gel section with an excisor into small pieces (approximately 3–4 mm × 3–4 mm), and transfer them to an empty Eppendorf (*see* **Note 13**).

3.3 Protein Digestion

1. Wash the gel sections with 50 μL of wash solution and incubate for 15 min.
2. Add 50 μL of ACN and incubate for 15 min.
3. Remove supernatant and repeat washing (**steps 1** and **2**).
4. Remove supernatant.
5. Add 50 μL of ACN and incubate for 10 min (*see* **Note 14**).
6. Remove the ACN and dry the spots in a vacuum evaporator, such as SpeedVac.
7. For disulfide bond reduction, add 50 μL of DTT to dried gels, and incubate at 60 °C for 1 h (*see* **Note 15**).
8. Remove supernatant, add 50 μL of iodoacetamide, and incubate at room temperature for 30 min in the dark to promote alkylation of free-sulfhydryl groups (*see* **Note 16**).
9. Wash the gel sections with 50 μL of wash solution and incubate for 15 min.
10. Add 50 μL of ACN and incubate for 15 min.
11. Remove supernatant and repeat washing (**steps 10** and **11**).
12. Remove supernatant. Add 50 μL of ACN and incubate for 10 min.
13. Remove the ACN and dry the spots in a vacuum evaporator.
14. For protein in-gel digestion with trypsin, add 25 μL of trypsin, and incubate at 37 °C for 60 min (*see* **Note 16**).
15. After 1 h, add wash solution until all the spots are submerged and re-incubate overnight at 37 °C.
16. After approx. 18 h, perform the acid extraction of the digested peptides.
17. Collect the supernatant to an empty Eppendorf.
18. Add 25 μL of FA to the spots and incubate for 30 min.
19. Collect the supernatant to the same Eppendorf as before.

20. Add 25 μL of FA and 25 μL of ACN and incubate for 30 min.
21. Collect the supernatant to the same Eppendorf as before and repeat step 20.
22. Collect the supernatant to the same Eppendorf as before, and dry the collected solutions using the vacuum evaporator.
23. Samples might be cleaned up with Zip-Tips, following manufacturer's instructions (*see* **Note 17**).
    (a) In brief, prepare the sample by adding 100 μL of 2% ACN and 1% FA to the peptide pellet, and then sonicate this mixture for 2 min (20% amplitude 1 s on 1 s off cycle).
    (b) Activate Zip-Tip by picking up a C18 OMIX tip, add from above the tip 100 μL of 50% ACN, and discard the flow through. Repeat this step one more time.
    (c) Equilibrate the tip by adding, from above, 100 μL of 2% ACN 1% FA.
    (d) Add to the tip, from above, 100 μL of 2% ACN and 1% FA, pull through the tip, and discard the flow through. Repeat this step two more times.
    (e) Add the sample to the tip from above, pull the sample, and discard to the sample Eppendorf. Repeat this **step 4** more times (*see* **Note 18**).
    (f) Add to the tip 100 μL of 2% ACN and 1% FA, pull through the tip, and discard the flow through to a clean Eppendorf.
    (g) Add to the tip, from above, 100 μL of 70% ACN and 0.1% FA. Pull through the tip, and recover the flow through to a new Eppendorf. Repeat this **step 3** more times (*see* **Note 19**).
    (h) Concentrate the eluted peptides by drying in a vacuum evaporator (e.g., SpeedVac).

3.4 LC Separation and MS Analysis

1. Separation and analysis of tryptic peptides are performed in a nano-HPLC-UltiMate 3000 connected to Probot™.
2. Define the separation program in Chromeleon.
3. Add the tryptic digests to autosampler racks.
4. Prepare eluent A and eluent B. Then, filter and degas with a 0.22 μm polyethersulfone membrane in a traditional kitasato-based vacuum system.
5. Define Chromeleon separation program: 7 °C for autosampler temperature, 25 °C for column oven temperature, 214 nm for UV detector, 30 μL for loading pump flow rate, 0.3 μL micro pump flow rate, 1–2 for inject valve position, five syringe wash cycles, 12 min for wait time before starting signal acquisition, 95% of eluent A for initial conditions.
6. Connect the HPLC column to the fraction collector μ-tee using a fused capillary: 30 μm I.D.

7. Prepare the Probot™ using μCarrier software, and fill the syringe with MALDI matrix solution.
8. Purge the line until eliminate all bubbles.
9. Dispense matrix to attest that the line is completely full.
10. Define the matrix addition flow rate, collection time per fraction, and number of spots using the application editor, and wait for the signal (defined on Chromeleon program) to start the fraction collection.
11. Prepare the sample by solubilizing it in 4 μL of solubilizing solution, sonicate for 30 s, and spin down in a microcentrifuge.
12. Dilute the sample by adding 20 μL of eluent A, sonicate and spin down in a microcentrifuge at maximum speed for 3 min, and place it in the autosampler (*see* **Note 20**).
13. Set the initial program parameters: column oven 25 °C, LoadingPump.Flow = 30 [μL/min], MicroPump.Flow = 0.3 [μL/min], and MicroPump.%B = 5.0 [%].
14. Start the acquisition/fraction collection following the gradient as defined in Table 3.

3.5 Protein Identification

1. Prepare mass spectrometer for measurement according to manufacturer's instructions, and calibrate the instrument using the Calmix 5.
2. Acquire the spectra in the MS positive reflector mode using 1200 laser shots in the m/z range between 700 and 4500 Da. MS/MS analysis of automatically selected precursors is performed at collision energy of 2 kV with air as collision gas at a pressure of 2×10^{-7} Torr. MS spectra are internally calibrated using Glu-Fib (m/z 1570.68). Up to 16 of the

Table 3
Gradient of LC mobile phase

Time (min)	B %
0	5
3	5 (valve shift)
35	45
40	80
45	5
50	5 (valve shift)
55	5

most intense ion signals per spot position with S/N above 50 are selected as precursors for MS/MS.

3. Identify the proteins doing a search against an appropriate database (e.g., Swiss-Prot protein database) using the Mascot algorithm (*see* **Note 21**):
   (a) Open the TS2Mascot and select the spot set of interest.
   (b) Click in save peak list to create the .mgf file.
   (c) Select the location to save the .mgf file.
   (d) Open Mascot web page: http://www.matrixscience.com/.
   (e) Browse and select .mgf file for search.
   (f) Select the database that you want to search against the dataset.
   (g) Select the enzyme used for digestion (e.g., trypsin).
   (h) Select peptide tolerance and MS/MS tolerance at appropriate values (e.g., precursor tolerance 25 ppm and fragment tolerance 0.3 Da).
   (i) Select automatic decoy database to determine the false discovery rate (FDR) (*see* **Note 22**).
   (j) Start the search.

3.6 Data Analysis Using Bioinformatics Tools

ClueGO and CluePedia are two Cytoscape plug-ins that allow to retrieve biological meaning from proteomic data as interaction networks. ClueGO integrates Gene Ontology (GO) terms as well as KEGG/BioCarta pathways and creates a functionally organized GO/pathway term network. ClueGO also allows to compare clusters of genes and visualizes their functional differences [14]. CluePedia complements ClueGO information by providing a comprehensive view on a pathway or process by collecting experimental and in silico data from different perspectives, including protein-protein interactions, as well as the functional context [13, 16]. In this chapter, these two plug-ins were combined to explore the biological processes more prevalent in Sertoli cells. In this sense, proteome data was collected from literature [5] and exported to an Excel file (Supplementary Table S1) to exemplify the application of this bioinformatics tool.

1. Open Cytoscape 3.4.0.
2. Run ClueGO plug-in (Apps → ClueGO v2.3.3 + CluePedia v1.3.3).
3. After open ClueGO panel, it is necessary to define a number of variables: analysis type, cluster list(s), organism, identifiers type, ontology, statistical test, pV correction, advanced statistical options, network specificity, and advanced settings (*see* **Note 23**).
4. Keep the default analysis mode on "ClueGO: function."

5. Load the list of the proteins in the box under "Load Markers List(s)" identified by the gene name (*see* **Note 24**).
6. Select "*Mus musculus*" in the organism drop-down menu under "Load Marker List(s)" (*see* **Note 25**).
7. Select the identifiers type (e.g., AffymetrixID, AccessionID, SymbolID).
8. Select the ontology or ontologies, and select the desired level of evidence (e.g., experimental, inferred from expression pattern, genetic interaction, mutant phenotype) for the ontology repositories (*see* **Note 26**).
9. Pick the option "Show only Pathways with pV ≤," and select the maximum *p* value (pV) allowed. Under "Statistical Options," select the statistical test (*see* **Note 27**).
10. Define pV correction (Bonferroni, Bonferroni step-down, or Benjamini-Hochberg).
11. Select network specificity (global, medium, or detailed network) (*see* **Note 28**).
12. Start the analysis.
13. Open the CluePedia panel and update to visualize the proteins associated to each functional annotation/GO term. If more than one cluster was set at **step 5**, it is possible to attribute each protein and GO term to one or more clusters due to the color-based code system. This is because not only the terms' nodes but also the genes/proteins' nodes will be depicted with a cluster-dependent color.

The network created was enriched through new interaction files (subnetworks). For that, select the genes/proteins from the subnetwork and click "Enrich" (right mouse click on the subnetwork or in CluePedia Enrichment panel). Keep standard settings, set the number of genes, and color before click in the "Start" button. This analysis evidenced the biological processes more prevalent in SCs such as "pyruvate dehydrogenase metabolism," "negative regulation of protein dephosphorylation," "regulation of cysteine-type endopeptidase activity involved in apoptotic process," and "cell recognition" (Fig. 2). SCs have a high glycolytic activity, which is mediated by specific signal transduction pathways, such as the ones involving kinases as AMP-activated protein kinase (AMPK) [7]. Data analysis with ClueGO highlights the serine/threonine-protein kinase OSR1 in the regulation of SCs metabolism (Fig. 2).

Other bioinformatics tools that might complement this information are SecretomeP (http://www.cbs.dtu.dk/services/SecretomeP/) and SignalP (http://www.cbs.dtu.dk/services/SignalP/), which allow to predict the potential secreted proteins by classical and nonclassical pathways, respectively. The same

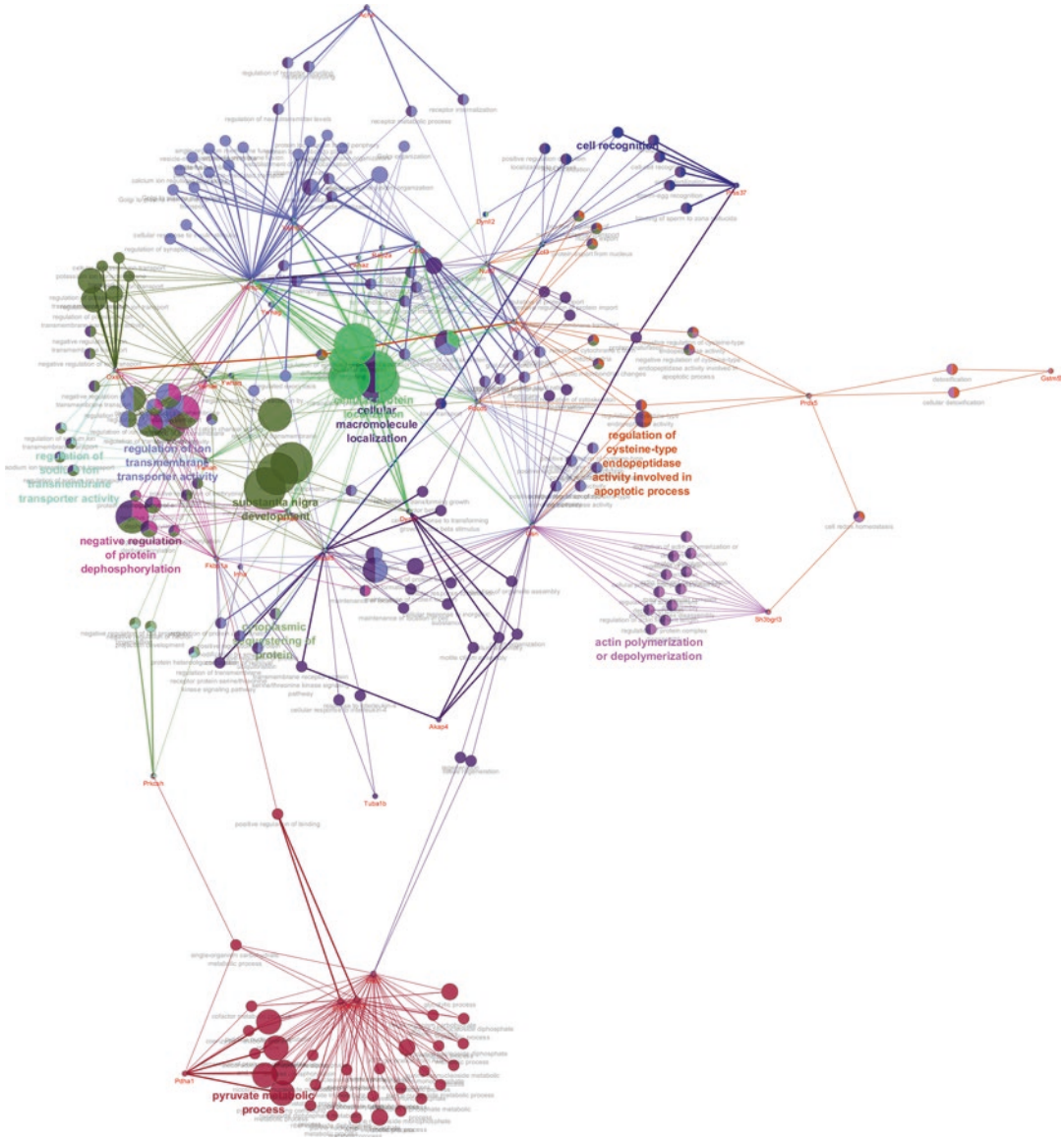

Fig. 2 ClueGO + CluePedia analyses of mouse SCs proteome using biological processes as the selected ontology

protein list (Supplementary Table S1) was used in this analysis; however, data was first converted to FASTA format.

1. Access to Uniprot (http://www.uniprot.org/) and select "Retrieve/ID mapping."
2. Copy the list of accession numbers from excel and pass to "1. Provide your identifiers."
3. Select in "2. Select options" UniProtKB AC/ID and UniProtKB and "Go."

4. In the new page, select "Download" and in the "Format" FASTA (canonical).
5. Paste data retrieved to an Excel file.
6. In http://www.cbs.dtu.dk/services/SecretomeP/, paste data to the "Submission" window (*see* **Note 29**).
7. Select "mammalian" and submit.
8. Copy the list of retrieved proteins to Excel (Supplementary Table S2).
9. In http://www.cbs.dtu.dk/services/SignalP/, paste the same data to "Submission" window.
10. All the other parameters are selected by default.
11. Then "Submit."
12. Copy the list of retrieved proteins to Excel (Supplementary Table S2).

A total of 18 proteins were assigned as secreted by the classical pathway, and 14 proteins were predicted to be secreted through membrane transporters or exosomes (Supplementary Table S2). One of the proteins putatively secreted by the classical and non-classical pathways is acetylcholinesterase. The presence of cholinergic molecules was previously reported to play a role in cell-to-cell communications affecting testicular cell differentiation and function [17]. Another example of a protein predicted to be secreted by both pathways is inhibin alpha chain, a growth factor mainly synthesized in Sertoli cells. This peptide has been found to regulate pituitary secretion of follicle-stimulating hormone (FSH) and to be essential for gonadal tumor suppression, as inhibin-deficient mice developed uni- or bilateral gonadal stromal tumors [18].

Hence, after completing the characterization of Sertoli cell's proteome, bioinformatics analyses can be of great interest: first, to understand the biological phenomena (pathways, metabolism, cell functions) taking place in these cell entities; second, already in a pathological basis, GO enrichment analysis with ClueGO + CluePedia will allow the comprehension of the disease mechanisms; and finally, crossing the information of ClueGO + CluePedia (i.e., deregulated biological processes linked to a subset of proteins) with the output of SecretomeP + SignalP (i.e., proteins predicted to be secreted through classical and nonclassical pathways) will help defining surrogate biomarkers for the diagnosis, prognosis, or therapy monitoring of conditions directly affecting Sertoli cells.

4 Notes

1. The pH of this solution is approximately 8.6 but there is no need to adjust it. This solution is usually stored concentrated at room temperature and should be diluted 1:10 before its use.

2. This solution should be stored at 4 °C during no more than 6 months.
3. Store at room temperature and assure that it has not solidified before its use.
4. A pellet of 15×10^4 to 20×10^4 SCs should be used to get around 50 μg of protein for SDS-PAGE-LC-MS/MS. These cells might be isolated following the procedure already described [19]. A variety of methods for protein extraction might be considered, mechanical (e.g., sonication) and/or buffer systems (e.g., Triton X-100, 8 M urea). Protease inhibitor cocktails should be added to prevent undesirable proteolysis of extracted proteins if samples are expected to be stored for a long period. Nevertheless, all experimental procedures should be performed at 4 °C to avoid undesirable proteolysis.
5. This commercial kit is based on biuret method and is suitable for the sample preparation procedure proposed. Nevertheless, other methods could be used such as Bradford, Lowry, or bicinchoninic acid (BCA). Its choice depends on the sample preparation method and on the predicted protein concentration in sample extracts.
6. The thickness of the gel depends on the sample volume to be loaded. No more than 25 μL of sample can be loaded in a gel with 0.75 mm thickness, using a 10-well comb.
7. The percentage of acrylamide depends on the expected protein molecular weight range distribution in sample extracts.
8. Molecular weight marker only allows to have an idea of protein distribution according to their molecular weight.
9. Samples might have to be diluted in Buffer SG to guarantee the same protein concentration. Then, a certain sample volume containing 40 μg of protein should be diluted with Laemmli buffer (1:2) and incubated at 100 °C for 5 min to assure protein denaturation. So, the sample volume loaded in the gel will be the same. A maximum of 25 μL should be loaded into gel wells to avoid contamination of the other wells.
10. This step assures that all proteins enter in the running gel and also allows some separation of SCs' proteome. However, proteins might be fractionated to varying degrees depending on sample complexity and experiment goal.
11. Other staining methods might be selected such as Coomassie Blue or mass spectrometry-compatible fluorescent dyes. If silver staining is chosen, it is imperative to follow a methodology compatible with MS analysis (the cross-linker glutaraldehyde should be avoided).
12. **Steps 13–15** might be skipped once the obtained image provides a rough idea of proteome separation.

13. Smaller gel pieces increase the efficiency of trypsin digestion.
14. After the addition of ACN, the bands/spots should be dehydrated and become white.
15. The steps of reduction and alkylation can be skipped. DTT promotes the reduction of disulfide bonds and formation of thiols (-SH). Iodoacetamide blocks thiols by alkylation and also prevents reoxidation of proteins by the formation of S-carboxyamidomethylcysteine (CAM; adduct: CH_2CONH_2). The specific mass of the amino acid cysteine is thereby increased from 103.01 to 160.03 Da.
16. Trypsin is usually chosen because it is highly specific and relatively inexpensive and by cleaving at arginine and lysine residues ensures a positive charge at the C-terminus (besides to the N-terminus), resulting in double-charged peptides. Trypsin is also active in several basic buffers. Nevertheless, other enzymes (such as Lys-C and Arg-C) might be used instead of trypsin; however, the optimal conditions of each enzyme should be adjusted with respect to the solubilization buffer, incubation temperature, and time of incubation.
17. This step might lead to peptide loss but prevents small polyacrylamide gel particles from entering LC system and damaging it. Moreover, this step improves spectral quality by eliminating interfering ions.
18. By discarding the flow-through to the same Eppendorf, sample loss can be minimized.
19. Before adding 70% ACN 0.1% FA, place an Eppendorf below the tip to avoid losses due to the low capillary strength of the solution.
20. Be careful and avoid bubbles while sample is being transferred to sample vial.
21. Mascot Server has been the standard software for protein identification using peak lists from instruments manufactured by different companies. Nevertheless, other algorithms might be chosen such as PatternLab [20], an integrated computational environment for analyzing shotgun proteomic data. PatternLab contains modules that allow, for example, formatting sequence databases, performing peptide spectrum matching, statistically filtering and organizing shotgun proteomic data, and performing similarity-driven studies with de novo sequencing data.
22. False discovery rate (FDR) is associated with the similarity score of a peptide spectrum match (PSM). FDR is estimated by searching the experimental data against a randomized peptide or protein sequence database (a decoy database). A decoy search can be automatically performed in Mascot by selecting

the Decoy checkbox on the search form. Nevertheless, other decoy databases can be created to estimate FDR.

23. ClueGO integrates GO terms as well as KEGG/BioCarta pathways and creates a functionally organized GO/pathway term network. It can analyze one or compare two lists of genes and comprehensively visualizes functionally grouped terms. GO defines concepts/classes used to describe gene products in terms of their associated biological processes, cellular components, and molecular functions (http://geneontology.org/). KEGG is a database resource for understanding biological systems from molecular level information (http://www.genome.jp/kegg/). BioCarta is a community-fed database that provides maps depicting common metabolic pathways, signal transduction pathway, as well as other biochemical pathways (https://www.hsls.pitt.edu/obrc/index.php?page=URL1151008585). ClueGO represents an open-source Java tool that extracts the non-redundant biological information for large clusters of genes, using all these databases [14].
24. If different conditions/samples are compared, more clusters can be added by pressing on "+." This will allow GO enrichment analysis and not only the mapping of ontologies for a subset of genes.
25. *Mus musculus* was selected as the reference species because more extensive annotation data are available for this species than for rat or sheep [5].
26. Do not forget to update GO categories in the "show ontology update" options.
27. The standard test is hypergeometric test two-sided, which allows to look at significant over- and underrepresented GO terms.
28. The "global network" provides a general biological information, whereas the "detailed network" shows more specific and informative ontologies underlying particular aspects of the studied gene product [21].
29. The maximum number of entries in FASTA format is 100 and the minimum is 40.

Acknowledgments

The authors thank Portuguese Foundation for Science and Technology (FCT), European Union, QREN, FEDER, and COMPETE for funding the iBiMED (UID/BIM/04501/2013), QOPNA (UID/QUI/00062/2013), UnIC (UID/IC/00051/2013), research project (POCI-01-0145-

FEDER-016728; PTDC/DTP-DES/6077/2014), and RV's (IF/00286/2015) and FT's (SFRH/BD/111633/2015) fellowship grants.

References

1. Li X, Wang W, Chen J (2015) From pathways to networks: connecting dots by establishing protein-protein interaction networks in signaling pathways using affinity purification and mass spectrometry. Proteomics 15(2–3):188–202. https://doi.org/10.1002/pmic.201400147
2. Zheng B et al (2015) Quantitative proteomics reveals the essential roles of stromal interaction molecule 1 (STIM1) in the testicular cord formation in mouse testis. Mol Cell Proteomics 14(10):2682–2691. https://doi.org/10.1074/mcp.M115.049569
3. Jegou B (1993) The Sertoli-germ cell communication network in mammals. Int Rev Cytol 147:25–96
4. Stanton PG, Sluka P, Foo CF, Stephens AN, Smith AI, McLachlan RI, O'Donnell L (2012) Proteomic changes in rat spermatogenesis in response to in vivo androgen manipulation; impact on meiotic cells. PLoS One 7(7):e41718. https://doi.org/10.1371/journal.pone.0041718
5. Chalmel F, Com E, Lavigne R, Hernio N, Teixeira-Gomes AP, Dacheux JL, Pineau C (2014) An integrative omics strategy to assess the germ cell secretome and to decipher sertoli-germ cell crosstalk in the Mammalian testis. PLoS One 9(8):e104418. https://doi.org/10.1371/journal.pone.0104418
6. Com E, Melaine N, Chalmel F, Pineau C (2014) Proteomics and integrative genomics for unraveling the mysteries of spermatogenesis: the strategies of a team. J Proteome 107:128–143. https://doi.org/10.1016/j.jprot.2014.04.013
7. Rato L, Alves MG, Socorro S, Duarte AI, Cavaco JE, Oliveira PF (2012) Metabolic regulation is important for spermatogenesis. Nat Rev Urol 9(6):330–338. https://doi.org/10.1038/nrurol.2012.77
8. Yates JR, Ruse CI, Nakorchevsky A (2009) Proteomics by mass spectrometry: approaches, advances, and applications. Annu Rev Biomed Eng 11:49–79. https://doi.org/10.1146/annurev-bioeng-061008-124934
9. Padrao AI, Vitorino R, Duarte JA, Ferreira R, Amado F (2013) Unraveling the phosphoproteome dynamics in mammal mitochondria from a network perspective. J Proteome Res 12(10):4257–4267. https://doi.org/10.1021/pr4003917
10. Aslam B, Basit M, Nisar MA, Khurshid M, Rasool MH (2017) Proteomics: technologies and their applications. J Chromatogr Sci 55(2):182–196. https://doi.org/10.1093/chromsci/bmw167
11. Paulo JA (2016) Sample preparation for proteomic analysis using a GeLC-MS/MS strategy. J Biol Methods 3(3). https://doi.org/10.14440/jbm.2016.106
12. Chen C, Huang H, Wu CH (2011) Protein bioinformatics databases and resources. Methods Mol Biol 694:3–24. https://doi.org/10.1007/978-1-60761-977-2_1
13. Bindea G, Galon J, Mlecnik B (2013) CluePedia Cytoscape plugin: pathway insights using integrated experimental and in silico data. Bioinformatics. https://doi.org/10.1093/bioinformatics/btt019
14. Bindea G et al (2009) ClueGO: a Cytoscape plug-in to decipher functionally grouped gene ontology and pathway annotation networks. Bioinformatics 25(8):1091–1093. https://doi.org/10.1093/bioinformatics/btp101
15. Bendtsen JD, Jensen LJ, Blom N, Von Heijne G, Brunak S (2004) Feature-based prediction of non-classical and leaderless protein secretion. Protein Eng Des Sel 17(4):349–356. https://doi.org/10.1093/protein/gzh037
16. Bindea G, Galon J, Mlecnik B (2013) CluePedia Cytoscape plugin: pathway insights using integrated experimental and in silico data. Bioinformatics 29(5):661–663. https://doi.org/10.1093/bioinformatics/btt019
17. Palmero S, Bardi G, Coniglio L, Falugi C (1999) Presence and localization of molecules related to the cholinergic system in developing rat testis. Eur J Histochem 43(4):277–283
18. Matzuk MM, Finegold MJ, Su JG, Hsueh AJ, Bradley A (1992) Alpha-inhibin is a tumour-suppressor gene with gonadal specificity in mice. Nature 360(6402):313–319. https://doi.org/10.1038/360313a0
19. Tripathi UK et al (2014) Differential proteomic profile of spermatogenic and Sertoli cells from peri-pubertal testes of three different

bovine breeds. Front Cell Dev Biol 2:24. https://doi.org/10.3389/fcell.2014.00024

20. Carvalho PC et al (2016) Integrated analysis of shotgun proteomic data with PatternLab for proteomics 4.0. Nat Protoc 11(1):102–117. https://doi.org/10.1038/nprot.2015.133

21. Killcoyne S, Carter GW, Smith J, Boyle J (2009) Cytoscape: a community-based framework for network modeling. Methods Mol Biol 563:219–239. https://doi.org/10.1007/978-1-60761-175-2_12

Chapter 14

Gene Silencing of Human Sertoli Cells Utilizing Small Interfering RNAs

Hong Wang, Qingqing Yuan, Minghui Niu, Liping Wen, Hongyong Fu, Fan Zhou, Weihui Zhang, and Zuping He

Abstract

Sertoli cells, as the unique somatic cells within the seminiferous tubules, play essential roles in regulating normal spermatogenesis. In addition, recent studies have demonstrated that Sertoli cells could have significant applications in regenerative medicine due to their great plasticity. However, the roles of genes in controlling the fate determinations of human Sertoli cells remain largely unknown. Silencing genes of human Sertoli cells utilizing small interfering RNAs (siRNAs) is an important method to explore their functions and mechanisms in human Sertoli cells. We isolated and identified human Sertoli cells. RNA interference (RNAi) was employed to probe the roles and signaling pathways of BMP6 and BMP4 in mediating the proliferation and apoptosis of human Sertoli cells. Specifically, siRNAs against BMP6 and BMP4 were used to knock down the expression levels of BMP6 and BMP4 and examine the function and mechanism in controlling the fate decisions of human Sertoli cells. In this chapter, we provided the detailed methods of RNAi in silencing BMP6 gene of human Sertoli cells. Quantitative real-time PCR demonstrated that the designed BMP6 siRNAs apparently silenced BMP6 mRNA in human Sertoli cells at 24 h after transfection. Western blots showed that the siRNAs silenced the expression of BMP6 protein effectively at 48 h after transfection. In summary, siRNAs can *effectively* and specifically knock down targeting genes at both transcriptional and translational levels utilizing RNAi in human Sertoli cells.

Key words Human Sertoli cells, Gene silencing, RNA interference, Gene and protein knockdown, Functions and mechanisms

1 Introduction

As the unique and important somatic cells of the testicular microenvironment or niche, Sertoli cells can secrete many important growth factors, e.g., GDNF, SCF, and BMP4, which regulate the fate determinations of spermatogonial stem cells [1, 2]. Sertoli cells are the main component of *blood-testis barrier*, which provides a stable internal environment for spermatogenesis [3]. It has been shown that each Sertoli cell supports the appropriate number of male germ cells, whereas the quantity and quality abnormality of Sertoli cells may lead to the dyszoospermia [4]. Moreover, Sertoli

Marco G. Alves and Pedro F. Oliveira (eds.), *Sertoli Cells: Methods and Protocols*, Methods in Molecular Biology, vol. 1748, https://doi.org/10.1007/978-1-4939-7698-0_14,

cells can be reprogrammed to become multipotent neural stem cells and Leydig cells [5, 6], reflecting that Sertoli cells have clinical applications in regenerative medicine.

RNA interference (RNAi) has previously been proposed to manipulate gene expression in the nematode *Caenorhabditis elegans*, and its function depends on an antisense mechanism between the endogenous messenger RNA transcripts and the exogenous RNA [7–9]. RNAi was regarded as the most prominent achievement by *Science* in 2002, and notably, it has been demonstrated to be a powerful tool to reveal the novel functions and mechanisms of genes in regulating various kinds of biological processes. The mechanism of RNAi has been illustrated in Fig. 1. Briefly, the double-stranded RNA (dsRNA) is degraded by Dicer enzyme, an RNase III-type protein, to 21–25 nucleotides length of small interfering RNAs (siRNAs) [10]. The siRNA-induced silencing complex (RISC) is composed of the guiding siRNA and Dicer and other proteins and enzymes, and the RISC degrades the homologous single-stranded messenger RNA (mRNA) to malfunctioning mRNA. RNAi method has certain advantages over other technologies of gene interference [7, 11–13]: (a) RNAi, as a posttranscriptional gene silencing (PTGS), specifically combines with its targeting mRNA and promotes mRNA degradation without affecting DNA and microRNA, and thus the roles and mechanisms of the interfering genes could be defined; (b) the efficiency of interference by RNAi is prominent and obvious, and a small dose of siRNA can effectively silence the expression of targeting mRNA; (c) RNAi can silence the targeting genes instantly without causing fetal death that is associated with gene knockout; and (d) RNAi was economical, and it takes less consumption of time compared to other gene editing techniques. Therefore, RNAi has been used extensively in studies on gene function and *gene therapy* [12, 14].

RNAi is a promising method to edit genes in humans, rodents, and other species. We have successfully silenced the expression levels of bone morphogenetic protein 6 (BMP6) and BMP4 using RNAi in human Sertoli cells to probe their functions and mechanisms underlying the development and maturity of Sertoli cells [15, 16]. BMP6 belongs to the member of the transforming growth factor-β (TGF-β) superfamily, and it plays essential roles in mediating the fate decisions of various kinds of stem cells [17–22]. In addition, the abnormal expression of BMP6 may cause skeletal deformities, heritable and metabolic disorders, cancer, and cardiovascular disease [23–25]. However, the function and mechanism of BMP6 in regulating the fate determinations of human Sertoli cells remain to be elucidated. In the following sections, we provide detailed information on the procedures of silencing BMP6 in human Sertoli cells utilizing RNAi: (1) two-step enzymatic digestion and differential plating to obtain a high purity Sertoli cells, (2) the procedures and notes of RNAi, and (3) the verification of the

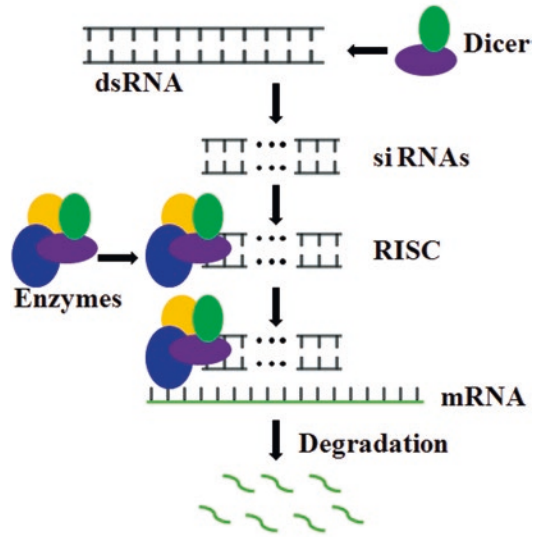

Fig. 1 The schematic diagram showed the mechanism by which siRNAs knock down the expression of genes

silencing efficiency of BMP6 at transcriptional and translational levels in human Sertoli cells. Two-step enzymatic digestion and followed by the differential plating can obtain a high purity of human Sertoli cells. Using these procedures, it is feasible to effectively silence the expression of numerous genes to probe their functions and molecular mechanisms underlying the development of human Sertoli cells.

2 Materials

2.1 Procurement of Human Testicular Tissues

1. Human testicular tissues were obtained from OA (obstructive azoospermia) patients who underwent microdissection and sperm extraction. All OA patients' pathologies were confirmed histologically, and they had normal spermatogenesis. All experimental protocols were performed in accordance with relevant guidelines and regulations of the Institutional Ethical Review Committee of Ren Ji Hospital (license number of ethics statement: 2012-01).
2. Phosphate-buffered saline (PBS).
3. Penicillin and streptomycin.
4. Dulbecco's modified Eagle medium F-12 (DMEM/F-12).
5. Dimethyl sulfoxide (DMSO).

2.2 Enzymatic Digestion of Human Testis Tissues to Obtain Testicular Cells

1. Enzymatic digestion solution I: 15 ml DMEM/F-12 with 2 mg/ml collagenase IV and 1 μg/μl DNase I.
2. Enzymatic digestion solution II: 15 ml DMEM/F-12 with 4 mg/ml collagenase IV, 2.5 mg/ml hyaluronidase, 2 mg/ml trypsin, and 1 μg/μl DNase I.

2.3 Obtaining Human Sertoli Cells with Differential Plating Technique

1. DMEM/F-12 medium supplemented with 10% FBS (complete medium).
2. Gelatin.

2.4 Identification of Human Sertoli Cells Using RT-PCR and Immunocytochemistry (ICC)

1. Trizol.
2. Chloroform, isopropyl alcohol, anhydrous ethanol.
3. Agarose gel.
4. The first strand cDNA synthesis kit.
5. PCR Premix Taq™.
6. Gengreen.
7. 4% paraformaldehyde (PFA).
8. PBS.
9. Triton X-100.
10. BSA.
11. Fluorescein isothiocyanate (FITC).
12. 4, 6-diamidino-2-phenylindole (DAPI).

2.5 BMP6 Silencing Using BMP6 siRNAs and the Viability Evaluation of Human Sertoli Cells After BMP6 siRNAs Transfection by Trypan Blue Staining

1. The siRNAs targeting human BMP6 were purchased from GenePharma, Suzhou, China.
2. Transfection reagent: lipofectamine 2000.
3. Opti-MEM I reduced serum medium.
4. Trypan blue.

2.6 The Transfection Efficiency of BMP6 siRNAs Using Quantitative Real-Time PCR and Western Blots

1. Power SYBR® Green PCR Master Mix.
2. Step one plus real-time PCR system.
3. RIPA buffer.
4. BCA kit.
5. 10% SDS-PAGE.
6. Methyl alcohol.
7. The XCell SureLock Mini-Cell apparatus.
8. Tris-buffered saline (TBS).
9. Tween.

10. Nonfat dry milk.
11. Horseradish peroxidase-conjugated anti-rabbit immunoglobulin G (IgG).
12. Chemiluminescence.

3 Methods

3.1 Procurement of Testes from OA Patients

The human testis tissues from OA patients were placed in human tubal fluid (HTF) immediately after surgery, and they were sent to laboratory as soon as possible. The testicular tissues were washed with PBS containing 2% penicillin and streptomycin to remove the rudimental serum. After being cut into small pieces, the tissues were frozen in 1 ml mixture of 10% DMSO, 80% FBS, and 10% DMEM/F-12 in liquid nitrogen for long-time storage, and the integrity of the tissues was excellent.

3.2 Enzymatic Digestion of Human Testis Tissues to Obtain Human Sertoli Cells

1. The hood was sterilized with UV light for at least 30 min.
2. Thirty milligrams (mg) of collagenase IV was weighed and put in a 15 ml conical tube. This was the enzyme I.
3. In total, 60 mg of collagenase IV, 37.5 mg of hyaluronidase, and 30 mg of trypsin were weighed and then placed in a 15 ml conical tube. This was the enzyme II.
4. Enzyme I (from **step 2**) was dissolved in 15 ml of DMEM/F-12 to obtain a 2 mg/ml collagenase IV solution. Solution I was filtered with a sterile Acrodisc syringe filter (5 μm) for sterilizing, and DNase I was added to it and mixed gently with pipette to yield 1 μg/μl DNase I. This was marked with enzyme I solution.
5. Enzyme II (from **step 3**) was dissolved in 15 ml of DMEM/F-12 to obtain 4 mg/ml collagenase IV, 2.5 mg/ml hyaluronidase, and 2 mg/ml trypsin solution. This solution was filtered with a sterile Acrodisc syringe filter (5 μm) for sterilizing, and DNase I was added to it and mixed gently with pipette to yield 1 μg/μl DNase I. This was marked with enzyme II solution.
6. Human testis tissues were cut into approximately 3 × 3 × 3 mm small pieces and washed with PBS for three times.
7. The testis tissues were minced by scissors to become a semiliquid state. After adding 15–20 ml DMEM/F-12, testis tissues were transferred into a 50 ml conical tube. After being mixed gently with 10 ml glass pipette and sedimentation for 5 min, the supernatant was discarded with 25 ml glass pipettes.
8. Enzyme I solution (from **step 4**) was added to the testis tissues (from **step 7**) and incubated in a shaking water bath at 34 °C for 10 min–15 min.

9. The digested testis tissues were examined under a microscope to ensure that there were only seminiferous tubules without gross lumps. The solution containing seminiferous tubules was transferred to a new 50 ml conical tubes, and 30 ml DMEM/F12 containing 10% FBS was added to the seminiferous tubules to stop the digestion. After 5 min of sedimentation, the supernatant was removed with a 25 ml pipette. The seminiferous tubules were washed with DMEM/F-12 extensively to remove the Leydig cells and interstitial cells.
10. Enzyme II solution (from **step 5**) was added to the seminiferous tubules (Fig. 2a, from **step 9**) and incubated in a shaking water bath at 34 °C for about 10 min–15 min at 100 cycles/min.
11. After digestion with enzyme solution II, the cell mixture containing male germ cells and Sertoli cells was pipetted with 10 ml glass tube for several times without producing air bubbles.
12. The effectiveness of enzyme II solution digestion was detected with a drop of the mixture under a microscope. If some seminiferous tubules existed the mixture was incubated for another 10–15 min in a shaking water bath at 34 °C until it was completely digested to single cells. Then, 30 ml DMEM/F-12 and 10% FBS were added to the mixture to stop the enzyme digestion and allowed 10 min of sedimentation.
13. The supernatant containing with germ cells and Sertoli cells was transferred to a new 50 ml conical tube, and the sediment was discarded.
14. The cell mixture with male germ cells and Sertoli cells (Fig. 2b) was pipetted with 10 ml glass tube to single cells, and it was filtered through a 40 μm nylon mesh to remove cell aggregates.
15. The cell mixture after filtration was centrifuged at 1000 rpm for 5 min, and the cell pellet was suspended in fresh DMEM/F-12 supplemented with 10% FBS.

3.3 Differential Plating to Obtain Human Sertoli Cells

The cells from **step 15** containing with male germ cells and Sertoli cells were seeded in a 15-cm diameter tissue culture dish pre-coated with 0.1% gelatin. After 3–6 h of culture, human Sertoli cells were attached with the dish (Fig. 2c), and male germ cells remained in suspension and removed.

3.4 Identification of Human Sertoli Cells

3.4.1 Identification of Human Sertoli Cells Using RT-PCR

1. Total RNA of human Sertoli cells was extracted using Trizol reagent according to the methods as described previously [15].
2. Reverse transcription (RT) was performed using first strand cDNA synthesis kit, and PCR was performed using PCR Premix Taq™. The amplification program was started at 94 °C

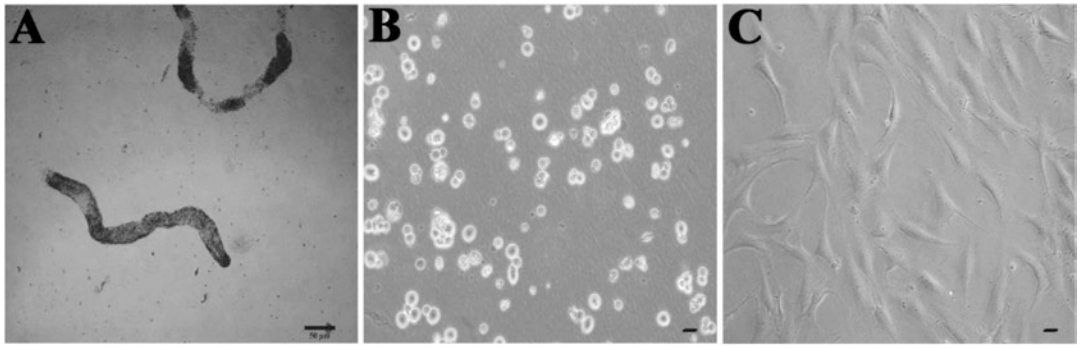

Fig. 2 The isolation and culture of human Sertoli cells. (**a**) Human seminiferous tubules were separated by digestion by enzymatic I. (**b**) The cell mixture containing human Sertoli cells and germ cells was obtained after enzymatic I and II enzymatic digestions. (**c**) Human Sertoli cells were obtained after differential plating. Scale bar in **a** = 50 μm; scale bars in **b** and **c** = 20 μm

for 3 min and performed in terms of the following conditions: denaturation at 94 °C for 30 s, annealing at 55–60 °C for 45 s, and elongation at 72 °C for 45 s. After 35 cycles, the samples were incubated for 5 min at 72 °C. The detailed information on the primer sequences of chosen genes for identification of human Sertoli cells could be found in Table S1 of ref. 16.

3. PCR products were separated by electrophoresis in 2.0% agarose gel and visualized with ethidium bromide.
4. The intensities of cDNA bands were analyzed using chemiluminescence (*see* Fig. 1A in ref. 16).

RT-PCR revealed that a number of genes for Sertoli cells [26–28], e.g., *GDNF*, *SOX9*, *BMP4*, *WT1*, *GATA4*, *GATA1*, *SCF*, *FGF2*, and *AR*, were expressed in the isolated human Sertoli cells, whereas *VASA*, a specific gene for male germ cells [26–28], was undetected in these cells.

3.4.2 Identification of Human Sertoli Cells Using Immunocytochemistry

1. Human Sertoli cells were seeded on glass slides in DMEM/F-12 supplemented with 10% FBS to allow the cells to attach to the slides.
2. The cell slides were washed with PBS for three times per 5 min, and they were fixed with 4% paraformaldehyde (PFA) for 30 min at room temperature. After extensive washes with PBS, the cells were permeabilized with 0.3% triton X-100 for 15 min at room temperature, and they were blocked with 5% BSA for 1 h at room temperature.
3. These cells were incubated with primary antibodies (the detailed information on the primary antibodies were referred to Table S2 of ref. 16) at 4 °C overnight.
4. After washing with PBS for three times per 5 min, the cells were incubated with the secondary antibody, namely, IgGs

conjugated with fluorescein isothiocyanate (FITC), at a 1:200 dilution for 1 h at room temperature.

5. To label the nuclei, DAPI (1:500) was used to stain the cells for 5 min at room temperature.
6. After washing with PBS, the images were captured with a Nikon microscope.

As shown in Fig. 1 of ref. 16, immunocytochemistry showed that WT1, SOX9, BMP4, GDNF, SCF, OCLN, ZO1, and VIM were expressed in the isolated Sertoli cells.

3.5 The Expression of BMP6 in Human Sertoli Cells Using RT-PCR, Western Blots, and Immunocytochemistry

The expression of BMP6 ligand was found in human Sertoli cells using RT-PCR (Fig. 3), Western blots (Fig. 2B in ref. 16), and immunocytochemistry (Fig. 2C, 2I, and 2L in ref. 16). The Western blot protocol was performed in terms of the method as described previously [15]. In summary, RT-PCR, Western blots, and immunocytochemistry demonstrated that BMP6 was present in human Sertoli cells.

3.6 Silencing BMP6 of Human Sertoli Cells Utilizing RNAi

1. Human Sertoli cells were seeded in 24-well plates at 2.0×10^5 cells/well in DMEM/F-12 supplemented with 10% FBS for overnight to reach a cell confluence of about 70%–90%.
2. In total, 60 pmol of FAM-labeled siRNA, negative control siRNA, and BMP6 siRNA-1, siRNA-2, siRNA-3, and siRNA-4 were diluted in 100 μl Opti-MEM I Reduced Serum Medium, respectively, and they were mixed gently (the detailed information on BMP6 siRNAs were referred to Table S3 of ref. 16).
3. In general, 2 μl lipofectamine 2000 were diluted in 100 μl Opti-MEM I Reduced Serum Medium and incubated for 5 min at room temperature. The appropriate ratio of siRNA and lipofectamine 2000 was crucial to achieve high transfection efficiency. It was recommended that the ratio of siRNA to lipofectamine 2000 was 1:0.01–1:0.1 (pmol: μl).
4. After incubation for 5 min at room temperature, the siRNA and lipofectamine 2000 solutions from **step 2** and **step 3** were mixed gently, and they were incubated for 15 min–20 min at room temperature.
5. The culture medium was changed with 400 μl fresh DMEM/F-12 without antibiotic and with 1% FBS before transfection, and the oligomer-lipofectamine 2000 complexes (from **step 4**) were added to each well and mixed gently.
6. Six hours after transfection of BMP6 siRNAs, the transfection efficiency was evaluated using Nikon fluorescence microscope. As shown in Fig. 4A of ref. 16, the transfection efficiency of BMP6 siRNAs in human Sertoli cells was above 80%.

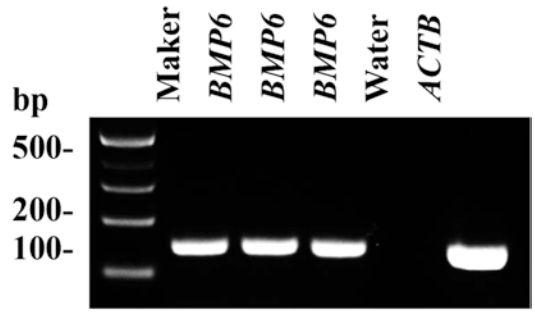

Fig. 3 The expression of BMP6 transcripts in human Sertoli cells. RT-PCR revealed the expression of *BMP6* mRNA in human Sertoli cells. Water without cDNA served as a negative control, and *ACTB* was used as a loading control for total RNA

7. The quantity of siRNA and lipofectamine 2000 can be adjusted slightly within the suggested ranges (Table 1) to achieve great transfection efficiency of siRNAs.
8. Trypan blue staining was performed to assess the viability of the cells after transfection BMP6 siRNAs. Briefly, the cells were incubated with 0.4% trypan blue for 3–5 min, and the viability of these cells was evaluated by the percentage of the cells excluding trypan blue staining and total cells counted. The viability of human Sertoli cells after transfection of BMP6 siRNAs was over 96%.
9. The cells were harvested to detect the BMP6 transcriptional and translational levels at 24 h or 48 h after transfection of BMP6 siRNAs.

3.7 The Knockdown Efficiency of BMP6 at Transcriptional and Translational Levels

3.7.1 The Silencing Efficiency of BMP6 mRNA by BMP6 siRNAs in Human Sertoli Cells

Quantitative real-time PCR reaction was performed using Power SYBR® Green PCR Master Mix and a 7500 Fast Real-Time PCR System to detect the efficiency of *BMP6* transcription (Fig. 4B in ref. 16). To quantify the products, the comparative CT (threshold cycle) method was used as described previously [29]. Quantitative real-time PCR showed that BMP6 siRNA-1, siRNA-2, siRNA-3, and siRNA-4 could effectively decrease the transcriptional levels of *BMP6* in human Sertoli cells at 24 h after transfection, while the silence efficiency of BMP6 siRNA-1 was the most prominent. Compared to the control siRNA, the BMP6 siRNA-1 reduced the BMP6 mRNA by 88.2% ± 2.4%.

3.7.2 The Silence Efficiency of BMP6 Protein by BMP6 siRNAs in Human Sertoli Cells

Western blots were used to detect the efficiency of BMP6 siRNAs on the translational levels of BMP6 in human Sertoli cells. As shown in Fig. 4E and F in ref. 16, BMP6 siRNA-1 diminished the expression of BMP6 protein by 300.0% ± 27.7% at 48 h after transfection.

Table 1
Optimal conditions of siRNA transfection in human Sertoli cells

Culture plate	siRNA doses (pmol)	siRNA ranges (pmol)	Total volumes of culture medium(μl)	Lipofectamine 2000 (μl)	Lipofectamine 2000 ranges(μl)
96-well	5	2.5–10	100	0.25	0.1–0.5
24-well	20	10–40	500	1	0.5–2
12-well	140	20–80	1000	2	1–4
6-well	100	50–200	2000	5	2.5–10
35 mm	100	50–200	2000	5	2.5–10
60 mm	600	300–1200	5000	10	5–20

4 Notes

1. The isolation and culture of adult human Sertoli cells were performed according to the notes we described previously [30].
2. The siRNA oligonucleotides are stable for 2 weeks at 4 °C and 6 months at −20 °C, and they should be avoided for repeated freeze-thaw cycles. A concentration of 20 μM siRNA is recommended for storage.
3. The dry powder of siRNA oligo is easily spread, and thus it should be centrifuged before opening the tube containing siRNA oligo.
4. FAM-labeled siRNA should be protected from light.
5. The viability of human Sertoli cells is critical to enhance transfection efficiency of siRNAs, and thus the transfection of siRNAs should be completed when the cells reach a 70%–90% confluence.
6. To ensure the repeatability of RNAi, the quantity of human Sertoli cells, subculture times, and culture conditions of these cells should be maintained consistently.
7. The effects of RNAi depend on siRNA sequences other than the increases of siRNA concentrations.
8. Negative siRNA controls without targeting the sequences of genes were essential for determining whether silencing of target genes by RNAi were specific or artificial.

References

1. Meng X et al (2000) Regulation of cell fate decision of undifferentiated spermatogonia by GDNF. Science 287(5457):1489–1493
2. Ohta H, Yomogida K, Dohmae K, Nishimune Y (2000) Regulation of proliferation and differentiation in spermatogonial stem cells: the role of c-kit and its ligand SCF. Development 127(10):2125–2131
3. Hofmann MC (2008) Gdnf signaling pathways within the mammalian spermatogonial stem cell niche. Mol Cell Endocrinol 288(1-2):95–103. https://doi.org/10.1016/j.mce.2008.04.012. S0303-7207(08)00153-6 [pii]
4. Orth JM, Gunsalus GL, Lamperti AA (1988) Evidence from Sertoli cell-depleted rats indicates that spermatid number in adults depends on numbers of Sertoli cells produced during perinatal development. Endocrinology 122(3):787–794. https://doi.org/10.1210/endo-122-3-787
5. Sheng C et al (2012) Direct reprogramming of Sertoli cells into multipotent neural stem cells by defined factors. Cell Res 22(1):208–218. https://doi.org/10.1038/cr.2011.175
6. Zhang L et al (2015) Reprogramming of Sertoli cells to fetal-like Leydig cells by Wt1 ablation. Proc Natl Acad Sci U S A 112(13):4003–4008. https://doi.org/10.1073/pnas.1422371112
7. Fire A, Xu S, Montgomery MK, Kostas SA, Driver SE, Mello CC (1998) Potent and specific genetic interference by double-stranded RNA in Caenorhabditis Elegans. Nature 391(6669):806–811. https://doi.org/10.1038/35888
8. Fire A, Albertson D, Harrison SW, Moerman DG (1991) Production of antisense RNA leads to effective and specific inhibition of gene expression in C. Elegans muscle. Development 113(2):503–514
9. Guo S, Kemphues KJ (1995) Par-1, a gene required for establishing polarity in C. Elegans embryos, encodes a putative Ser/Thr kinase that is asymmetrically distributed. Cell 81(4):611–620
10. Bernstein E, Caudy AA, Hammond SM, Hannon GJ (2001) Role for a bidentate ribonuclease in the initiation step of RNA interference. Nature 409(6818):363–366. https://doi.org/10.1038/35053110
11. Nykanen A, Haley B, Zamore PD (2001) ATP requirements and small interfering RNA structure in the RNA interference pathway. Cell 107(3):309–321
12. Elbashir SM, Harborth J, Lendeckel W, Yalcin A, Weber K, Tuschl T (2001) Duplexes of 21-nucleotide RNAs mediate RNA interference in cultured mammalian cells. Nature 411(6836):494–498. https://doi.org/10.1038/35078107
13. Bass BL (2001) RNA interference. The short answer. Nature 411(6836):428–429. https://doi.org/10.1038/35078175
14. Scherr M, Battmer K, Winkler T, Heidenreich O, Ganser A, Eder M (2003) Specific inhibition of bcr-abl gene expression by small interfering RNA. Blood 101(4):1566–1569. https://doi.org/10.1182/blood-2002-06-1685
15. Hai Y, Sun M, Niu M, Yuan Q, Guo Y, Li Z, He Z (2015) BMP4 promotes human Sertoli cell proliferation via Smad1/5 and ID2/3 pathway and its abnormality is associated with azoospermia. Discov Med 19(105):311–325
16. Wang H et al (2017) BMP6 regulates proliferation and apoptosis of human Sertoli cells via Smad2/3 and Cyclin D1 pathway and DACH1 and TFAP2A activation. Sci Rep 7:45298. https://doi.org/10.1038/srep45298
17. Crews L et al (2010) Increased BMP6 levels in the brains of Alzheimer's disease patients and APP transgenic mice are accompanied by impaired neurogenesis. J Neurosci 30(37):12252–12262. https://doi.org/10.1523/JNEUROSCI.1305-10.2010. 30/37/12252 [pii]
18. Peretto P, Cummings D, Modena C, Behrens M, Venkatraman G, Fasolo A, Margolis FL (2002) BMP mRNA and protein expression in the developing mouse olfactory system. J Comp Neurol 451(3):267–278. https://doi.org/10.1002/cne.10343
19. He Z, Subramaniam D, Zhang Z, Zhang Y, Anant S (2013) Honokiol as a Radiosensitizing agent for colorectal cancers. Curr Colorectal Cancer Rep 9(4). https://doi.org/10.1007/s11888-013-0191-4
20. Xie T, Spradling AC (1998) Decapentaplegic is essential for the maintenance and division of germline stem cells in the drosophila ovary. Cell 94(2):251–260. S0092-8674(00)81424-5 [pii]
21. Sekiya I, Colter DC, Prockop DJ (2001) BMP-6 enhances chondrogenesis in a subpopulation of human marrow stromal cells. Biochem Biophys Res Commun 284(2):411–418. https://doi.org/10.1006/bbrc.2001.4898. S0006-291X(01)94898-3 [pii]

22. Zhang J et al (2003) Identification of the haematopoietic stem cell niche and control of the niche size. Nature 425(6960):836–841. https://doi.org/10.1038/nature02041. nature02041 [pii]
23. Massague J, Blain SW, Lo RS (2000) TGFbeta signaling in growth control, cancer, and heritable disorders. Cell 103(2):295–309. S0092-8674(00)00121-5 [pii]
24. Asanbaeva A, Masuda K, Thonar EJ, Klisch SM, Sah RL (2008) Regulation of immature cartilage growth by IGF-I, TGF-beta1, BMP-7, and PDGF-AB: role of metabolic balance between fixed charge and collagen network. Biomech Model Mechanobiol 7(4):263–276. https://doi.org/10.1007/s10237-007-0096-8
25. Tobin JF, Celeste AJ (2006) Bone morphogenetic proteins and growth differentiation factors as drug targets in cardiovascular and metabolic disease. Drug Discov Today 11(9-10):405–411. https://doi.org/10.1016/j.drudis.2006.03.016.S1359-6446(06)00060-2 [pii]
26. Gonen N, Quinn A, O'Neill HC, Koopman P, Lovell-Badge R (2017) Normal levels of Sox9 expression in the developing mouse testis depend on the TES/TESCO enhancer, but this does not act alone. PLoS Genet 13(1):e1006520. https://doi.org/10.1371/journal.pgen.1006520
27. Guo Y, Hai Y, Yao C, Chen Z, Hou J, Li Z, He Z (2015) Long-term culture and significant expansion of human Sertoli cells whilst maintaining stable global phenotype and AKT and SMAD1/5 activation. Cell Commun Signal 13:20. https://doi.org/10.1186/s12964-015-0101-2
28. Castrillon DH, Quade BJ, Wang TY, Quigley C, Crum CP (2000) The human VASA gene is specifically expressed in the germ cell lineage. Proc Natl Acad Sci U S A 97(17):9585–9590. https://doi.org/10.1073/pnas.160274797
29. He Z, Jiang J, Hofmann MC, Dym M (2007) Gfra1 silencing in mouse spermatogonial stem cells results in their differentiation via the inactivation of RET tyrosine kinase. Biol Reprod 77(4):723–733. https://doi.org/10.1095/biolreprod.107.062513
30. He Z, Kokkinaki M, Jiang J, Zeng W, Dobrinski I, Dym M (2012) Isolation of human male germ-line stem cells using enzymatic digestion and magnetic-activated cell sorting. Methods Mol Biol 825:45–57. https://doi.org/10.1007/978-1-61779-436-0_4

Chapter 15

Testicular Cell Selective Ablation Using Diphtheria Toxin Receptor Transgenic Mice

Diane Rebourcet, Annalucia Darbey, Michael Curley, Peter O'Shaughnessy, and Lee B. Smith

Abstract

Testis development and function is regulated by intricate cell-cell cross talk. Characterization of the mechanisms underpinning this has been derived through a wide variety of approaches including pharmacological manipulation, transgenics, and cell-specific ablation of populations. The removal of all or a proportion of a specific cell type has been achieved through a variety of approaches. In this paper, we detail a combined transgenic and pharmacological approach to ablate the Sertoli or germ cell populations using diphtheria toxin in mice. We describe the key steps in generation, validation, and use of the models and also describe the caveats and cautions necessary. We also provide a detailed description of the methodology applied to characterize testis development and function in models of postnatal Sertoli or germ cell ablation.

Key words Cre/lox, Transgenic, Diphtheria, Sertoli cells, Testis, Mouse

1 Introduction

Testis development and function is regulated by intricate cell-cell cross talk and through communications along the hypothalamo-pituitary-gonad axis. Elucidation of the mechanisms underpinning these processes has been derived through a wide variety of approaches including both systemic pharmacological treatments to block specific functions and more recently the development of transgenic and knockout mouse models to examine the role of specific genes in specific cell types [1, 2].

Another approach that has been widely and successfully utilized to examine testis development and function is induced cell ablation, that is, completely or partially removing a cell type from the testis, with a view to determining the multiple roles that particular cell type plays. In testis biology, cell ablation has been a powerful technique to elucidate testis development and function. For example, the cytotoxic chemotherapeutic drug busulfan has been widely used as a method to remove germ cells in

Marco G. Alves and Pedro F. Oliveira (eds.), *Sertoli Cells: Methods and Protocols*, Methods in Molecular Biology, vol. 1748, https://doi.org/10.1007/978-1-4939-7698-0_15,

transplantation studies [3, 4]. The use of other cytotoxins such as ethane dimethane sulfonate (EDS) to specifically ablate Leydig cells and liposome-entrapped dichloromethylene diphosphonate to remove macrophages is also well described in the literature and reviewed in [5]. Together these cell ablation approaches have provided major insights into (1) the development and origin of the adult Leydig population [6, 7], (2) the regulation of steroidogenesis by Leydig cell-macrophage interactions [8, 9] and (3) the influence of germ cells on other cell types in the testis [10].

Another approach that has been exploited in the testis more recently is the use of the potently cytotoxic diphtheria toxin (DTX). This was first used in targeted chemotherapy in the 1970s, where the toxin was coupled to an antibody raised against a specific antigen of the mumps virus [11]. In the past decade, this approach to induce cell death has been refined using the Cre/loxP system giving rise to two different models. Upon Cre recombinase-mediated activation, the first model (which we call DTA) expresses the catalytic unit of the DTX, the A subunit (DTA) [12], within target cells, triggering apoptosis. The cell-specificity is determined by the localization of Cre expression. The second model (which we call DTR) is based on the observation that mice are naturally resistant to diphtheria toxin [13]. This means that transgenically introducing the human or simian receptor for DTX (HB-EGF receptor) [14, 15] will render cells in the mice expressing the receptor sensitive to DTX, and cell death will occur upon injection/delivery of the toxin, at a time of the researcher's choosing. The natural resistance of the mouse to DTX also means that other cells are unaffected. In combination, the two models permit the induction of cell death directly in utero (DTA) (because DTX does not cross the placenta) and at any time in postnatal life (DTR + DTX injection).

We recently initiated a study to determine whether Sertoli cells, besides their well-described importance in testis differentiation and spermatogenesis, had further roles in testis biology. Conscious that no model of acute ablation specific to postnatal Sertoli cells existed, we combined Sertoli cell-specific recombinase Cre, Amh-Cre, or germ cell-specific Stra8-Cre, with the DTR model to specifically ablate Sertoli cells or germ cells, respectively, at key stages of postnatal life. In the present chapter, we provide a detailed description of the methodology developed and applied to generate and characterize models of postnatal Sertoli or germ cell ablation and which has led to a major reassessment of Sertoli cell functions [16, 17].

2 Materials

2.1 Validation of the Cre Lines

Mice were housed and bred under standard conditions of care. Experiments passed local ethical review and were conducted with licensed permission under the UK Animal Scientific Procedures Act (1986) (Home Office license number PPL 60/4200).

2.1.1 Mouse Lines

1. Amh-Cre animals [18].
2. Stra8-Cre animals [19].
3. Reporter lines: R26R-EYFP line [20], tdTomato line [21].
4. HB-EGF (DTR) line [14].

2.1.2 Genotyping

1. Genomic DNA extraction: Tris EDTA (TE) Tween buffer (fresh), proteinase K (10 mg/ml), filter disc 0.2 μM.
2. PCR reagents: BioMix, sterile water, primers (Table 1), thermocycler, QIAxcel reagents, capillary electrophoresis QIAxcel device.

2.1.3 Assessment of the Reporter Expression Using Epifluorescence

1. Gross morphology analysis: Cold phosphate buffered saline 1× (PBS), Leica MZFLIII fluorescence stereomicroscope with YFP/GFP/RFP filter system linked to CoolSNAP camera.

2.1.4 Assessment of Reporter Expression Using Immunohistochemistry Techniques

1. Fixation and embedding: Bouin's fixative, alcohol, xylene, paraffin, resin, microtome, charged slides, coverslips.
2. Histology: Xylene, histology glassware, alcohol, hematoxylin, acid alcohol; 1% concentrated hydrochloric acid in 70% alcohol, Scott water, eosin, mounting media Pertex.
3. Immunohistochemistry/immunofluorescence: Xylene, gradient of alcohol (absolute alcohol to 75%), citrate buffer, pressure cooker, hydrogen peroxide, Tris buffered saline (TBS), normal serum, primary and secondary antibodies [16, 17, 22], streptavidin biotin, chromogen diaminobenzidine (DAB), fluorophore-tagged Tyramide amplification system, SYTOX green, aqueous media Permafluor, Provis microscope, LSM 710 confocal microscope.
4. Software: Adobe package, GraphPad Prism, Minitab.

2.2 Cell-Specific Ablation Transgenic Model

2.2.1 Diphtheria Toxin (DTX) Preparation and Injection

1. Handling and preparation of DTX: Gloves, face masks, hood, DTX, sterile water.
2. Intratesticular injection of DTX: Anesthetic rig with anesthetic chamber allowing unrestricted movement, small face mask anesthetic system for rodents, anesthetic (isoflurane), warming pad, alcohol, sterile surgical tools, sterile sutures, analgesic (buprenorphine 0.05 mg/kg).

2.2.2 Assessment and Validation of the Cell-Specific Ablation Model

1. Gross analysis and collection of the transgenic animals: Microbalance, electronic digital calipers, dissection tools, alcohol, Bouin's fixative, dry ice.
2. Histological analysis of the phenotype (*see* Subheading 2.1.4 for materials).
3. Stereological analysis of the phenotype (*see* Subheading 2.1.4 for materials).

Table 1

Primers used for genotyping and qRT-PCR

Gene symbol	Primers 5′-3′
HB-EGF (DTR) mutant HB-EGF (DTR) common HB-EGF (DTR) wild type	cat caa gga aac cct gga cta ctg aaa gtc gct ctg agt tgt tat gga gcg gga gaa atg gat atg
Stra8-Cre	gtg caa gct gaa caa cag ga agg gac aca gca ttg gag tc
Amh-Cre	cac atc agg ccc agc tct at gtg tac agg atc ggc tct gc
YFP WT	gga gcg gga gaa atg gat atg aaa gtc gct ctg agt tgt tat
YFP mut	aag acc gcg aag agt ttg tc
tdTomato WT	aag gga gct gca gtg gag ta ccg aaa atc tgt ggg aag tc
tdTomato Ai14 mut	ctg ttc ctg tac ggc atg g ggc att aaa gca gcg tat cc
Fshr	ggc cag gtc aac ata ccg ctt g tgc ctt gaa ata gac ttg ttg caa att g
Wt1	gct cca gct cag tga aat gga cag aa ggc cac tcc aga tac acg ccg
Cnn1	caa gct ggc cca gaa ata cga cc tct tca cag aac ccg gct gca g
Myh11	ctg cac aac ctg agg gag cga tac t aat ggc ata gat gtg agg cgg c
Mc2r	att agt gac aaa gcc aag gag agg agc a ggg tgg tgt ttg ccg ttg act tac
Sult1e1	tgt tga aat gtt ctt ggc aag gcc cat cct cct tgc att ttt cca cat ca
Cyp11a1	cac aga cgc atc aag cag caa aa gca ttg atg aac cgc tgg gc
Stra8	gaa ggt gcat ggt tca ccg tgg gct cga tgg cgg gcc tgt g

(continued)

Table 1
(continued)

Gene symbol	Primers 5′-3′
Sog1	gag cca gaa cgg aac ccg ga
	gac atc ggg ctg ggt cct cc
Tp1	ggc gat gat gca agt cgc aa
	cca ctc tga tag gat ctt tgg ctt ttg g
Tnfa	ccc aga ccc tca cac tca gat catc
	cca cta gtt ggt tgt ctt tga gat cca tg
Dkkl1	gag cca gaa cgg aac ccg ga
	gac atc ggg ctg ggt cct cc
Dhh	aga aca gcg gcg cag acc g
	gcc ttc gta gtg gag tga atc ctg tg
Ptm2	ggc ggc atc gca gag gct gc
	cac atg atg ttg ctt ggg cag gt
Cd31	caa agt gga atc aaa ccg tat ctc caa a
	tga agt tgg cta cag gtg tgc cc
Cdh5	tcc cca gat aga cac ccc caa ca
	gca cat act tag cat tct ggc ggt tc
Hsd3b1	cct cct aag ggt tac cct ata tca tac cag ct
	gtc tcc ttc caa cac tgt cac ctt gg

4. Blood-testis barrier analysis: Tight junction functional biotin tracer and biotin assay EZ (*see* Subheading 2.1.4 for materials).
5. Molecular analysis of the phenotype: RNA extraction kit, NanoDrop 1000 spectrophotometer, SuperScript® VILO™ cDNA Synthesis Kit Luciferase mRNA SYBR master mix, primers designed using Primer Express 2.0 (Table 1).
6. Hormonal analysis: Heparin, 1 ml syringes: and 23G 0.6 × 25 mm needles, ELISA Kits (FSH, LH, T), microplate spectrophotometer reader.

3 Methods

3.1 Validation of the Cre Models

Genetically targeting/deleting a specific cell population is dependent upon the site of Cre recombinase expression as it is the Cre activity within cells that will activate DTR expression and thus render cells sensitive to DTX. Consequently, prior to any in-depth analysis,

careful evaluation of the spatial and temporal expression of the Cre line to be used is necessary to identify all sites of Cre expression and thus possibilities for unwanted off-target effects [2]. This is essential in the case of planned DTX-mediated cell ablation studies, where accidental induction of cell death in other essential body systems could lead to unintended sickness or even death of experimental animals. Our study aimed at determining whether Sertoli cells had other roles in testis development and function besides orchestrating testis differentiation and spermatogenesis [23, 24] using a well characterized and established Sertoli cell-specific mouse line the Amh-Cre line [18]. As we predicted that loss of Sertoli cells would also lead to loss of germ cells, in parallel we also used a Stra8-Cre line [19] which selectively and exclusively targets germ cells from 3 dpn (day postnatal). To confirm the cell-specific nature of the Cre expression, we bred hemizygous males from these Cre lines to homozygous females carrying a lineage-tracing reporter transgene (R26R-EYFP, tdTomato) [20, 21] which allowed us to track Cre expression through identification of daughter cells expressing YFP or RFP. This breeding strategy also controlled for any incidence of random induction of YFP or RFP expression, as 50% of offspring did not inherit the Cre transgene.

To generate our experimental models, we then bred hemizygous males from the Amh-Cre or Stra8-Cre line to females hemizygous for the HB-EGF (DTR) transgene, to obtain offspring with the four genotypes, Amh-Cre+/−;DTR−/−, Amh-Cre−/−;DTR−/−, Amh-Cre−/−;DTR+/−, and Amh-Cre+/−;DTR+/−, and following a single subcutaneous injection of vehicle (water) or DTX (100 ng), we were able to use them to assess (1) induction of DTR expression by Cre recombinase, (2) the cell-type specificity of the targeting, (3) the toxicity of the toxin in nontarget tissues (potential off-target induction of cell death), and (4) whether Cre recombinase expression alone leads to a phenotype, as described below.

3.1.1 Breeding to a Reporter Line

1. Mate a hemizygous Cre (Amh-Cre+/− or Stra8-Cre+/−) adult male (>50 dpn) with a homozygous female R26R-EYFP+/+ or tdTomato. To maximize the matings, use at least two females per male.
2. The Mendelian ratio of transgene segregation from this breeding will result in half of the litter being Cre+/−;YFP+/− and the other half Cre−/−;YFP+/−. Verify the genotype of the offspring by PCR using specific primers (Table 1). The protocol for genotyping is described in Subheading 3.1.2 (*see* **Note 1**). As only one copy of the reporter is required for lineage tracing, no additional breeding for further generations is necessary.

3.1.2 Genotyping

1. Mouse genotyping can be undertaken from any tissue, but either ear clip or tail genomic DNA is normally used (*see* **Note 1**).
2. Genomic DNA is prepared using Tris EDTA (TE) Tween buffer made fresh. In a sterile 50 ml Falcon tube, add 2.5 ml of 1 M Tris (pH 8.0), 100 μl of 0.5 M EDTA (pH 8.0), and 250 μl of Tween, and fill-up to 50 ml with dH20. Filter-sterilize the mixed solution with a tube top filter disc (0.2 μm) into a fresh sterile 50 ml Falcon tube.
3. For single ear clips, add 25 μl of TE Tween supplemented with 2 μl proteinase K (10 mg/ml) per ear clip.
4. For tail tips (~3 mm in length): Add 50 μl of TE Tween plus 4 μl proteinase K per tail clip, into 0.2 ml PCR tubes.
5. Incubate tissues at 55 °C for 1 h in a PCR machine (heated lid prevents evaporation) and then at 95 °C for 7 min (to destroy enzymatic function), and cool to room temperature (RT).
6. Vortex tubes to finalize disruption of the tissue.
7. Centrifuge briefly to pulse down the pellet of undigested tissue.
8. In a new 0.5 ml tube, add 90 μl of sterile water, and add 10 μl of the supernatant from 7.
9. Keep at 4 °C for short-term (2–3 days) storage and at −20 °C for longer-term storage.
10. Perform PCR on DNA sample. Prepare a mix with 5 μl of BioMix and 0.1 μl of each primer (20 μM) (Table 1), and make up to 9 μl with sterile water. Add 1 μl of DNA sample and amplify by PCR.
11. Amplified products are separated and visualized on a capillary electrophoresis QIAxcel device. Alternatively, products can be visualized on a 1% agarose gel [16].

3.1.3 Assessment of Reporter Expression Using Epifluorescence: Collection and Tissue Preparation

1. Cull animals at different time points (neonatal, prepubertal, and adulthood) according to the age of interest for the study.
2. Dissect out reproductive organs (testes/ovary, epididymis/uterus, seminal vesicle, prostate), endocrine-related tissues (pituitary, adrenal …), and extra nonreproductive tissues (heart, liver, brain …).
3. Place the collected tissues in cold sterile PBS 1× on ice.
4. Under an epifluorescent dissecting microscope, assess the YFP or RFP fluorescence from each tissue and capture images. Under certain circumstances, some tissues can autofluoresce, especially under high laser power. It is therefore essential that YFP or RFP expressing samples (from Cre+/−;YFP+/− or Cre+/−;RFP+/− animals) are imaged next to control samples (from Cre−/−;YFP+/− or Cre−/−;RFP+/− animals). Both

bright field and fluorescent images should be taken of the same samples in the same position to aid orientation of the viewer in subsequent analysis/publications (Fig. 1a, b).

5. Fix tissues in Bouin's fixative for 6 h (maximum up to 24 h, longer fixations are likely to affect any subsequent immunohistochemistry studies), and then move the tissue into 70% alcohol until processed for embedding (*see* **Notes 2** and **3**).
6. Embed tissue in paraffin.
7. Using a microtome, cut 5 μm section, and bind the section onto a charged slide (charging promotes tissue adhesion).

3.1.4 Assessment of Reporter Expression Using Immunofluorescence

1. Dewax slides of interest under the hood, by incubating in two successive washes of xylene contained in histology glass troughs for 5–10 min. Drain excess xylene.
2. Rehydrate slides through alcohol washes (going from absolute alcohol to 70% alcohol, each for 20 s incubation), and rinse in tap water. Do not let slides dry at any stage of **steps 1** and **2**.
3. Using a pressure cooker, perform a heat-induced epitope retrieval in citrate buffer (*see* **Note 4**).

   0.1 M Citrate buffer 10× stock: add 84.04 g citric acid (monohydrate), and dissolve in 3.5 l of deionized water. Adjust the solution pH to 6 at RT, and add distilled water to a final volume of 4 l.
4. Cool slides under running tap water.
5. Block the endogenous peroxidase by incubating slides in 3% v/v hydrogen peroxide in 1× TBS for 30 min on a rocker at RT.

   Stock solution 20×: add 48 g of Tris HCl (formula weight 157.6 g), add 11.2 g Tris base (formula weight 121.1 g), and add 176 g NaCl (formula weight 58.4 g). Dissolve in 900 ml distilled water. Adjust the pH of the solution at 7.6 at RT, and add distilled water to a final volume of 1 l.

   Working solution 1× TBS: dilute the stock solution 20 times.
6. Wash the slides in three successive 1× TBS washes for 5 min each on a rocker at RT.
7. Place slides in a humid chamber, and block the non-specific IgG sites to reduce background staining by incubating sections for 30 min at RT in 10% normal goat serum diluted in 1× TBS and 1% BSA (*see* **Note 5**).
8. Remove the serum from the sections; add the primary antibody, rabbit-raised anti-YFP or rabbit-raised anti-tRFP, in normal goat serum; and incubate overnight at 4 °C in a humid chamber. Include a negative control where the primary solution is replaced by serum alone (*see* **Note 6**).
9. Rinse in three successive washes of 1× TBS for 5 min each on a rocker at RT.

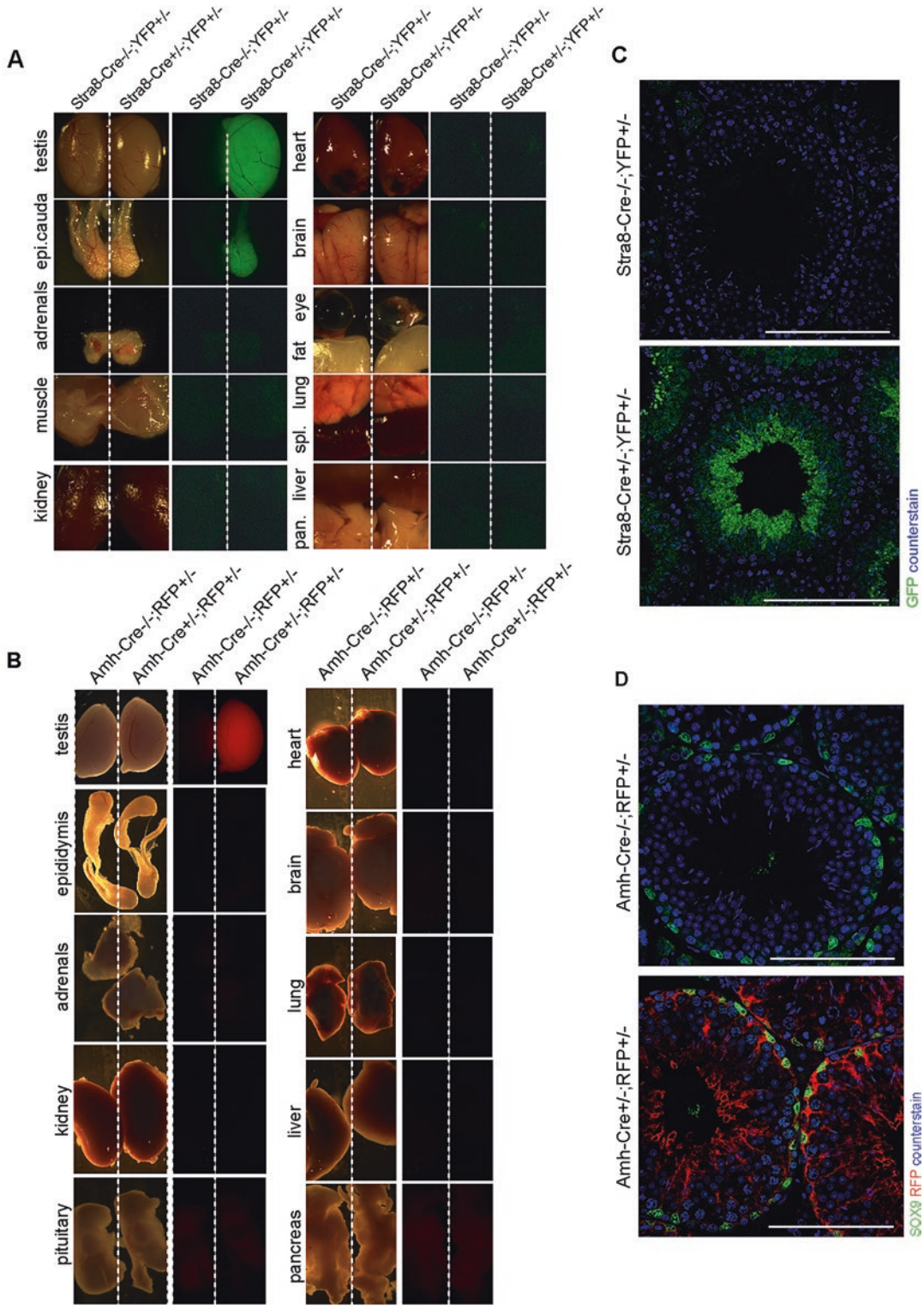

Fig. 1 Localization of the Cre recombinase expression. Assessment of the Cre localization by fluorescence using a YFP or RFP filter shows expression of (**a**) Stra8-Cre specially in testis and cauda epididymis in Stra8-Cre+/–; YFP+/– males and absence in Stra8-Cre–/–; YFP+/– animals and (**b**) in testis only in Amh-Cre+/–; YFP+/– males. Immunolocalization of the Cre by assessing the reporter expression (green or red) is confined (**c**) to germ cells in the testis for the Stra8-Cre+/–; YFP+/– (scale bar: 100 μm) and (**d**) to Sertoli cells in the testis for the Amh-Cre+/–; YFP+/– when compared to SOX9 staining (scale bar, 100 μm). Epi, epididymis; spl, spleen; and pan, pancreas

10. Incubate all sections with the secondary antibody (goat-raised anti-rabbit coupled to peroxidase) in normal goat serum for 30 min at RT in a humid chamber.
11. Rinse in three successive washes of 1× TBS for 5 min each on a rocker at RT.
12. Incubate sections with Tyramide diluted 1/50 in buffer for 10 min at RT in a humid chamber as per manufacturer's instructions (*see* **Note 7**).
13. Rinse in three successive washes of 1× TBS for 5 min each on a rocker at RT protected from the light.
14. Incubate sections with SYTOX green diluted 1/1000 for 10 min at RT in a humid chamber.
15. Rinse in three successive washes of 1× TBS for 5 min each on a rocker at RT protected from the light.
16. Mount with aqueous media and coverslip the slides with caution.
17. Protect the slides from light in cardboard slide holder in tinfoil or in an opaque slide box, and store at 4 °C until images are captured on a confocal microscope (Fig. 1c, d).

3.2 Setting-Up and Validating the Cell-Specific Ablation Model

3.2.1 Breeding Strategies

1. Mate heterozygous Cre (Amh-Cre+/− or Stra8-Cre+/−) animals (male or female) with heterozygous DTR+/− animals (female or male).
2. Verify the genotype of the offspring as described in Subheading 3.1.2. Offspring Cre+/−;DTR+/, Cre−/−;DTR+/, Cre+/−;DTR−/−, and Cre−/−;DTR−/− are obtained from the initial breeding pairs and will be used for initial validation of the experiment: refer to Subheading 3.3 (*see* **Note 8**).
3. For the Amh-Cre; DTR line only, set up breeding pairs to obtain a colony of homozygous animal for both the Amh-Cre and the DTR allele (*see* **Note 9**). *Warning*: As the Stra8-Cre transgene is expressed in germ cells, we did not breed a second generation, in order to avoid inducing ubiquitous DTR expression.

3.2.2 Genotyping

See Subheading 3.1.2.

3.2.3 Assessment of the Expression of the Receptor DTR

1. Collect tissues (reproductive organs and nonreproductive organs) from superfluous males Amh-Cre+/−; DTR+/− and Amh-Cre; DTR+/− (postnatal age).
2. Fix in Bouin's fixative for 6 h, and then place in 70% alcohol until processed for embedding. Process samples as described in Subheading 3.1.3, **step 6** onward.
3. Dewax and rehydrate slides of interest. Antigen retrieved, inactivate the endogenous peroxidase, and block the non-specific

sites in 10% normal goat serum as described in Subheading 3.1.4, **steps 1–8**.

4. Remove the serum from the sections, add the primary antibody (mouse-raised anti-HB-EGF, [16]) diluted 1/50 in normal goat serum, and incubate overnight at 4 °C in a humid chamber. Include a negative control where the primary antibody solution is replaced by serum.
5. Rinse in three successive washes of 1× TBS for 5 min each on a rocker at RT.
6. Incubate all sections with a secondary antibody (goat-raised anti-mouse biotinylated) diluted 1/500 in normal goat serum, and incubate for 30 min at RT in a humid chamber.
7. Rinse in three successive washes of 1× TBS for 5 min each on a rocker at RT.
8. Incubate sections with horseradish peroxidase-conjugated streptavidin, a biotin-binding protein, diluted 1/1000 in 1× TBS for 30 min at RT in a humid chamber.
9. Rinse in three successive washes of 1× TBS for 5 min each on a rocker at RT.
10. Incubate sections with DAB. Following the manufacturer's instructions, add one drop of concentrate per ml of reaction buffer, and incubate for 1–5 min while carefully monitoring the intensity of brown staining and background under the microscope.
11. Rinse in running water for 5 min to stop the reaction.
12. Counterstain in hematoxylin (purple nuclear stain) for 30 s, and rinse in running water.
13. Dip the slides quickly once or twice into acid-alcohol solution to remove excess dye from tissues and to define the nuclei, and then rinse in running tap water.
14. If running tap water is soft (low in minerals), incubate slides for 10–20 s in a blueing solution Scott's water, and rinse in tap water. Drain any water excess.
15. Dehydrate slides in subsequent washes of increasing concentration of alcohol (from 70% alcohol to absolute alcohol) each for 20 s incubation, and rinse in tap water. Do not let slides dry during **steps 15** and **16**.
16. Incubate in two successive washes of xylene for 5 min each.
17. Mount in Pertex and coverslip the slides with caution, avoiding any bubbles.
18. After drying the slides, capture pictures on a light microscope as detailed in [16].

3.3 Validation of the Model: Assessment of the Toxicity of the Toxin

3.3.1 Preparation of the Toxin (See Note 10)

1. Stock solution (solution A): 2 mg of diphtheria toxin is reconstituted in 1 ml of sterile water and aliquoted into 50 µl stock samples.
2. Storage solution (solution B): dilute stock solution A to obtain a 20 µg/ml solution, aliquot into 100 µl samples, and store at −80 °C until needed.
3. Working solution: DTX is quite unstable and should be prepared on the day of the experiment. Add 900 µl of sterile water to 100 µl of solution B to obtain a 2 ng/µl solution (solution C).
4. Injection dose: inject animals subcutaneously with 100 ng of DTX (50 µl of solution C). This dose is sufficient to ablate all Sertoli cells in both neonate and adult animals without inducing side effects. The injection dose can be diluted further for induction of partial ablation (removal of just a proportion of the target cell population).

3.3.2 Assessment of the Toxicity Following Injection of DTX

1. To verify the toxicity and the specificity of the model, select neonatal (2 dpn) and adult males (50 dpn) Amh-Cre+/−;DTR+/−, Amh-Cre−/−;DTR+/−, Amh-Cre+/−;DTR−/−, and Amh-Cre−/−;DTR−/− originating from the first generation of breeding.
2. Inject subcutaneously with 100 ng/50 µl DTX.
3. Dissect animals 1 day, 3–7 days, and 30 days later. Collect reproductive and nonreproductive tissue including the heart and liver (known target organs of the toxin) (*see* **Note 11**).
4. Fix tissue in Bouin's fixative for 6 h and process as described in Subheading 3.2.1.

3.3.3 Assessment of the Tissue by Histopathology Following Injection of DTX

Hematoxylin-eosin (HE) staining is commonly used to assess tissue morphology [25]. Bouin's fixation helps retain the cells' nuclear morphology and maintains the architecture of the seminiferous tubules. Combined with HE staining, which stains nuclei blue (hematoxylin) and cytoplasm pink (eosin), testis composition and cell organization can be quickly assessed.

1. Process slides of interest as described in Subheading 3.2.3, **steps 12–14**.
2. Incubate sections in eosin solution for 10–30 s.
3. Rinse in running water for 5 min.
4. Dehydrate slides and mount as described in Subheading 3.2.3, **step 15**.
5. After drying the slides, capture pictures on a light microscope to assess the histopathology as demonstrated in [16, 17].

3.3.4 Assessment of the Specificity of the Targeting Following Injection of DTX

1. Assess apoptosis by immunohistochemistry using cleaved caspase 3, and co-stain for specific Sertoli cells and germ cell markers (*see* Subheadings 3.2.1 and 3.2.2) (Fig. 2).

3.4 Characterization of Total Sertoli Cell Ablation: Characterizing the Model

We confirmed that treatment of WT animals (Amh-Cre−/−; DTR+/−, Amh-Cre+/−;DTR−/− and Amh-Cre−/−;DTR−/−) with 100 ng of DTX had no impact on testis nor on nonreproductive organs and that the ablation in Amh-Cre+/−;DTR+/− animals was specific to Sertoli cells. In order to reduce animal numbers, we bred the line to a fixed double homozygous colony (Amh-Cre+/+;DTR+/+), which could be treated with either vehicle or with DTX (*see* Subheading 3.1.1). To cover different aspects of testis development and function, we targeted Sertoli cells at different time points throughout testis development: 2 dpn (neonatal), 18 dpn (prepubertal), and 50 dpn (adult) (Fig. 3). To be able to distinguish between phenotypic effects due to Sertoli cell ablation from germ cell ablation, we also added a cohort of animals where only germ cells were ablated (Stra8-Cre;DTR+/− or WT animals treated with busulfan) [16, 17, 22]. When ablating an entire population, we anticipated that the impacts on the morphology and composition of the organ would be significant. The first step in examination of the phenotype was qualitative and focused on

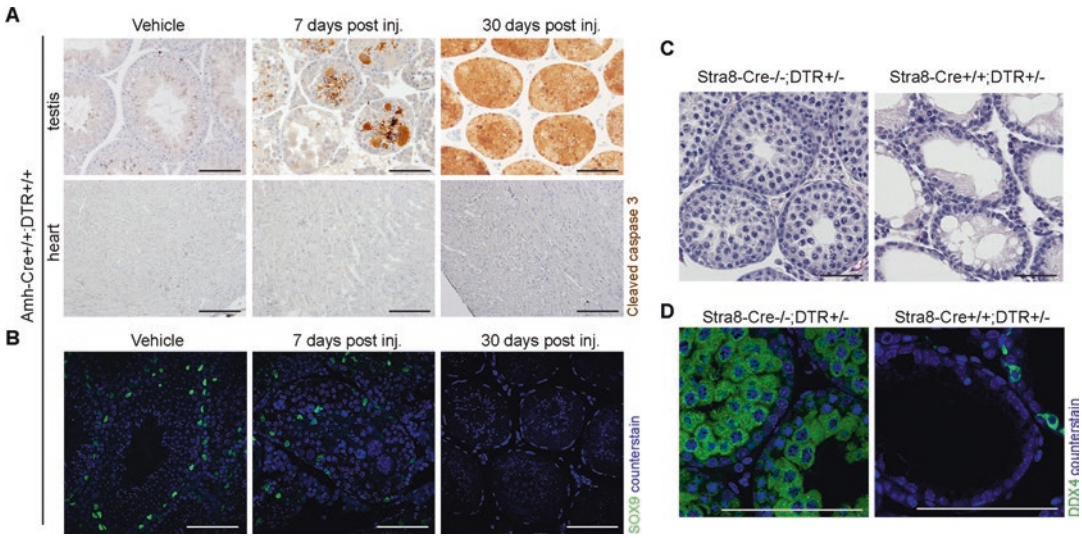

Fig. 2 Assessment of the DTX-induced apoptosis. (**a**) Immunolocalization of cleaved caspase 3 following DTX injection in adulthood shows that apoptosis is restricted to Sertoli cells, whereas no staining is observed in the heart confirming the absence of off-target effects. (**b**) SOX9 expression is reduced 7 days after Sertoli cell ablation and completely absent 30 days later confirming the specificity of the DTX targeting (scale bar, 100 μm). (**c**) Testicular histology using hematoxylin-eosin staining shows Sertoli cells only in tubules following germ cell ablation (scale bar, 100 μm). (**d**) Immunolocalization of DDX4 confirms the specific depletion of germ cells (scale bar, 100 μm)

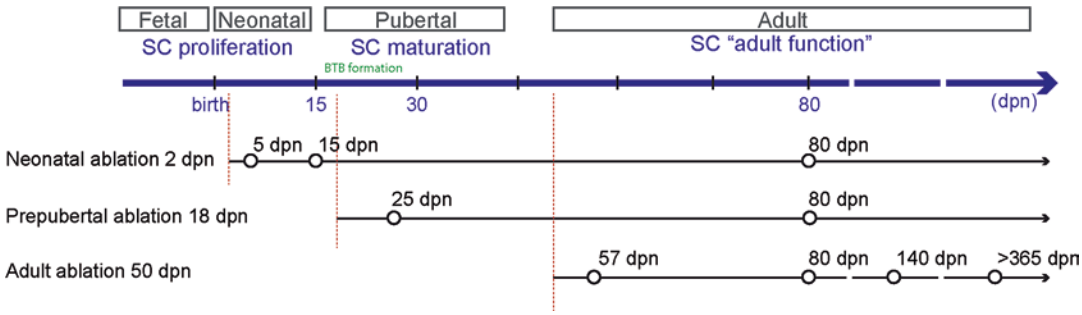

Fig. 3 Schematic representation of the total Sertoli cell ablation study. The study end points are shown as circles at different times after DTX injection

morphological analysis using histology approaches. However, because changes in testis size, shape, and cellular content may be challenging to assess, the qualitative analysis should be supported by quantitative analysis (stereological cell counting) based either on cell morphology or using specific markers to identify the cell type [26, 27].

3.4.1 Assessment of Neonatal, Prepubertal, and Adult Sertoli Cell Ablation: Gross Morphological Analysis

1. Inject mice subcutaneously with 100 ng/50 μl to induce total ablation (or <10 ng/50 μl for partial ablation). Treat at ages 2 dpn, 18 dpn, and 50 dpn (cf. Subheading 3.6).
2. Collect animals at different time points following injection (1, 7, 15, 23, 50 days … post injection) and in adulthood.
3. Prior to culling the animals, coat syringes and needles with heparin.
4. Collect blood by cardiac puncture with the coated syringes, and centrifuge the blood samples at full speed (17,000 rcf) for 10 min at 4 °C.
5. Collect the sera into a new tube, and freeze at −80 °C until further analysis (cf. Subheading 3.4.6).
6. Dissect out the reproductive system (including seminal vesicle, prostate, testes, epididymis, and bladder), and assess the gross morphology of the reproductive system (*see* **Note 12**). Weigh the seminal vesicles (pair) and the testes (individual) (*see* **Note 13**). Also collect nonreproductive tissues including the heart and liver for further assessment by histopathology.
7. Fix a piece of tissue in Bouin's fixative for 6 h, and freeze another piece of tissue for molecular analysis.

3.4.2 Assessment of Neonatal, Prepubertal, and Adulthood Sertoli Cell Ablation: Histological Analysis

First, we analyzed the histology of testis and the content of epididymis (in adult animals) following Sertoli cell ablation. We noticed that the impact of Sertoli cell ablation on testis histology differed according to the time point of injection as summarized in

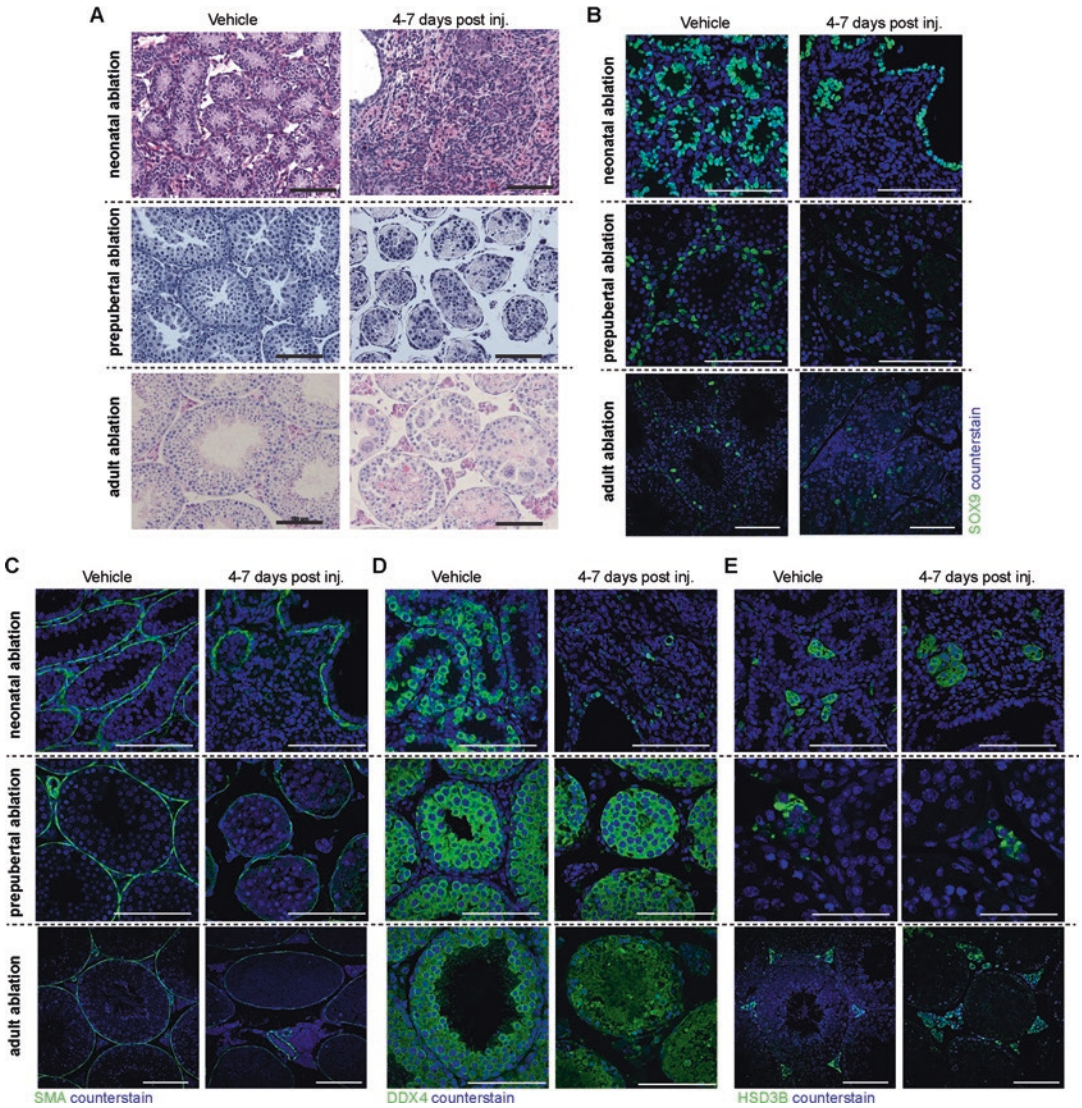

Fig. 4 Effect of total Sertoli cell ablation on the testis—example of a typical analysis. (**a**) Testicular histology using hematoxylin-eosin staining shows impact on testis architecture and seminiferous tubules composition 7 days after neonatal or prepubertal or adult Sertoli cell ablation. Note the difference of severity relating to the endpoint of ablation. Immunolocalization of (**b**) SOX9, (**c**) SMA, (**d**) DDX4, and (**e**) HSD3B confirms the depletion of Sertoli cells and shows impact on the other testicular cell types (scale bar, 100 μm)

[16, 17]. The preliminary observations were further characterized using specific markers by immunohistochemistry.

1. Following fixation and processing of the tissue (*see* Subheading 3.2.1), assess the histology of each tissue using HE staining (*see* Subheading 3.3.3) (Fig. 4a, b).
2. Undertake analysis for apoptosis (cleaved caspase 3 staining) and for Sertoli cell markers (cf. Subheading 3.3.4).

3.4.3 Assessment of Neonatal, Prepubertal, and Adult Sertoli Cell Ablation: Immunohistochemistry Analysis

To examine the status (development and function) of each of the cell type in more detail, we used specific markers for each cell type: Leydig cells, peritubular myoid cells, blood vessels, and immune cells by immunohistofluorescence/fluorescence:

1. Proceed as described in Subheading 3.1.4 (Fig. 4c–e).

3.4.4 Assessment of Neonatal, Prepubertal, and Adult Sertoli Cell Ablation: Cell Numerical Density, Volume Analysis

1. Following fixation, testis from at least six animals for each endpoint and treatment is embedded in resin.
2. Cut 20 μm sections using a motorized microtome, *see* Subheading 3.2.1.
3. Stain with HE.
4. Estimate the total testis volume using the Cavalieri's principle [28]. The slides used to estimate the number of cells are also used to estimate testis volume.
5. The optical dissector technique [29] is used to count the number of Leydig cells and Sertoli cells in each testis based on their morphology. Leydig cells are identified by their position within the interstitial tissue, by their round nuclei and prominent nucleoli, and, normally, by the presence of abundant cytoplasm and Sertoli cells by the tripartite nucleoli and nuclear shape [30, 31].
6. The numerical density of the Leydig cells is estimated using an Olympus BX50 microscope fitted with a motorized stage and Stereologer software.

3.4.5 Assessment of Neonatal, Prepubertal, and Adulthood Sertoli Cell Ablation: Gene Expression Analysis

To complete the analysis of the development status and function of each testicular cell type, we also analyzed mRNA transcript levels of specific markers for Sertoli cells, Leydig cells, PTM cells, immune cells, and blood vessels by qPCR (Table 1):

1. Extract testis RNA using a tissue disrupter and TRIzol following manufacturer's instructions.
2. Add luciferase mRNA (5 ng) as an external standard to each sample at the start of the RNA extraction procedure [32] (*see* **Note 14**).
3. Reverse transcribe isolated RNA using random hexamers and Moloney murine leukemia virus reverse transcriptase.
4. For real-time PCR, mix SYBR master mix with primer (100 nM) and template in a total volume of 10 μl, and amplify with an Agilent MX3000 cycler. All primers were designed by Primer Express 2.0 [33] and are shown in Table 1.

3.4.6 Assessment of Neonatal, Prepubertal, and Adult Sertoli Cell Ablation: Hormone Profile

Testis endocrine function and spermatogenesis are regulated by the hypothalamic-pituitary-gonad axis [34]. The hypothalamus through pulsatile secretion of gonadotrophin-releasing hormone (GnRH) stimulates release of luteinizing hormone (LH) and follicle-stimulating hormone (FSH) by the pituitary, and each

hormone has a specific action on the gonad [35–40], and this hormonal interplay is controlled by feedback regulations, where testosterone and inhibin negatively regulate gonadotrophin secretion, which also means that changes in hormonal profile could stem from hypothalamic/pituitary or gonadal defects. The first step of the hormonal profile was to analyze FSH-circulating levels to confirm our model and later to establish circulating LH and androgen status in basal and stimulated conditions.

1. Following blood collection, sera were separated and stored at −20 °C until measured (*see* Subheading 3.2.1).
2. Serum testosterone was measured using a Mouse testosterone commercial kit under basal condition or after human chorionic gonadotropin (hCG) stimulation (*see* **Note 15**).
3. Serum LH and FSH were measured using a Mouse LH and FSH commercial kit following manufacturer's instructions.
4. ELISA plates are assessed on a multi-wave length microplate spectrophotometer to read the optical density (*see* **Note 16**).

3.4.7 Assessment of Neonatal, Prepubertal, and Adult Sertoli Cell Ablation: Blood-Testis Barrier Function Analysis

At puberty during their maturation phase, Sertoli cells undergo fundamental changes which include the formation of inter-Sertoli cell junctional complexes to create the blood-testis barrier (BTB) [41, 42]. The barrier is crucial to spermatogenesis as it inhibits immune cell infiltration into the adluminal compartment of the seminiferous tubules and creates a unique environment for germ cell meiosis. We wanted to determine the contribution of PTM cells to the BTB and therefore undertook analysis of biotin infiltration through the BTB following biotin injection.

1. Prepare on the day of use a biotin solution (10 mg/ml) in a freshly made solution of 1× PBS containing $MgCl_2$ (10 mM).
2. Collect adult males and dissect out the testes. Place the testes in a petri dish on ice.
3. Inject 10–15 μl of biotin solution into freshly collected testis, aim for the interstitial space, and avoid targeting seminiferous tubules. Inject 10–15 μl of 1× PBS containing $MgCl_2$ into the contralateral testis as a control.
4. Leave testes in the petri dish on ice for 30 min.
5. Then fix in Bouin's and proceed to Subheading 3.1.3, **step 6** onward.
6. Dewax and rehydrate slides of interest. Antigen retrieved, inactivate the endogenous peroxidase, and block the non-specific sites in 10% normal chicken serum as described in Subheading 3.1.4, **steps 1–8**.
7. To detect the biotin first, add a conjugate streptavidin-alexa-488 diluted 1/200 in normal chicken serum overnight at 4 °C in a humid chamber (or 1 h at RT). Include a negative control where the primary solution is replaced by serum.

8. Rinse in three successive washes of 1× TBS for 5 min each on a rocker at RT.
9. Apply Subheading 3.1.4, **step 7** onwards. Blocking in 10% normal chicken serum, incubate sections successively with primary antibody (mouse-raised anti-SMA, [17]), secondary antibody (chicken-raised anti-mouse coupled to peroxidase), and Tyramide-Cy5, diluted 1/50, and use DAPI as counterstain (*see* **Note 17**).

3.5 Characterization of Partial Sertoli Cell Ablation: Phenotyping the Model

Controlled ablation of Sertoli cells was possible through regulation of the amount of DTX injected using similar volume of toxin to treat animals, as mentioned in Subheading 3.4.1 (Fig. 5). We first characterized and analyzed the degree of ablation in response to different doses of DTX (*see* **Note 18**), and then we carried out an analysis of the proportion of Sertoli cells within the testis (*see* **Note 19**). We observed that, within doses, animal response to the DTX tended to show quite marked variation, whereas, in contrast, total ablation was always achieved when the DTX dose is in excess (100 ng) (Fig. 6). Therefore it was crucial for our experiments to measure Sertoli cell number and to use Sertoli cell-specific transcripts (SOX9, WT1…) in order to relate data to Sertoli cell number. To characterize this model more in depth, we then used similar methods to those described previously (Subheadings 3.4) (*see* **Note 20**).

3.6 Targeting Other Testicular Cell Types

Controlled cell ablation using the Cre/loxP system is a powerful technique that depends highly on the spatiotemporal expression pattern of the Cre. In the testis, several Cre recombinase lines are available that target either germ cells or somatic cells [5]. However, to counteract the extra-gonadal expression of certain Cre lines (e.g., to permit targeting of Leydig cells, where the majority of Leydig Cre lines would also target the adrenal), we also developed intratesticular injection delivery of the toxin. Targeting the testis directly by surgically exposing the organ through the scrotum or

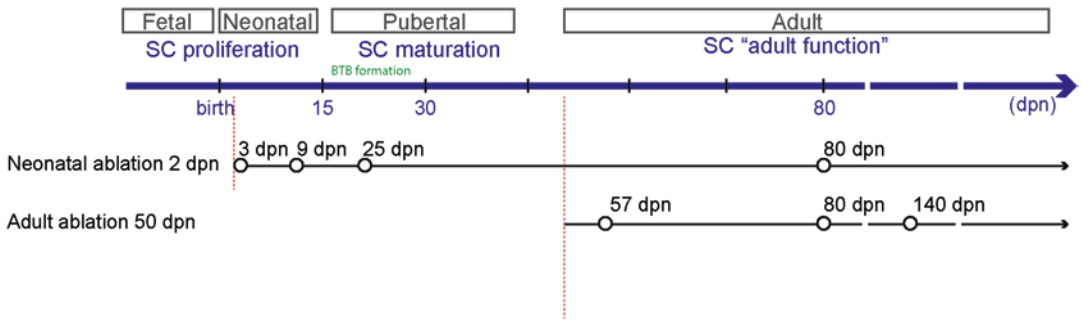

Fig. 5 Schematic representation of the partial Sertoli cell ablation study. The study end points are shown as circles at different times after DTX injection

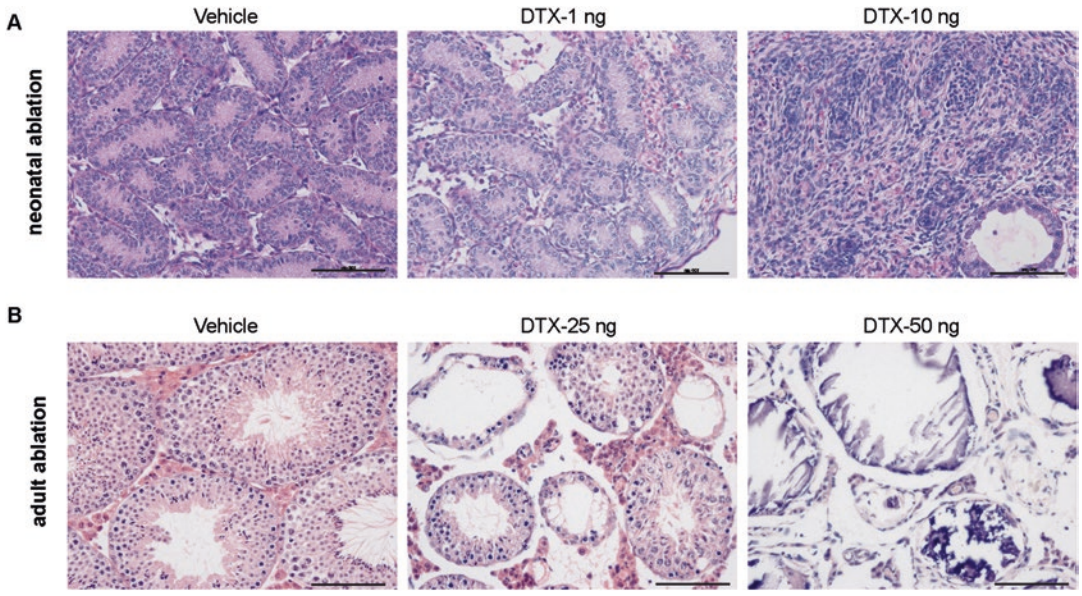

Fig. 6 Assessment of the DTX dose to induce partial ablation. Testicular histology using hematoxylin-eosin staining shows dose-response effect on testis architecture and seminiferous tubules composition 7 days after neonatal or adult Sertoli cell partial ablation (scale bar, 100 μm). Note the markedly different outcomes depending on age of the animals and dose of DTX injected (scale bar, 100 μm)

abdomen has previously been described for virus delivery [43]. To assess the possibility for targeted cell ablation through this route, we first validated that low-dose intratesticular DTX injection could induce cell death in the targeted testis but did not induce cell death in the non-injected contralateral testis.

3.6.1 Validation of the Intratesticular Injection

1. Doses <10 ng (in up to 10 μl water) of DTX is administered to adult mice (>50 dpn) and prepubertal mice (<50 dpn) via a single injection to the testes.
2. Place mice into an anesthetic chamber with unrestricted movement, and anesthetize them using inhalation of isoflurane.
3. Following induction of anesthesia, move mice to a warming pad and anesthesia maintained using a small face mask.
4. Shave and sterilize by swabbing with ethanol the area of interest. Make a single 1 cm incision into the scrotum, and expose one testis.
5. Inject DTX directly through the tunica wall using a 31G insulin needle.
6. Reinsert the testis, and carry out the same procedure on the contralateral testis, but use saline instead of toxin (*see* **Note 21**).
7. Reinsert testis within the scrotum and close the incision with sterile sutures.

8. Inject the mice subcutaneously with buprenorphine 0.05 mg/kg while still anesthetized, and allow to recover while being monitored.
9. Closely monitor mice over the next 24 h for any welfare problems and twice daily from then onward.
10. Cull mice at the end of the experiment.
11. Collect blood by cardiac puncture immediately after culling.
12. Recover tissues for postmortem analysis (*see* Subheading 3.2.1) (Fig. 7).

4 Notes

1. At weaning (21 dpn) animals are ear marked; therefore the ear clip is conserved and used for genotyping. For any collection endpoints earlier than 21 dpn, the animal genotype is unknown and so determined from a tail tip after culling.
2. Bouin's fixative (recipe: under hood mix 75 ml of picric acid (saturated) with 25 ml of formaldehyde (37–40%) and 5 ml of glacial acetic acid) is preferred to PFA fixation for testis histology as it preserves the nuclear structure. This is especially important for germ cells as it is a criterion for seminiferous epithelium staging. The time of fixation is minimum of 6 h, up to 24 h (no more than 48 h); once you select a fixation time, you need to apply this to all your samples for consistency of subsequent staining. For testis fixation, we cut the testis in half 4 h into the full 6-h process of tissue fixation.
3. The picric acid stain (yellow color) will extravasate from the tissue and be removed during the processing procedure. However, you can also reduce the yellow color using several washes in 70% alcohol. No interference with downstream protocols and analysis has been found if this is not carried out.
4. Not all antibodies require antigen retrieval. The manufacturers will indicate on the antibody technical datasheet whether retrieval is required and also the type of application the antibody has been tested for and a recommended range of dilution. However, before initiating a study, the antibody must be optimized, and different conditions should be assessed (test for requirement of citrate retrieval, titer for antibody dilution, pH of the citrate buffer, amplification system, permeabilization).
5. To reduce the background due to potential non-specific binding of the secondary antibodies, we select the species of the normal serum according to the species in which the secondary is raised.

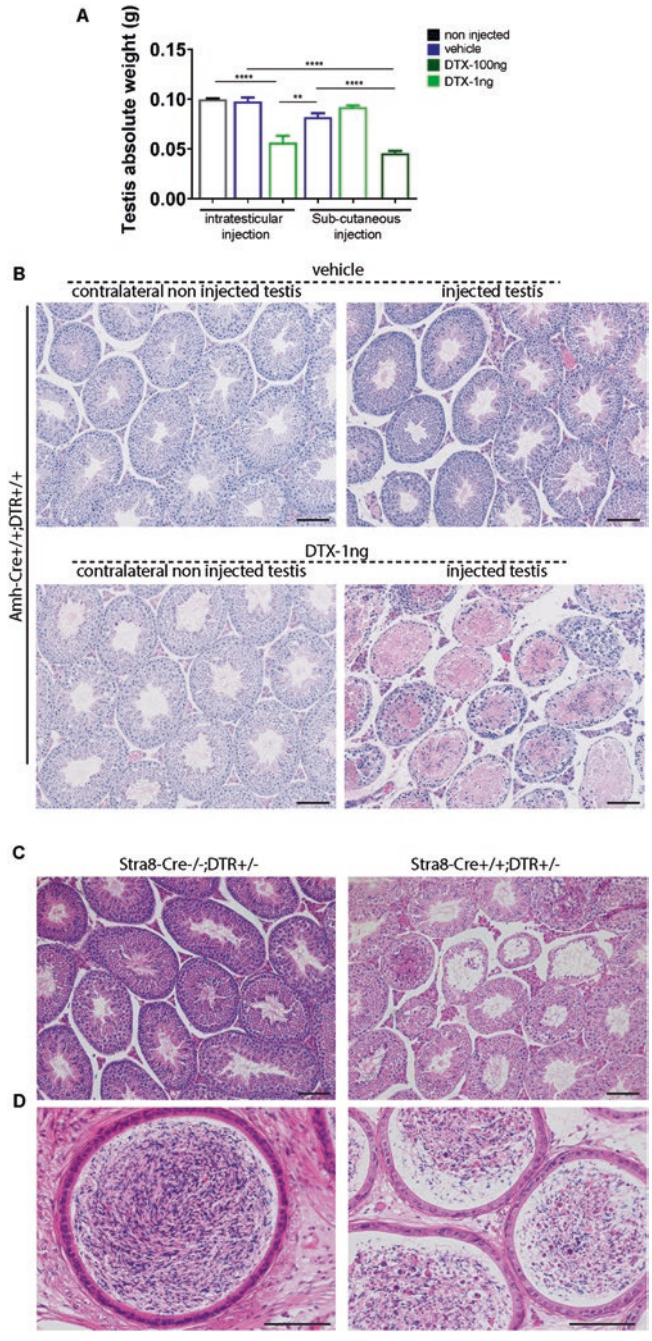

Fig. 7 Validation of intratesticular cell ablation. (**a**) Using the Amh-Cre+/+;DTR+/+ line, testis weight reduction following intratesticular-induced Sertoli cell ablation using 1 ng is comparable to the level of impact following subcutaneous induced ablation using 100 ng. (ANOVA, $^{**}P<0.01$, $^{****}P<0.0001$). (**b**) Testicular histology shows no impact on the composition of the non-injected contralateral testes following vehicle or DTX-1 ng treatment, confirming the absence of leakage from one testis to the other. The 1 ng injection in the testis of interest is sufficient to alter and deplete seminiferous tubules in a similar pattern as the subcutaneous induced ablation 7 days after (scale bar, 100 μm). (**c**) Similar approach was used in the Stra8-Cre+/−;DTR+/− line, and testicular histology shows depletion in germ cells in not all the tubules 7 days following intratesticular injection. (**d**) Abnormal residual germ cells were identified in the cauda epididymis among spermatozoa (scale bar, 100 μm)

6. A negative control is important for the validation of the localization and specificity of the staining [44]. For well-characterized antibodies, we use a non-primary control; if the protein is not well known, then complementary controls should be added to the optimization (negative control, peptide block, IgG control).
7. The tyramide amplification system can be conjugated to different fluorophores which allow double or triple staining.
8. Because the parents are Amh-Cre+/−; DTR−/− and Amh-Cre−/−;DTR+/−, all the required genotypes for the validation of the model should be obtained from the same litters. Due to the efficiency of the targeting system, one copy of the receptor is sufficient to induce cell death.
9. Once the model is validated, to minimize the number of animals, we used a homozygous population Amh-Cre+/+;DTR+/+ which was either treated with 100 ng DTX or vehicle for the rest of the study. To optimize our breeding strategies and save time and cost, we bred a maximum of pairs (1 male with 2 females) and let the first two rounds of litter age for the adult ablation. We then started the earlier ablation endpoints (prepubertal and neonatal).
10. While mice are resistant to diphtheria toxin, humans are extremely sensitive. It is essential to follow local and national health and safety guidelines when using diphtheria toxin, both in terms of personal protective equipment and preparation for hazardous spills or ingestion.
11. Diphtheria toxin is an extremely potent cytotoxic protein. Low concentrations in some mammalian species are enough to induce death (a few μg/kg BW in human and monkeys…). The toxin is composed of two linked A and B peptide subunits with the B subunit able to bind to the HB-EGF receptor. Upon binding of the toxin to its receptor, the complex internalizes and releases the catalytic subunit A leading to cell death. Even though diphtheria toxin has no specific target organ, it appears the heart, liver, and muscle are first affected. In the preliminary analysis, we want to assess whether the toxin is affecting organs in the absence of the receptor and to confirm specific targeting within the testis with no leakage. For these reasons we collected both nonreproductive organs and reproductive organs.
12. Gross morphological assessment of the reproductive organ (testis, seminal vesicle, and epididymis) is a quick way to evaluate the function of the reproductive system. The size of the tissues/organs will tell you immediately whether the development of the testes and/or secondary sexual organs has been affected by the cell ablation and whether there is disrupted

androgen action (*see* **Notes 13** and **14**). In our study, for example, the testes collected in adulthood, following Sertoli cell depletion, were significantly smaller than controls, and the respective epididymides exhibited an empty cauda although seminal vesicle size did not seem to change.

13. The seminal vesicle (SV) is an androgen-responsive organ, and its weight is used as a biomarker for circulating androgens and therefore varies accordingly [45]. Approximately 80–90% of testis weight is determined by its content of germ cells. In our model, ablating Sertoli cells also affects germ cell content, and we, therefore, observed a dramatic reduction in testis weight.
14. The addition of luciferase mRNA serves as controls for the efficiency of RNA extraction, RNA degradation, and the reverse transcription step and allows specific transcript levels to be expressed per testis (an important benchmark when cell composition inside the testis has changed).
15. To assess Leydig cell function in response to stimulation, we treated males with human chorionic gonadotrophin (hCG), which is an agonist of the LHCGR, and then measured testosterone production. Following cell ablation in adulthood (50 dpn), Amh-Cre+/+;DTR+/+ adult males (80 dpn) were injected intraperitoneally with 20IU of hCG 16 h before culling and their sera assessed by ELISA for testosterone concentration.
16. The testosterone, LH, and FSH assays are conducted routinely by a service to which we have access.
17. In this study, the entire Sertoli cell population is depleted, and we wanted to assess the peritubular myoid cell contribution to BTB. Therefore, in parallel with assessing the biotin infiltration, we also marked the peritubular myoid cells. In conditions where Sertoli cells are still present in the seminiferous tubules, we would also assess the presence of tight junctions using immunohistochemistry.
18. In neonates a DTX dose of 10 ng induced a total Sertoli cell depletion, and we therefore used lower concentrations for partial ablation. In adulthood, we had to use a dose <50 ng to induce partial Sertoli cell ablation.
19. The assessment of the dose response on Sertoli cell number could also have been completed by determining the portion of apoptotic Sertoli cells 1–3 days following injection, using cleaved caspase 3 staining. Our aim, however, was to determine the density of the final population and to be able to correlate this with other somatic and germ cells.
20. The partial ablation did not induce visible gross morphology defects.

21. In the first validation approach, the contralateral testis was not injected as we wanted to assess whether DTX leakage from the injected testis occurs. In parallel a batch of animal was injected with water to assess the impact on the testis following the surgical procedure and route of injection.

Acknowledgments

We thank Lyndsey Cruickshanks, Nathan Jeffery, Sarah Smith, Laura Milne, Laura O'Hara, Yi Ting Tsai, Rod Mitchell, Mike Millar, Forbes Howie, Mike Dodds, and Ana Monteiro for technical support. The work described in this article was funded by a Biotechnology and Biological Sciences Research Council (BBSRC) Project Grant [BB/J015105/1 to L.B.S., P.O'S.] and a Medical Research Council (MRC) Programme Grant [MR/N002970/1 to L.B.S.].

References

1. Allan CM, Haywood M, Swaraj S, Spaliviero J, Koch A, Jimenez M, Poutanen M, Levallet J, Huhtaniemi I, Illingworth P, Handelsman DJ (2001) A novel transgenic model to characterize the specific effects of follicle-stimulating hormone on gonadal physiology in the absence of luteinizing hormone actions. Endocrinology 142(6):2213–2220. https://doi.org/10.1210/endo.142.6.8092
2. Smith L (2011) Good planning and serendipity: exploiting the Cre/Lox system in the testis. Reproduction 141(2):151–161. https://doi.org/10.1530/REP-10-0404
3. Yoshida S (2010) Stem cells in mammalian spermatogenesis. Dev Growth Differ 52(3):311–317.https://doi.org/10.1111/j.1440-169X.2010.01174.x
4. Brinster RL (2002) Germline stem cell transplantation and transgenesis. Science 296(5576):2174–2176. https://doi.org/10.1126/science.1071607
5. Smith LB, O'Shaughnessy PJ, Rebourcet D (2015) Cell-specific ablation in the testis: what have we learned? Andrology 3(6):1035–1049. https://doi.org/10.1111/andr.12107
6. Stanley E, Lin CY, Jin S, Liu J, Sottas CM, Ge R, Zirkin BR, Chen H (2012) Identification, proliferation, and differentiation of adult Leydig stem cells. Endocrinology 153(10):5002–5010. https://doi.org/10.1210/en.2012-1417
7. Sharpe RM, Maddocks S, Kerr JB (1990) Cell-cell interactions in the control of spermatogenesis as studied using Leydig cell destruction and testosterone replacement. Am J Anat 188(1):3–20. https://doi.org/10.1002/aja.1001880103
8. Gaytan F, Bellido C, Morales C, Garcia M, van Rooijen N, Aguilar E (1996) In vivo manipulation (depletion versus activation) of testicular macrophages: central and local effects. J Endocrinol 150(1):57–65
9. Bergh A, Damber JE, van Rooijen N (1993) Liposome-mediated macrophage depletion: an experimental approach to study the role of testicular macrophages in the rat. J Endocrinol 136(3):407–413
10. O'Shaughnessy PJ, Hu L, Baker PJ (2008) Effect of germ cell depletion on levels of specific mRNA transcripts in mouse Sertoli cells and Leydig cells. Reproduction 135(6):839–850. https://doi.org/10.1530/REP-08-0012
11. Moolten FL, Cooperband SR (1970) Selective destruction of target cells by diphtheria toxin conjugated to antibody directed against antigens on the cells. Science 169(3940):68–70
12. Brockschnieder D, Lappe-Siefke C, Goebbels S, Boesl MR, Nave KA, Riethmacher D (2004) Cell depletion due to diphtheria toxin fragment A after Cre-mediated recombination. Mol Cell Biol 24(17):7636–7642. https://

doi.org/10.1128/MCB.24.17.7636-7642.2004

13. Cha JH, Chang MY, Richardson JA, Eidels L (2003) Transgenic mice expressing the diphtheria toxin receptor are sensitive to the toxin. Mol Microbiol 49(1):235–240
14. Buch T, Heppner FL, Tertilt C, Heinen TJ, Kremer M, Wunderlich FT, Jung S, Waisman A (2005) A Cre-inducible diphtheria toxin receptor mediates cell lineage ablation after toxin administration. Nat Methods 2(6):419–426. https://doi.org/10.1038/nmeth762
15. Saito M, Iwawaki T, Taya C, Yonekawa H, Noda M, Inui Y, Mekada E, Kimata Y, Tsuru A, Kohno K (2001) Diphtheria toxin receptor-mediated conditional and targeted cell ablation in transgenic mice. Nat Biotechnol 19(8):746–750. https://doi.org/10.1038/90795
16. Rebourcet D, O'Shaughnessy PJ, Monteiro A, Milne L, Cruickshanks L, Jeffrey N, Guillou F, Freeman TC, Mitchell RT, Smith LB (2014) Sertoli cells maintain Leydig cell number and peritubular myoid cell activity in the adult mouse testis. PLoS One 9(8):e105687. https://doi.org/10.1371/journal.pone.0105687
17. Rebourcet D, O'Shaughnessy PJ, Pitetti JL, Monteiro A, O'Hara L, Milne L, Tsai YT, Cruickshanks L, Riethmacher D, Guillou F, Mitchell RT, van't Hof R, Freeman TC, Nef S, Smith LB (2014) Sertoli cells control peritubular myoid cell fate and support adult Leydig cell development in the prepubertal testis. Development 141(10):2139–2149. https://doi.org/10.1242/dev.107029
18. Lecureuil C, Fontaine I, Crepieux P, Guillou F (2002) Sertoli and granulosa cell-specific Cre recombinase activity in transgenic mice. Genesis 33(3):114–118. https://doi.org/10.1002/gene.10100
19. Sadate-Ngatchou PI, Payne CJ, Dearth AT, Braun RE (2008) Cre recombinase activity specific to postnatal, premeiotic male germ cells in transgenic mice. Genesis 46(12):738–742. https://doi.org/10.1002/dvg.20437
20. Srinivas S, Watanabe T, Lin CS, William CM, Tanabe Y, Jessell TM, Costantini F (2001) Cre reporter strains produced by targeted insertion of EYFP and ECFP into the ROSA26 locus. BMC Dev Biol 1:4
21. Madisen L, Zwingman TA, Sunkin SM, Oh SW, Zariwala HA, Gu H, Ng LL, Palmiter RD, Hawrylycz MJ, Jones AR, Lein ES, Zeng H (2010) A robust and high-throughput Cre reporting and characterization system for the whole mouse brain. Nat Neurosci 13(1):133–140. https://doi.org/10.1038/nn.2467
22. Rebourcet D, Wu J, Cruickshanks L, Smith SE, Milne L, Fernando A, Wallace RJ, Gray CD, Hadoke PW, Mitchell RT, O'Shaughnessy PJ, Smith LB (2016) Sertoli cells modulate testicular vascular network development, structure, and function to influence circulating testosterone concentrations in adult male mice. Endocrinology 157(6):2479–2488. https://doi.org/10.1210/en.2016-1156
23. Cool J, DeFalco T, Capel B (2012) Testis formation in the fetal mouse: dynamic and complex de novo tubulogenesis. Wiley Interdiscip Rev Dev Biol 1(6):847–859. https://doi.org/10.1002/wdev.62
24. Sekido R, Lovell-Badge R (2013) Genetic control of testis development. Sex Dev 7(1–3):21–32. https://doi.org/10.1159/000342221
25. Fischer AH, Jacobson KA, Rose J, Zeller R (2008) Hematoxylin and eosin staining of tissue and cell sections. CSH Protoc 2008:prot4986. https://doi.org/10.1101/pdb.prot4986
26. O'Shaughnessy PJ, Monteiro A, Abel M (2012) Testicular development in mice lacking receptors for follicle stimulating hormone and androgen. PLoS One 7(4):e35136. https://doi.org/10.1371/journal.pone.0035136
27. Russell LD, Ren HP, Sinha Hikim I, Schulze W, Sinha Hikim AP (1990) A comparative study in twelve mammalian species of volume densities, volumes, and numerical densities of selected testis components, emphasizing those related to the Sertoli cell. Am J Anat 188(1):21–30. https://doi.org/10.1002/aja.1001880104
28. O'Shaughnessy PJ, Baker PJ, Heikkila M, Vainio S, McMahon AP (2000) Localization of 17beta-hydroxysteroid dehydrogenase/17-ketosteroid reductase isoform expression in the developing mouse testis--androstenedione is the major androgen secreted by fetal/neonatal leydig cells. Endocrinology 141(7):2631–2637. https://doi.org/10.1210/endo.141.7.7545
29. Shima Y, Miyabayashi K, Haraguchi S, Arakawa T, Otake H, Baba T, Matsuzaki S, Shishido Y, Akiyama H, Tachibana T, Tsutsui K, Morohashi K (2013) Contribution of Leydig and Sertoli cells to testosterone production in mouse fetal testes. Mol Endocrinol 27(1):63–73. https://doi.org/10.1210/me.2012-1256
30. Sharpe RM, McKinnell C, Kivlin C, Fisher JS (2003) Proliferation and functional maturation of Sertoli cells, and their relevance to disorders of testis function in adulthood. Reproduction 125(6):769–784
31. Auharek SA, Lara NL, Avelar GF, Sharpe RM, Franca LR (2012) Effects of inducible nitric oxide

synthase (iNOS) deficiency in mice on Sertoli cell proliferation and perinatal testis development. Int J Androl 35(5):741–751. https://doi.org/10.1111/j.1365-2605.2012.01264.x

32. Baker PJ, O'Shaughnessy PJ (2001) Expression of prostaglandin D synthetase during development in the mouse testis. Reproduction 122(4):553–559
33. Vergouwen RP, Jacobs SG, Huiskamp R, Davids JA, de Rooij DG (1991) Proliferative activity of gonocytes, Sertoli cells and interstitial cells during testicular development in mice. J Reprod Fertil 93(1):233–243
34. O'Shaughnessy PJ (2014) Hormonal control of germ cell development and spermatogenesis. Semin Cell Dev Biol 29:55–65. https://doi.org/10.1016/j.semcdb.2014.02.010
35. Mendis-Handagama SM, Ariyaratne HB (2001) Differentiation of the adult Leydig cell population in the postnatal testis. Biol Reprod 65(3):660–671
36. Haider SG (2004) Cell biology of Leydig cells in the testis. Int Rev Cytol 233:181–241. https://doi.org/10.1016/S0074-7696(04)33005-6
37. Saez JM (1994) Leydig cells: endocrine, paracrine, and autocrine regulation. Endocr Rev 15(5):574–626. https://doi.org/10.1210/edrv-15-5-574
38. Regueira M, Artagaveytia SL, Galardo MN, Pellizzari EH, Cigorraga SB, Meroni SB, Riera MF (2015) Novel molecular mechanisms involved in hormonal regulation of lactate production in Sertoli cells. Reproduction 150(4):311–321. https://doi.org/10.1530/REP-15-0093
39. Walker WH, Cheng J (2005) FSH and testosterone signaling in Sertoli cells. Reproduction 130(1):15–28
40. O'Shaughnessy PJ, Monteiro A, Verhoeven G, De Gendt K, Abel MH (2010) Effect of FSH on testicular morphology and spermatogenesis in gonadotrophin-deficient hypogonadal mice lacking androgen receptors. Reproduction 139(1):177–184. https://doi.org/10.1530/REP-09-0377
41. Stanton PG (2016) Regulation of the blood-testis barrier. Semin Cell Dev Biol 59:166–173. doi:S1084-9521(16)30179-3 [pii]
42. Elkin ND, Piner JA, Sharpe RM (2010) Toxicant-induced leakage of germ cell-specific proteins from seminiferous tubules in the rat: relationship to blood-testis barrier integrity and prospects for biomonitoring. Toxicol Sci 117(2):439–448. https://doi.org/10.1093/toxsci/kfq210
43. Willems A, Roesl C, Mitchell RT, Milne L, Jeffery N, Smith S, Verhoeven G, Brown P, Smith LB (2015) Sertoli cell androgen receptor signalling in adulthood is essential for post-meiotic germ cell development. Mol Reprod Dev 82(9):626–627. https://doi.org/10.1002/mrd.22506
44. Burry RW (2011) Controls for immunocytochemistry: an update. J Histochem Cytochem 59(1):6–12. https://doi.org/10.1369/jhc.2010.956920
45. Porter JC, Melampy RM (1952) Effects of testosterone propionate on the seminal vesicles of the rat. Endocrinology 51(5):412–420. https://doi.org/10.1210/endo-51-5-412

Chapter 16

Regulation of Blood-Testis Barrier (BTB) Dynamics, Role of Actin-, and Microtubule-Based Cytoskeletons

Qing Wen, Elizabeth I. Tang, Nan Li, Dolores D. Mruk, Will M. Lee, Bruno Silvestrini, and C. Yan Cheng

Abstract

The blood-testis barrier (BTB) is an important ultrastructure in the testis that supports meiosis and postmeiotic spermatid development since a delay in the establishment of a functional Sertoli cell barrier during postnatal development in rats or mice by 17–20 day postpartum (dpp) would lead to a delay of the first wave of meiosis. Furthermore, irreversible disruption of the BTB by toxicants also induces infertility in rodents. Herein, we summarize recent findings that BTB dynamics (i.e., disassembly, reassembly, and stabilization) are supported by the concerted efforts of the actin- and microtubule (MT)-based cytoskeletons. We focus on the role of two actin nucleation protein complexes, namely, the Arp2/3 (actin-related protein 2/3) complex and formin 1 (or the formin 1/spire 1 complex) known to induce actin nucleation, respectively, by conferring plasticity to actin cytoskeleton. We also focus on the MT plus (+)-end tracking protein (+TIP) EB1 (end-binding protein 1) which is known to confer MT stabilization. Furthermore, we discuss in particular how the interactions of these proteins modulate BTB dynamics during spermatogenesis. These findings also yield a novel hypothetical concept regarding the molecular mechanism that modulates BTB function.

Key words Testis, Sertoli cell, Blood-testis barrier, Spermatogenesis, Ectoplasmic specialization, Tight junction, Gap junction, Desmosome, Seminiferous epithelial cycle

1 Introduction

The blood-testis barrier (BTB) is constituted by multiple junction types at the base of the seminiferous epithelium between adjacent Sertoli cells near the basement membrane, which include the actin-based tight junction (TJ) and gap junction (GJ). These junctions, in turn, are supported by coexisting basal ectoplasmic specialization (ES, a testis-specific actin-rich adherens junction (AJ)) and the intermediate filament-based desmosome (Fig. 1a, b) [1–4]. Recent studies have shown that the actin- and microtubule (MT)-based cytoskeletons in the seminiferous epithelium are playing a crucial role to the homeostasis of the BTB in the mammalian testis, in particular the cytoskeletal elements at the basal ES

Marco G. Alves and Pedro F. Oliveira (eds.), *Sertoli Cells: Methods and Protocols*, Methods in Molecular Biology, vol. 1748, https://doi.org/10.1007/978-1-4939-7698-0_16,

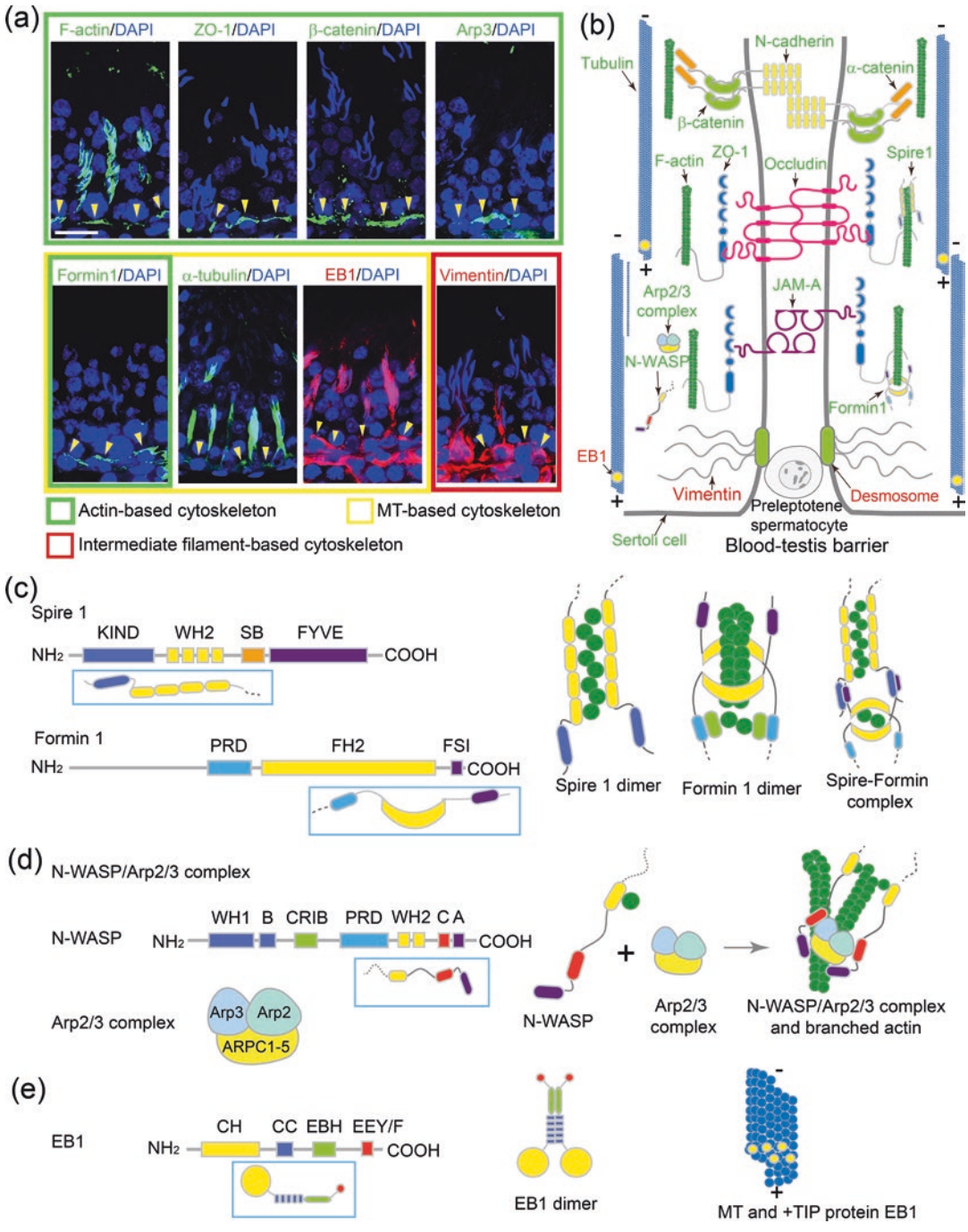

Fig. 1 Illustrations on the relative localization of F-actin-, MT-, and vimentin-based cytoskeletons in the testis and selected regulatory and structural proteins plus their functional domains and organization. (**a**) The relative localization of F-actin network and the basal ES/BTB proteins ZO-1 and ß-catenin and nucleation proteins Arp3 and formin 1 in cross sections of adult rat testes *vs.* the MT (α-tubulin)- and intermediate filament (vimentin)-based cytoskeletons and EB1 (a +TIP protein) using corresponding specific antibodies was performed by immunofluorescence analysis as earlier described [15, 17, 18, 81]. The relative location of the BTB is annotated by the yellow arrowheads. It is noted that F-actin, MT, and intermediate filaments also form some track-like structures that lay perpendicular to the basement membrane to support germ cell and organelle transport.

[5–11]. Specifically, it was shown that besides serving as the attachment sites for the adhesion protein complexes at the BTB, these cytoskeletons also provide the track-like structures to support (1) intracellular trafficking of endocytic vesicles and other cargoes (e.g., phagosomes, endosomes) and (2) the paracellular transport of preleptotene spermatocytes connected in clones across the immunological barrier at stage VIII of the epithelial cycle in rodent testes [12–14]. This conclusion is supported based on studies by disrupting these track-like structures such as through a transient knockdown of nucleation protein formin 1 (Fig. 1c) by RNAi. It is now known that in the testis, formin 1, likely working in concert with other actin regulatory proteins, such as plastin 3 (an actin bundling protein) and the Arp2/3 complex (a branched actin nucleation protein complex which effectively converts an actin microfilament to a branched configuration), are crucial to support the generation of linear actin microfilaments across the Sertoli cells to confer the establishment of actin microfilaments at the basal ES [15–18] (Fig. 1c, d). This coordinated effort is necessary to support the timely transport of step 19 spermatids across the epithelium in stage VII–VIII tubules to prepare for their release at spermiation in stage VIII tubules [19, 20]. But they are also necessary to facilitate the timely remodeling of the BTB to support the transport of preleptotene spermatocytes across the immunological barrier at stage VIII of the epithelial cycle [15, 16]. Studies have shown that these two cellular events that take place at the opposite ends of the seminiferous epithelium are coordinated at stage VIII of

Fig. 1 (continued) Cell nuclei were visualized by DAPI staining. Scale bar, 80 μm, which applies to all other micrographs. (**b**) This is a schematic drawing illustrating the intact BTB of a stage VII to early stage VIII tubule and the association of different regulatory and nucleation proteins with the corresponding F-actin- and MT-based cytoskeletons. Also shown are the structural adhesion proteins of the BTB. (**c**) Functional domains of nucleation proteins spire 1 and formin 1 and the simplified models of the two proteins (boxed in rectangles). (**d**) Functional domains of barbed end nucleation protein complex N-WASP/Arp2/3 and the simplified model of N-WASP (boxed in rectangle). (**e**) Functional domains of MT regulatory protein EB1, a +TIP protein known to stabilize MTs, and the simplified model of EB1. For (**c**–**e**), the illustrations on the right panels illustrate the models by which the corresponding proteins function in tissues including the seminiferous epithelium in the rat testis. Abbreviations: *+TIP* plus (+)-end microtubule tracking protein, *A* acidic domain, *Arp2/3 complex* actin-related protein 2 and 3 complex, *B* basic domain, *C* central region, *CC* coiled-coil domain, *CH* calponin homology, *CID* α-catenin interacting domain, *CRIB* Cdc42/Rac-interactive binding, *DAD* diaphanous autoregulatory domain, *DD* dimerization domain, *DID* diaphanous inhibitory domain, *EB1* end-binding protein 1 (a +TIP protein), *EBH* end-binding protein homology, *EEY/F* C-terminal EEY/F motif, *EF hand* calcium-binding motif, *FH* formin homology, *FSI* formin-spire interaction motif, *FYVE* Fab1/YOTB/Vac1/EEA1 zinc-binding domain, *GBD* GTPase-binding domain, *KIND* kinase noncatalytic C-lobe domain, *MTB* microtubule-binding domain, *PRD* proline-rich domain, *N-WASP* neuronal Wiskott-Aldrich syndrome protein, *SB* spire box, *WH1 domain* WASP homology domain 1, *WH2 domain* WASP homology domain 2, *ZO-1* zonula occludens 1

the epithelial cycle [9, 21, 22]. On the other hand, studies have shown that formin 1 is capable of binding to microtubules (MT) [15], possibly through the presence of a MT-binding domain near the N-terminus of formin 1 as earlier reported [23]. In fact, it was recently shown that a loss of formin 1 in the testis in vivo by RNAi led to a gross disruption of MT-based cytoskeletal network across the entire seminiferous epithelium in virtually all stages of the tubules [15]. Additionally, studies based on the use of the adjudin model have also shown that a disruption of the MT-based tracks mediated by changes in the spatiotemporal expression of EB1 (end-binding protein 1, an MT plus (+)-end tracking protein (TIP)) (Fig. 1e) also perturbed the transport of step 19 spermatids across the epithelium in stage VII–VIII tubules [13]. Adjudin also induced disruptive changes in the actin-based cytoskeleton mediated by its effects on the actin regulatory proteins such as Arp2/3 complex (a branched actin polymerization protein) (Fig. 1d), Eps8 (an actin barbed end capping and bundling protein) [13, 17, 24], and palladin (an actin-bundling protein) [25]. In both animal models, namely, the adjudin and the formin 1 knockdown model, step 19 spermatids are persistently found in the seminiferous epithelium that are trapped near the base of the epithelium in stage IX–XII tubules until they are eliminated by the Sertoli cell through lysosomal degradation, sometimes through the appearance of multinucleated round and/or spermatocytes [13, 15, 16], as noted in other toxicant-induced aspermatogenesis models [26–29].

On the other hand, recent studies have shown that BTB dynamics in the rat testis are supported and regulated by local functional axis involving biologically active fragments released from the apical ES (at the Sertoli-spermatid interface in the adluminal compartment from step 8–19 spermatids) such as the F5 peptide from the laminin chains [30–32], and also peptides from the collagen α3 (IV) chain (e.g., non-collagenous 1, NC1, domain peptide) [33] and laminin α2 chain (e.g., 80 kDa fragment) [34, 35]. These findings are also supported by studies using toxicant-induced Sertoli cell injury animal models, such as the use of phthalates [36, 37]. More important, these biologically active fragments released from the constituent components of the apical ES (e.g., laminin γ3 chain) and the basement membrane (e.g., collagen α3 (IV) chain, laminin α2 chain) through the plausible action of MMP 2 (matrix metalloprotease 2) [38] and MMP 9 [39] at the corresponding site are shown to exert their regulatory effects through their action on the actin- and/or MT-based cytoskeletons [31, 32, 34, 35]. Collectively, these findings illustrate that the actin- and MT-based cytoskeletons are

working in concert to maintain the homeostasis of the BTB dynamics to support spermatogenesis.

Herein, we briefly review these recent data to provide a molecular model regarding the regulation of BTB dynamics by the local area regulatory networks besides the hormonal hypothalamic-pituitary-testicular axis [40–44] which have been reviewed by other investigators.

2 Actin and Microtubule (MT) Networks and BTB Homeostasis

Blood-tissue barriers such as the blood-brain barrier (BBB) and the blood-retinal barrier (BRB) are created by tight junction (TJ) barrier between adjacent endothelial cells of the microvessels and supported by pericytes in the brain and the eye, respectively [45–48]. The BTB, however, is contributed almost exclusively by the coexisting TJ and basal ES between adjacent Sertoli cells near the base of the seminiferous tubule in the mammalian testis, whereas endothelial cells of the microvessels in the interstitium contribute to relatively little barrier function [1, 11, 49]. In rodent testes, but not in primates, the peritubular myoid cells in the tunica propria also play a role in conferring the barrier function at the BTB [1, 50]. As such, the Sertoli cells in the testis, in particular in primates and humans, are the major players of the BTB function. As noted in Fig. 1a, b, the Sertoli cell is supported by the extensive networks of the actin- and MT-based cytoskeletons across the cell cytosol, which together with the intermediate filament-based desmosome [4, 51] constitute the BTB such as shown in the rat testis (Fig. 1a, b). This unusual extensive networks of F-actin and MTs that contribute to the strength of the BTB, making it one of the tightest blood-tissue barriers in the mammalian body, are not static ultrastructures. Instead, these actin microfilaments and MTs continuously remodel, undergoing rapid disassembly and reassembly to support the transport of preleptotene spermatocytes across the immunological barrier (Fig. 2). Recent studies have shown that several actin-binding and regulatory proteins as well as MT-binding and regulatory proteins are crucial to modulate the dynamic conversion of actin microfilaments or MTs between their bundled, unbundled/branched, and/or truncated/defragmented state. These changes thus confer plasticity to these cytoskeletons, supporting their continuous remodeling during the epithelial cycle of spermatogenesis when preleptotene spermatocytes transformed from type B spermatogonia are being transported across the immunological barrier. Below is a critical review of these findings.

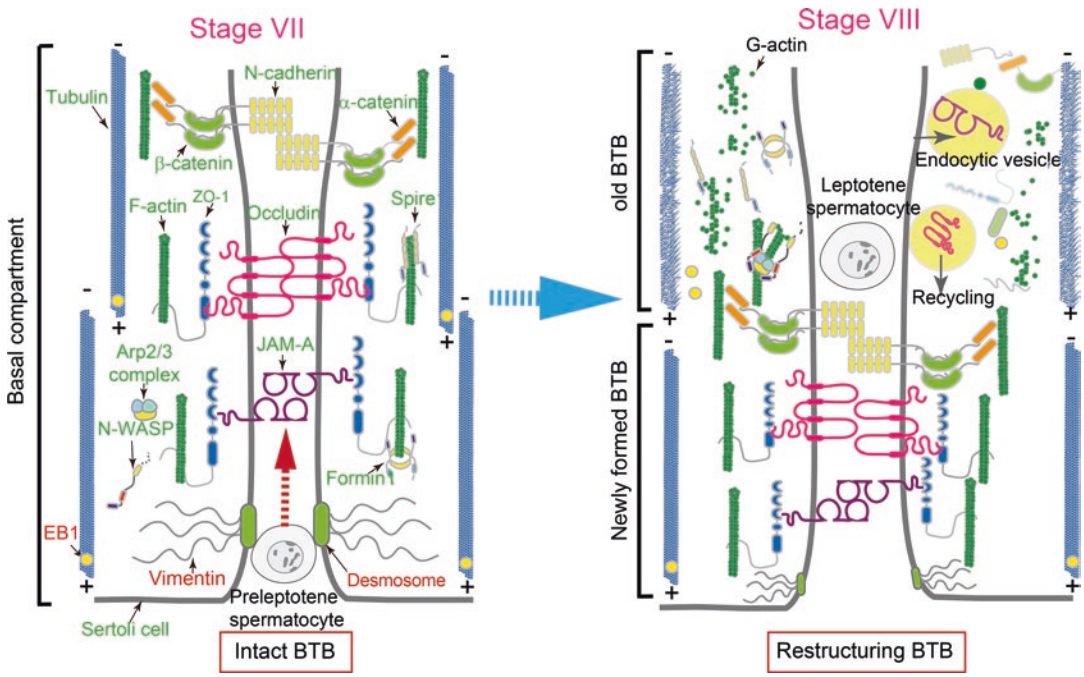

Fig. 2 A schematic drawing that illustrates the dynamic BTB restructuring is mediated by changes in the spatial expression of actin- and MT-binding/regulatory and nucleation proteins. The left panel depicts a schematic stage VII (or early stage VIII) tubule with an intact BTB supported by proper organized F-actin and MT networks. At stage VIII (right panel), the N-WASP/Arp2/3 complex is activated, causing actin microfilaments to assume a branched configuration, no longer capable of supporting the actin filaments to assume a bundled configuration. EB1 is also moving away from MTs, failing to stabilize the MT network and causing a disruption of the "old" BTB to facilitate the transport of preleptotene spermatocytes across the immunological barrier with a concomitant assembly of a "new" BTB behind the preleptotene spermatocyte. *See* text for details

3 Actin-Based Cytoskeleton

Actin in Sertoli cells, similar to other mammalian cells, is organized as either filamentous actin (F-actin) or globular actin (G-actin). F-actin is a polymer and an intrinsic polarized structure formed by G-actin subunits assembled from the fast-growing end (also called the barbed end or plus (+) end) through the action of nucleation proteins *vs.* the slow-growing end known as the pointed end or minus (−) end [10, 52, 53]. In order for actin to undergo continuous remodeling, actin microfilaments undergo rapid changes including polymerization (or nucleation), depolymerization, bundling, severing (or cleavage), capping, and branching via the action of different actin-binding and regulatory proteins. Herein we discuss some recent findings based on studies of the following selected actin-binding/regulatory proteins in the testis and how these proteins work alone or in concert with others to modulate the organization of actin microfilaments, most notably at the ES to regulate (1) spermatid adhesion and transport and (2) BTB dynamics to

facilitate the transport of preleptotene spermatocytes across the immunological barrier. Other regulatory proteins such as actin-bundling proteins plastin 3, Eps8, ezrin, and palladin and regulatory protein kinases (e.g., FAK, c-Src, c-Yes) pertinent to the regulation of spermatogenesis have recently been reviewed [14, 19], and thus, they are not being discussed herein to avoid redundancy. Instead, we focus on a group of actin nucleation proteins; however, these actin nucleation proteins are grouped into two types: one confers branched actin nucleation (e.g., the Arp2/3 complex), whereas the other type confers linear actin nucleation (e.g., formin 1 and Spire 1). Their concerted effects thus generate either a branched actin network or actin microfilaments that can be bundled by actin cross-linking/bundling proteins to facilitate ES degeneration or integrity to support ES breakdown or integrity in the seminiferous epithelium during the epithelial cycle. These changes in turn support germ cell transport across the epithelium.

3.1 The Arp2/3 Complex

The Arp2/3 (actin-related protein 2/3) complex is an actin nucleation protein composed of Arp2, Arp3, and ARPC1-5 (actin-related protein 2/3 complex components 1–5). In short, the Arp2/3 is a protein complex composed of seven different proteins. Its intrinsic activity is to bind onto the barbed end of an existing actin microfilament, upon activation by N-WASP (neuronal Wiskott-Aldrich syndrome protein), and the N-WASP/Arp2/3 complex rapidly induces branched actin nucleation [54–59] (Fig. 1d). Thus, the Arp2/3 complex is effective in converting actin microfilaments from a bundled to a branched/unbundled configuration. The net result of these changes thus destabilizes the ES, facilitating internalization of adhesion protein complexes at the site via endocytosis. This thus promotes endocytic vesicle trafficking so that proteins at the ES, such as at the apical ES near the tubule lumen in a late stage VIII tubule getting ready for spermiation, can be endocytosed and recycled to assemble new apical ES to support newly differentiated step 8 spermatid. This notion is supported by the presence of an extensive network of proteins that are found at the apical ES near the concave (ventral) side of spermatid head, also known as the apical tubulobulbar complex (apical TBC) [60]. In fact, the apical ES is an ultrastructure that supports endocytic vesicle-mediated protein trafficking [61], which is being used to support the assembly of newly formed apical ES at the interface of step 8 spermatids and the Sertoli cell in stage VIII tubules. Similar events also take place at the BTB to support the transport of preleptotene spermatocytes across the immunological barrier in which adhesion proteins located above the preleptotene spermatocytes connected in clones via intercellular bridges are also rapidly endocytosed, creating an ultrastructure known as basal TBC [62], which is readily detected by electron microscopy [63]. As such, adhesion proteins (e.g.,

N-cadherin, occludin, JAM-1, ZO-1) can be rapidly endocytosed at the "old" BTB site located above preleptotene spermatocytes and recycled to the site behind the preleptotene spermatocytes for the assembly of a "new" BTB (Fig. 2). It is envisioned that the "new" BTB requires the rapid assembly of adhesion protein complexes at the site (e.g., N-cadherin/ß-catenin, occludin/ZO-1, JAM-1/ZO-1) through endocytosis and recycling, and this extensive series of protein trafficking events are supported by the actin network at the apical ES/apical TBC and basal ES/basal TBC. Furthermore, linear actin microfilaments through the action of actin nucleators formin 1 and possibly spire 1 are also required for the assembly of actin microfilament bundles at the "new" apical ES and "new" basal ES/BTB [15, 18].

3.2 Formin 1 and Spire 1

Formin 1 is a member of the morphoregulatory protein family called formins, and due to its intrinsic activity as an actin nucleator, it is capable of inducing actin polymerization from the fast-growing barbed end of an actin filament, forming a long stretch of linear actin microfilament [55, 64–66]. Thus, formins are essential actin nucleation proteins for cytoskeletal organization during development [64, 67]. A functional formin 1 molecule is a dimer in which two formin 1 polypeptide chains are recruited adjacent to one another via their coiled-coil (CC) domains and dimerization (DD) domains. These polypeptides in turn dimerize via their formin homology (FH) 2 domains at the barbed end of an actin microfilament [68, 69]. The dimerized formin 1 promotes addition of actin monomers from the barbed end using G-actin/profilin complexes so that long stretches of actin filaments can be rapidly formed [70]. Thus allows formation of actin microfilaments that can be assembled to actin filament bundles to support the ES through the action of actin bundling proteins such as palladin and Eps8 (epidermal growth factor receptor pathway substrate 8) in the testis. Additionally, formin 1 also possesses intrinsic actin-bundling activity via its FH2 domain [68, 71, 72] (Fig. 1c), capable of inducing actin microfilaments into bundled structures. It also possesses a prominent microtubule-binding (MTB) domain near its N-terminus [23, 69, 71], illustrating it may also be involved in MT organization. On the other hand, spire 1 is also an actin nucleator known to nucleate actin polymerization as a monomeric nucleator via a mechanism different from either formin 1 or the Arp2/3 complex [55, 73]. Spire 1 induces actin polymerization through its central four tandem WH2 domains including the linker-3 (between WH2 domains 3 and 4) [55] (Fig. 1c). Studies in *Drosophila* oocytes have shown that cappuccino (formin) and spire, however, form a functional complex to induce actin nucleation [74, 75] (Fig. 1c). Emerging evidence has shown that formins (e.g., formin 1) and spire proteins (e.g., spire 1) create a spire/formin actin nucleator complex in mammalian cells other than the oocyte to

induce actin polymerization [76–78]. This is made possible due to the presence of a FSI (formin-spire interaction) motif near the C-terminus of formin 1 [76] (Fig. 1c). However, formation of this complex blocks the intrinsic nucleation and barbed end-binding activities of formins, but the spire nucleation activity is considerably enhanced [74, 75]. This is due to the assembly of a dimeric spire upon binding onto formins instead of a monomeric spire protein; thus, there are eight WH2 repeats in tandem to facilitate the recruitment of actin monomers to be polymerized to create long stretches of actin microfilaments across the cell (Fig. 1c) [76]. However, it remains to be investigated if spire/formin complex is a regulatory actin nucleation complex in the mammalian testis.

Studies in the testis have shown that formin 1 is highly expressed at the basal ES at the BTB and also the apical ES, colocalizing with F-actin in adult rat testes [15, 18]. At the basal ES/BTB, the expression of formin 1 remains high in all stages of the epithelial cycle except at stage VIII when its expression is considerably diminished to an almost nondetectable level [15, 18], coinciding with the remodeling of the BTB at this stage to facilitate the transport of preleptotene spermatocytes across the immunological barrier [22]. At the apical ES, formin 1 expression is robust and prominent but limited mostly to stage VII tubules when elongated (step 19) spermatids firmly anchor onto the Sertoli cell in the epithelium [15, 18], requiring formin 1 to promote the generation of actin microfilaments to sustain apical ES function. In this context, it is of interest to note that at stage VII, extensive F-actin remodeling also takes place at the concave (ventral) side of spermatid heads known as the apical TBC – the site where formin 1 is highly expressed – to facilitate the endocytic vesicle-mediated trafficking events such as endocytosis and recycling [60, 61, 79, 80]. This thus requires an elevated expression of formin 1 to sustain actin microfilament turnover at the apical TBC. However, formin 1 expression at the apical ES diminished to an almost undetectable level in stage VIII tubules during apical ES degeneration to support the release of sperm at spermiation [15, 18]. In short, these findings suggest that the spatiotemporal expression of formin 1 at the apical and basal ES is to support (or promote) the integrity or its turnover (but not degeneration) of the actin microfilaments at the ES. Due to its intrinsic actin polymerization and bundling activity, a knockdown of formin 1 by RNAi in Sertoli cells cultured in vitro with an established functional TJ barrier has thus shown to perturb the Sertoli cell TJ permeability barrier function [18]. Formin 1 knockdown in Sertoli cell epithelium has also shown to downregulate the kinetics of actin polymerization and the overall Sertoli cell actin-bundling activity [18]. Thus, it is not unexpected that formin 1 knockdown in the testis in vivo considerably perturbed the transport of elongating/elongated spermatids across the seminiferous epithelium so that some fully developed elon-

gated spermatids (i.e., spermatozoa) fail to lineup at the luminal edge of the apical compartment for their release into the tubule lumen at spermiation [15, 18]. Instead, step 19 spermatids are routinely found embedded deep inside the epithelium; some are even close to the basement membrane in formin 1 silenced adult rat testes in stage IX–X tubules, and phagosomes also fail to be transported to the base of the epithelium in stage IX and X tubules for their eventual degradation by the Sertoli cell [15, 18]. This is likely due to defects in proper organization of F-actin network in the seminiferous epithelium in response to changes in stages of the epithelial cycle to support these cellular events. For instance, a knockdown of formin 1 considerably disrupts the track-like structures conferred by F-actin that lay across the epithelium such as in stage VIII tubules to support spermatid and phagosome transport [15].

4 MT-Based Cytoskeleton

The MT- and actin-based cytoskeletons are two distinctive cytoskeletal networks, supported by different binding and regulatory proteins in the testis [5, 8, 9, 20]. However, these two cytoskeletal networks are intimately associated structurally and functionally to support spermatogenesis [9, 19]. Interestingly, studies have shown that both cytoskeletal networks can be modulated by the same proteins. For instance, it has recently been shown that EB1 (end-binding protein 1, a +TIP (plus (+)-end tracking protein)) (Fig. 1e) modulates MT and F-actin organization since its knockdown by RNAi perturbs the organization of MTs and actin microfilaments in Sertoli cells [81]. On the other hand, formin 1, an actin nucleator which also possesses an MT-binding domain near its N-terminus [23] to confer its ability to bind to MTs [15], has also been shown to modulate both F-actin and MT organization in Sertoli cells [15, 18]. In fact, a knockdown of formin 1 in the testis in vivo was shown to induce extensive disorganization of MTs in the seminiferous epithelium in which the MT-conferred tracks were grossly disrupted, no longer stretched across the epithelium prominently as found in control testes transfected with nontargeting negative control siRNA duplexes besides perturbing F-actin organization [15]. Under electron microscopy, MTs lay adjacent to the actin microfilaments at the ES [9, 11], suggesting that these two cytoskeletons are likely working in concert to support the ES function. MTs, similar to F-actin, are also polymers, constituted by the α- and ß-tubulins that serve as the building blocks, and are polarized structures with the plus (+) and the minus (−) ends as the fast-growing and the slow-growing ends, respectively [5, 9]. A recent report has shown that germ cell transport across the seminiferous epithelium during the epithelial cycle requires the support of the

actin- and MT-based cytoskeletons [13]. Based on the study using the adjudin model wherein rats were treated with a single dose of adjudin at 50 mg/kg b.w. by oral gavage, this male contraceptive drug was found to induce apical ES disruption, causing germ cell exfoliation across the entire seminiferous epithelium [13]. However, many step 19 spermatids were trapped deep inside the epithelium even though the apical ES that anchored these spermatids were degenerated. The inability of these spermatids to be empty into the tubule lumen was due to the absence of tracks conferred by MTs. As such, even though the apical ES function had been compromised following adjudin treatment, losing the ability to anchor spermatids onto the Sertoli cell in the epithelium, these step 19 spermatids were entrapped inside the epithelium because tracks were missing to support their transport to the adluminal edge for their release into the tubule lumen [13]. In short, there were no MT-conferred tracks that support the transport of these elongated spermatids to the tubule lumen [13], illustrating these two cytoskeletons are working in concert to support spermatid transport. This observation has also been reproduced in rats subjected to RNAi using testes transfected with formin 1-specific siRNA duplexes *vs.* nontargeting control siRNA duplexes in control testes [15]. For instance, many step 19 spermatids are found deeply embedded into the seminiferous epithelium in stage IX and X tubules when spermiation has already occurred [15]. A careful examination on the distribution and organization of MTs across the epithelium in these testes has noted that testes following formin 1 knockdown display gross disorganization of MTs so that the track-like structures are considerably diminished or virtually not existed [15]. This thus disables elongated spermatids from being transported to the adluminal edge of the apical compartment to be emptied into the tubule lumen at spermiation, as well as the transport of preleptotene spermatocytes across the immunological barrier. In short, the basal and apical ES rely heavily on the integrity of the actin- and MT-based cytoskeletons to support the transport of spermatids and other organelles (e.g., residual bodies and phagosomes), which are essential to maintain spermatogenesis.

5 Concluding Remarks and Future Perspectives

As briefly discussed above, the actin- and MT-based cytoskeletons are playing a crucial role to support BTB dynamics (i.e., disassembly, reassembly, and stabilization) to facilitate the paracellular transport of preleptotene spermatocytes across the Sertoli cell immunological barrier, such as at stage VIII of the epithelial cycle. The two actin nucleation protein complexes, namely, the Arp2/3 complex and formin 1 (or the spire/formin complex) that induce branched actin polymerization and linear actin filament polymer-

ization, respectively, are working in concert with other actin regulatory proteins (e.g., actin-bundling proteins, cleavage and depolymerization proteins) to confer the plasticity of F-actin network in the Sertoli cell. On the other hand, MTs are also modulated by other MT-binding/regulatory proteins, such as EB1 which is known to induce MT stabilization [82–84]. However, formin 1, an actin nucleation protein, is also recently shown to modulate Sertoli cell MT organization, illustrating these two cytoskeletons are intimately engaged in the testis to support BTB dynamics during spermatogenesis. In fact, a recent report using the adjudin model has demonstrated the actin- and MT-based cytoskeletons are working closely together to support both germ cell adhesion and the transport of germ cells and other organelles (e.g., residual bodies, phagosomes, endocytic vesicles) across the seminiferous epithelium including the BTB during the epithelial cycle of spermatogenesis [13]. Future research shall explore the signaling molecules and/or pathways that are involved in modulating these actin- and MT-binding/regulatory proteins.

Acknowledgments

This work was supported by grants from the National Institutes of Health (NICHD R01 HD056034 to C.Y.C.; U54 HD029990 Project 5 to C.Y.C.); Hong Kong Research Grants Council (RGC)/National Natural Science Foundation of China Joint Research Scheme (N_HKU 717/12) to W.M.L., and Hong Kong University Seed Funding to W.M.L.; W.Q. was supported in part from The F. Lau Memorial Fellowship, The Noopolis Foundation, and The Economic Development Council.

References

1. Cheng CY, Mruk DD (2012) The blood-testis barrier and its implication in male contraception. Pharmacol Rev 64:16–64
2. Pelletier RM (2011) The blood-testis barrier: the junctional permeability, the proteins and the lipids. Prog Histochem Cytochem 46:49–127
3. Stanton PG (2016) Regulation of the blood-testis barrier. Semin Cell Dev Biol 59:166–173. https://doi.org/10.1016/j.semcdb.2016.06.018
4. Mruk DD, Cheng CY (2015) The mammalian blood-testis barrier: its biology and regulation. Endocr Rev 36(5):564–591. https://doi.org/10.1210/er.2014-1101
5. O'Donnell L, O'Bryan MK (2014) Microtubules and spermatogenesis. Semin Cell Dev Biol 30:45–54. https://doi.org/10.1016/j.semcdb.2014.01.003
6. O'Donnell L (2014) Mechanisms of spermiogenesis and spermiation and how they are disturbed. Spermatogenesis 4(2):e979623. https://doi.org/10.4161/21565562.2014.979623
7. Tang EI, Mruk DD, Cheng CY (2013) MAP/microtubule affinity-regulating kinases, microtubule dynamics, and spermatogenesis. J Endocrinol 217:R13–R23
8. Tang EI, Mruk DD, Lee WM, Cheng CY (2015) Cell-cell interactions, cell polarity, and the blood-testis barrier. In: Ebnet K (ed) Cell polarity 1. Springer International Publishing, Geneva, pp 303–326. https://doi.org/10.1007/978-3-319-14463-4_13

9. Tang EI, Mruk DD, Cheng CY (2016) Regulation of microtubule (MT)-based cytoskeleton in the seminiferous epithelium during spermatogenesis. Semin Cell Dev Biol 59:35–45. https://doi.org/10.1016/j.semcdb.2016.01.004
10. Lie PPY, Mruk DD, Lee WM, Cheng CY (2010) Cytoskeletal dynamics and spermatogenesis. Philos Trans R Soc Lond B Biol Sci 365:1581–1592
11. Vogl AW, Vaid KS, Guttman JA (2008) The Sertoli cell cytoskeleton. Adv Exp Med Biol 636:186–211
12. Wen Q et al (2016) Transport of germ cells across the seminiferous epithelium during spermatogenesis—the involvement of both actin- and microtubule-based cytoskeletons. Tissue Barriers 4(4):e1265042. https://doi.org/10.1080/21688370.2016.1265042
13. Tang EI, Lee WM, Cheng CY (2016) Coordination of actin- and microtubule-based cytoskeletons supports transport of spermatids and residual bodies/phagosomes during spermatogenesis in the rat testis. Endocrinology 157(4):1644–1659. https://doi.org/10.1210/en.2015-1962
14. Li N, Wong CK, Cheng CY (2016) Plastins regulate ectoplasmic specialization via its actin bundling activity on microfilaments in the rat testis. Asian J Androl 18:716–722. https://doi.org/10.4103/1008-682X.166583
15. Li N, Mruk DD, Tang EI, Lee WM, Wong CK, Cheng CY (2016) Formin 1 regulates microtubule and F-actin organization to support spermatid transport during spermatogenesis in the rat testis. Endocrinology 157:2894–2908. https://doi.org/10.1210/en.2016-1133
16. Li N, Lee WM, Cheng CY (2016) Overexpression of plastin 3 in Sertoli cells disrupts actin microfilament bundle homeostasis and perturbs the tight junction barrier. Spermatogenesis 6(1):e1206353. https://doi.org/10.1080/21565562.2016.1206353
17. Lie PPY, Chan AYN, Mruk DD, Lee WM, Cheng CY (2010) Restricted Arp3 expression in the testis prevents blood-testis barrier disruption during junction restructuring at spermatogenesis. Proc Natl Acad Sci USA 107:11411–11416
18. Li N, Mruk DD, Wong CKC, Han D, Lee WM, Cheng CY (2015) Formin 1 regulates ectoplasmic specialization in the rat testis through its actin nucleation and bundling activity. Endocrinology 156:2969–2983
19. Li N, Mruk DD, Cheng CY (2015) Actin binding proteins in blood-testis barrier function. Curr Opin Endocrinol Diabetes Obes 22:238–247
20. Li N, Tang EI, Cheng CY (2016) Regulation of blood-testis barrier by actin binding proteins and protein kinases. Reproduction 151(3):R29–R41. https://doi.org/10.1530/REP-15-0463
21. Hess RA, de Franca LR (2008) Spermatogenesis and cycle of the seminiferous epithelium. Adv Exp Med Biol 636:1–15
22. Xiao X, Mruk DD, Wong CKC, Cheng CY (2014) Germ cell transport across the seminiferous epithelium during spermatogenesis. Physiology 29(4):286–298. https://doi.org/10.1152/physiol.00001.2014
23. Zhou F, Leder P, Martin SS (2006) Formin-1 protein associates with microtubules through a peptide domain encoded by exon-2. Exp Cell Res 312(7):1119–1126. https://doi.org/10.1016/j.yexcr.2005.12.035
24. Lie PPY, Mruk DD, Lee WM, Cheng CY (2009) Epidermal growth factor receptor pathway substrate 8 (Eps8) is a novel regulator of cell adhesion and the blood-testis barrier integrity in the seminiferous epithelium. FASEB J 23:2555–2567
25. Qian X, Mruk DD, Wong EWP, Lie PPY, Cheng CY (2013) Palladin is a regulator of actin filament bundles at the ectoplasmic specialization in the rat testis. Endocrinology 154:1907–1920
26. Johnson KJ (2014) Testicular histopathology associated with disruption of the Sertoli cell cytoskeleton. Spermatogenesis 4:e979106. https://doi.org/10.4161/21565562.2014.979106
27. Heindel JJ (2006) Role of exposure to environmental chemicals in the developmental basis of reproductive disease and dysfunction. Semin Reprod Med 24:156–167
28. Boekelheide K (1993) Sertoli cell toxicants. In: Russell L, Griswold M (eds) The sertoli cell. Cache River Press, Clearwater, pp 551–575
29. Boekelheide K et al (2003) 2,5-Hexanedione-induced testicular injury. Annu Rev Pharmacol Toxciol 43:125–147
30. Yan HHN, Mruk DD, Wong EWP, Lee WM, Cheng CY (2008) An autocrine axis in the testis that coordinates spermiation and blood-testis barrier restructuring during spermatogenesis. Proc Natl Acad Sci USA 105:8950–8955
31. Su L, Mruk DD, Lie PPY, Silvestrini B, Cheng CY (2012) A peptide derived from laminin-γ3 reversibly impairs spermatogenesis in rats. Nat Communs 3:1185. https://doi.org/10.1038/ncomms2171
32. Gao Y, Mruk DD, Lui WY, Lee WM, Cheng CY (2016) F5-peptide induces aspermatogenesis by disrupting organization of actin- and microtubule-based cytoskeletons in the testis. Oncotarget 7:64203–64220
33. Wong EWP, Cheng CY (2013) NC1 domain of collagen α3(IV) derived from the basement membrane regulates Sertoli cell blood-testis

barrier dynamics. Spermatogenesis 3:e25465. https://doi.org/10.4161/spmg.25465. PMID:23885308; PMCID:PMC23710226

34. Gao Y, Mruk D, Chen H, Lui WY, Lee WM, Cheng CY (2017) Regulation of the blood-testis barrier by a local axis in the testis: role of laminin alpha2 in the basement membrane. FASEB J 31:584–597. https://doi.org/10.1096/fj.201600870R
35. Gao Y, Chen H, Lui WY, Lee WM, Cheng CY (2017) Basement membrane laminin α2 regulation of BTB dynamics via its effects on F-actin and microtubule (MT) cytoskeletons is mediated through mTORC1 signaling. Endocrinology 158:963–978. https://doi.org/10.1210/en.2016-1630
36. Yao PL, Lin YC, Richburg JH (2010) Mono-(2-ethylhexyl) phthalate-induced disruption of junctional complexes in the seminiferous epithelium of the rodent testis is mediated by MMP2. Biol Reprod 82:516–527
37. Yao PL, Lin YC, Richburg JH (2009) TNFα-mediated disruption of spermatogenesis in response to Sertoli cell injury in rodents is partially regulated by MMP2. Biol Reprod 80:581–589
38. Siu MKY, Cheng CY (2004) Interactions of proteases, protease inhibitors, and the β1 integrin/laminin γ3 protein complex in the regulation of ectoplasmic specialization dynamics in the rat testis. Biol Reprod 70:945–964
39. Siu MKY, Lee WM, Cheng CY (2003) The interplay of collagen IV, tumor necrosis factor-α, gelatinase B (matrix metalloprotease-9), and tissue inhibitor of metalloprotease-1 in the basal lamina regulates Sertoli cell-tight junction dynamics in the rat testis. Endocrinology 144:371–387
40. Chen H, Mruk DD, Xiao X, Cheng CY (2017) Human spermatogenesis and its regulation. In: Winters SJ, Huhtaniemi IT (eds) Male hypogonadism, contemporary endocrinology. Springer International Publishing AG, New York, pp 1–24. https://doi.org/10.1007/978-3-319-53298-1_3
41. Sharpe RM (1994) Regulation of spermatogenesis. In: Knobil E, Neill JD (eds) The physiology of reproduction. Raven Press, New York, pp 1363–1434
42. O'Donnell L, Meachem SJ, Stanton PG, McLachlan RI (2006) Endocrine regulation of spermatogenesis. In: Neill JD (ed) Physiology of reproduction, 3rd edn. Elsevier, Amsterdam, pp 1017–1069
43. O'Donnell L, Robertson KM, Jones ME, Simpson ER (2001) Estrogen and spermatogenesis. Endocr Rev 22:289–318
44. McLachlan RI, O'Donnell L, Meachem SJ, Stanton PG, de Kretser DM, Pratis K, Robertson DM (2002) Hormonal regulation of spermatogenesis in primates and man: insights for development of the male hormonal contraceptive. J Androl 23:149–162
45. Easton AS (2012) Regulation of permeability across the blood-brain barrier. Adv Exp Med Biol 763:1–19
46. Campbell M, Humphries P (2012) The blood-retina barrier: tight junctions and barrier modulation. Adv Exp Med Biol 763:70–84
47. Dore-Duffy P, Cleary K (2011) Morphology and properties of pericytes. Methods Mol Biol 686:49–68. https://doi.org/10.1007/978-1-60761-938-3_2
48. Winkler EA, Bell RD, Zlokovic BV (2011) Central nervous system pericytes in health and disease. Nat Neurosci 14(11):1398–1405. https://doi.org/10.1038/nn.2946
49. Cheng CY, Mruk DD (2010) A local autocrine axis in the testes that regulates spermatogenesis. Nature Rev Endocrinol 6:380–395
50. Setchell BP (2008) Blood-testis barrier, functional and transport proteins and spermatogenesis. Adv Exp Med Biol 636:212–233
51. Mruk DD, Cheng CY (2011) Desmosomes in the testis. Moving into an unchartered territory. Spermatogenesis 1:47–51
52. Livne A, Geiger B (2016) The inner workings of stress fibers—from contractile machinery to focal adhesions and back. J Cell Sci 129(7):1293–1304. https://doi.org/10.1242/jcs.180927
53. Spence EF, Soderling SH (2015) Actin out: regulation of the synaptic cytoskeleton. J Biol Chem 290(48):28613–28622. https://doi.org/10.1074/jbc.R115.655118
54. Pizarro-Cerda J, Chorev DS, Geiger B, Cossart P (2017) The diverse family of Arp2/3 complexes. Trends Cell Biol 27(2):93–100. https://doi.org/10.1016/j.tcb.2016.08.001
55. Dominguez R (2016) The WH2 domain and actin nucleation: necessary but insufficient. Trends Biochem Sci 41(6):478–490. https://doi.org/10.1016/j.tibs.2016.03.004
56. Cheng CY, Mruk DD (2011) Regulation of spermiogenesis, spermiation and blood-testis barrier dynamics: novel insights from studies on Eps8 and Arp3. Biochem J 435:553–562
57. Qian X, Mruk DD, Cheng YH, Cheng CY (2013) Actin cross-linking protein palladin and spermatogenesis. Spermatogenesis 3:e23473. https://doi.org/10.4161/spmg.23473
58. Qian X, Mruk DD, Cheng YH, Cheng CY (2013) RAI14 (retinoic acid induced protein 14) is an F-actin regulator—lesson from the testis. Spermatogenesis 3:e24824
59. Li SY, Mruk DD, Cheng CY (2013) Focal adhesion kinase is a regulator of F-actin dynamics: new insights from studies in the testis. Spermatogenesis 3(3):e25385. https://doi.org/10.4161/spmg.25385

60. Vogl AW, Young JS, Du M (2013) New insights into roles of tubulobulbar complexes in sperm release and turnover of blood-testis barrier. Int Rev Cell Mol Biol 303:319–355
61. Vogl AW, Du M, Wang XY, Young JS (2014) Novel clathrin/actin-based endocytic machinery associated with junction turnover in the seminiferous epithelium. Semin Cell Dev Biol 30:55–64
62. Russell LD (1979) Observations on the interrelationships of Sertoli cells at the level of the blood-testis barrier: evidence for formation and resorption of Sertoli-Sertoli tubulobulbar complexes during the spermatogenic cycle of the rat. Am J Anat 155:259–279
63. Xiao X, Mruk DD, Wong EWP, Lee WM, Han D, Wong CKC, Cheng CY (2014) Differential effects of c-Src and c-Yes on the endocytic vesicle-mediated trafficking events at the Sertoli cell blood-testis barrier: an in vitro study. Am J Physiol Endocrinol Metab 307:E553–E562
64. Zeller R et al (1999) Formin defines a large family of morphorgulatory genes and functions in establishment of the polarising region. Cell Tissue Res 296:85–93
65. Baarlink C, Brandt D, Grosse R (2010) SnapShot: formins. Cell 142:172
66. Grikscheit K, Grosse R (2016) Formins at the junction. Trends Biochem Sci 41(2):148–159. https://doi.org/10.1016/j.tibs.2015.12.002
67. Woychik RP, Maas RL, Zeller R, Vogt TF, Leder P (1990) 'Formins': proteins deduced from the alternative transcripts of the limb deformity gene. Nature 346:850–853
68. Kobielak A, Pasolli HA, Fuchs E (2004) Mammalian formin-1 participates in adherens junctions and polymerization of linear actin cables. Nat Cell Biol 6:21–30
69. Li N, Mruk DD, Tang EI, Wong CKC, Lee WM, Silvestrini B, Cheng CY (2015) Formins: actin nucleators that regulate cytoskeletal dynamics during spermatogenesis. Spermatogenesis 5:e1066476. https://doi.org/10.1080/21565562.2015.1066476
70. Goode BL, Eck MJ (2007) Mechanism and function of formins in the control of actin assembly. Annu Rev Biochem 76:593–627
71. Breitsprecher D, Goode BL (2013) Formins at a glance. J Cell Sci 126(Pt 1):1–7. https://doi.org/10.1242/jcs.107250
72. Bohnert KA, Willet AH, Kovar DR, Gould KL (2013) Formin-based control of the actin cytoskeleton during cytokinesis. Biochem Soc Trans 41(6):1750–1754. https://doi.org/10.1042/BST20130208
73. Quinlan ME, Heuser JE, Kerkhoff E, Mullins RD (2005) *Drosophila* spire is an actin nucleation factor. Nature 433:382–388
74. Vizcarra CL et al (2011) Structure and function of the interacting domains of Spre and Fmn-family formins. Proc Natl Acad Sci U S A 108:11884–11889
75. Quinlan ME, Hilgert S, Bedrossian A, Mullins RD, Kerkhoff E (2007) Regulatory interactions between two actin nucleators, Spire and Cappuccino. J Cell Biol 179:117–128
76. Dietrich S, Weiβ S, Pleiser S, Kerkhoff E (2013) Structural and functional insights into the Spir/formin actin nucleator complex. Biol Chem 394(12):1649–1660. https://doi.org/10.1515/hsz-2013-0176
77. Carlier MF, Husson C, Renault L, Didry D (2011) Control of actin assembly by the WH2 domains and their multifunctional tandem repeats in Spire and Cordon-Bleu. Int Rev Cell Mol Biol 290:55–85. https://doi.org/10.1016/B978-0-12-386037-8.00005-3
78. Carlier MF, Pernier J, Montaville P, Shekhar S, Kuhn S, Cytoskeleton D, Motility G (2015) Control of polarized assembly of actin filaments in cell motility. Cell Mol Life Sci 72(16):3051–3067. https://doi.org/10.1007/s00018-015-1914-2
79. Xiao X, Wong EWP, Lie PPY, Mruk DD, Wong CKC, Cheng CY (2014) Cytokines, polarity proteins and endosomal protein trafficking and signaling—the Sertoli cell blood-testis barrier *in vitro* as a study model. Methods Enzymol 534:181–194
80. Su WH, Mruk DD, Cheng CY (2013) Regulation of actin dynamics and protein trafficking during spermatogenesis—insights into a complex process. Crit Rev Biochem Mol Biol 48:153–172
81. Tang EI, Mok KW, Lee WM, Cheng CY (2015) EB1 regulates tubulin and actin cytoskeletal networks at the Sertoli cell blood-testis barrier in male rats—an in vitro study. Endocrinology 156:680–693
82. Akhmanova A, Steinmetz MO (2015) Control of microtubule organization and dynamics: two ends in the limelight. Nat Rev Mol Cell Biol 16(12):711–726. https://doi.org/10.1038/nrm4084
83. Nehlig A, Molina A, Rodrigues-Ferreira S, Honore S, Nahmias C (2017) Regulation of end-binding protein EB1 in the control of microtubule dynamics. Cell Mol Life Sci 74(13):2381–2393. https://doi.org/10.1007/s00018-017-2476-2
84. Bowne-Anderson H, Hibbel A, Howard J (2015) Regulation of microtubule growth and catastrophe: unifying theory and experiment. Trends Cell Biol 25(12):769–779. https://doi.org/10.1016/j.tcb.2015.08.009

Chapter 17

Monitoring the Integrity of the Blood-Testis Barrier (BTB): An In Vivo Assay

Haiqi Chen, Wing-yee Lui, Dolores D. Mruk, Xiang Xiao, Renshan Ge, Qingquan Lian, Will M. Lee, Bruno Silvestrini, and C. Yan Cheng

Abstract

The blood-testis barrier is a unique ultrastructure in the mammalian testis, located near the basement membrane of the seminiferous tubule that segregates the seminiferous epithelium into the basal and the adluminal (apical) compartment. Besides restricting paracellular and transcellular passage of biomolecules (e.g., paracrine factors, hormones), water, electrolytes, and other substances including toxicants and/or drugs to enter the adluminal compartment of the epithelium, the BTB is an important ultrastructure that supports spermatogenesis. As such, a sensitive and reliable assay to monitor its integrity in vivo is helpful for studying testis biology. This assay is based on the ability of an intact BTB to exclude the diffusion of a small molecule such as sulfo-NHS-LC-biotin ($C_{20}H_{29}N_4NaO_9S_2$, Mr. 556.59, a water-soluble and membrane-impermeable biotinylation reagent) from the basal to the apical compartment of the seminiferous epithelium. Herein, we summarize the detailed procedures on performing the assay and to obtain semiquantitative data to assess the extent of BTB damage when compared to positive controls, such as treatment of rats with cadmium chloride ($CdCl_2$) which is known to compromise the BTB integrity.

Key words Testis, Blood-testis barrier, Spermatogenesis, Sertoli cells, Tight junction, Ectoplasmic specialization, Actin filaments, Assay

1 Introduction

When small electron-dense substances are loaded into the blood vessel, the blood-testis barrier (BTB) is known to exclude their diffusion across the barrier from entering the seminiferous tubules for more than a century (for reviews, *see* [1, 2]). For instance, when peroxidase was injected into the testicular interstitium, the majority of the enzyme was accumulated in the lamina propria of the seminiferous tubules, in the intercellular spaces of the Leydig cells and in the lymphatic capillaries, and virtually no peroxidase was detected in the adluminal (apical) compartment of the seminiferous tubules [3]. The BTB is almost exclusively contributed by Sertoli cells which are the epithelial cells of the seminiferous epithelium even though peritubular myoid cells in rodents

Marco G. Alves and Pedro F. Oliveira (eds.), *Sertoli Cells: Methods and Protocols*, Methods in Molecular Biology, vol. 1748, https://doi.org/10.1007/978-1-4939-7698-0_17,

(but not primates) are known to confer part of the barrier function (for a review, *see* [1]). Studies have shown that the BTB is constituted by coexisting actin-based tight junction (TJ), basal ectoplasmic specialization (basal ES, a testis-specific atypical adherens junction) and gap junction, as well as intermediate filament-based desmosome [2, 4–8]. Under physiological conditions, the BTB is under precise regulation by different signaling molecules and signal pathways [9, 10], so that it remains tightly "sealed" at different stages of the seminiferous epithelial cycle including stage VIII when preleptotene spermatocytes connected in clones via intercellular bridges are to be transported across the immunological barrier [11–13]. Nonetheless, the BTB can be compromised during virus infection such as Zika [14] and HIV [15] such that these viruses can use the testis as a safe haven. In fact, the testis serves as one of the viral reservoirs, preventing HIV-1 eradication even though the serum viral load is virtually undetectable [16, 17]. Additionally, environmental toxicants (e.g., cadmium, bisphenol A, PFOS) are also known to induce BTB disruption [18, 19]. Studies have shown that scrotal heat stress [20], electromagnetic pulse irradiation [21], and reduced intratesticular testosterone level [22, 23] also play a role in perturbing the Sertoli cell BTB function in vivo. More importantly, BTB disruption is often associated with impaired spermatogenesis in particular germ cell exfoliation and hence subfertility and/or infertility [24, 25]. Collectively, these findings illustrate that a simple, reliable, and noninvasive assay that monitors BTB integrity in vivo would be of great help to investigators in the field.

An earlier version of the in vivo BTB integrity assay requires the use of a small fluorescence probe such as FITC (Mr 389.39) alone or inulin-FITC (Mr ~5 kDa) which was administered into the rats via the jugular vein under anesthesia using ketamine HCl/xylazine [26, 27]. This assay is based on the ability of an intact BTB to block the diffusion of either FITC or inulin-FITC conjugate from entering the apical compartment from the interstitial space so that the fluorescence tag was limited to the basal compartment near the basement membrane in the tunica propria. The extent of the BTB disruption is thus quantified by comparing the distance traveled by FITC or inulin-FITC *versus* the radius of the seminiferous tubule. However, this is an invasive procedure that requires an administration of either FITC or inulin-FITC via the jugular vein. The procedure is time-consuming and requires researchers to receive relevant recovery surgical training. Moreover, since FITC or inulin-FITC is released into the whole body through circulation following administration, the amount of FITC or inulin-FITC that eventually accumulates around the seminiferous tubules in the testis is limited, making the green fluorescence tracking by fluorescence microscopy less optimal and requiring a lengthy exposure time of ~10–15 s to capture optimal images. Herein, we describe an easy to perform and highly reproducible procedure of the BTB integrity assay based on two earlier reports with minor

modifications [23, 28]. Instead of using FITC or inulin-FITC, a membrane-impermeable protein biotinylation reagent sulfo-NHS-LC-biotin is used based on the similar idea that biotin can be retained by an intact BTB. This assay is easy to manage since the sulfo-NHS-LC-biotin is aqueous soluble and a small aliquot of the biotin reagent can be loaded onto the testis under the tunica albuginea through the scrotum using a 28-gauge needle. Furthermore, since the sulfo-NHS-LC-biotin is loaded directly into the testis locally instead of through the systemic circulation, relatively small amount of the reagent is needed. Thereafter, cross sections of testes are obtained using frozen testes in a cryostat, and fluorescence signal is considerably enhanced by incubating cross sections with fluorophore-conjugated streptavidin.

2 Materials

2.1 Animal Surgical Procedures

1. Ketamine hydrochloride (800 mg)/xylazine hydrochloride (120 mg) mixture in 10-ml double distilled water (note: xylazine is an analgesic and a muscle relaxant).
2. EZ-Link™ Sulfo-NHS-LC-Biotin.
3. Cadmium chloride.
4. Insulin syringe (28 gauge).

2.2 Sample Preparation and Image Requisition

1. Standard cryostat operating at −22 °C.
2. Paraformaldehyde.
3. Streptavidin, Alexa Fluor® 555 conjugate (red fluorescence) (streptavidin conjugated with other types of fluorophore is also suitable based on specific experimental needs).
4. Standard wide-field microscope or confocal microscope.

3 Methods

3.1 Pre-surgery Setup

1. Treat a group of adult Sprague-Dawley male rats (or other rodents based on specific experimental needs) (n = 3, ~270–300 gm b.w.) with $CdCl_2$ (3 mg/kg b.w., i.p.) which is known to induce irreversible BTB disruption [29, 30] about 2 to 3 days before surgery. This group of rats serves as a positive control.
2. On the day of surgery, each rat (~270–300 gm b.w.) receives 400 μl mixture of ketamine hydrochloride with xylazine hydrochloride so that the final concentration of ketamine hydrochloride is 32 mg per rat (i.e., 80 mg/ml) and the xylazine hydrochloride is 4.8 mg per rat (i.e., 12 mg/ml).

3. Clean area for surgery with Betadine, to be followed by 70% ethanol, and cover the area with clean tissue towel. Turn on a heat lamp to maintain proper temperature of the surgical area. Use sterile scissors and forceps for all procedures.
4. Maintain a clean rest area (with animal beddings) with a heat lamp so that anesthetized rats can maintain its body temperature.
5. Freshly prepare a stock of 10 mg/ml EZ-Link™ sulfo-NHS-LC-biotin in PBS (10 mM sodium phosphate, 0.15 M NaCl) containing 1 mM $CaCl_2$.

3.2 Surgery

1. Weigh rats and record.
2. Inject ketamine/xylazine anesthetic mixture (~400 μl per rat at ~300 gm b.w.) intramuscularly onto his right thigh using the 28-gauge insulin needle. It usually takes ~1–2 min before rats are under anesthesia. Turn on heat lamp to maintain normal body temperature of the anesthetized rats. Keep rats in a clean rest area (with animal beddings).
3. Allow injected rats to rest for 5–10 min. Observe the loss of eye reflex response and maintenance of a steady breathing pattern to ensure rats are under complete anesthesia. Move rats to the surgery area, with their head/eye area covered with a moist tissue paper to avoid eye injury.
4. Ensure both testes have descended to the scrotum. Rinse scrotal area with 70% ethanol.
5. Expose testes by making a small incision of approximately 1 cm in the middle of the scrotum.
6. Load 100 μl of EZ-Link™ sulfo-NHS-LC-biotin (at 10 mg/ml, biotin reagent dissolved in PBS containing 1 mM $CaCl_2$) stock gently under the tunica albuginea using a 28-gauge insulin syringe.
7. After biotin reagent administration, move rats to a clean rest area.
8. Allow rats to rest for 30 min. These rats remain under anesthesia for at least ~40–50 min.

3.3 Sample Preparation

1. After 30 min, euthanize rats by CO_2 asphyxiation using slow displacement of chamber air with compressed carbon dioxide from a CO_2 tank at 20–30% per min.
2. Following euthanasia, remove testes from the scrotum using a pair of sharp scissors, immediately rinse each testis in ~20-ml ice-cold PBS in a Petri dish to remove any blood contamination (only handle the testis with a pair of forceps, avoiding touching the organ with hands).

3. Snap-freeze each testis in liquid nitrogen and store them in labeled specimen bags at −80 °C.
4. Cut 7 μm-thick frozen cross sections of the testes in a cryostat at −22 °C.
5. Fix frozen cross sections of the testes at room temperature (RT) in 4% PFA (paraformaldehyde) (in PBS, 10 mM sodium phosphate, 0.15 M NaCl, pH 7.4 at 22 °C) (w/v) for 10 min.
6. Wash cross sections with PBS, three times at RT.
7. Stain cross sections with Alexa Fluor 555-streptavidin at a dilution of 1:250 for 30 min at RT.
8. Wash cross sections with PBS for three times at RT.
9. Stain cell nuclei in cross sections with 4′,6-diamidino-2-phenylindole (DAPI).

3.4 Image Requisition and Data Analysis

1. Acquire images using a standard fluorescence microscope or confocal microscope. Typical images are shown in Fig. 1, illustrating the intact BTB in normal rat testes which blocks the diffusion of biotin across the barrier to enter the adluminal compartment. However, the BTB which has been disrupted by cadmium treatment fails to block the diffusion of biotin across the immunological barrier.
2. To semi-quantify the extent of BTB damage, measure the distance traveled by biotin in the tubule (D_{Biotin}) and the radius of the same tubule (D_{Radius}). For an oval-shaped tubule, the radius is the average of the shortest and the longest distance of the tubule. The extent of the BTB damage (E) can be expressed in percentage (n = 3 rats, a total of ~150–300 randomly selected tubules) as:

$$\mathrm{E} = \left[D_{\text{Biotin}} / D_{\text{Radius}} \right] \times 100\%$$

3. At least 50–100 tubules are randomly selected and quantified from a total of n = 3 rats with a total of 150–300 tubules.
4. Calculate the E for each experimental group, and compare each group using appropriate statistical method.

Acknowledgments

This work was supported by grants from the National Institutes of Health, NICHD R01 HD056034 to C.Y.C., and U54 HD029990 Project 5 to C.Y.C.; Hong Kong Research Grants Council (RGC)/National Natural Science Foundation of China Joint Research Scheme (N_HKU 717/12) to W.M.L., Hong Kong RGC Grant GRF17100816 to W.Y.L. and GRF 771513 to W.M.L., Hong

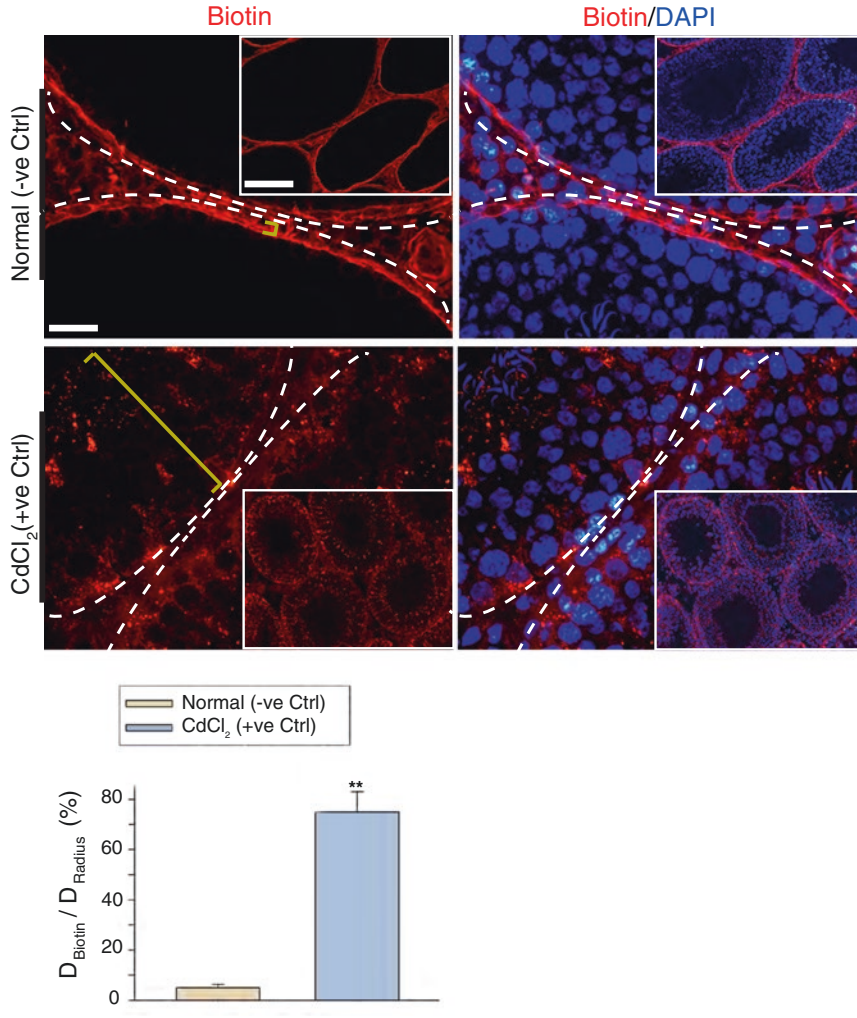

Fig. 1 A study to assess the BTB integrity based on an in vivo functional assay. A membrane-impermeable protein biotinylation reagent sulfo-NHS-LC-biotin was loaded under the tunica albuginea of the rat testis under anesthesia using ketamine HCl/xylazine. The sulfo-NHS-LC-biotin rapidly diffused across the entire testis. An intact BTB blocked the passage of biotin into the apical compartment of the seminiferous epithelium. Thus, the biotin (red fluorescence) was detected near the basement membrane of the seminiferous tubules and the interstitial space as noted in the normal (−ve Ctrl) testis group. However, in the positive control group wherein rats were treated with $CdCl_2$ at 3 mg/kg b.w. by i.p. (for 3 days) which was earlier shown to induce irreversible disruption of the BTB [29, 31], biotin diffused into the apical compartment of the seminiferous epithelium. The yellow bracket indicates the distance traveled by biotin. Basement membrane was annotated by dashed white lines. Image in inset is the lower magnified view of the testis cross section. Scale bar, 30 μm; 220 μm in insets. The bar graph below summarizes the semi-quantified data regarding the extent of BTB damage (E) shown in the representative micrographs above between normal (−ve Ctrl) group and $CdCl_2$-treated (+ve Ctrl) group. D_{Biotin}, Distance traveled by biotin in the tubule; D_{Radius}, the radius of the same tubule. **, $p < 0.01$ by student's *t*-test

Kong University Seed Funding to W.Y.L. and W.M.L.; NSFC Grant 81730042 to R.S.G. and NSFC Grant 31371176 to X.X., and Zhejiang Province Department of Science Technology Funding 2016F10010 to X.X.; H.C. was supported in part by The S.Y. Law Memorial Fellowship and The F. Lau Memorial Fellowship.

References

1. Setchell BP (2008) Blood-testis barrier, functional and transport proteins and spermatogenesis. Adv Exp Med Biol 636:212–233
2. Cheng CY, Mruk DD (2012) The blood-testis barrier and its implication in male contraception. Pharmacol Rev 64:16–64
3. Aoki A, Fawcett DW (1975) Impermeability of sertoli cell junctions to prolonged exposure to peroxidase. Andrologia 7:63–76
4. Mruk DD, Cheng CY (2004) Sertoli-Sertoli and Sertoli-germ cell interactions and their significance in germ cell movement in the seminiferous epithelium during spermatogenesis. Endocr Rev 25:747–806
5. Pelletier RM (2011) The blood-testis barrier: the junctional permeability, the proteins and the lipids. Prog Histochem Cytochem 46:49–127
6. Franca LR, Auharek SA, Hess RA, Dufour JM, Hinton BT (2012) Blood-tissue barriers: morphofunctional and immunological aspects of the blood-testis and blood-epididymal barriers. Adv Exp Med Biol 763:237–259
7. Kaur G, Thompson LA, Dufour JM (2014) Sertoli cells–immunological sentinels of spermatogenesis. Semin Cell Dev Biol 30:36–44
8. Stanton PG (2016) Regulation of the blood-testis barrier. Semin Cell Dev Biol 59:166–173. https://doi.org/10.1016/j.semcdb.2016.06.018
9. Li N, Tang EI, Cheng CY (2016) Regulation of blood-testis barrier by actin binding proteins and protein kinases. Reproduction 151(3):R29–R41. https://doi.org/10.1530/REP-15-0463
10. Lie PPY, Cheng CY, Mruk DD (2013) Signalling pathways regulating the blood-testis barrier. Int J Biochem Cell Biol 45:621–625
11. Xiao X, Mruk DD, Wong CKC, Cheng CY (2014) Germ cell transport across the seminiferous epithelium during spermatogenesis. Physiology 29(4):286–298. https://doi.org/10.1152/physiol.00001.2014
12. Chen H, Cheng CY (2016) Planar cell polarity (PCP) proteins and spermatogenesis. Semin Cell Dev Biol 59:99–109. https://doi.org/10.1016/j.semcdb.2016.04.010
13. Smith BE, Braun RE (2012) Germ cell migration across Sertoli cell tight junctions. Science 338:798–802
14. Govero J et al (2016) Zika virus infection damages the testes in mice. Nature 540:438–442
15. Jenabian MA et al (2016) Immune tolerance properties of the testicular tissue as a viral sanctuary site in ART-treated HIV-infected adults. AIDS 30(18):2777–2786. https://doi.org/10.1097/QAD.0000000000001282
16. Darcis G, Coombs RW, Van Lint C (2016) Exploring the anatomical HIV reservoirs: role of the testicular tissue. AIDS 30(18):2891–2893. https://doi.org/10.1097/QAD.0000000000001281
17. Eisele E, Siliciano RF (2012) Redefining the viral reservoirs that prevent HIV-1 eradication. Immunity 37:377–388
18. Siu ER, Mruk DD, Porto CS, Cheng CY (2009) Cadmium-induced testicular injury. Toxicol Appl Pharmacol 238(3):240–249
19. Wan HT, Mruk DD, Wong CKC, Cheng CY (2014) Perfluorooctanesulfonate (PFOS) perturbs male rat Sertoli cell blood-testis barrier function by affecting F-actin organization via p-FAK-Tyr^{407}–an *in vitro* study. Endocrinology 155:249–262
20. Cai H et al (2011) Scrotal heat stress causes a transient alteration in tight junctions and induction of TGF-beta expression. Int J Androl 34:352–362
21. Hou WG, Zhao J, Li Z, Li W, Li T, Xiong LZ, Zhang YQ (2012) Effects of electromagnetic pulse irradiation on the mouse blood-testicle barrier. Urology 80(1):225 e221–225 e226
22. Smith LB, Walker WH (2014) The regulation of spermatogenesis by androgens. Semin Cell Dev Biol 30:2–13. https://doi.org/10.1016/j.semcdb.2014.02.012
23. Meng J, Holdcraft RW, Shima JE, Griswold MD, Braun RE (2005) Androgens regulate the permeability of the blood-testis barrier. Proc Natl Acad Sci U S A 102:16696–16700
24. Xiao X et al (2014) N-wasp is required for structural integrity of the blood-testis barrier. PLoS Genet 10:e1004447
25. Mruk DD, Cheng CY (2015) The mammalian blood-testis barrier: its biology and regulation. Endocr Rev 36:564–591
26. Li MW et al (2006) Tumor necrosis factor {alpha} reversibly disrupts the blood-testis

barrier and impairs Sertoli-germ cell adhesion in the seminiferous epithelium of adult rat testes. J Endocrinol 190:313–329

27. Sarkar O, Mathur PP, Cheng CY, Mruk DD (2008) Interleukin 1 alpha (IL1A) is a novel regulator of the blood-testis barrier in the rat. Biol Reprod 78:445–454
28. Furuse M et al (2002) Claudin-based tight junctions are crucial for the mammalian epidermal barrier: a lesson from claudin-1-deficient mice. J Cell Biol 156:1099–1111
29. Wong CH, Mruk DD, Lui WY, Cheng CY (2004) Regulation of blood-testis barrier dynamics: an *in vivo* study. J Cell Sci 117:783–798
30. Lui WY, Lee WM, Cheng CY (2001) Transforming growth factor-b3 perturbs the inter-Sertoli tight junction permeability barrier *in vitro* possibly mediated via its effects on occludin, zonula occludens-1, and claudin-11. Endocrinology 142:1865–1877
31. Lui WY, Wong CH, Mruk DD, Cheng CY (2003) TGF-b3 regulates the blood-testis barrier dynamics via the p38 mitogen activated protein (MAP) kinase pathway: an *in vivo* study. Endocrinology 144:1139–1142

Chapter 18

Computational Methods Involved in Evaluating the Toxicity of the Reproductive Toxicants in Sertoli Cell

Pranitha Jenardhanan, Manivel Panneerselvam, and Premendu P. Mathur

Abstract

The Sertoli cell, the somatic component of seminiferous tubule, provides nutritional support and immunological protection and supports overall growth and division of germ cells. Cytoskeletons, junction proteins, and kinases in Sertoli cells are prime targets for reproductive toxicants and other environmental contaminants. Among the varied targets, the kinases that are crucial for regulating varied activities in spermatogenesis such as assembly/disassembly of blood-testis barrier and apical ES and those that are involved in conferring polarity are highly targeted. In an attempt to study the effect of toxicants on these kinases, the present chapter deals with computational methodology concerning their three-dimensional structure prediction, identification of inhibitors, and understanding of conformational changes induced by these inhibitors.

Key words Sertoli cells, Reproductive toxicants, Tyrosine kinases, Serine/threonine kinases, Type II and type III kinase inhibitors, Nonhormonal male contraceptives

1 Introduction

The Sertoli cell is the only somatic component in the seminiferous tubules of the testis that serves to support the growth, division, differentiation, maturation, and release of sperms into the lumen [1]. Each Sertoli cell supports 30–50 germ cells through elaborate network of cell junctions that provide structural, communicational, and signaling support [2]. The Sertoli cell also provides nutritional support and immunological protection to the germ cell [3–5]. Unique to the Sertoli cell are the shape of its nucleus, thin cytoplasmic arms, intricate physical associations with germ cells, and spermatid disengagement complex [6]. The Sertoli cell remains as the unique niche surrounding which the entire events of spermatogenesis takes place, which was also observed to be the crucial target for any kind of disruptions that are targeted to affect spermatogenesis [7]. Precisely, the testis-specific features such as blood-testis barrier, apical ES, and cytoskeletons including actin, microfilament,

Marco G. Alves and Pedro F. Oliveira (eds.), *Sertoli Cells: Methods and Protocols*, Methods in Molecular Biology, vol. 1748, https://doi.org/10.1007/978-1-4939-7698-0_18,

and microtubule were observed to be the key targets for any kind of spermatogenesis disruptors [4, 8–15].

Adjacent Sertoli cells in the seminiferous epithelium form the tight testis-specific barrier called blood-testis barrier (BTB), which is formed by the coexisting tight junctions, basal ectoplasmic specializations (ES) (testis-specific actin-rich adherens junctions), gap junctions, and desmosomes. BTB divides the seminiferous epithelium into basal and adluminal compartments, thus rendering the self-renewal of spermatogonial stem cells (SSC) and spermatogonial cells and differentiation of type B spermatogonia into preleptotene spermatocytes to take place in basal compartment, while meiosis, spermiogenesis, and spermiation take place in adluminal compartment. This specific segregation by BTB helps in providing immunological protection to the developing germ cells in adluminal compartment [9, 13]. Throughout the stages of seminiferous epithelial cycle (SE), germ cells remain attached to the Sertoli cells, and this peculiar connection is mediated predominantly by apical ES and to some extent by desmosomes [16]. Typical assembly and disassembly of components at BTB remain crucial for propagation of preleptotene and leptotene spermatids toward the adluminal compartment [17]. Similarly, assembly and disassembly of apical ES are important for holding and transportation of round, elongating, and elongated spermatids across adluminal compartment toward the lumen. During this journey, germ cells undergo maturation via spermiogenesis, and finally the disassembly of apical ES aids in releasing matured elongated spermatids into the lumen by the process called spermiation [18]. Along with apical ES, which is the actin-rich component of the testis, microtubules, motor proteins, and intermediate filaments also help in orchestration and transportation of spermatids across the adluminal compartment [19–22].

Regulation of BTB, apical ES, and microtubule functions was proven to be crucial for successful completion of spermatogenesis, making them targets for several drugs and toxicants that disrupt spermatogenesis. Among various structural proteins that regulate BTB, apical ES, and microtubules, kinases play a major role, whose disruption is observed to result in premature release of immature spermatids into lumen of SE [23–25]. For instance, the MAPK kinases, FAK, c-SRC, and c-Yes, were observed to play role in regulating the assembly and disassembly of apical ES and BTB [25–27], while MARK4 is shown to impart polarity to developing spermatids as well as its involved in regulating the functions of both microtubule and microtubule-associated proteins [28]. Disruption of kinase activity of these kinases has sufficiently shown to be enough for affecting the spermatogenesis. These kinases were also found to be promising drug targets for design of potential nonhormonal male contraceptives by temporarily disrupting spermatogenesis.

In an attempt to understand the effects of toxicants on altering the morphology and function of Sertoli cells, it becomes crucial to understand how these toxicants impart structural changes on the protein in Sertoli cells. In view of this, the present chapter discusses the methodology involved in predicting the structure and understanding the conformational properties of important kinases in their inactive state and finally will be involved in understanding how the structure of these kinases will be modified by the association of kinase inhibitors. Since both kinase inhibitors and environmental toxicants hamper the kinase activity of these proteins, the structural changes imparted by inhibitors can be potentially used as reference data to assess the changes imparted by other reprotoxicants and also provide hints for developing nonhormonal male contraceptives.

2 General Criteria to Be Considered Before Commencing Protein Structure Prediction

The success of protein structure modelling depends on the availability of high-quality template that covers all the available folds/domains in the target. A quality template, with homology generally more than 30%, is selected as the standard criterion for obtaining reasonable model. The principle belief stating that sequences with high homology shares structural and functional similarity lies in the heart of comparative modelling. Nevertheless, sequences with more homology, i.e., more than 50% of sequence identity, will render better resolution structures with less than 1.0 RMSD. In general, the selection of the template solely depends on the objective of the study. As in case of the present context, the objective is to decipher the inactive state of kinases, which can be achieved by selecting the template sequence sharing identity to corresponding kinase domain of target (protein of interest). However, when the objective is to understand complete conformational changes taking in entire span of structure, the templates need to cover the full span of target sequence. The problem arises here is the availability of such templates. Complete understanding of the biological aspects of target and templates is highly essential before commencement with selection of proper template. Particularly, when dealing with kinases in the Sertoli cell/testis, several aspects have to be taken in consideration. For instance, the following hints provide few clues over the important aspects that are needed to be understood before commencement with template search.

2.1 Understanding the Class, Family, Superfamily, and Hierarchy of Target Kinases

Kinases such as FAK, a member of non-receptor protein tyrosine kinase family [29], c-Src, and C-Yes were members of SRC family of non-receptor tyrosine kinase [30], while MARK4 falls under the serine/threonine family of kinases. The general topology and domain organization of each kinases differ [31]. For instance,

although FAK, c-Src, and C-Yes kinases fall under one family of non-receptor tyrosine kinases, they differ in domain organization. In case of c-Src and c-Yes, they contain an SH2, an SH3 domain, and a kinase domain, while FAK has N-terminal sequence followed by FERM domain (band 4.1 protein, ezrin, radixin, moesin homology), a linker region, a central kinase domain, proline-rich low-complexity region, and a C-terminal focal adhesion targeting (FAT) domains [32–34]. Similarly, although MARK4 falls under the general class of ser/thr kinase family, it differs in its domain organization by holding N-terminal Kinase domain, followed by a linker region that has CD motif, UBA domain, a spacer region, and a terminal KA domain [31, 35, 36]. Hence, while template selection, the template should be ensured to possess similar domain organization as the target.

A second important criterion is the knowledge over the presence of specific form of kinase in the Sertoli cell/testis. In case of MARK4, it has two isoforms, short and long isoform, and the long isoform alone is testis-specific [35, 36]. Similarly, testis-specific isoform of FAK is found to have exons 15 and 16 [37], and similarly c-SRC [38], Fyn [39], HCK [40], and protein Kinase A (PKA) [41] all were found to have testis-specific isoforms. For instance, two different entries for human FAK are available in UniProt, and FAK2 is the one which corresponds to the protein that is expressed in the testis (UniProt ID: Q14289). Hence, when considering the respective sequence for protein structure prediction, the difference between the isoforms has to be analyzed, and the sequence of the proper isoform that expresses in the testis has to be selected. In case of predicting the active state conformation, the knowledge over the specific residue that gets phosphorylated is to be understood. For instance, several phosphorylated forms of FAK are known to exist in different cells; however, in the testis, p-FAK-Tyr397 and p-FAK-Tyr407 were found to be functionally important [42]. Hence, only the specific residues have to be phosphorylated in the predicted model.

The knowledge over the specific functions of each domain in respective kinase and the effect of mutation on such domains over the kinase activity has to be understood. This knowledge will facilitate the design of allosteric inhibitors for inhibiting kinase activity. For instance, in MARK4, the CD motif located in the linker region is proven to be essential for protein-protein interaction, and mutation in this region is observed to affect the architecture of kinase domain [43].

Finally, the knowledge over the specific structural features of the kinase domain has to be understood. Since the prime objective of this chapter is to predict the structure for kinase domain and to understand the effect of chemical modulators on kinase domain, the detailed understanding of domain-specific structural features is essential. Precisely, the kinase domain holds many key structural

fingerprints. Whether it is non-receptor tyrosine kinases or serine/threonine kinases, their catalytic domains share similar architecture. In general, catalytic domain has bilobed architecture with smaller N-lobe and larger C-lobe connected by a hinge region. The space between the lobes constitutes the catalytic cleft, where the ATP binds. The structural fingerprints include the hinge region and phosphate-binding loop (P-Loop) which will hold catalytic lysine residue, core helix αC, the T-loop/activation loop that has characteristic DFG motif and the key threonine/tyrosine residue, the phosphorylation of which will activate the kinase domain, and the catalytic C-loop with conserved RD motif. In the inactive state, the T-loop will be folded toward the catalytic cleft; the DFG motif will exhibit characteristic DFG-out mode (Asp-Phe-Glyresiudes) which hinders the interaction of incoming ATP into inactive state of kinase domain. However, upon phosphorylation, T-loop orientation will be relocated such that the T-loop will be folded away the cleft therein opening the cleft for the entry of ATP; meanwhile, the core helix αC will be shifted toward the cleft; therein the conserved glutamate residue in helix αC will establish salt-bridge interaction with conserved lysine in the β3 strand of N-lobe (DFG-in mode). This general understating of structural features in catalytic domain can help in the structural analysis of kinase domains.

These specific details will help in gaining firsthand knowledge over the structural and functional aspects of the target kinases. The following will provide other important factors that are to be considered before commencement of protein structure prediction.

Identification and understanding of structural and nonstructural regions in the selected kinase targets: majority of human proteome is now recognized to have unstructured regions, named as intrinsically disordered regions that are located throughout the proteins or located in the specific regions of proteins such as linker and spacer regions in kinases. Even within the catalytic domain, the T-loop or activation loop is completely disordered. For instance, in FAK2, except FERM domain (141–260), kinase domain (425–679), and low-complexity region (431–443, 712–725, 926–934), the remaining regions were disordered. Hence, such knowledge will help in deciding the choice of method for predicting the structure for those regions. In case of T-loop, the amino acid number will be less in number, and hence there is no need for employing other specific methods such as ab initio prediction; however, when we need to model the structure for spacer regions, the resulting amino acids will be longer which requires employing combination of comparative modelling and ab initio modelling techniques. Since most of the templates from RCSB are crystallized proteins, they will not hold regions identical to these disordered regions, and alignment of such hits with target protein will affect the overall identity score. A prior knowledge of these regions will help in proper selection of templates. In most cases, UniProt database

[44] itself provides data on such regions; however, if they are not available, it can be obtained from PFAM search [45] and can be cross validated by submitting the sequence to DisProt disorder predicting tool [46].

Following disorder prediction, the secondary structure prediction for the structured regions needs to be accomplished. Several standard secondary structure prediction tools are available, and one such is PSIPRED [47]. With the knowledge of secondary structure, understanding of class, architecture, topology, and homologous superfamily can be performed using CATH software [48]. These details have to be considered in selection of right templates. Mere sequence identity might mislead in template identification, in such cases, the knowledge on secondary structure, and CATH details will help to identify most closely related hits based on the secondary structure and topology information. On the other hand, the comparison of CATH details for both template and target can also be used to validate template selection, such as when two proteins share similar secondary structure content, architecture and topology will definitely hold similar fold and share similar function. Similarly, the knowledge of domains located on both proteins as obtained from literature knowledge and PFAM details can be used to compare template with target and justify the selection of template.

The knowledge on posttranslational modification and protein phosphorylation also needs to be accounted, so as those regions of protein sequence that are unrelated with functional form of protein can be eradicated during BLAST search [49]. Details on protein phosphorylation can be useful if such data is unavailable, and in case of kinases, such data is necessary when the objective is to predict the structure for kinase in active state conformation. Several tools listed in ExPASy can be used for this prediction.

Finally, the knowledge on functional unit of protein and the details on the necessity of cofactors, metals required for functional form of protein has to be gained from literature data. Such knowledge can be used to predict monomeric/dimeric/trimeric/hexameric forms of protein along with presence of metals/cofactors. Since most of the protein structures were determined by X-ray crystallography, the selected hits were found mostly to be in monomeric/dimeric/trimeric/hexameric forms which are basically defined by the unit cell arrangement, which is entirely different from the functional unit of the molecule, for example, the crystal structure c-SRC kinase represented by the PDB ID: 4MXO has two molecules per unit cell connected by the crystallographic contacts; however, the functional unit of the protein is monomeric; thus while predicting the structure for c-SRC, only the monomeric form should be used. Similarly, the precipitant and supernatant solutions used in crystallizations are sometimes enriched with peculiar metals or other chemical substances to act as catalyst to

favor the crystallization of proteins. Hence, such molecules that are functionally unrelated to the protein of interest are to be eliminated. On the other hand, several proteins function only in association with metals and cofactors such as active state of kinase domains that contains Mg; hence, they have to be included in the predicted model if the objective becomes modelling the active state of proteins. Thus, such knowledge is crucial to eliminate or to include functionally related chemical moieties in the predicted model. Finally, in case of predicting active state kinase conformations, the phosphorylated residues in the template will be denoted in unique forms in PDB files, and such data will be not accepted by Modeller software [50] that will result in error conditions. Such residues should be modified immediately after modelling so as to make them compatible for the software input format.

3 Methods

3.1 Selection of Suitable Templates for Selected Targets

1. The amino acid sequence for the selected kinase targets has to be retrieved from the UniProt database and subjected to the BLASTp search against the Protein Data Bank (PDB) [51].
2. With reference to the objective of the study, the respective sequence for the target protein has to be submitted. For instance, the objective of the current study lies in predicting the kinase domain conformation for prediction of kinase-specific inhibitors to inhibit at inactive state; hence, the respective sequence for kinase domain is used for structure prediction. Apart from the use of conventional BLASTp search, user can employ DELTA-BLAST to get hits based on the identity to individual domains. For instance, in a search against the Protein Data Bank for predicting structure for Rat c-SRC kinase, the DELTA-BLAST [52] will pull out specific hits for the kinase domain rather than for the entire protein.
3. The conventional sequence identity, query coverage, and E-value are to be considered in selection of hits for template. In case of searching templates for kinase domain of Rat c-SRC kinase, when the full length sequence is submitted, the only few of the obtained hits were appeared to cover the full length sequence, and such hits possess high sequence identity and good E-value. On the other hand, hits that correspond to the kinase domain alone exhibit less sequence identity. Hence when the objective is only to model the structure for kinase domain, the input should be the sequence for the kinase domain alone. Only then the true identity of the hits to the kinase domain can be obtained which can facilitate the selection of right template.

4. The next step is the careful examination of the templates before their selection. For instance, many of the obtained hits to Rat c-SRC were of diverged categories. Few hits like PDB ID: 3GEQ which refers to the mechanism behind the chemical rescue of kinase activity, PDB ID: 4MXZ which corresponds to the double mutant form of human c-SRC, and PDB ID: 2QQ7 which refers to the drug-resistant form of c-SRC were all found to share 98% identity. However these templates correspond to diverged functional objectives, and hence their selection should be avoided if the objective of the study lies in determining the native functional state of c-SRC kinase domain. Indeed, the PDB hit PDB ID: 1FMK sharing 99% identity alone corresponds to the closed inactive state of c-SRC kinase; hence, such template can be selected for further analysis.
5. With the identification of specific template, the homology in terms of structural organization as defined by CATH, the secondary structure architecture has to be analyzed.
6. In certain cases, like in modelling the structure of mouse MARK4 kinase domain, the obtained hits show human MARK4 kinase domain structure along with inhibitor (PDB ID: 5ES1): however, when the objective becomes to model the native inactive conformation of MARK4 kinase domain, the templates should be devoid of any such inhibitor, and in this case the structures of kinase domain in inactive state are available for MARK1, MARK2, and MARK3 with respective identities in the range of 84–86% identity. The literature data states that although MARK4 is observed to play role in spermatogenesis, the structural architecture of kinase domain is found to be similar for all four isoforms. Hence all three templates corresponding to wild-type kinase domain of MARK1, MARK2, and MARK3 can be used, and multi-template-based modelling can be used for predicting the three-dimensional structure for mouse MARK4.
7. In other cases, even when the resulting templates share identity in the range of 50–70%, multiple templates can be selected. While selecting multiple templates, care should be taken that each template refers to different protein and not to the same protein sequence, which was pulled from different crystal structures pertaining to same protein. In many cases, same protein might have been crystallized under different conditions, and in case of kinases, several structures will be available in data bank. Each structure may refer to the same protein; however, the functional objective behind each crystal structure will be different, and in addition they might be co-crystallized with different inhibitors. Hence, multiple templates that are to be selected should not correspond to

diverged functional objectives, and they should not contain the mixture of active and inactive states, which may eventually result in erroneous structure for target.

8. When the structure corresponding to the native inactive state is not available and when the user is forced to use the crystal structure co-crystallized with inhibitors, the knowledge on the native state should be gained, and the literature corresponding to the obtained hit should be read carefully so as to understand if the co-crystallized inhibitor has imposed conformational changes in the kinase domain. If any such conformational changes are there, then the inhibitor has to be removed, and the structure has to be subjected to molecular dynamics (MD) study so as to gain the features native form of protein. If, in case, the co-crystallized chemical molecule is not observed to make major or minor conformational changes, rather it remains simply to inhibit the kinase activity, then such ligands should be removed before structure prediction, and the resulting structure should also be subjected to energy minimization and molecular dynamics simulation studies to ensure the stability of the secondary and tertiary structure.
9. Similarly, many crystallographic structures might represent the functional form prior to the activation of protein, or they might correspond to the form involved in interaction with partner protein. The functional objective and crystallization conditions of such hits should be carefully studied from the associated literature, and only if such forms agree with the objective of the present study, they should be considered; else they should be avoided even if they possess high sequence identity/similarity.
10. Concerning to the functional unit of selected kinase region, the literature knowledge should be acquired, and when no such data is available, the literature data of the obtained hits should be carefully studied, and clear data on quaternary arrangement corresponding to the functional unit and unit cell should be understood.
11. Only after careful execution of **steps 1–10**, the corresponding hit/hits should be selected.
12. Finally, prior to commencement of protein structure prediction, the text file of PDB hits should be carefully checked for errors using various programs mentioned in WHATIF web interface such as analyses of atomic contacts, structure validation, rotamer, cysteine-related checks, and finally check structure options. If any such errors are reported, they should be fixed, and options for correcting and fixing models were also available in WHATIF web interface (http://swift.cmbi.ru.nl/servers/html/index.html). Finally fixed and corrected and

validated structures corresponding to templates should be carried forward for structure predictions.

13. In case of unavailability of potential hits with considerable identity/similarity, such as when the resulting hits fall in twilight zone, i.e., when the identity is less than the 30%, the decision should be taken to proceed for threading or ab initio programs. ITASSER [53] and ROBETTA software [54] suite are well utilized for threading and ab initio programs.
14. In case, when majority of the submitted sequences receive justifiable hits and regions such as disordered regions are present, the models for such disordered regions should be modelled separately using ROBETTA; and for generating the full length, the respective BLAST hits along with ROBETTA models should be used as multiple templates to predict the structure for the input target.

3.2 Generation of Three-Dimensional Structures, Model Validation, and Model Refinement

1. Conventional Modeller software can be used for predicting the three-dimensional structure of the selected kinase targets. Multalin interface [55] can be used to generate the target-template alignment; the resulting alignment can be conventionally used as alignment file as per instructions provided in Modeller manual. Then the prediction can be performed as per the instructions given in the Modeller file; rather than using automated scripts for template-target structure alignment such as Align2D, manual alignment will ensure careful generation of structures, although it may appear tricky and time-consuming. More than 20 models can be generated, and based on resulting DOPE and MOLPDF scores, best models can be selected for further analysis.
2. Modeller software can be conventionally used for generating models based on multi-template, multichain, multi-template/multichain with ligands, and multi-template/multichain with structural/functional water molecules.
3. In case of sequences with less identity that is below 70% and when low resolution crystal structures were used as templates, problems could arise in loops, and in such cases inbuilt loop refinement scripts of Modeller should be used to refine the loop structures.
4. Final, resultant models should be subjected to check and repair options in WHATIF web interface, and based on the resulting validation report and by comparison with crystallographic structure, the decision for selection of refinement programs should be made. In general, when template-target identity is far below, 70% refinement procedure is advisable. Particularly, structure should be carefully checked for the permissible geometric features of peptide phi/psi angle, side-chain rotamer,

C-beta deviation, sequence-structure compatibility, Asn and Gln flippers, etc. In case of inconsistency, the generated models should be subjected to energy minimization programs to check if the minimization ensures validity of the generated models.

3.3 Understanding the Conformational Changes in the Predicted Model

Once the predicted model is refined and validated, the next step is to understand its conformational changes. In general pertaining to the kinases, when the predicted model involves only the catalytic domain, much data cannot be gathered from understanding the conformational dynamics. Nevertheless, molecular dynamics study can be performed to study the stability of structural features of the kinase domain. With the understanding of kinase domain structural features, the molecular dynamics study can be performed to understand the stability of these features.

1. Molecular dynamics simulation (MDS) studies: Initially, the selection of MD suite can be made over the expertise. In our studies we have used GROMACS molecular dynamics suite [56, 57]. The general protocol of molecular dynamics study is utilized, where the predicted model is first typed with appropriate force field, generally the AMBER force field. Then simulation box type is defined; the choice of the box type is made according to the number of residues in the protein structure. In general, when the total residues is far above 300 amino acids, the box type can be defined to be cubic, and when small protein is used, triclinic box type can be used. The protein is to be placed in the center of the box with the distance of 1.0 nm; therein it will reduce the number of water molecules and can speed up the simulations. In the next step, the simulation box has to be filled with water model, and in general TIP3P water model is used. Later, the charge of the system has to be calculated, and the respective ions have to be added to make it neutral. The Neutralized system will be then subjected to energy minimization and then subjected to the equilibration step, where the system will be equilibrated under standard NVT and NPT ensembles for the time period of 1 ns. The final MD will be carried out for 50 ns, which will be sufficiently enough for understanding the stability of the predicted structural features.
2. When coming to the analysis part of MD results, the RMSD, RMSF, and radius of gyration (Rg) have to be analyzed, and the principal component analysis (PCA) has to be performed. In general, PCA analysis is a useful method to study the structural transitions taking place in the input structure as it elucidates the large-scale collective motions that represents the functional state of the molecule taking place in the structure. The high-amplitude concerted motions denoted by PCA were

captured by eigenvalues, and hence, initially the covariance matrix will be generated and diagonalized using g_covarscript of GROMACS. The output of g_covar will include eigenvalues, eigenvectors, and covariance matrix derived from the coordinates of protein. Later the g_aneig script will be used to analyze the eigenvalues and eigenvectors and create two-dimensional and three-dimensional projections along eigenvectors. The g_analyze script will give cosine values for each eigenvectors, and only those eigenvectors with less cosine values can be used for the analysis. In general, the cosine content derived from the coordinates of the target protein determines if the motion captured along the eigenvector really represents functionally important conformational changes or just the random fluctuations. The principal components with less cosine value, i.e., lesser than 1, were generally considered for analyzing the dominant motions which have taken place in the structure. The g_aneig script can also be used to create extreme projections along the selected eigenvector. The projection of top 10 eigenvectors onto each other can be used as a measure to understand the stability of the system in the given time scale. Meanwhile, the extreme projections retrieved along each eigenvectors (that has low cosine values) can be used to study the conformational changes along those eigenvectors. These changes can be conventionally studied by importing the PDF file of extreme projections in PyMOL, and by using the script called Modevector, the user can generate porcupine plots representing the extreme motions. The g_sham can be used to generate XPM matrix file for generating the free energy landscape, which can be conventionally used to analyze the transitions among the metastable states of the target protein under study.

3. In general while subjecting kinase domain in inactive state for MD simulation studies, the need for PCA analysis and FEL analysis is minimal. Nevertheless, the projections of top 10 eigenvectors onto each other can be used to assay the stability of the system. Since the system includes only the kinase domain, the most important objective at this level will be to assay the stability of the structural features in inactive state. In addition to RMSD, RMSF, and Rg plots, the distance between the conserved glutamate and lysine residues can be measured and the stability of the selective interaction that holds T-loop within the cleft and fluctuation of selected residues in catalytic loop, P-loop, T-loop, DFG motif, and hinge and core helix can be evaluated. The structures can be retrieved from 1 ns time interval and can be compared with starting structure to understand the stability of the selected structural features in catalytic domain.

4. In view of structural analysis, the final selected metastable structure from MD studies has to be compared with the template structure. For obtaining meaningful comparison, several protein structure viewing and analysis tools are available. One such is PyMOL viewer. It holds several options for analysis of structure. Using PyMOL, one can perform structural comparison based on combinatorial extension method; retrieve RMSD for every residue as well for whole protein; create surface around binding pocket, such as catalytic cleft in kinase domain; calculate volume and area; and so on. (For detailed information on the list of commands available for structural analysis, please refer to https://pymolwiki.org/index.php/Category:Commands, and for various tutorials refer to https://pymolwiki.org/index.php/Category:Tutorials.) PyMOL can also be used to take meaningful pictorial representation of several structural analyses performed on protein, such as display of protein in varied representation, superimposition of proteins, display of catalytic cleft, solvent accessible surface area, etc. Structural comparison of target kinase with its template and with other members of the same family will provide hints on the arrangement of DFG motif, T-loop, hinge region, P-loop, C-loop, and core helix. The unique arrangement of any of these features can define the unique nature of the target kinase under study. For instance, comparison of MARK4 inactive state kinase domain onto other members of PAR family of ser/thr kinase revealed that members of MARK family of kinase has unique kinase domain features defined by the presence of DFG-in/αC helix "out" conformation in the inactive state of kinase. This feature identifies MARK family of kinase as unique members that can facilitate the binding of ATP even in the inactive state; however, the stable interaction of ATP within the cleft will be established following the phosphorylation of threonine residue in activation loop.

3.4 Understanding of Structural Changes Imposed on Kinase Catalytic Domain by Chemical Entities

As mentioned in the objective, the main goal of this chapter is to elucidate how the chemical entities impose structural changes in kinase catalytic domain. On the other hand, the detailed understanding of such structural changes can also be used in designing promising leads that can be used as nonhormonal male contraceptives. Thus, this section will explain how to perform general docking studies of known kinase inhibitors with kinase and to develop a pharmacophore model, which can be used to screen kinase-specific inhibitor databases for identification of kinase-specific inhibitors. Detailed understanding of how these inhibitors interact and impose structural changes on kinase catalytic domain will be analogous to the effects imposed by environmental toxicants.

1. Initially, the structure for known kinase inhibitors, which were shown to be functional as catalytic site inhibitors, mostly type II kinase inhibitors that bind with inactive state of catalytic domain, should be identified from literature. Since in our earlier steps, we discussed on generation of three-dimensional structure for inactive state of kinase catalytic domain, we will proceed with discussion pertaining to type II kinase inhibitors and their interaction with inactive kinase. Other types of inhibitors that were available for inhibiting kinase were type I kinase inhibitors which act as ATP competitors and will bind with and inhibit the activity of kinase catalytic domain in its active state. Other options include the use of allosteric inhibitors that can bind at the site distant to the catalytic cleft, and finally the peptide molecules that mimic substrate peptide were also used as inhibitors to modulate the kinase activity. Nevertheless, the observed reprotoxicants are mostly observed to hinder the kinase activity indicating that they can perform similarly to both type I and type II kinase inhibitors. In view of this, we discuss here how to perform molecular docking studies of known type II kinase inhibitors and identification of new promising leads based on the pharmacophore features of known inhibitors.
2. The three-dimensional structure for such known type II kinase inhibitors should be prepared, which can be performed by retrieving canonical SMILES format from PubChem database [58], using which two-dimensional structure can be generated in ChemBioDraw software. The generated two-dimensional format can then be imported into Schrödinger's LigPrep module (Schrödinger Release 2017–1: LigPrep, Schrödinger, LLC, New York, NY, 2017), and minimized isoforms and tautomers for target ligand can be generated.
3. Initially, ligands will be typed with OPLS force field; ionization states will be generated at pH 7 with the options for generating isomers and tautomers. Nearly 32 possible conformations for each ligand will be generated with at least one low energy ring conformation per ligand.
4. Once the structure for known inhibitors was prepared, they should be docked into the catalytic domain of kinase domain. Since the docking is done with reference to type II kinase inhibitors and inactive state of kinase catalytic domain, the receptor grid is defined around the catalytic lysine residue and DFG motif, such that the grid covers the entire catalytic cleft including the residues of T-loop that were folded into the cleft.
5. The molecular docking of prepared type II kinase inhibitors with residues of catalytic cleft can be performed using Glide module of Schrödinger suite [59]. The interacting conformation can be generated by simple precision and extra precision XP modes with respective scorings. Since the inhibitors were

already proven to elicit inhibitory actions, they can be docked with XP mode. The best interacting conformations and their scores and structural changes imposed by them can be used as reference to select best leads from existing database of kinase inhibitors and also for designing best lead molecules.

6. Next step is to identify and generate best pharmacophoric hypothesis that explains how the known inhibitors bind with catalytic domain of kinase domain. Initially as mentioned in earlier steps, the best known type II kinase inhibitors that were shown to be specific for the target kinase under study should be identified in literature. The inhibition constant value for each of the selected inhibit should be retrieved from the literature.
7. The set of known kinase type inhibitors along with their IC_{50} values should be used to create the pharma set. Initially, the structures for these inhibitors should be prepared as mentioned in **step 2**, and their biological activity should be converted as—Log [concentration] values. The Phase module [60] of Schrödinger can be employed for generating pharmacophoric hypotheses.
8. Next step is involved in segregating the pharma set ligands as active or inactive based on their biological activity value. The threshold value is set to be—0.5, and those with values greater than threshold are defined as active and lesser than threshold as inactive. This segregation is important because the respective conformations of active ligand will alone be utilized for searching common pharmacophore features, and during aligning, the identified features will be aligned only with these molecules.
9. With segregation of active and inactive groups, the search for common pharmacophoric features will be initiated. In general, there are six common pharmacophoric features that include hydrogen bond acceptor (A), hydrogen bond donor (D), hydrophobic group (H), negatively charged group (N), positively charged group (P), and aromatic ring (R). These features will be used to generate pharmacophoric variants that define pharmacophoric hypotheses. Variants will be defined with a condition that they should possess maximum of five active and minimum of four active points and should match three of three active groups. A good hypothesis will be the variant with maximum site points, matched with all active groups, such that they cover all active pharmacophoric features.
10. Hypotheses generated will then be scored using the set of similar pharmacophoric features driven from other active site ligands.
11. Initially, the best aligned ligand and its pharmacophoric features will be used as reference. Other active ligands will be

aligned to the reference using the standard least square method. Alignment will be scored using alignment score, vector score, and volume score. If any non-reference ligand scored better than the reference one, then the respective non-reference ligand will be taken as reference, and the remaining ligands will be aligned to that so that all the active ligands and their pharmacophoric features will be aligned and scored.

12. The final survival score for each hypothesis will be generated, and the one with high survival score will be selected for virtual screening purpose.
13. Virtual screening and selection of potential hits will be the next major task, which can be performed using Schrodinger site. Initially, the pharmacophore selected from the above steps will be used to search against the compounds from the databases. The kinase-specific inhibitors will be the best option to search for potent inhibitors. Hence, the kinase-specific inhibitors can be retrieved from two databases, KINACore and KINASet from ChemBridge database.
14. The "Find match to best hypothesis" in Phase module will be used to screen and select the best ligands that match the matches of all the features in selected best hypothesis. The align score, fitness score, and matching score not less than 2.0 Å matching tolerance along with vector score and volume score not less than—1.0 and 0.0 will be used to score the alignment of ligands with hypothesis.
15. The selected hits that match to the best hypothesis will be taken up for the virtual screening protocol in Schrodinger. Initially, the selected ligands will be prepared and optimized using LigPrep module. Later, their "druggable" nature will be assayed using ADME filtering using QikProp (Schrödinger Release 2017–1: QikProp, Schrödinger, LLC, New York, NY, 2017), and the resulting hits that possess druggability nature with no toxicity will be selected for next level.
16. The selected hits will then be tested for their ability to bind with residues in the catalytic cleft. Before commencement of the protocol, the docking grid has to be defined, which is performed as mentioned in **step 4**. With the definition of grid, the docking of selected molecules with residues of catalytic cleft will be performed in three different accuracy levels, high-throughput virtual screening followed by simple precision and finally XP. After each level of docking, 50% of best scoring hits after post-minimization will be carried forward for the next level of docking.
17. The top docked conformations of the ligands will be selected based on the XP score, and in comparison with the reference molecule (as mentioned in **step 5**), the best hits will be selected. The free energy of binding will also be calculated and

will be compared with that of reference molecule. The duplicates in the resultant molecules will be eradicated, and the structure for the complex of kinase with docked hit will be retrieved.

18. The kinase hit complexes will then be subjected to the molecular dynamics simulation study.
19. The protocol for the MD simulation will be same, with inclusion of few steps. In case of protein-ligand complex, the topology for the ligand has to be generated separately and has to be merged with protein topology, which should be then carried forward for definition of simulation box and so on. Initially, the coordinates for the ligand has to be separated from the PDB file corresponding to the protein-ligand complex, and PDB file for protein alone has to be subjected to initial step of MD protocol, where it has to be typed with force filed, and topology file has to be generated. Meanwhile the ligand coordinated separated from complex has to be submitted to the PRODRG server [61], and their corresponding topology has to be generated. Later the prepared ligand structure has to be merged with PDB structure of protein, and two ligand topologies have to be included in the protein topology file. (Please refer to the detailed instructions given in the following tutorial, for detailed protocol on protein-ligand simulation studies using GROMACS: http://www.bevanlab.biochem.vt.edu/Pages/Personal/justin/gmx-tutorials/complex/) In general, the time scale for the kinase inhibitor complex simulation can be the same as that of native ligand-free kinase simulation as mentioned in Subheading 3.2.
20. The PCA analysis will provide detailed insights into the conformational changes taken in place of the inhibitor. Hence, as mentioned in Subheading 3.3, the user needs to create the covariance matrix and generate eigenvalues and eigenvectors. The cosine value for each eigenvectors needs to be generated. Only those eigenvectors with cosine value lesser than one should be considered for generating free energy landscapes. The extreme projections along the selected eigenvectors along with metastable states from FEL plot can be retrieved and imported into PyMOL and analyzed for the conformational changes taken place in N- and C-lobes of catalytic cleft.
21. The binding free energy associated with the binding of ligand with catalytic cleft can also be calculated, and calculations can be performed using various procedures mentioned in GROMACS. One fine method is to use the g_mmpbsa script. The result can give data on how the free energy of binding changes between the ligand and the protein as a function of the time. The stable

and increasing affinity will denote the potential of identified hit for inhibiting the kinase activity.

22. While coming to the analysis part of the MD results of kinase inhibitor complex, the following list elucidates the series of structural analysis that can be performed:

    (a) Analysis of RMSD, RMSF, and Rg plots with native undocked conformation.

        Initially, the RMSD graph representing the conformational deviation between kinase domain in the presence and absence of selected inhibitors will indicate if the kinase domain with inhibitor is stabilized in the given time scale. It also highlights the conformational differences in the kinase domain on comparison with native pre docked conformation. Detailed comparison of fluctuation in the residues and regions involved in interaction with ligand and with ligand free state of the protein would shed light on the differences in their intercation profile. The Rg plot will be critically measured, since its comparison might directly elucidate whether the structure has become compact in the presence of ligand. In general, the bound ligand will aid to pull the N- and C-lobes of catalytic cleft so as that it will close the cleft, therein blocking entry of any further chemical entities such as ATP into the cleft. Comparison of Rg plot can provide clear indication of such conformational change. Along with the RMSD of entire protein, RMSD plot can also be generated for the bound ligand, and the resulting plot if holds less deviation will indicate the stability of the docked conformation over the given time scale of simulation. If minor differences are observed, then the manual comparison of ligand conformation has to be made. In general, the structures at regular time interval can be retrieved and can be used for comparing the differences in the conformation of ligand.

    (b) Analysis of the non-covalent interactions observed between the ligand and the residues of catalytic cleft.

        The next critical analysis to be performed is to evaluate the stability of the observed non-covalent interactions between the ligand and the residues of catalytic cleft. Initially, the index file holding data on the atoms and residue involved in hydrogen bond, salt-bridge, and van der Waals interaction has to be made separately. The makendx script of GROMACS can be used to calculate such index file. The g_distance option of GROMACS can be used to evaluate the stability of the interactions which will take generated index file and the XTC file as inputs. The resulting plot can be plotted in xmgrace, and the stability of the interactions can be assayed. In case if the RMSD plot for

the ligand shows deviations, then the structures at regular time interval have to be retrieved, and manually the interactions has to be observed and to be noted. The list of new interactions has to be finally taken into account, and their stability can also be accessed in the same manner as mentioned earlier in this part. Finally based on these results, the list of stable interactions that aids to stabilize the association of ligand within the cleft has to be elucidated. Meanwhile, the structures retrieved at regular time intervals have to be imported into the PyMOL and to be compared with native docked conformation. For aligning the ligands, ligalign script of PyMOL can be used, and for aligning the structures, the CE align script of PyMOL can be used. By comparing the deviation in ligand, the user can understand which functional groups of ligand have flipped and deviated, and the consequence of such flip in case of affecting the existing non-covalent interactions and its influence over establishment of new interactions can be studied. Finally, the changes in the free energy of binding for each ligand also have to be calculated. This can be achieved by using g_mmpsa option of GROMACS; alternatively, the structures retrieved at regular time intervals can be imported in Maestro viewer of Schrödinger; dock and score option can be used, and prime MMGBSA values associated with binding can be evaluated.

(c) Analysis of structural changes in kinase domain.

When coming to the analysis of conformational changes in kinase domain, the essential features to be analyzed are the evaluation of structural changes in the fingerprints of kinase domain. Initially, the structures retrieved at regular time interval from total time frame of MD studies have to be imported into the PyMOL. Then the structure referencing to the pre-docked conformation and native docked pre-simulated conformation has also to be imported. The CE align script of PyMOL can be used to generate meaningful structural comparison. By comparing pre-simulated and post-simulated structures, respective changes in kinase fingerprints such as DFG motif, hinge region, activation loop, C-loop, and P-loop can be assayed. The individual RMSD based on reference on N- and C-lobes has to be taken individually. These data may elucidate the differences in the spatial orientation of these lobes. Meanwhile the movement in N- and C-lobes if observed can be further validated by comparing pre-docked and post-simulated structures. For acquiring detailed insights, the PCA and FEL analysis can be made used. The eigenvectors with cosine values lesser than one can be selected, and extreme

projections along the selected eigenvectors can be imported into the PyMOL. The Modevector script can be used to analyze the extreme projections. Analysis of extreme projections along the varied eigenvectors will elucidate the structural changes that strengthen the interction of lignad as well as the series of changes that help in the closure of catalytic cleft. Moreover, the FEL generation and structural analysis of structures corresponding to metastable states can also strengthen the observations made in eigenvector analysis. If, in case, the bound ligands tend to pull the N- and C-lobes, as observed in the case of search of inhibitors against MARK4 [62], the respective changes in the distance between the two lobes have to be calculated. For accomplishing this, the respective docked pre-simulated and post-simulated structures can be imported into the Chimera software. Then the axis has to be defined along the center of the N- and C-lobes, and then the distance between these axes can be calculated. The calculated distance can sufficiently provide hints on the changes observed in the distance between these lobes over the time scale of simulation. Another important structural feature associated with the movement of the N- and C-lobes is the closure of the catalytic cleft. To measure the closure of the cleft, the change in the area and volume occupied by the ligand inside the cleft has to be measured so that the get_area option of PyMOL and site_map option of Schrodinger Maestro viewer can be used. Initially, the total area of the residues in the cleft region, total area of the ligand, and total area of residues and ligand as a complex have to be calculated using the get_area option of PyMOL. Then subtracting the sum of total area for residues and ligand from the total area of ligand residue complex, the resulting the area of the cleft can be obtained. Meanwhile the total volume of binding site can be calculated from Site_map option [63]. Such calculation should be performed on the structures retrieved at regular time intervals of total simulation time scale. The resulting value when indicates substantial decrease in binding area and binding volume can substantially elucidate the closure in the cleft induced by the bound ligand. The substantial stability of ligand, the stability over the established non-covalent interactions, associated pulling of N- and C-lobes, and closure of cleft by ligand can justify that the bound ligand can actively arrest the kinase activity of the protein.

Other features that are to be assayed for justifying the inhibition profile of bound ligand is that their functional groups should introduce stable interactions with key residues of the

catalytic cleft, such as catalytic lysine, DFG motif, hinge region, and residues of core alpha helix. These interactions should function to block the access of these residues, and they should hold these regions strongly from preventing their transition upon activation of kinase. In addition, the bound ligand can be independent of T-loop conformation such that even after phosphorylation at T-loop, the bound ligand can actively protect transition in P-loop, core helix, DFG motif, and hinge region. In other case, bound ligand can also establish strong interactions with T-loop such that even after phosphorylation of threonine/tyrosine, the ligand can block the movement of T-loop away from the cleft. In order to assess these possibilities, the concerned residue at activation loop can be phosphorylated and can be further subjected to MD simulation studies. If the obtained results confirm the expected observations, then the bound ligands can be proposed to be the promising hits for inhibiting the kinase activity of selected kinases. These best scoring set of ligands that can potentially afftec the conformation of kinase in its inactive state can be seleced for further experimental validation for their potency to function as type II kinase inhibitors.

4 Other Possibilities to Hamper the Kinase Activity

Besides type II kinase inhibitors, kinase activity can be hampered by the use of allosteric inhibitors as well as by the compounds that can function as pseudo-substrates for the kinases. For instance in FAK, the space near the HRD motif acts as the site for binding of allosteric inhibitors [64]. The binding of type III kinase inhibitors, the allosteric inhibitors, at such site distant to the ATP binding site alters the kinase activity. Meanwhile, the peptide-based inhibitors that can act as pseudo-substrate for few protein tyrosine kinases have also been developed [65]. Concerning to the methodology for identification of such inhibitors, the general pharmacophoric features of substrate-binding region can be taken into account for design of novel inhibitors. Protein stucture-based pharmacophore along with ligand based pharmocophore (as defined in Subheading 3.4, **steps 7–12**) can be used to screen kinase-specific inhibitor libraries. The resulting hits can be further subjected to high-throughput virtual screening protocol, where the input conformation of protein has to be in the active state conformation, and best docking hits can be further subjected to molecular dynamics simulation studies. In case of screening inhibitors for targeting allosteric inhibitors, the pharmacophoric features in the allosteric region has to be understood, and the search for novel inhibitors has to be initiated. The general docking methodology combined

with Induced-Fit method can be employed. Concerning the input structure, the effect of allosteric inhibitor can be evaluated on both active and inactive states using the same methodology defined for docking and simulation studies.

5 Further Developments in Evaluating the Potency of the Selected Inhibitors

The stated methodology can be applied for computational evaluation of the effects induced by the inhibitors on the structure of the inactive state of kinase domain. Further, these analyses can also be taken as a reference for understanding the effect of various reprotoxicants on these kinases. Moreover, the inhibitors that can be selected from the virtual screening workflow can be further evaluated for their potency by using experimental studies. The methodology used in the studies to evaluate toxicity of reprotoxicants on Sertoli cells can be used as reference to evaluate the new potential kinase inhibitors. Moreover, their potency to establish direct interaction with selected kinases can be assayed by using isothermal calorimetric studies as well as by X-ray crystallization studies, and those compounds that exhibit potency for kinase-specific inhibition can be used to design non-hormonal male contraceptives with better specificity and efficacy.

References

1. Parvinen M (1982) Regulation of the seminiferous epithelium. Endocr Rev 3(4):404–417. https://doi.org/10.1210/edrv-3-4-404
2. Weber JE, Russell LD, Wong V, Peterson RN (1983) Three-dimensional reconstruction of a rat stage V Sertoli cell: II. Morphometry of Sertoli--Sertoli and Sertoli--germ-cell relationships. Am J Anat 167(2):163–179. https://doi.org/10.1002/aja.1001670203
3. Mital P, Kaur G, Dufour JM (2010) Immunoprotective sertoli cells: making allogeneic and xenogeneic transplantation feasible. Reproduction 139(3):495–504. https://doi.org/10.1530/REP-09-0384
4. Mruk DD, Cheng CY (2004) Sertoli-Sertoli and Sertoli-germ cell interactions and their significance in germ cell movement in the seminiferous epithelium during spermatogenesis. Endocr Rev 25(5):747–806. https://doi.org/10.1210/er.2003-0022
5. Sylvester SR, Griswold MD (1994) The testicular iron shuttle: a “nurse” function of the Sertoli cells. J Androl 15(5):381–385
6. Franca LR, Hess RA, Dufour JM, Hofmann MC, Griswold MD (2016) The Sertoli cell: one hundred fifty years of beauty and plasticity. Andrology 4(2):189–212. https://doi.org/10.1111/andr.12165
7. Oatley MJ, Racicot KE, Oatley JM (2011) Sertoli cells dictate spermatogonial stem cell niches in the mouse testis. Biol Reprod 84(4):639–645. https://doi.org/10.1095/biolreprod.110.087320
8. Cheng CY (2014) Toxicants target cell junctions in the testis: insights from the indazole-carboxylic acid model. Spermatogenesis 4(2):e981485. https://doi.org/10.4161/21565562.2014.981485
9. Cheng CY, Mruk DD (2012) The blood-testis barrier and its implications for male contraception. Pharmacol Rev 64(1):16–64. https://doi.org/10.1124/pr.110.002790
10. Gao Y, Mruk DD, Cheng CY (2015) Sertoli cells are the target of environmental toxicants in the testis - a mechanistic and therapeutic insight. Expert Opin Ther Targets 19(8):1073–1090. https://doi.org/10.1517/14728222.2015.1039513
11. Li N, Mruk DD, Lee WM, Wong CK, Cheng CY (2016) Is toxicant-induced Sertoli cell

injury in vitro a useful model to study molecular mechanisms in spermatogenesis? Semin Cell Dev Biol 59:141–156. https://doi.org/10.1016/j.semcdb.2016.01.003

12. Monsees TK, Franz M, Gebhardt S, Winterstein U, Schill WB, Hayatpour J (2000) Sertoli cells as a target for reproductive hazards. Andrologia 32(4–5):239–246
13. Wan HT, Mruk DD, Wong CK, Cheng CY (2013) The apical ES-BTB-BM functional axis is an emerging target for toxicant-induced infertility. Trends Mol Med 19(7):396–405. https://doi.org/10.1016/j.molmed.2013.03.006
14. Boekelheide K, Neely MD, Sioussat TM (1989) The Sertoli cell cytoskeleton: a target for toxicant-induced germ cell loss. Toxicol Appl Pharmacol 101(3):373–389
15. Johnson KJ (2014) Testicular histopathology associated with disruption of the Sertoli cell cytoskeleton. Spermatogenesis 4(2):e979106. https://doi.org/10.4161/21565562.2014.979106
16. Russell LD, Peterson RN (1985) Sertoli cell junctions: morphological and functional correlates. Int Rev Cytol 94:177–211
17. Mruk DD, Cheng CY (2015) The mammalian blood-testis barrier: its biology and regulation. Endocr Rev 36(5):564–591. https://doi.org/10.1210/er.2014-1101
18. Yan HH, Mruk DD, Lee WM, Cheng CY (2007) Ectoplasmic specialization: a friend or a foe of spermatogenesis? BioEssays 29(1):36–48. https://doi.org/10.1002/bies.20513
19. O'Donnell L, O'Bryan MK (2014) Microtubules and spermatogenesis. Semin Cell Dev Biol 30:45–54. https://doi.org/10.1016/j.semcdb.2014.01.003
20. Aumuller G, Schulze C, Viebahn C (1992) Intermediate filaments in Sertoli cells. Microsc Res Tech 20(1):50–72. https://doi.org/10.1002/jemt.1070200107
21. Wen Q et al (2016) Transport of germ cells across the seminiferous epithelium during spermatogenesis-the involvement of both actin- and microtubule-based cytoskeletons. Tissue Barriers 4(4):e1265042. https://doi.org/10.1080/21688370.2016.1265042
22. Guttman JA, Kimel GH, Vogl AW (2000) Dynein and plus-end microtubule-dependent motors are associated with specialized Sertoli cell junction plaques (ectoplasmic specializations). J Cell Sci 113(Pt 12):2167–2176
23. Jenardhanan P, Mathur PP (2014) Kinases as targets for chemical modulators: structural aspects and their role in spermatogenesis. Spermatogenesis 4(2):e979113. https://doi.org/10.4161/21565562.2014.979113
24. Wan HT et al (2014) Role of non-receptor protein tyrosine kinases in spermatid transport during spermatogenesis. Semin Cell Dev Biol 30:65–74. https://doi.org/10.1016/j.semcdb.2014.04.013
25. Chojnacka K, Mruk DD (2015) The Src non-receptor tyrosine kinase paradigm: new insights into mammalian Sertoli cell biology. Mol Cell Endocrinol 415:133–142. https://doi.org/10.1016/j.mce.2015.08.012
26. Almog T, Naor Z (2008) Mitogen activated protein kinases (MAPKs) as regulators of spermatogenesis and spermatozoa functions. Mol Cell Endocrinol 282(1–2):39–44. https://doi.org/10.1016/j.mce.2007.11.011
27. Gungor-Ordueri NE, Mruk DD, Wan HT, Wong EW, Celik-Ozenci C, Lie PP, Cheng CY (2014) New insights into FAK function and regulation during spermatogenesis. Histol Histopathol 29(8):977–989. https://doi.org/10.14670/HH-29.977
28. Tang EI, Mruk DD, Cheng CY (2013) MAP/microtubule affinity-regulating kinases, microtubule dynamics, and spermatogenesis. J Endocrinol 217(2):R13–R23. https://doi.org/10.1530/JOE-12-0586
29. Schaller MD, Borgman CA, Cobb BS, Vines RR, Reynolds AB, Parsons JT (1992) pp125FAK a structurally distinctive protein-tyrosine kinase associated with focal adhesions. Proc Natl Acad Sci U S A 89(11):5192–5196
30. Roskoski R Jr (2004) Src protein-tyrosine kinase structure and regulation. Biochem Biophys Res Commun 324(4):1155–1164. https://doi.org/10.1016/j.bbrc.2004.09.171
31. Marx A, Nugoor C, Panneerselvam S, Mandelkow E (2010) Structure and function of polarity-inducing kinase family MARK/par-1 within the branch of AMPK/Snf1-related kinases. FASEB J 24(6):1637–1648. https://doi.org/10.1096/fj.09-148064
32. Cowan-Jacob SW (2006) Structural biology of protein tyrosine kinases. Cell Mol Life Sci 63(22):2608–2625. https://doi.org/10.1007/s00018-006-6202-8
33. Hubbard SR, Till JH (2000) Protein tyrosine kinase structure and function. Annu Rev Biochem 69:373–398. https://doi.org/10.1146/annurev.biochem.69.1.373
34. Hall JE, Fu W, Schaller MD (2011) Focal adhesion kinase: exploring Fak structure to gain insight into function. Int Rev Cell Mol Biol 288:185–225. https://doi.org/10.1016/B978-0-12-386041-5.00005-4
35. Naz F, Anjum F, Islam A, Ahmad F, Hassan MI (2013) Microtubule affinity-regulating kinase

4: structure, function, and regulation. Cell Biochem Biophys 67(2):485–499. https://doi.org/10.1007/s12013-013-9550-7

36. Tang EI et al (2012) Microtubule affinity-regulating kinase 4 (MARK4) is a component of the ectoplasmic specialization in the rat testis. Spermatogenesis 2(2):117–126. https://doi.org/10.4161/spmg.20724
37. Corsi JM, Rouer E, Girault JA, Enslen H (2006) Organization and post-transcriptional processing of focal adhesion kinase gene. BMC Genomics 7:198. https://doi.org/10.1186/1471-2164-7-198
38. Al-Khalili O, Duke BJ, Zeltwanger S, Eaton DC, Spier B, Stockand JD (2001) Cloning of the proto-oncogene c-src from rat testis. DNA Seq 12(5–6):425–429
39. Kierszenbaum AL, Rivkin E, Talmor-Cohen A, Shalgi R, Tres LL (2009) Expression of full-length and truncated Fyn tyrosine kinase transcripts and encoded proteins during spermatogenesis and localization during acrosome biogenesis and fertilization. Mol Reprod Dev 76(9):832–843. https://doi.org/10.1002/mrd.21049
40. Bordeleau LJ, Leclerc P (2008) Expression of hck-tr, a truncated form of the src-related tyrosine kinase hck, in bovine spermatozoa and testis. Mol Reprod Dev 75(5):828–837. https://doi.org/10.1002/mrd.20814
41. Singh AK, Tasken K, Walker W, Frizzell RA, Watkins SC, Bridges RJ, Bradbury NA (1998) Characterization of PKA isoforms and kinase-dependent activation of chloride secretion in T84 cells. Am J Phys 275(2 Pt 1):C562–C570
42. Lie PP, Mruk DD, Mok KW, Su L, Lee WM, Cheng CY (2012) Focal adhesion kinase-Tyr407 and -Tyr397 exhibit antagonistic effects on blood-testis barrier dynamics in the rat. Proc Natl Acad Sci U S A 109(31):12562–12567. https://doi.org/10.1073/pnas.1202316109
43. Rovelet-Lecrux A et al (2015) De novo deleterious genetic variations target a biological network centered on Abeta peptide in early-onset Alzheimer disease. Mol Psychiatry 20(9):1046–1056. https://doi.org/10.1038/mp.2015.100
44. The UniProt C (2017) UniProt: the universal protein knowledgebase. Nucleic Acids Res 45(D1):D158–D169. https://doi.org/10.1093/nar/gkw1099
45. Finn RD et al (2014) Pfam: the protein families database. Nucleic Acids Res 42(Database issue):D222–D230. https://doi.org/10.1093/nar/gkt1223
46. Piovesan D et al (2017) DisProt 7.0: a major update of the database of disordered proteins. Nucleic Acids Res 45(D1):D1123–D1124. https://doi.org/10.1093/nar/gkw1279
47. Buchan DW, Minneci F, Nugent TC, Bryson K, Jones DT (2013) Scalable web services for the PSIPRED protein analysis workbench. Nucleic Acids Res 41(Web Server issue):W349–W357. https://doi.org/10.1093/nar/gkt381
48. Greene LH et al (2007) The CATH domain structure database: new protocols and classification levels give a more comprehensive resource for exploring evolution. Nucleic Acids Res 35(Database issue):D291–D297. https://doi.org/10.1093/nar/gkl959
49. Altschul SF, Gish W, Miller W, Myers EW, Lipman DJ (1990) Basic local alignment search tool. J Mol Biol 215(3):403–410. https://doi.org/10.1016/S0022-2836(05)80360-2
50. Sali A, Blundell TL (1993) Comparative protein modelling by satisfaction of spatial restraints. J Mol Biol 234(3):779–815. https://doi.org/10.1006/jmbi.1993.1626
51. Berman HM et al (2002) The protein data bank. Acta Crystallogr D Biol Crystallogr 58(Pt 6 No 1):899–907
52. Boratyn GM, Schaffer AA, Agarwala R, Altschul SF, Lipman DJ, Madden TL (2012) Domain enhanced lookup time accelerated BLAST. Biol Direct 7:12. https://doi.org/10.1186/1745-6150-7-12
53. Yang J, Yan R, Roy A, Xu D, Poisson J, Zhang Y (2015) The I-TASSER suite: protein structure and function prediction. Nat Methods 12(1):7–8. https://doi.org/10.1038/nmeth.3213
54. Kim DE, Chivian D, Baker D (2004) Protein structure prediction and analysis using the Robetta server. Nucleic Acids Res 32(Web Server issue):W526–W531. https://doi.org/10.1093/nar/gkh468
55. Corpet F (1988) Multiple sequence alignment with hierarchical clustering. Nucleic Acids Res 16(22):10881–10890
56. Hess B, Kutzner C, van der Spoel D, Lindahl E (2008) GROMACS 4: algorithms for highly efficient, load-balanced, and scalable molecular simulation. J Chem Theory Comput 4(3):435–447. https://doi.org/10.1021/ct700301q
57. Pronk S et al (2013) GROMACS 4.5: a high-throughput and highly parallel open source molecular simulation toolkit. Bioinformatics 29(7):845–854. https://doi.org/10.1093/bioinformatics/btt055
58. Kim S et al (2016) PubChem substance and compound databases. Nucleic Acids Res 44(D1):D1202–D1213. https://doi.org/10.1093/nar/gkv951

59. Halgren TA, Murphy RB, Friesner RA, Beard HS, Frye LL, Pollard WT, Banks JL (2004) Glide: a new approach for rapid, accurate docking and scoring. 2. Enrichment factors in database screening. J Med Chem 47(7):1750–1759. https://doi.org/10.1021/jm030644s
60. Dixon SL, Smondyrev AM, Knoll EH, Rao SN, Shaw DE, Friesner RA (2006) PHASE: a new engine for pharmacophore perception, 3D QSAR model development, and 3D database screening: 1. Methodology and preliminary results. J Comput Aided Mol Des 20(10–11):647–671. https://doi.org/10.1007/s10822-006-9087-6
61. Schuttelkopf AW, van Aalten DM (2004) PRODRG: a tool for high-throughput crystallography of protein-ligand complexes. Acta Crystallogr D Biol Crystallogr 60(Pt 8):1355–1363. https://doi.org/10.1107/S0907444904011679
62. Jenardhanan P, Mannu J, Mathur PP (2014) The structural analysis of MARK4 and the exploration of specific inhibitors for the MARK family: a computational approach to obstruct the role of MARK4 in prostate cancer progression. Mol BioSyst 10(7):1845–1868. https://doi.org/10.1039/c3mb70591a
63. Halgren TA (2009) Identifying and characterizing binding sites and assessing druggability. J Chem Inf Model 49(2):377–389. https://doi.org/10.1021/ci800324m
64. Iwatani M et al (2013) Discovery and characterization of novel allosteric FAK inhibitors. Eur J Med Chem 61:49–60. https://doi.org/10.1016/j.ejmech.2012.06.035
65. Al-Obeidi FA, Lam KS (2000) Development of inhibitors for protein tyrosine kinases. Oncogene 19(49):5690–5701. https://doi.org/10.1038/sj.onc.1203926

Chapter 19

A Stopped-Flow Light Scattering Methodology for Assessing the Osmotic Water Permeability of Whole Sertoli Cells

Anna Maggio, Raquel L. Bernardino, Patrizia Gena, Marco G. Alves, Pedro F. Oliveira, and Giuseppe Calamita

Abstract

Movement of water into and out of the cell is fundamental to life. In the male reproductive tract, at the level of the seminiferous epithelium, Sertoli cells are pivotal in mediating the movement of water into the luminal compartment, a process providing a means of transport of spermatozoa into the epididymal ducts. Here, we describe a stopped-flow light-scattering methodology to easily assess the Sertoli cell osmotic water permeability. The devised methodology is well suited for studying how the Sertoli cell's permeability changes following exogenous stimuli.

Key words Aquaporin channels, Male fertility, Membrane water permeability, Sertoli cells, Spermatogenesis

1 Introduction

Fluid reabsorption and secretion are essential processes in male reproductive tract physiology [1]. Water movements provide a means of transport to the spermatozoa into the epididymal ducts and are therefore essential for composition of the luminal fluids that fill the testicular ducts [2]. In this context, Sertoli cells play a critical role in regulating the amount of water and solutes that move from the interstitial fluid to the adluminal compartment, which is filled by the seminiferous tubular fluid [3]. The solute and water transporters at the Sertoli cell plasma membrane are influenced by various exogenous conditions [4–7]. Sertoli cells express various membrane transport proteins, allowing them to control both the seminiferous fluid composition and pH [2, 5, 8–10].

Anna Maggio and Raquel L. Bernardino contributed equally to this work.

Marco G. Alves and Pedro F. Oliveira (eds.), *Sertoli Cells: Methods and Protocols*, Methods in Molecular Biology, vol. 1748, https://doi.org/10.1007/978-1-4939-7698-0_19,

Stopped-flow light scattering (SFLS) is one of the most widely used approaches in measuring the osmotic and solute permeability of biological membranes. Depending on the solid shape of the cells, SFLS can be used to measure the membrane permeability of whole intact cells (cells of spheroidal shape) or that of vesicles prepared from any type of membrane (i.e., plasma membrane, microsomal membranes). SFLS can be also employed to measure the membrane permeability of isolated organelles such as mitochondria [11]. This chapter describes a SFLS-based methodology to measure the coefficient of osmotic water permeability (P_f; cm/s) of the Sertoli cell plasma membrane. The osmotic water permeability is assessed by measuring the cell shrinkage induced by imposing a hyperosmotic gradient (140 mosM) between the extracellular medium and the intracytoplasmic compartment of suspended Sertoli cells. Immediately, after applying the hypertonic gradient, water outflow occurs, and the cells shrink, causing an increase in scattered light intensity [12, 13]. The time course of cell volume change is followed from changes in intensity of scattered light at 20 °C (depending on the experimental need, the measurements can be done at lower or higher temperatures) at the wavelength of 530 nm using a stopped-flow reaction analyzer. The Sertoli cell's P_f value is calculated using the following equation:

$$P_f = k_i \times V_0 \,/\, A_v \times V_w \times \Delta C$$

where k_i is the fitted exponential rate constant, V_0 is the initial mean cell volume, A_v is the mean cell surface, V_w is the molar volume of water, and ΔC is the osmotic gradient [12].

2 Materials

2.1 Rat Sertoli Cell Culture

The preparation of solutions for rat Sertoli cell culture is done in a sterile environment, and ultrapure water should be used to prepare all solutions. This procedure is described in detail in another chapter.

1. Phosphate-buffered saline solution (PBS): 140 mM sodium chloride, 3 mM potassium chloride, 10 mM sodium phosphate dibasic, and 1.8 mM potassium phosphate monobasic anhydrous. Weigh all reagents into a 1 L graduated cylinder and dissolve in 900 mL of water. If necessary, the pH of the solution should be adjusted to 7.4, using concentrated solutions of hydrochloric acid and/or sodium hydroxide. Adjust the volume to 1 L with deionized water. The PBS should be filtered through a 0.2 μm mixed cellulose ester membrane filter using a vacuum filtration unit in the laminar flow chamber in a sterile environment and stored in a sterile glass bottle at 4 °C.

2. Culture medium: for the preparation of culture medium, add Dulbecco's Modified Eagle's Medium (DMEM) (with glucose and L-glutamine) with Nutrient Mixture F-12 Ham (with glucose and L-glutamine), and dissolve in 900 mL of water according to the manufacturer's recommendations. After, add 14 mM sodium hydrogen carbonate and 15 mM HEPES. If low-glucose DMEM medium is used, it should be supplemented with D-Glucose until reaching a final concentration of 18 mM. The pH of the medium should be adjusted to 7.4, using concentrated solutions of hydrochloric acid and/or sodium hydroxide. Adjust the volume to 1 L. This solution should be filtered through a 0.2 μm mixed cellulose ester membrane filter using a vacuum filtration unit in the laminar flow chamber in a sterile environment. Add to the sterile medium 100 mL fetal bovine serum (FBS) (10%), 50 μg/mL gentamicin, 50 U/mL penicillin, and 50 mg/mL streptomycin (all these reagents should be sterile). Store in a sterile bottle at 4 °C.
3. Trypsin EDTA solution.

2.2 Stopped-Flow Light Scattering

1. Isotonic medium (300 mosM): 220 mM mannitol, 70 mM sucrose, 20 mM Tris–HCl, 1 mM EDTA, and 5 mM EGTA, pH 7.4. Store at 4 °C.
2. Hypertonic solution (500 mosM): Weigh 1.822 g of mannitol and transfer to a 50 mL tube containing 50 mL of isotonic medium.
3. Hypotonic solution (220 mosM): Transfer 36.67 mL of isotonic medium to a 50 mL tube and add distilled water until 50 mL.
4. Distilled water.
5. Ethanol 70%.
6. Spectrophotometer (Jasco FP-6200).
7. Stopped-flow injection module.
8. Two 10 mL syringes for SFM-20.
9. Cryostat.

3 Methods

Here we describe the procedure for measuring the osmotic membrane permeability of Sertoli cells using the equipment already described in Subheading 2. The protocol for preparing the Sertoli cell cultures is described in detail in another chapter. In the procedure reported below, we used Sertoli cell cultures at about 80% confluence.

3.1 Sertoli Cell Cultures

1. Observe the cells using an inverted optical microscope.
2. Discard the culture medium.
3. Wash the cell culture three times with PBS (4 °C).
4. Trypsinize the cell culture during approximately 5 min (*see* **Notes 1** and **2**).
5. Stop the action of trypsin with FBS-containing culture medium (*see* **Note 3**).
6. Centrifuge the cellular suspension at 300 × *g* for 6 min at 4 °C and discard the related supernatant.

3.2 Stopped-Flow Light-Scattering Setup

1. Before starting the permeability measurements, wash the injection system thoroughly (*see* **Note 4**).
2. Set the cryostat temperature to 20 °C (*see* **Note 5**).
3. Initialize the injection system and the spectrophotometer using the appropriate software.
4. Set SFLS device parameters as follows:
   (a) Dead time: 1.6 ms.
   (b) 99% Mixing efficiency in <1 ms.
   (c) Mixing time: 20 ms.
   (d) Volume injected by syringe 1: 100 μL.
   (e) Volume injected by syringe 2: 100 μL.
   (f) Set the excitation and emission wavelength on the stopped-flow spectrophotometer to 450 nm. The bandwidth of excitation and emission must be set to 20 nm.

3.2.1 Sample Preparation and Stopped-Flow Light-Scattering Measurements

1. Resuspend the cellular pellet in hypotonic medium and mix by gently pipetting (*see* **Note 6**).
2. Measure the mean diameter of the cells using an inverted microscope with camera (*see* **Note 7**) (Fig. 1).
3. Prepare the cellular suspension for one of the syringes of the stopped-flow apparatus diluting 600 μL of the initial cell suspension into 2.5 mL of the hypotonic solution (*see* **Note 8**). Let the Sertoli cells equilibrate for 5 min (*see* **Note 9**), and then fill the syringe with this cellular suspension.
4. Fill the other syringe with the hypertonic solution (*see* **Note 8**).
5. Rapidly mix in a chamber the hypertonic solution (500 mosM) with the cell suspension (220 mosM) (osmotic gradient, 140 mosM) (Fig. 2).
6. After applying a hypertonic gradient, water outflow occurs leading to cell shrinkage and causing an increase in scattered light intensity (I) over time (s).

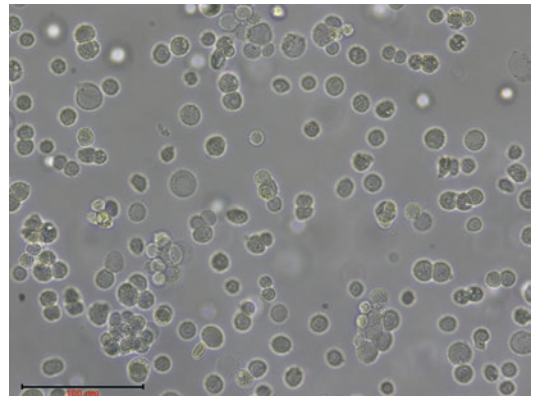

Fig. 1 Representative image of the rat Sertoli cell suspension. Rat Sertoli cells resuspended and equilibrated in hypotonic solution (220 mosM) during 5 min. Scale bar, 100 μm

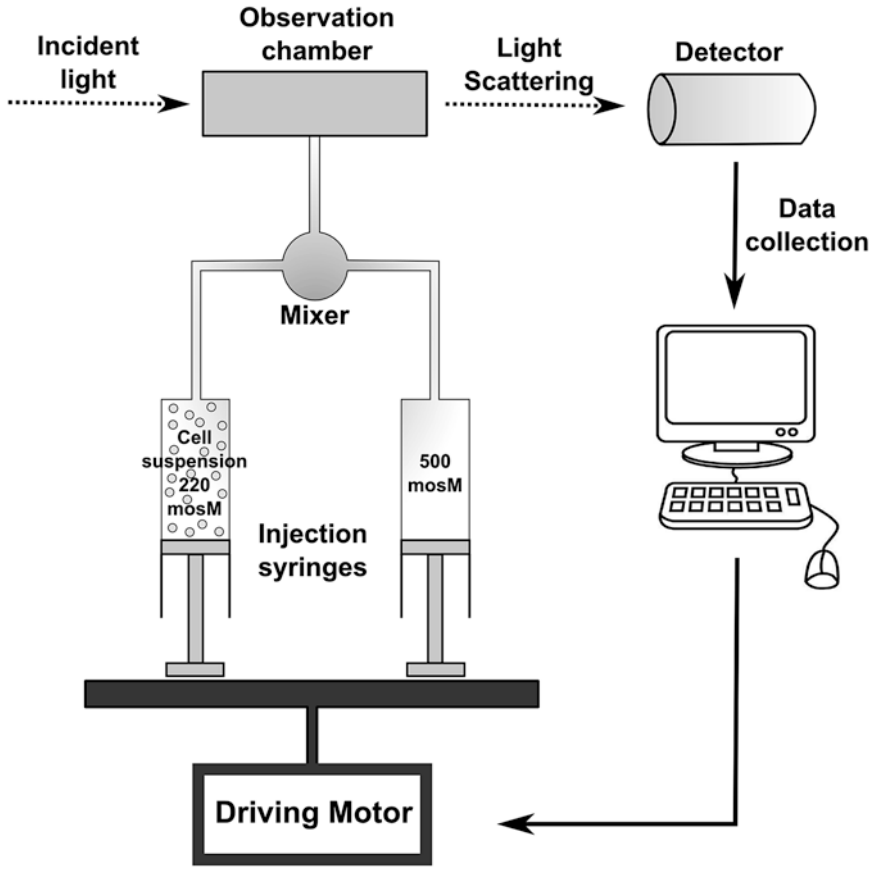

Fig. 2 Schematic diagram of the stopped-flow light scattering system used for measuring the osmotic permeability of the rat Sertoli cells. A driving motor triggers the syringe pistons allowing the solutions to move from syringes to a mixer. The mixture passes through an observation chamber, irradiated with light. The detector is connected to the computer in order to collect the data

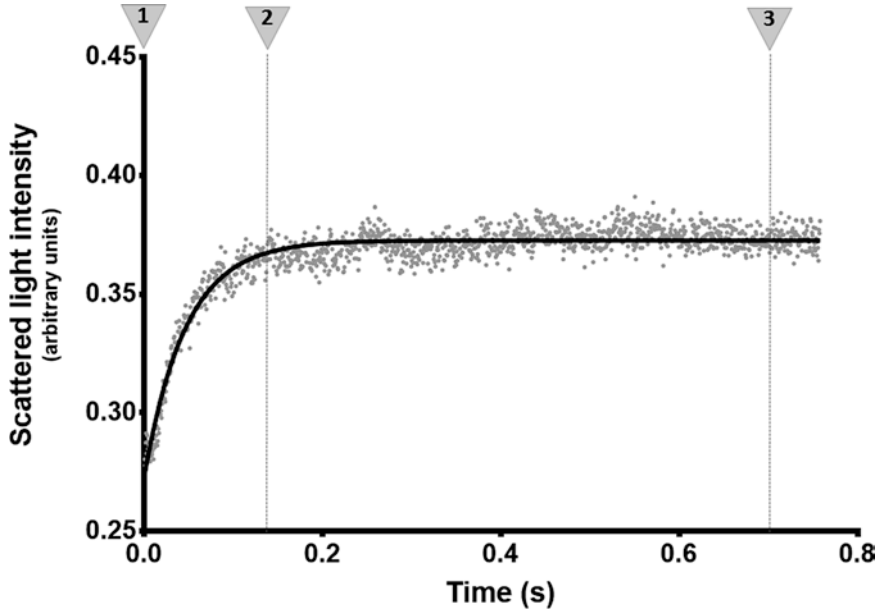

Fig. 3 Representative trace of a time course of scattered light intensity along with single exponential fits of Sertoli cells exposed to a 140 mosM hyperosmotic gradient. Lines 1 and 2 represent the start and the end of the exponential phase, respectively. Line 3 is the end of the equilibrium phase

3.3 Results Analysis

The fitting of the curve data using a single exponential function allows the determination the related time constant (ki, s^{-1}) of cell shrinkage.

1. Analyze the kinetics of the fitted curve by placing three vertical bars: (1) at the beginning of the exponential phase of the curve, (2) at the end of the exponential phase of the curve, and (3) at the end of the equilibrium phase (plateau phase) (Fig. 3).
2. With these points, the appropriate software (Bio-Kine32) automatically calculates the ki of the curve, which is directly related to the slope of the curve.
3. The k_i value is used for calculation of water permeability as described in Subheading 1.

4 Notes

1. The trypsin solution should cover the entire surface of the flask.
2. The time of incubation with trypsin should be sufficient to have the cell isolated in suspension.
3. The quantity of FBS-containing culture medium should be equal to the volume of trypsin.

4. For both syringe housings, perform three washings with distilled water, 70% ethanol, and distilled water, respectively. Repeat these steps at the end of the procedures.
5. It is advisable to start the measurements once the device reaches the selected temperature. Measurements can be done at different temperatures, although for the procedure described in this chapter, we worked at 20 °C.
6. The cells are equilibrated in a slightly hypotonic solution to increase cell turgidity. The volume of the hypotonic solution should be adjusted to the number of the cells. In average one T75 flask with 80% confluence contains about 1×10^7 Sertoli cells (e.g., the pellet obtained the six T75 flasks with 80% confluence should be diluted in approximately 2 mL of hypotonic solution).
7. Capture the images with a microscope equipped with a camera, and measure the cell diameter with an appropriate software.
8. Prepare fresh hypotonic and hypertonic solutions before doing experiment.
9. Equilibration of Sertoli cells in the 220 mosM solution and osmotic shock 500 mosM (equal volumes of cell suspension and hypertonic solution upon mixing) leads to an outwardly directed osmotic gradient of 140 mosM.

Acknowledgment

This work was supported by the "Fundação para a Ciência e a Tecnologia" (FCT) (PTDC/BBB-BQB/1368/2014), UMIB (PEst-OE/SAU/UI0215/2014). R.L. Bernardino was also financed by (SFRH/BD/103105/2014).

References

1. Martins AD, Bernardino RL, Neuhaus-Oliveira A, Sousa M, Sá R, Alves MG, Oliveira PF (2014) Physiology of Na+/H+ exchangers in the male reproductive tract: relevance for male fertility. Biol Reprod 91(1):11–16. Article 11
2. Rato L, Socorro S, Cavaco JE, Oliveira PF (2010) Tubular fluid secretion in the seminiferous epithelium: ion transporters and aquaporins in Sertoli cells. J Membr Biol 236(2): 215–224
3. Bernardino R et al (2013) Molecular basis of bicarbonate membrane transport in the male reproductive tract. Curr Med Chem 20(32): 4037–4049
4. Bernardino RL, Martins AD, Jesus TT, Sá R, Sousa M, Alves MG, Oliveira PF (2015) Estrogenic regulation of bicarbonate transporters from SLC4 family in rat Sertoli cells. Mol Cell Biochem 408(1–2):47–54
5. Bernardino RL et al (2016) Estradiol modulates Na+−dependent HCO3− transporters altering intracellular pH and ion transport in human Sertoli cells: a role on male fertility? Biol Cell 108(7):179–188
6. Jesus TT, Bernardino RL, Martins AD, Sá R, Sousa M, Alves MG, Oliveira PF (2014) Aquaporin-4 as a molecular partner of cystic fibrosis transmembrane conductance regulator

in rat Sertoli cells. Biochem Biophys Res Commun 446(4):1017–1021

7. Jesus TT, Bernardino RL, Martins AD, Sá R, Sousa M, Alves MG, Oliveira PF (2014) Aquaporin-9 is expressed in rat Sertoli cells and interacts with the cystic fibrosis transmembrane conductance regulator. IUBMB Life 66(9): 639–644
8. Bernardino RL et al (2016) Hepatocyte and sertoli cell aquaporins, recent advances and research trends. Int J Mol Sci 17(7):1096
9. Oliveira PF, Sousa M, Barros A, Moura T, Da Costa AR (2009) Membrane transporters and cytoplasmatic pH regulation on bovine Sertoli cells. J Membr Biol 227(1):49
10. Oliveira PF, Sousa M, Barros A, Moura T, da Costa AR (2009) Intracellular pH regulation in human Sertoli cells: role of membrane transporters. Reproduction 137(2):353–359
11. Mathai JC, Sprott GD, Zeidel ML (2001) Molecular mechanisms of water and solute transport across archaebacterial lipid membranes. J Biol Chem 276(29):27266–27271
12. Calamita G et al (2008) Altered expression and distribution of aquaporin-9 in the liver of rat with obstructive extrahepatic cholestasis. Am J Physiol Gastrointest Liver Physiol 295(4):G682–G690
13. Calamita G, Ferri D, Gena P, Liquori GE, Cavalier A, Thomas D, Svelto M (2005) The inner mitochondrial membrane has aquaporin-8 water channels and is highly permeable to water. J Biol Chem 280(17):17149–17153

Chapter 20

Cryopreservation of Human Testicular Tissue by Isopropyl-Controlled Slow Freezing

Yoni Baert, Jaime Onofre, Dorien Van Saen, and Ellen Goossens

Abstract

Tissue cryopreservation uses very low temperatures to preserve structurally intact living cells in their natural microenvironment. Cell survival is strongly influenced by the biophysical effects of ice during both the freezing and the subsequent thawing. These effects can be controlled by optimizing the fragment size, type of cryoprotectant, and cooling rate. The challenge is to determine cryopreservation parameters that suit all cell types present in the tissue. Here we describe a quick and convenient protocol for the cryopreservation of testicular tissue using an isopropyl-insulated freezing device, which was validated in both a mouse and a human model.

Key words Mouse, Human, Testicular tissue, Cryopreservation, Isopropyl, Slow freezing

1 Introduction

There are two basic approaches to cryopreservation: freeze-thaw procedures and vitrification. Basically, during freezing-thawing, the extracellular solution is frozen, but steps are taken to minimize the probability of lethal intracellular ice formation. During vitrification, there is an attempt to rapidly achieve the noncrystalline glass phase and completely avoid ice formation [1]. Nevertheless, cryopreservation protocols for both techniques typically involve loading the sample with cryoprotectants (CPAs), such as dimethyl sulfoxide (DMSO) and sucrose, and then cooling to storage temperature. Upon removal from storage, the sample is thawed and cryoprotectants are removed from the system by dilution [2].

Although many biophysical processes remain relevant when scaling-up cryopreservation protocols from a microscopic cellular level to a macroscopic tissue scale, new problems are introduced related to the heterogeneous composition of the tissues (optimal cryopreservation parameters may vary between cell types) as well as

Marco G. Alves and Pedro F. Oliveira (eds.), *Sertoli Cells: Methods and Protocols*, Methods in Molecular Biology, vol. 1748, https://doi.org/10.1007/978-1-4939-7698-0_20,

to the heat and mass transfer phenomena in larger systems. It is key to achieve equal distribution with rapid diffusion of CPAs and uniform temperature exchange to limit cryoinjury (Fig. 1) [3].

First protocols for freezing testis biopsies aimed at preserving testicular spermatozoa as part of the assisted reproduction program for couples with azoospermia. Later on, it was shown that spermatogenesis could be restored after transplanting cryopreserved spermatogonial stem cells in the seminiferous tubules of sterilized mice [4]. It was then quickly recognized that testicular tissue cryopreservation could also be helpful to save the genetic pool of endangered animals and the fertility of boys and men facing spermatogonial stem cell loss when sperm banking is not applicable [5, 6]. Therefore, adapted testicular tissue cryopreservation protocols were needed with a focus on preserving spermatogonial stem cells and their supportive cells rather than mature germ cells.

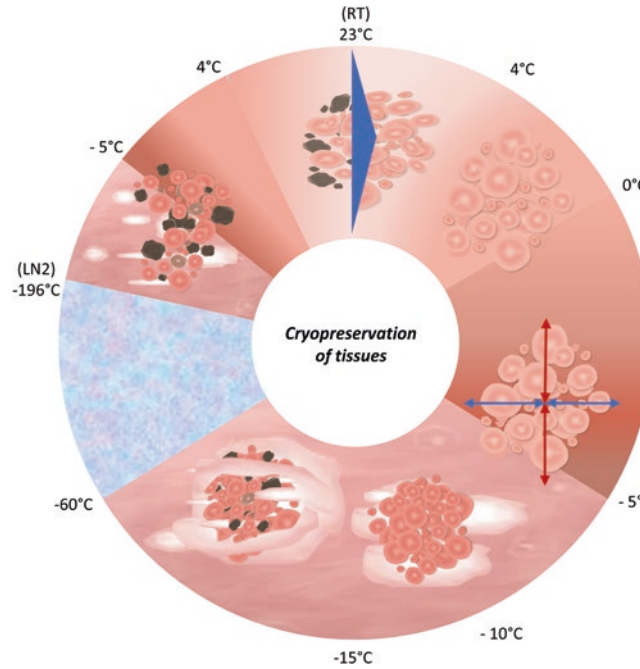

Fig. 1 Sequence of events underlying the freezing of tissue. Along cooling, tissues lose osmotic equilibrium within their medium. At around −5 °C, intra- and extratissular heat (red arrows) and mass (blue arrows) transfer permits equilibration between the tissue and the medium. Between −5 and −15 °C, extracellular ice grows, and therefore solute (electrolyte) concentration increases causing tissue to shrink due to dehydration. From −15 to −60 °C, ice crystals grow larger resulting in intracellular freezing (major degree of cryopreservation-induced tissue damage) and cell death (dark-stained cells). During warming, this sequence of events is reversed, prompting cumulated cryopreservation-induced damage to result in tissue cracking and cell death

Slow freezing has been successfully applied in several animal models [7]. In mice, healthy offspring were obtained from immature frozen-thawed allografts [8]. In humans, slow-frozen prepubertal tissue maintained its integrity and activity in short-term organotypic culture and during long-term xenografting [9–11], making it a well-established and widely used method to bank human testicular tissue for fertility preservation. Indeed, slow freezing was applied to cryopreserve testicular tissue for over 260 patients in clinics worldwide [12, 13]. However, the majority of slow freezing protocols makes use of a time-consuming freezing program provided by rather expensive biofreezers needing liquid nitrogen supply. Consequently, such protocols do not easily allow collection and cryopreservation of testicular tissue at a procurement site distant from the banking and transplantation site nor open doors to laboratories in developing countries willing to offer testicular tissue banking. Hence, we studied two alternative cryopreservation methods, which are more convenient than biofreezers-controlled slow freezing, i.e., isopropyl-controlled slow freezing and solid-surface vitrification. Although solid-surface vitrification preserved the spermatogenic potential of immature mouse testicular tissue, which restored spermatogenesis in sterilized mice, it could not protect human testicular tissue from cryoinjury [14, 15]. In contrast, isopropyl-controlled slow freezing did not only perform well in the mouse model [14], it also protected the integrity of adult human testicular tissue and maintained cell dynamics in long-term propagation culture similar to fresh controls [15, 16]. This chapter describes the isopropyl-controlled slow freezing protocol for the cryopreservation of human testicular tissue.

2 Materials

2.1 Preparation of Cryopreservation Medium

1. Balance.
2. Sterile 15 ml/50 ml polypropylene tubes.
3. Sterile pipette 5/10/25 ml.
4. Injekt™ 20 ml eccentric syringe.
5. Sterile syringe filter unit, pore size 0.22 μm, diam. 33 mm.
6. Sterile 1000 μl pipette tips.
7. 1 ml syringe with 26G × 0.375″ needle.
8. DMEM/F12.
9. Sterile DMSO.
10. Human serum albumin.

11. Sucrose.

2.2 Cryopreservation of Testicular Tissue

1. DMEM/F12.
2. Sterile high-security vials.
3. Cryo labels.
4. Sodium chloride.
5. Sterile water.
6. Sterile pipette 10/25 ml.
7. Sterile 1000 µl pipette tips.
8. Sterile surgical tweezers and scissor or scalpel.
9. Petri dishes with a diameter of 100 mm.
10. Sealing machine.
11. Nalgene® Cryo 1 °C "Mr. Frosty" freezing container.
12. 100% isopropyl alcohol.
13. 70% ethanol.
14. −80 °C freezer.
15. Liquid nitrogen cryotank.
16. Water bath.

3 Methods

3.1 Preparation of Cryopreservation Medium

1. Dissolve 2.55 g sucrose in 40 ml DMEM/F12 (=0.15 M) in a sterile 50 ml polypropylene tube.
2. Filter the solution in another 50 ml polypropylene tube (*see* **Note 1**).
3. Add 5 ml sterile HSA (=10% v/v) and 5 ml sterile DMSO (=1.5 M) with a sterile 5 ml pipette.
4. Store at 4 °C (*see* **Note 2**).

3.2 Cryopreservation of Testicular Tissue

1. The testicular biopsy is collected in a sterile 0.9%NaCl solution in a sterile recipient and transported to the lab on melting ice (Fig. 2a).
2. Clean working space (*see* **Note 3**).
3. Prepare the cryopreservation medium fresh or complete the frozen working solution (*see* Subheading 3.1).
4. Put three sterile dishes (diameter 100 mm) on ice and fill them with 15 ml DMEM/F12.
5. Transfer the testicular biopsy from the sterile recipient to the first dish filled with DMEM/F12 using sterile tweezers.

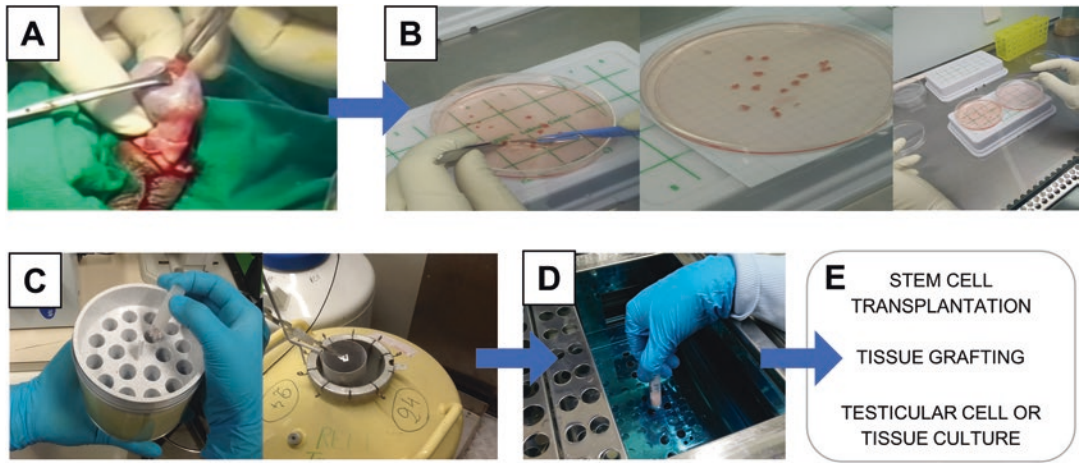

Fig. 2 Testicular tissue cryopreservation procedure. (**a**) Testicular tissue biopsies are retrieved. (**b**) The testicular biopsy is fragmented (6 mm^3 pieces). (**c**) Tissue fragments are transferred to cryovials and loaded to an isopropyl-insulated freezing device, which is placed at −80 °C. After overnight freezing, the cryovials are transferred to liquid nitrogen for long-term storage. (**d**) Thawing is performed at 37 °C in a water bath. (**e**) The recovered tissue is available for downstream applications

6. Transfer the testicular biopsy to the second dish filled with DMEM/F12 (*see* **Note 4**).
7. Divide the testicular biopsy in fragments by using sterile scissors or a scalpel. Remove remnants of the tunica albuginea if present. Keep one larger fragment as fresh control (*see* **Note 5**). Divide the rest into fragments of approximately 6 mm^3 (*see* **Note 6**) (Fig. 2b).
8. Transfer the fragments to the last dish filled with DMEM/F12.
9. Put the cryovials at 4 °C. Fill each vial with 800 µl of cryopreservation medium (*see* **Note 7**).
10. Transfer two testicular fragments to each cryovial.
11. Keep the vials at 4 °C for 15 min.
12. Label the vials.
13. Put the vials in the Mr. Frosty freezing container, and put the freezing container in a −80 °C freezer for a minimum of 4 h (*see* **Note 8**) (Fig. 2c).
14. After incubation in −80 °C, the samples can be transferred to liquid nitrogen for long-term storage (*see* **Note 9**).
15. Thaw the samples in a water bath at 37 °C until all the ice has melted (about 2 min) (Fig. 2d).
16. Spray the vials abundantly with 70% ethanol.
17. Dilute the CPAs by doubling the volume with DMEM/F12 supplemented with 10% (v/v) HSA, and incubate at 4 °C for 5 min.

18. Remove the CPAs by transferring the fragments to fresh DMEM/F12.
19. The fragments are now ready to use (Fig. 2e).

4 Notes

1. DMSO must be added after filtration because this can damage the syringe filter. Also, freeze-thawing cycles of HSA should be avoided. Therefore, these supplements should be added freshly to the cryopreservation medium.
2. The cryopreservation medium can either be prepared fresh at the day of testicular tissue freezing or the DMEM-sucrose solution can serve as a stock solution and be stored at −20 °C. The day of cryopreservation the stock solution (e.g., 8 ml) can be thawed and further prepared by adding DMSO (1 ml, collect with 1 ml sterile syringe) and HSA (1 ml).
3. The procedure needs to be performed in aseptic conditions in a cleaned laminar airflow (LAF). Clear the LAF and all devices inside of it. Wear sterile gloves during the whole procedure.
4. Use different tweezers to avoid carry-over of possible contamination in the transport medium to the sterile dish filled with DMEM/F12.
5. One larger fragment is reserved as fresh control. This fragment is fixed and embedded in paraffin by using a standard fixation protocol. Histological and immunohistochemical analysis can be performed to evaluate the histology of the tissue before cryopreservation (Fig. 3a–c).
6. The size of the pieces should not be too large because the cryopreservation solution should be able to enter the tissue. If pieces are too large, cryodamage might occur at the cellular and subcellular level (Fig. 3c–f).
7. Contact with liquid nitrogen during storage should be prevented to avoid possible contamination. Preferably, high-security tubes are used which can be sealed using a sealing machine. Alternatively, vials can be used with internally threaded caps.
8. Dry the vials before putting them in the freezing container since during incubation in the −80 °C freezer, ice formation can make the vials stick to the freezing container and thus hamper the transfer to liquid nitrogen. The isopropyl alcohol in the Mr. Frosty freezing container should be refilled after every five uses of the freezing container.
9. To avoid potential transfer of contaminations between vials, it is recommended to store them in the vapor phase of liquid nitrogen.

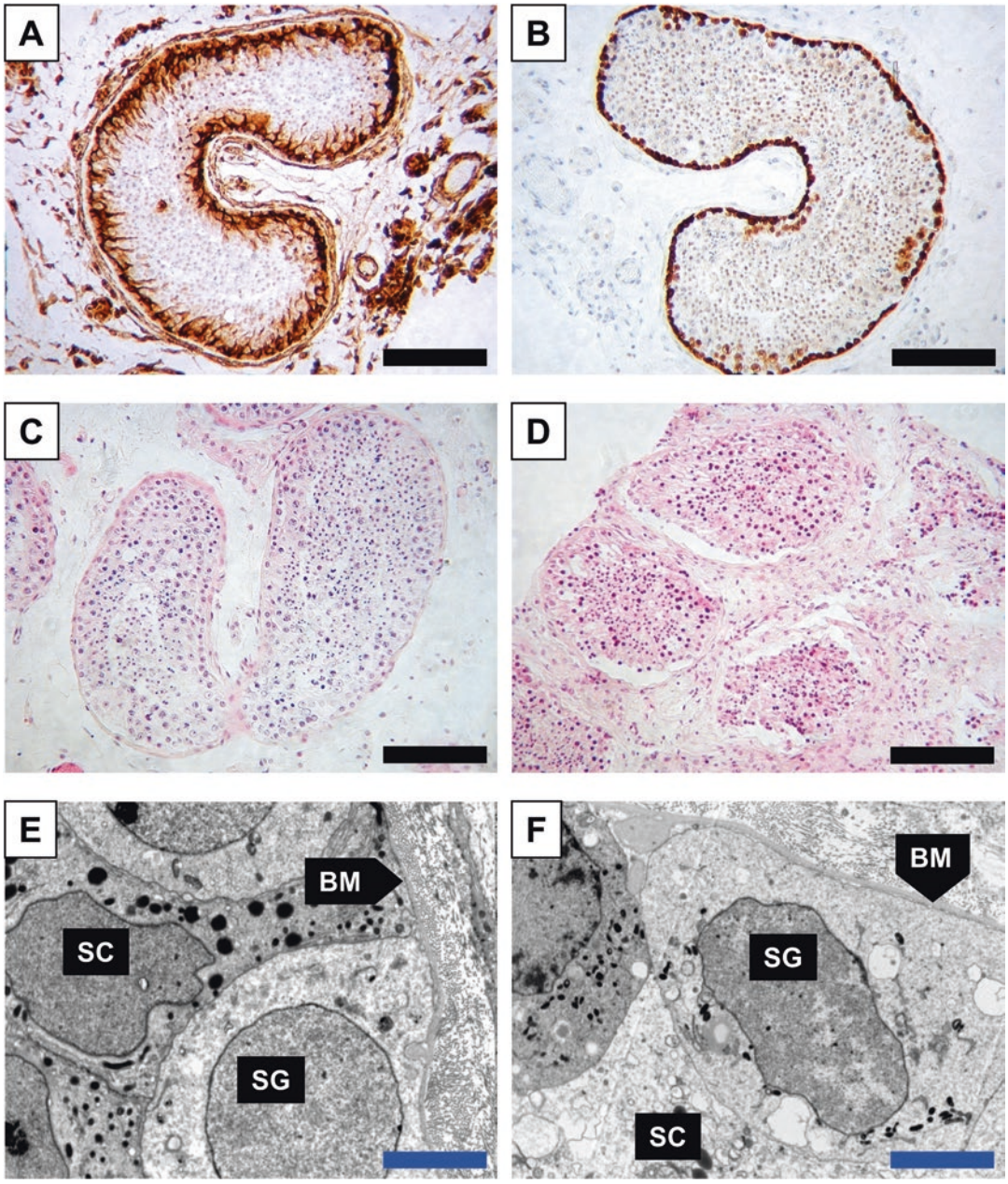

Fig. 3 Immunostainings for vimentin (**a**) and MAGE-A4 (**b**) can be used to evaluate the somatic cells and spermatogonia, respectively (**c** and **d**). Hematoxylin-eosin staining (**c** and **d**) and transmission electron microscopy (**e** and **f**) of fresh (**c** and **e**) and frozen-thawed (**d** and **f**) testicular tissue. Cryopreserving too large fragments might induce cryoinjury, e.g., rupture of the seminiferous epithelium (**d**) or ultrastructural changes to cellular organelles (**f**). *BM* Basal membrane, *SC* Sertoli cell, *SG* spermatogonium, black scale bars: 100 μm, green scale bars: 5 μm

Acknowledgments

This work was supported by a PhD grant from the Agency for Innovation by Science and Technology and research grants from the European Commission Research and Innovation Marie Sklodowska Actions (MSCA)s Seventh Framework program (FP7-People-2013-ITN-603568), the Flemish League against Cancer-Public Utility Foundation, the Scientific Research Foundation Flanders (FWO), University Hospital Brussels (fund Willy Gepts), and the Vrije Universiteit Brussel (Methusalem grant). Y.B. and D.V.S. are postdoctoral fellows of the FWO.

References

1. Yavin S, Arav A (2007) Measurement of essential physical properties of vitrification solutions. Theriogenology 67:81–89
2. Mazur P (1970) Cryobiology: the freezing of biological systems. Science 168:939–949
3. Karlsson JOM, Toner M (1996) Long-term storage of tissues by cryopreservation: critical issues. Biomaterials 17:243–256
4. Avarbock MR, Brinster CJ, Brinster RL (1996) Reconstitution of spermatogenesis from frozen spermatogonial stem cells. Nat Med 2:693–696
5. Nugent D, Meirow D, Brook PF, Aubard Y, Gosden RG (1997) Transplantation in reproductive medicine: previous experience, present knowledge and future prospects. Hum Reprod Update 3:267–280
6. Thuwanut P, Srisuwatanasagul S, Wongbandue G, Tanpradit N, Thongpakdee A, Tongthainan D, Manee-in S, Chatdarong K (2013) Sperm quality and the morphology of cryopreserved testicular tissues recovered post-mortem from diverse wild species. Cryobiology 67:244–247
7. Onofre J, Baert Y, Faes K, Goossens E (2016) Cryopreservation of testicular tissue or testicular cell suspensions: a pivotal step in fertility preservation. Hum Reprod Update 22:744–761
8. Shinohara T, Inoue K, Ogonuki N, Kanatsu-Shinohara M, Miki H, Nakata K, Kurome M, Nagashima H, Toyokuni S, Kogishi K et al (2002) Birth of offspring following transplantation of cryopreserved immature testicular pieces and in-vitro microinsemination. Hum Reprod 17:3039–3045
9. Curaba M, Poels J, van Langendonckt A, Donnez J, Wyns C (2011) Can prepubertal human testicular tissue be cryopreserved by vitrification? Fertil Steril 95:2123.e9–2123.12
10. Keros V, Hultenby K, Borgstrom B, Fridstrom M, Jahnukainen K, Hovatta O (2007) Methods of cryopreservation of testicular tissue with viable spermatogonia in pre-pubertal boys undergoing gonadotoxic cancer treatment. Hum Reprod 22:1384–1395
11. Wyns C, Van Langendonckt A, Wese F-X, Donnez J, Curaba M (2008) Long-term spermatogonial survival in cryopreserved and xenografted immature human testicular tissue. Hum Reprod 23:2402–2414
12. Picton HM, Wyns C, Anderson RA, Goossens E, Jahnukainen K, Kliesch S, Mitchell RT, Pennings G, Rives N, Tournaye H et al (2015) A European perspective on testicular tissue cryopreservation for fertility preservation in prepubertal and adolescent boys. Hum Reprod 30:2463–2475
13. Valli H, Gassei K, Orwig KE (2015) Stem cell therapies for male infertility: where are we now and where are we going? Bienn Rev Infertil 4:1017–1039
14. Baert Y, Goossens E, Van Saen D, Ning L, in't Veld P, Tournaye H (2012) Orthotopic grafting of cryopreserved prepubertal testicular tissue: in search of a simple yet effective cryopreservation protocol. Fertil Steril 97:1152-7–1152-2
15. Baert Y, Van Saen D, Haentjens P, in't Veld P, Tournaye H, Goossens E (2013) What is the best cryopreservation protocol for human testicular tissue banking? Hum Reprod 28:1816–1826
16. Baert Y, Braye A, Struijk RB, van Pelt AMM, Goossens E (2015) Cryopreservation of testicular tissue before long-term testicular cell culture does not alter in vitro cell dynamics. Fertil Steril 104:1244-1252–1244-1254

INDEX

Marco G. Alves and Pedro F. Oliveira (eds.), *Sertoli Cells: Methods and Protocols*, Methods in Molecular Biology, vol. 1748, https://doi.org/10.1007/978-1-4939-7698-0, © Springer Science+Business Media, LLC 2018

T

V

W